Synthesis and characterisation of bifunctional MRI contrast agents

Thesis

UNRESTRICTED

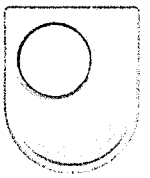

Synthesis and Characterisation of Bifunctional MRI Contrast Agents

by

Patrick J. O'Connell

A thesis submitted in requirement for the degree of

Doctor of Philosophy

Department of Chemistry and Analytical Sciences

The Open University

March 2009

Submission date: 31 January 2007
Date of award: 8 September 2009

DECLARATION

I declare that the work presented in this thesis is the result of my own investigations, and where the work of others is cited, it is fully acknowledged. The material embodied in the thesis has not been submitted, nor is currently submitted for any other degree.

Part of this work was presented as a poster communication: P.J. O'Connell, J.I. Bruce, M. Mortimer, *Synthesis and characterisation of Magnetic Resonance Imaging (MRI) contrast agents,* American Chemical Society (ACS) National Meeting, September 2005, Washington D.C.

.....

Patrick J. O'Connell

ACKNOWLEDGMENTS

I would like to thank my supervisors, Dr James Bruce and Dr Mike Mortimer for their help, guidance and support throughout the PhD. I am grateful to The Open University for financial support and for giving me the opportunity to study for a PhD.

I would like to thank Mr Graham Jeffs for keeping the mass spectrometer alive as cyclen chemistry is impossible without it ! I am grateful to Dr Glen Gibson for his practical help, and to Dr Alan Bowden for help with NMR, and to Mr Pravin Patel and Mr Colin Haynes for their technical support.

Thanks to David Smith for his company in the lab and the lively discussions. Finally, I would like to thank my sister, Dr Ann Marie O'Connell, who is a consultant radiologist, for her kind donation of Magnevist.

Abstract

Macrocyclic ligands based on cyclen form lanthanide complexes with good thermodynamic stability and kinetic inertness due to the large degree of preorganization of the ligand. Conversely, it is these favourable properties which have impeded their development as magnetopharmaceuticals as the functionalization of cyclen remains synthetically challenging. This thesis describes the development of new synthetic routes to substituted cyclen ligands, which after complexation with Gd(III), could have potential as MRI contrast agents.

At present, cyclen is primarily functionalized by alkylation with halide substrates. In an attempt to prepare bifunctional ligands, cyclen was alkylated with derivatised amino acids. Elimination of the halide substrate to give the corresponding alkene was found to be a significant problem using this approach.

As an alternative route to functionalized macrocycles, the Michael addition of cyclen to activated alkenes was investigated. The aza-Michael addition of cyclen to acrylamide was found to be regioselective with the tri-amide substituted cyclen (DO3PAM) being the major product. Hydrolysis of DO3PAM with 12M HCl gave the corresponding tri-acid substituted cyclen (DO3P) in a yield of 90 %. DO3P is an analogue of the important cyclen ligand, DO3A, which has three acetate substituents. Trifluoromethanesulfonic acid was found to catalyse the conjugate addition of mono-*N*-Z-cyclen to methyl-2-acetamidoacrylate under mild conditions. This methodology of mono-Z-protection followed by acid-catalysed addition and deprotection offers a new and versatile route to tri-*N*-substituted cyclen derivatives. The addition of cyclen to ethyl-*cis*-β-cyanoacrylate was regioselective as addition occurred exclusively at the carbon β to the nitrile group.

The ligands DO3P and DO3PAM were complexed with gadolinium(III) and the T_1 spin-lattice relaxation times of the complexes were measured. The corresponding T_1-relaxivity values (r_1) of Gd(DO3P) and Gd(DO3PAM) were determined to be 4.0 and 4.6 $mM^{-1} s^{-1}$ (60 MHz, 25 °C), respectively. These complexes provide significantly better relaxivity values than that of the best-selling MRI contrast agent, Magnevist (Gd-DPTA), which has an r_1 value of 2.8 $mM^{-1} s^{-1}$ (60 MHz, 25 °C).

List of Abbrevations

Å	Angstom
Ac	Acetyl
B_0	Strength of main magnetic field
BBB	Blood brain barrier
BFCA	Bifunctional chelating agent
Boc	*t*-Butoxycarbonyl protecting group
Boc_2O	Di-*tert*-butyldicarbonate
1,2-DB	1,2-dibromotetrachloroethane
CA	Contrast agent
DCC	1,3-Dicyclohexylcarbodiimide ($C_6H_{11}N{=}C{=}NC_6H_{11}$)
DCM	Dichloromethane
DIPEA	Di-*iso*propylethylamine
DMF	*N*,*N*-Dimethylformamide
DO3PAM	1,4,7,10-Tetrazacyclododecane-4,7,10-tripropanamide
DO3P	1,4,7,10-Tetrazacyclododecane-4,7,10-tripropanoate
DOTA	1,4,7,10-Tetra(carboxymethyl-1,4,7,10-etraazocyclododecane)
DPPE	1,2-Bis(diphenylphosphino)ethane
DTPA	Diethylenetriaminepentaacetic acid
EDCI	1-(3-Dimethylaminopropyl)-3-ethylcarbodiimide
eq.	Equivalent
ES-MS	Electrospray mass spectroscopy
EtOAc	Ethyl acetate
Et_3N (TEA)	Triethylamine
Et_2O	Diethyl ether
EtOH	Ethanol
FID	Free induction decay
FT-IR	Fourier-Transform Infra-Red
HR-MS	High-resolution mass spectrometry
i$PrNH_2$	*iso*propylamine
LC-MS	Liquid chromatography-mass spectrometry
LR-MS	Low-resolution mass spectrometry
LSME	L-serine methyl ester

McAb	Monoclonal antibody
$[M]^+$	Molecular ion
MeCN	Acetonitrile
MeOH	Methanol
m.p.	Melting point
MS	Mass spectrometry
MsCl	Methanesulfonyl chloride
MRI	Magnetic Resonance Imaging
m/z	Mass to charge ratio
NMR	Nuclear Magnetic Resonance
NMV	Net magnetisation vector
PG	Protecting group
p-TSA	*p*-Toluenesulfonic acid
q	Number of bound water molecules per Gd^{3+}
RF	Radiofrequency pulse
R_f	Retention factor (TLC)
RT	Room temperature
SBM	Solomon-Bloembergen-Morgan equations
SNR	Signal-to-noise ratio
SPIO	Superparamagnetic iron oxide
T_1	Spin-lattice (longitudinal) relaxation time constant
T_2	Spin-spin (transverse) relaxation time constant
TEA	Triethylamine
TFA	Trifluoroacetic acid
TLC	Thin layer chromatography
TPP	Triphenylphosphine
τ_R	Rotational correlation time
Z (Cbz)	Benzyloxycarbonyl protecting group

Table of Contents

Chapter 1

Introduction

1.0 Introduction

Magnetic resonance imaging (MRI) is a powerful and non-invasive diagnostic technique useful in providing images of the inside of the human body [1]. It has become widely used in hospitals around the world, since it received FDA approval for clinical use in 1985. It is a clinical imaging technique, which relies on the detection of NMR signals emitted by hydrogen protons in the body when placed in a magnetic field. MRI is based on the principles of nuclear magnetic resonance (NMR), a spectroscopic technique used by chemists to obtain structural information about molecules. In 2003, Paul C. Lauterbur and Sir Peter Mansfield won the Nobel Prize in physiology and medicine for their discoveries concerning MRI because it can be widely used for the non-invasive diagnosis and monitoring of human diseases, such as heart disease and cancer.

Nowadays, around 40 % of all MRI scans are performed employing a contrast agent, which is an exogenous compound able to enhance the relaxation rates of water protons [2]. In this way, the quality of the MRI images obtained can be greatly improved (Figure 1.1).

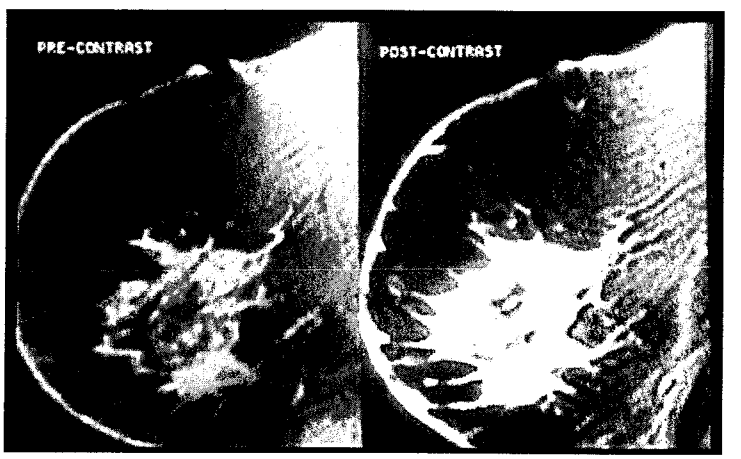

Figure 1.1 Enhancement of cancer imaging with a gadolinium-based contrast agent [3].
(*Left*) MRI before contrast agent is administered
(*Right*) MRI with contrast agent

Polyaminopolycarboxylic complexes of gadolinium(III) (Gd^{3+}), which are administered intravenously, are the most widely used contrast agents in MRI (Figure 1.2) [4].

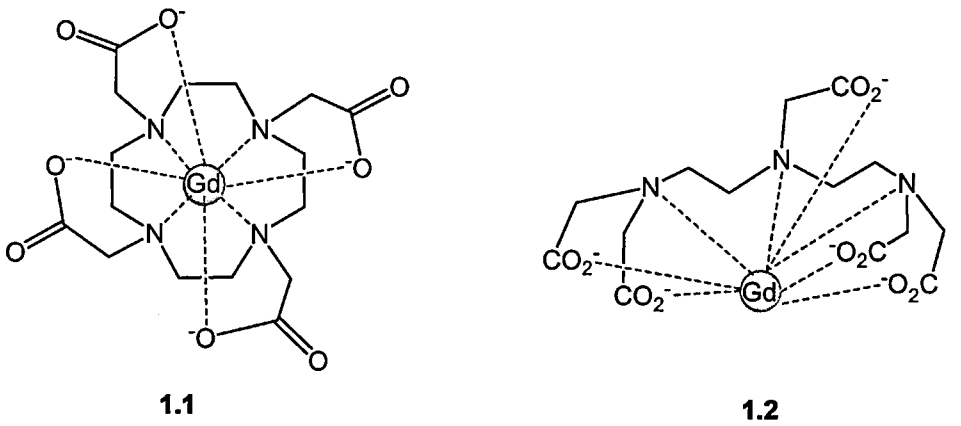

1.1 **1.2**

Figure 1.2 Structure of Gd-DOTA (**1.1**) and Gd-DPTA (**1.2**).

These first generation contrast agents currently in clinical use are small-molecular, extracellular (systemic) agents such as Gd-DTPA and Gd-DOTA[a] (Figure 1.2). They distribute non-specifically throughout plasma and interstitial spaces and are rapidly excreted via the kidneys, or in the case of lipophilic hepatobiliary agents, via the liver. The next generation of contrast agents are geared towards more specific or directed functional imaging. With this in mind, the aim of this project was to synthesise new ligands/complexes with improved targeting properties.

In the following sections of this chapter, the theory of MRI is introduced. It is then outlined how gadolinium-based contrast agents improve the detail of MRI scans. After the different types of contrast agents are reviewed, an account of cyclen chemistry is given. The chapter concludes with a section outlining the aims of the thesis.

[a] DTPA refers to diethylenetriaminepentaacetic acid,
DOTA refers to 1,4,7,10-tetra(carboxymethyl)-1,4,7,10-tetraazocyclododecane [3].

1.1 Basic principles of NMR and MRI

The property of Nuclear Magnetic Resonance (NMR) was first described by Purcell and Bloch in 1946 [5]. Since then, NMR has become a powerful tool in the analysis of chemical composition and structure. In 1973, Lauterbur used the principles of NMR to describe a technique (essentially Magnetic Resonance Imaging or MRI) for determining physical structure [6]. This work led to the development of MRI for applications in biomedical imaging. The MRI technique is based upon the interaction of the magnetic moment of ^{1}H nuclei with the main magnetic field of an MRI scanner [7-9].

As a result of its nuclear spin (I = 1/2) and positive charge (+1), a proton has an intrinsic magnetic moment (μ). The magnetic moments of hydrogen nuclei causes them to behave like tiny compass needles. Other nuclei with an odd number of protons also have net magnetic moments and are candidates for magnetic resonance (see Table 1.1).

Table 1.1 The frequency of nuclei in a magnetic field [8].

Nucleus	Magnetic field (Tesla)	Larmor frequency (MHz)
^{1}H	0.15	6.4
	0.5	21.3
	1.0	42.6
	1.5	63.9
^{13}C	1.0	10.71
^{31}P	1.0	17.25

Nuclei with no spin include ^{12}C, ^{16}O, ^{18}O, ^{40}Ca.

When a proton is placed into a strong external magnetic field, it experiences a turning force, known as a torque, which makes it precess (rotate) around the direction of the field (Figure 1.3).

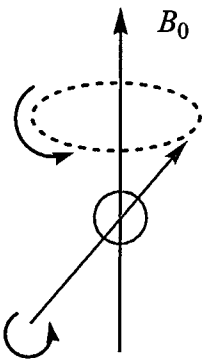

Figure 1.3 A spinning nucleus precesses in an applied magnetic field at its characteristic Larmor frequency.

The precessional frequency, ν, of the proton is found to be directly proportional to the external magnetic field, given by *the Larmor equation*:

$$\nu = \frac{\gamma B_0}{2\pi} \tag{1.1}$$

where ν = Larmor frequency (in Hz or MHz)

B_0 = applied magnetic field (in Tesla)

γ = magnetogyric ratio which is specific for different nuclei (e.g. the value of $\gamma/2\pi$ for protons is 42.58 MHz/T).

The spin of a proton is quantized and in the presence of an external magnetic field can exist in either one of two states (Figure 1.4) [1]. The spin-up (or α-state) is aligned parallel to the main field while the spin-down (or β-state) aligns anti-parallel to it. The frequency required to induce a transition from the α to the slightly higher energy β-state corresponds to the precessional frequency of the nucleus in question; that is, its Larmor frequency;

$$\Delta E = h\nu = h\left(\frac{\gamma B_0}{2\pi}\right) \tag{1.2}$$

where ΔE = energy of transition,

h = Planck's constant (6.63×10^{-34} J s),

For an NMR instrument with a magnetic field strength of 7.0 Tesla, radiofrequency irradiation of approximately 300 MHz is needed to effect a spin-state transition for a proton (Figure 1.4). In MRI, the magnetic field is not as strong and the energy required to effect a spin-state transition is consequently lower. For example, a scanner with a magnetic field strength of 1.4 Tesla, requires irradiation at 60 MHz to effect a spin-state transition in a proton.

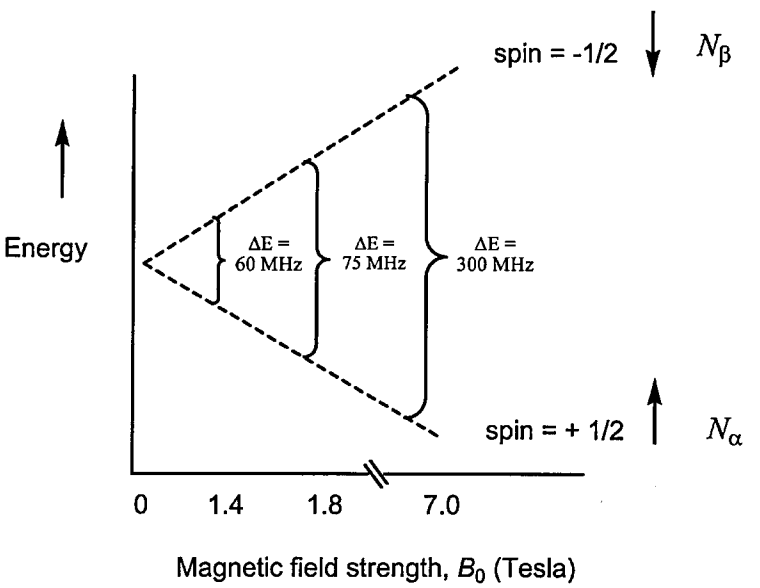

Figure 1.4 Proton energy levels at different magnetic field strengths in ^{1}H NMR.

When an MRI or NMR spectrum is being recorded, the population difference between the α and β states is being sampled. The population difference at equilibrium between the two states is described by *the Boltzmann equation*:

$$\frac{N_\alpha}{N_\beta} = \exp\left(\frac{-\Delta E}{kT}\right) = \exp\left(\frac{-h\nu}{kT}\right) \qquad (1.3)$$

where N = number of nuclei in spin state (α = spin-up, β = spin-down)
k = Boltzmann constant (1.3806×10^{-23} J K^{-1})
T = temperature

For both NMR and MRI, the population differences between the two states are only in the order of 1 part in 10^5 even with the strongest available field strengths. As a consequence, one of the practical problems of both NMR and MRI is that they are inherently insensitive techniques. From eqn 1.3, it can be seen that the only 2 variables influencing the population difference is the field strength and temperature. In MRI, body temperature cannot be changed so increasing the field strength is the only way to improve net magnetization and the strength of the MR signal. High field strengths (> 1.0 T), which have better signal to noise (SNR) ratios, are generated with superconducting magnets [10].

Inside the bore of an MRI scanner, the main magnetic field runs straight down the centre of the tube in which the patient is placed. This means that if a patient is lying on his or her back in the scanner, the hydrogen protons in his or her body will line up in the direction of either the feet or the head [5]. The vast majority of these protons will cancel out each others magnetic effects but a slight excess fraction of the hydrogen nuclei will be aligned with the main magnetic field termed B_0. At body temperature (37 °C) and in a 1.5T scanner, the population difference works out at about 1.000004, which means that for every million protons in the spin-down direction there are a million-and-four protons in the spin-up direction. This results in a net magnetisation vector (NMV) as shown in Figure 1.5(a).

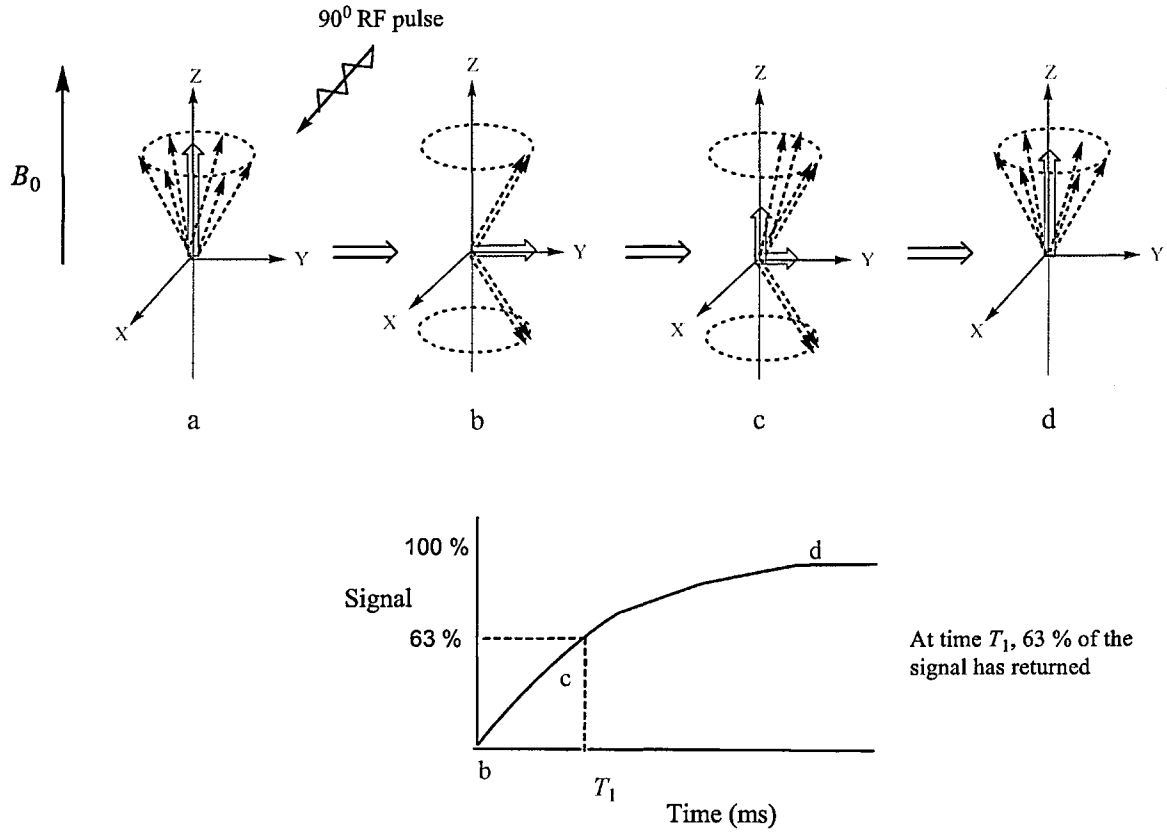

Figure 1.5 The net magnetization vector and its behaviour following a 90° RF pulse [7].

In Figure 1.5(a), the hydrogen nuclei precess around the main magnetic field (B_0) in the longitudinal plane: for clarity, only the excess protons in spin-up alignment are shown. Since the external magnetic field (provided by the static magnet) is much greater than the sample's net magnetization, it is not possible to detect the sample's small magnetization in this state. The sample magnetization must be separated from the external magnetic field by applying a secondary magnetic field perpendicular at a 90° angle to the external field. An RF pulse applied along the +X axis instantaneously creates a secondary magnetic field that causes the magnetic moments to tip away from the equilibrium state. The combined precession of many spins generates a small but detectable excess oscillating magnetic field in the X-Y plane perpendicular to the external magnetic field (i.e. the transverse plane). These oscillations induce an alternating voltage (the NMR signal) in a detection coil.

Application of the RF pulse at the same precessional frequency of the nuclei (i.e. their resonance frequency) promotes them to an excited state. After the RF pulse is switched off, the protons 'relax' back to their original aligned state parallel to B_0 (Figure 1.5, b-d). This longitudinal relaxation along the longitudinal plane (Z-axis) is called T_1-relaxation (*spin-lattice relaxation*). This relaxation process involves transfer of energy from the protons to the surroundings (Figure 1.6).

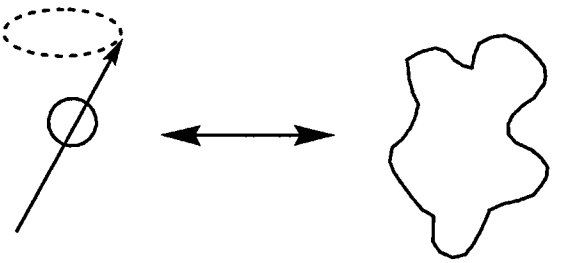

Figure 1.6 Spin-lattice (T_1) relaxation; where spins transfer energy to the surrounding lattice.

A second relaxation process in the sample is the de-phasing of the individual precessing spins that combine to make the NMV. This relaxation along the transverse plane is called T_2 relaxation (*spin-spin relaxation*) and involves changes in precessional frequency due to the interaction between spins in close proximity to one another (Figure 1.7).

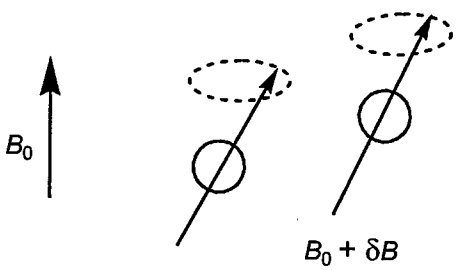

Figure 1.7 Spin-spin (T_2) relaxation; One spin in close proximity to another experiences a change in magnetic field strength which changes its precessional frequency.

When analyzing the structure of chemical compounds in laboratory NMR instruments, samples are placed in a highly uniform static magnetic field so that a single line (or multiplet) for each chemically different proton may be obtained for analysis. A different resonance frequency (or chemical shift) is observed for each chemically different nucleus because it is surrounded by different electron densities and as a result experiences a unique local magnetic field. In contrast, Magnetic Resonance Imaging (MRI) makes use of linear field gradients in order to obtain an image. In 1973, Paul Lauterbur showed that the Larmor equation could be used to obtain geometric information if the magnetic field was made inhomogeneous in a controlled way [6]. Using magnetic field gradients, he showed that the frequency of a signal can be used to convey the location of protons within the field. This effect is demonstrated in Figure 1.8 [11].

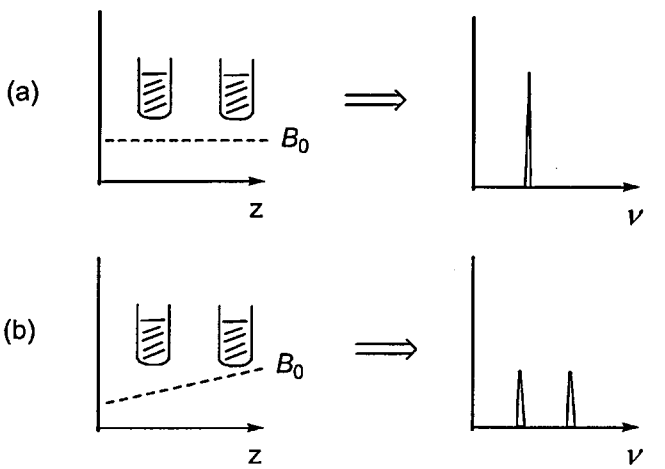

Figure 1.8 **(a)** A spectrum obtained from 2 tubes of water in a constant magnetic field will display only one frequency when Fourier-transformed. **(b)** If the signal is acquired in the presence of a magnetic field gradient, the frequency spectrum will show 2 frequencies, with a separation that depends on their spatial separation.

This basic idea can be elaborated so spatial information can be imparted to NMR signals in order to create an MRI image. This is achieved by varying the pattern and timing of the RF pulse and the use of three-dimensional magnetic field gradients.

1.2 Relaxivity in tissues

Differentiation between biological tissues is the primary objective for imaging use in clinical diagnosis, and requires that the ^1H signal intensities vary depending on tissue type. Most human soft tissues contain about the same amount of water and therefore do not allow tissue differentiation on the basis of water content alone. However, the T_1 (longitudinal) and T_2 (transverse) relaxation times of water protons vary markedly depending on tissue type, and therefore, may be used as the source of contrast in MR images (Table 1.2).

Table 1.2 NMR values for tissue at 10 MHz and 37 °C [12].

Tissue	T_1 (msec)	T_2 (msec)	Proton content (%, relative)
blood	720	175	90
muscle	435	40	84
lung	595	90	72
adipose	170	130	86
water	2500	2500	100

Examination of Table 1.2 shows that protons in biological tissues usually have shorter T_1 and much shorter T_2 than pure water. T_1 depends on tissue composition, structure and surroundings [13]. When the lattice consists of mostly water, it is difficult for the protons to dissipate their energy as the small water molecules move too rapidly. Thus, water has a long T_1. On the other hand, protons attached to discrete fat or protein molecules tumble near the Larmor frequency [1, 7]. Consequently, T_1 relaxation is much more efficient resulting in short T_1 times. T_1 is also longer in a strong magnetic field as the protons precess faster. This results in inefficient energy transfer from the relaxing protons to the lattice with more slowly fluctuating magnetic fields.

1.3 The contrast agent effect

The image contrast in MRI is typically classified according to its sensitivity to the three tissue parameters, proton density (ρ), the longitudinal (or spin-lattice) relaxation times T_1, and the transverse (or spin-spin) relaxation times T_2 [14]. Using different RF pulse sequences, image intensity can be weighted with respect to T_1 or T_2. In MRI, relaxation times are relatively slow (0.1 to 2 sec), increasing the time required to obtain clinically useful images and negatively affecting image quality. As the NMR signal is intrinsically weak, the observed spectra suffer from a poor signal-to-noise ratio (SNR). This can be mitigated by signal averaging, that is, adding the spectra from repeated measurements.

Since paramagnetic ions like Gd^{3+} significantly shorten the T_1 of protons in the tissues where they accumulate, the use of contrast agents in MRI accelerates the signal averaging technique. The Gd^{3+} ion behaves like any magnetic field inhomogeneity but acts over a very small distance. Tissues which take up the agent have an enhanced signal intensity on T_1-weighted images. In Figure 1.1, this effect can be clearly seen. Tumours have more blood-carrying vessels than normal tissues and appear very bright on T_1-weighted images after a contrast agent is injected.

1.4 Properties of gadolinium complexes

The chemical and physical properties of Gd^{3+} complexes and the parameters affecting relaxivity have recently been discussed by Caravan [15] and Aime [4]. However, a brief review of these parameters is necessary here in order to gain some understanding of the rationale behind the design of new gadolinium-based MRI contrast agents.

1.4.1 Physico-chemical properties of gadolinium

The first requirement for a successful MR imaging contrast agent is to be able to interact magnetically with hydrogen nuclei [16]. As single unpaired electrons have magnetic dipole moments that are 657 times stronger than the magnetic dipole moment of protons, the magnetic effects of unpaired electrons dominate the magnetic effects of the atom. Since the relaxation properties of hydrogen nuclei vary as the square of the magnetic dipole moment (of the atom or molecule used as a contrast agent), it is the number of unpaired electrons in the outer shell of an atom that principally determines its effect as a relaxation contrast agent. Gd^{3+} has seven unpaired electrons (unlike any other ion) which results in a magnetic moment of 7.9 magnetons (Table 1.3).

Table 1.3 Electronic configuration and magnetic moments of metal ions [17].

Atomic number	Ion	3d	4f	Magnetic moment (Magneton [b])
24	Cr^{3+}	↑↑ ↑		3.8
25	Mn^{2+}	↑↑ ↑↑ ↑		5.9
26	Fe^{3+}	↑↑ ↑↑ ↑		5.9
29	Cu^{2+}	↓↑ ↓↑ ↓↑ ↓↑ ↑		1.7 - 2.2
63	Eu^{3+}		↓↑ ↑↑ ↑↑ ↑↑	6.9
64	Gd^{3+}		↑↑ ↑↑ ↑↑ ↑	7.9
66	Dy^{3+}		↓↑ ↓↑ ↑↑ ↑↑ ↑	5.9

Gadolinium is a member of the 14 lanthanides or 'rare-earth' elements [18]. The most common and usually the most stable oxidation state of the lanthanides is the trivalent state. Lanthanide cations like Gd^{3+} are hard acids and tend to bind most effectively to hard bases. Like other cations in this category, Gd^{3+} shows a marked preference for oxygen ligands and especially chelating ligands.

[b] One magneton is the magnetic dipole moment of a single free electron [16].

Hard Acids: Gd^{3+}, Na^{+}, Mg^{2+}, Ca^{2+}, Al^{3+}, Fe^{3+}

Hard Bases: H_2O, NH_3, OH^-, ROH, RO^-, CO_3^{2-}, F^-, Cl^-

In an aqueous solution of paramagnetic metal chelate, there is a dipolar magnetic interaction between the electronic magnetic moment of the paramagnetic atom and the much smaller magnetic moments of the protons belonging to nearby water molecules. Gd^{3+} reduces T_1 significantly and T_2 slightly. The overall effect is highly dependent on the Gd^{3+} concentration and concentrations of approximately 0.5M are required to provide significant improvement in tissue contrast.

Gd^{3+} is a very efficient water relaxation catalyst for nuclear magnetic resonance (NMR) due to its high magnetic moment and very labile water coordination [19]. Each Gd^{3+} ion can influence the relaxation of the protons of more than 106 water molecules per second. Gd^{3+} is largely insoluble above pH 6, where it hydrates to produce insoluble oxides and hydroxides. It also readily precipitates with carbonate and phosphate ions, both ubiquitous in blood and tissues. Furthermore, like other heavy metals, it is also capable of competing for binding sites normally occupied by endogenous biological cations such as Zn^{2+} and Ca^{2+}.

1.4.2 The use of cyclen-based ligands in contrast agents

As the naked Gd^{3+} ion is very toxic, it must be wrapped in a tightly-bound organic ligand framework; in other words, it must be chelated [c]. Simple monodentate or even bidentate ligands will not suffice because they do not remain bound to Gd^{3+} in solution. Ligands with higher coordination numbers are therefore required. The obvious candidate is $EDTA^{4-}$, ethylenediaminetetraacetate, which is a commonly employed hexadentate ligand used to

[c] A chelate is a multidentate ligand which contains more than one donor atom coordinated to a metal ion. A complex, in contrast, may be a metal ion with just one water molecule ligand [19].

complex transition metals. However, gadolinium tends to favour high coordination numbers of 8 and 9 in aqueous media due to its large size. Ligands such as DOTA, which are prepared from cyclen (1,4,7,10-tetraazacyclododecane), provide a stable framework for the coordination of the Gd^{3+} ion (Figure 1.9).

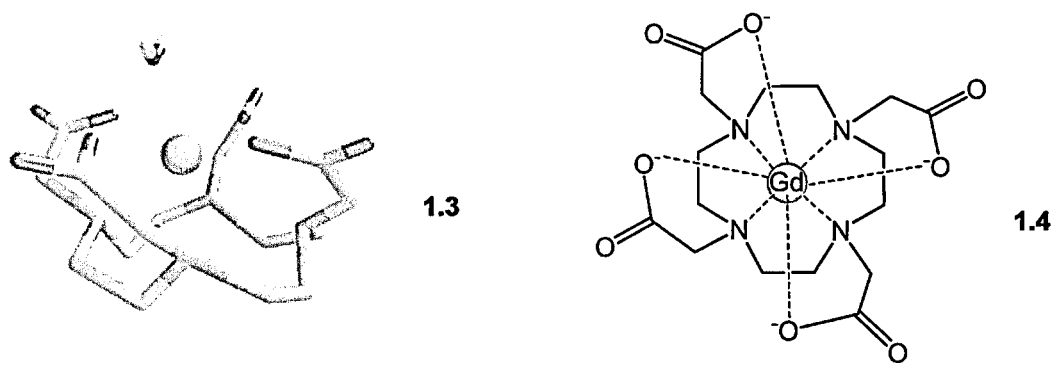

Figure 1.9 X-ray structure[20] of $[Gd(DOTA)]^-$ (**1.3**) and schematic representation (**1.4**).

The DOTA ligand binds to Gd^{3+} through four oxygen atoms of the carboxylates and four nitrogen atoms of the amines. Chelation to DOTA increases the solubility of the Gd^{3+} at the body's neutral pH and still allows for the paramagnetic effect required for an MRI contrast agent. DOTA simultaneously binds the Gd^{3+} ion tenaciously and yet permits one water molecule to coordinate to Gd^{3+}.

Substitution of the nitrogen atoms of cyclen by pendant arms containing donor groups is essential in order to ensure a thermodynamically stable and kinetically inert Gd^{3+} complex [21]. Several functional groups have been used, such as carboxylates, phosphonates, amides and alcohols. Generally, carboxylates are preferred as the resulting complexes are thermodynamically more stable. *N*-functionalized cyclens form exceedingly stable and inert lanthanide complexes due to the stable [3.3.3.3]-square conformation adopted by cyclen in the complexes [22]. Figure 1.9 shows how the DOTA ligand adopts a wrapping conformation to encapsulate the metal cation.

1.5 Relaxivity theory

The presence of a Gd^{3+} ion increases the longitudinal and transverse relaxation rates, $1/T_1$ and $1/T_2$, respectively, of water protons. The observed solvent relaxation rate, $(1/T_i)_{obs}$ is the sum of the diamagnetic $(1/T_i)_d$ and paramagnetic $(1/T_i)_p$ relaxation rates where the subscript i refers to either the longitudinal $(1/T_1)$ or the transverse rate $(1/T_2)$:

$$(1/T_i)_{obs} = (1/T_i)_d + (1/T_i)_p \quad (1.4)$$

The diamagnetic term $(1/T_i)_d$ corresponds to the relaxation rate of the solvent (water) protons in the absence of the paramagnetic solute. The paramagnetic term $(1/T_i)_p$ gives the relaxation rate enhancement caused by the paramagnetic substance, which is linearly proportional to the concentration of the paramagnetic species, $[Gd^{3+}]$:

$$(1/T_i)_{obs} = (1/T_i)_d + r_i [Gd^{3+}] \quad (1.5)$$

According to Equation 1.5, a plot of the observed relaxation rate versus the gadolinium concentration is linear with a slope that defines the relaxivity, r_i. The unit of relaxivity is $mM^{-1} s^{-1}$.

1.5.1 Paramagnetic relaxation enhancement

The relaxivity of a paramagnetic Gd^{3+} complex depends on the magnitude of the magnetic dipole-dipole interaction between the electron spin on the metal and the proton spin on the water molecule coordinated to the metal [23]. A fast exchange (on the NMR time scale) between the inner-sphere water and the bulk water then results in propagation of the paramagnetic influence to the solvent (Figure 1.10).

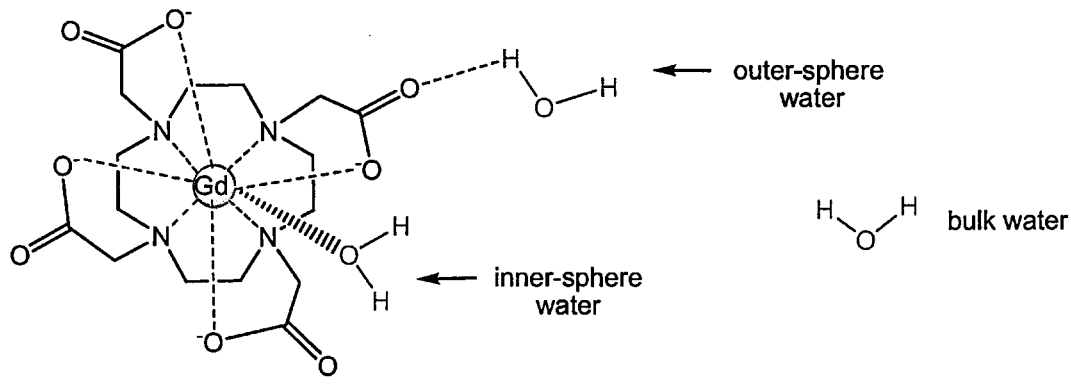

Figure 1.10 Three classes of water: inner-sphere (directly coordinated to Gd^{3+}), outer-sphere (hydrogen-bonded to the complex) and bulk water.

The total paramagnetic relaxation enhancement due to the paramagnetic agent can be divided into two components, inner-sphere and outer-sphere as in Equation (1.6), or expressed in relaxivities as in Equation (1.7):

$$(1/T_i)_p = (1/T_i)^{IS} + (1/T_i)^{OS} \quad (1.6)$$

$$r_i = r_i^{IS} + r_i^{OS} \quad (1.7)$$

where the superscripts 'IS' and 'OS' refer to the inner and outer sphere, respectively.

1.5.2 Inner sphere relaxation

Efficient catalysis of relaxation by a dilute metal complex in 55.5 M water requires that a water molecule reside at the metal no longer than necessary to be relaxed [9]. The change observed in T_1 of bulk water protons in the presence of a dissolved Gd^{3+} complex can be described by Equation (1.8):

$$r_{1p}^{IS} = \left(\frac{1}{T_1}\right)_{obs} - \left(\frac{1}{T_1}\right)_{W} = \frac{[M]\ q}{55.5\ (T_{1M} + \tau_m)} \qquad (1.8)$$

where
- r_{1p}^{IS} = Inner-sphere relaxivity
- $(1/T_1)_{obs}$ = reciprocal of the observed T_1
- $(1/T_1)_w$ = reciprocal of T_1 of the bulk water
- [M] = molar concentration of paramagnetic complex
- q = number of bound water molecules per Gd^{3+}
- T_{1M} = longitudinal relaxation time of the bound water protons
- τ_m = lifetime of the water molecule in coordination site (which is the reciprocal of the solvent exchange rate, k_{ex})

T_{1M} for protons on water coordinated to Gd^{3+} are on the order of microseconds. If τ_m is long relative to T_{1M}, 'slow exchange' conditions exist and no communication between the lanthanide and bulk water occurs. Examples of such systems include tetra-amide gadolinium complexes, in which the overall relaxivity is almost entirely due to the outer-sphere contribution [24]. 'Fast exchange' conditions exist when $\tau_m \ll T_{1M}$.

The term $1/T_{1M}$ is composed of a dipole-dipole term (DD) and a scalar term (SC) (Equation 1.9).

$$\frac{1}{T_{1M}} = \frac{1}{T_1^{DD}} + \frac{1}{T_1^{SC}} \qquad (1.9)$$

As the scalar term becomes negligible at magnetic field strengths above 0.2 T and since most clinical experimental MR images are acquired at field strengths higher than 0.2 T, the scalar term is not an important factor in proton relaxation [25]. Thus, $1/T_{1M}$ is essentially determined by the $1/T_1^{OD}$ term. The dipole-dipole (through space) and scalar (through bonds) interaction between the protons on coordinated water and gadolinium complexes is described by the Solomon-Bloembergen-Morgan (SBM) equations [26, 15]. SBM theory predicts a maximum relaxivity of 100 $mM^{-1}s^{-1}$ for a small-molecular gadolinium complex with a hydration number of one [27]. The relaxivity of a water molecule by a Gd^{3+} complex is a multi-faceted and complex phenomenon with at least eleven inter-dependent parameters describing water relaxation at a given magnetic field strength [15].

1.5.3 Outer sphere relaxation

Contrast agents can display relaxivity even when $q = 0$ (For example, see Egad in Figure 1.20 on Page 32). As there is no water in the inner coordination sphere, the relaxivity must come from outer sphere contributions. These can take two forms;

(i) second sphere relaxation where water molecules hydrogen bonded to the carboxylate oxygen atoms are relaxed via dipolar mechanisms, and

(ii) outer sphere relaxation which arises due to diffusion of water molecules in the bulk near to the Gd^{3+} complex (see Figure 1.10).

For small-sized complexes, it is estimated that the outer-sphere contribution may account for up to 50 % of the overall relaxivity [28]. However, the outer sphere contribution to relaxivity is not very well understood, as it is difficult to quantify the number of second-sphere water molecules [15].

1.6 Enhancement of relaxivity

Figure 1.11 schematically describes the molecular parameters that influence inner- and second-sphere relaxivity. In Figure 1.11, the hydrogen nuclei are small magnetic dipoles denoted by the small vectors whereas the Gd^{3+} ion has a much larger vector. There are q waters in the inner-sphere with a Gd–H distance r and a residency time τ_m, and q' waters in the second-sphere at a Gd–H distance r' and residency time τ_m'. k_{ex} refers to the water exchange rate and is equal to $1/\tau_m$. τ_R refers to the molecular rotational correlation time.

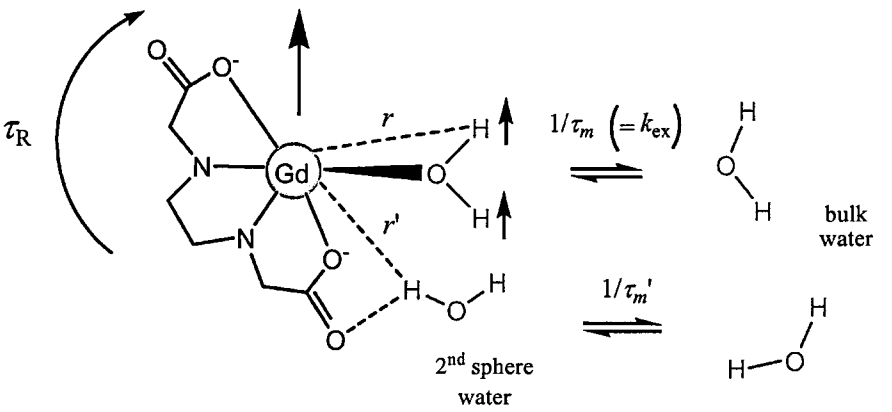

Figure 1.11 Schematic representation of a Gd^{3+} chelate with one inner-sphere water molecule, surrounded by bulk water [15].

Relaxivity arising from the inner-sphere water(s) is given by eqn (1.10), which incorporates 2-site exchange where T_{1m} is the T_1 of the water hydrogen in the inner-sphere and $[H_2O]$ is the water concentration in mM [15]. In order to increase relaxivity, one can increase q or decrease T_{1m} or τ_m.

$$r_{1p}^{IS} = \frac{q\,[H_2O]}{(T_{1M} + \tau_m)} \qquad (1.10)$$

1.6.1 Hydration number (*q*)

For a small monomeric Gd^{3+} complex, a primary determinant of relaxivity is its hydration number [29]. Clinically-available agents are all nine-coordinate, with the polyamino-polycarboxylato ligand providing 8 donors, and a water molecule occupying the ninth coordination site ($q = 1$). Heptadentate ligands allow the coordination of 2 water molecules in the inner sphere of the metal and consequently yield higher relaxivity with respect to Gd^{3+} complexes of octadentate ligands. For example, removing an acetate arm from $[Gd(DOTA)(H_2O)]_2$ to give $[Gd(DO3A)(H_2O)_2]$ doubles the hydration number but still results in a stable complex (Figure 1.12) [15].

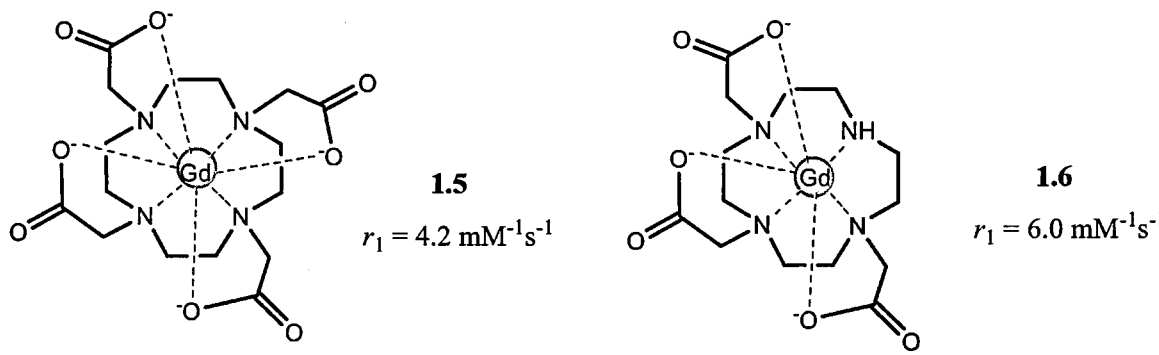

Figure 1.12 Structures of $[Gd(DOTA)(H_2O)]$ and $[Gd(DO3A)(H_2O)_2]$.

Unfortunately, the water molecules in $[Gd(DO3A)(H_2O)_2]$ can be displaced by binding from anions found *in vivo* such as phosphate and bicarbonate (Scheme 1.1).

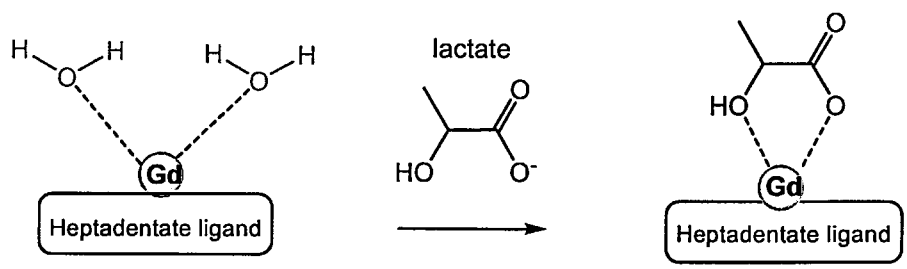

Scheme 1.1 Schematic diagram of the displacement of inner-sphere water molecules upon lactate binding [27].

1.6.2 Rotational correlation time (τ_R)

At the magnetic field strengths used in MRI scans (0.5-1.5 T, 20-60 MHz), the longitudinal relaxation times of the bound water protons, T_{1m}, is dominated by the molecular reorientation (rotational correlation) time, τ_R. If the rotation or tumbling rate of a complex is reduced, the rotational correlation time is longer leading to faster relaxation rates and hence higher relaxivities [15]. Therefore, slowing the rotational correlation time by increasing the molecular weight of a complex or by chelating the metal ion with bulky ligands will optimize the rotational correlation time. This method of improving relaxivity was substantiated by the work of Tweedle *et al.* [30]. They found that relaxivity per Gd^{3+} ion was found to correlate well with molecular weight up to 5 kDa for a series of monomeric and multimeric Gd^{3+} chelates. Their results are reproduced in Figure 1.13 below.

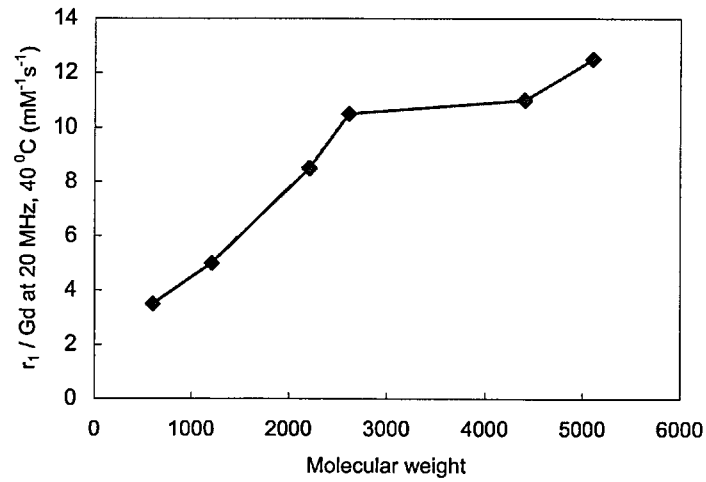

Figure 1.13 Relaxivity per Gd^{3+} ion versus molecular weight for various multimeric complexes [30].

1.7 Contrast agent design

1.7.1 Attributes of MRI contrast media

Like other pharmaceutical products, contrast agents (CAs) must satisfy a number of requirements including target specificity to minimise dose. They must be excreted within a reasonable length of time to minimise toxicity but remain *in vivo* long enough for images to be produced. Other criteria for clinical contrast agents include:

- adequate *in vivo* relaxation enhancement
- high water solubility
- low osmotic potential (osmolality)
- acceptably low toxicity and high thermodynamic stability
- *in vivo* specificity, appropriate lipophilicity and biodistribution
- easy to synthesize

1.7.2 Small molecule or macromolecular contrast agents ?

Macromolecular contrast agents may be defined as paramagnetic compounds of sufficient molecular weight, generally >20,000 Da, that demonstrate prolonged vascular retention. Often based on nanoparticles, dendrimers, antibodies, and proteins, they have a high relaxivity relative to traditional contrast agents. The rotational correlation time of Gd^{3+} in small complexes is generally too fast, in the order of 10^{-10} s, to be optimally effective. Slowing the rotational correlation time to approximately 10^{-8} s will tend to improve the relaxation effectiveness of each Gd^{3+} ion. Fortunately, an increased molecular size results in a slowing of molecular rotation. Thus, macromolecular contrast agents with molecular weights greater than 10,000 daltons will tend to have higher proton T_1 relaxivity than small molecular Gd^{3+} complexes. The relaxation effectiveness of each Gd^{3+} ion can be increased

three- to fourfold by linking the Gd^{3+} complex to a bulky macromolecular carrier (Table 1.4).

Table 1.4 Properties of selected macromolecular contrast media [31].

	Gd-DTPA	Albumin-Gd-DTPA	Dextran-Gd-DTPA
Gd^{3+} ions per molecule	1	30	15
molecular weight (Da)	538	92,000	75,000
r_1 in H_2O per Gd^{3+}	3.7	14.4	10.5
r_1 in H_2O per molecule	3.7	432	157

Macromolecules demonstrate a wide range of possibilities in molecular imaging. However, disadvantages of macromolecular contrast agents include lengthy and expensive preparations, limited shelf-life, and potential immunogenicity [32]. Their size can also prevent effective cellular delivery.

In contrast to the larger macromolecules, smaller molecular contrast agents like Gd-DTPA (MW = 547 Da) rapidly equilibriate between the blood and extravascular interstitial space. They have promising targeting ability due to their high diffusion rates and ability to penetrate tissues. However, the relaxivity of these agents is limited and research is ongoing to increase their sensitivity.

1.7.3 Acyclic or macrocyclic contrast agents ?

All gadolinium chelates currently in clinical use are based on either the acyclic DTPA ligand or the macrocyclic DOTA ligand (Figure 1.14). DTPA (**1.7**) is the first and most widely used acyclic chelator for the complexation of Gd^{3+}. DTPA is an octadentate ligand and when it is complexed with Gd^{3+} accumulates non-specifically and is excreted rapidly [33].

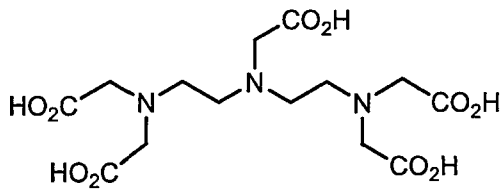

1.7

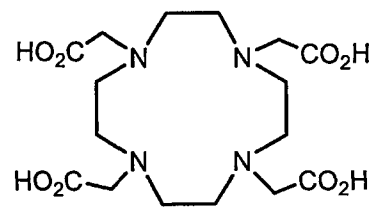

1.8

Figure 1.14 Structure of the ligands DTPA (**1.7**) and DOTA (**1.8**).

The macrocyclic ligand, DOTA (**1.8**), is one of the most frequently employed chelating agents, primarily because of the high stability and kinetic inertness of its metal complexes. Both these properties are crucial but kinetic inertness is essential. This stability and inertness has been ascribed to the macrocyclic structure of the ligands. The *macrocyclic effect* states that complexes of macrocyclic ligands are more stable than those with polydentate ligands of similar binding ability (or similar donor atoms) [34]. The stability of the majority of macrocyclic gadolinium chelates is higher than that of complexes derived from acyclic ligands. Conformationally constrained ligands are preferred because it is considered;

(i) a certain degree of preorganisation [d] should favour the complexation process, and

(ii) decomplexation should be disfavoured due to the presence of steric barriers.

[d] Preorganised means that the donor atoms are held in the correct spatial positions for coordination to a metal [19].

Additionally, DOTA-type complexes are kinetically more stable because the rigid ring structure of the macrocycle prevents release of the metal, as at least five coordination sites would have to break simultaneously, whereas in Gd-DTPA, it is possible to envisage sequential breaking of the coordination sites [35]. The gadolinium chelate of DOTA is currently used as an MRI contrast agent under the brand name Dotarem (Guerbet, France). DOTA is the parent molecule of an ever-growing family of macrocyclic lanthanide (III) chelating agents [33].

1.8 Types of contrast agents

There are a number of ways in which contrast agents (CAs) can be classified. For example, it may be based on clinical applications, target organ, chemical composition, and so on. MRI contrast agents can be classified as positive (appearing bright on MRI) or negative (appearing dark on MRI), T_1 or T_2, contrast agents. T_1 agents containing Gd^{3+} and Mn^{2+} are usually preferred to T_2 contrast agents like SPIO (Superparamagnetic iron oxide) particles as a positive contrast enhancement is often more easily detected than a negative one. The first generation of contrast agents (Figure 1.2) are all non-specific, even if their distribution in the body is far from homogenous [32]. They reside mainly in the blood stream because of their hydrophilic nature. There remains a need for more selective and efficient contrast media that would aid radiologists in making more accurate diagnoses [36]. These second generation agents will be able to selectively visualise for instance, the liver or cardiovascular system.

In this section, CAs conjugated to targeting biomolecules will be discussed in Section 1.8.2 and are referred to as targeted contrast agents. Activatable contrast agents, by comparison,

are switched on by a specific environmental factor and are chemically responsive to physiological states within tissues (Section 1.8.3).

1.8.1 Blood-pool contrast agents

Many injuries and diseases such as atherosclerosis manifest themselves through abnormalities of the blood vasculature [37]. Also, abnormal angiogenesis (blood vessel growth) is observed in the development of most tumours. In order to efficiently image blood vessels, compounds need to stay in the circulation and should not partition into the interstitial space. Filtration by the glomeruli in the kidney defines the molecular weight of blood pool agents to be > 20,000 [38]. High molecular weight macromolecules have been investigated in recent years as potential blood pool imaging agents. Macromolecular molecules cannot be eliminated by glomerular filtration and have much longer dwell times in the body. Furthermore, due to longer rotational correlational times (τ_r), high molecular weight agents based on Gd^{3+} are characterised by higher relaxivities (see Section 1.7.2).

For example, Gd-DTPA covalently bonded to albumin was found to provide excellent enhancement of blood in rats [24]. However, retention of Gd^{3+} *in vivo* for several weeks raised concerns of the contrast agent's long term toxicity. The long residence time of macromolecules in the body improves their susceptibility for cell uptake. Additionally, large molecules are more likely to be antigenic than small molecules, leading to drug-directed antibodies and potentially anaphylaxis [e]. Probably as a result of these concerns, no macromolecular agents have as yet advanced to human trials. One non-macromolecular compound with good potential as a blood pool imaging agent is MS-325 or AngioMARK (Figure 1.15).

[e] Anaphylaxis is an acute, systemic (multi-system) and severe Type I hypersensitivity allergic reaction [34].

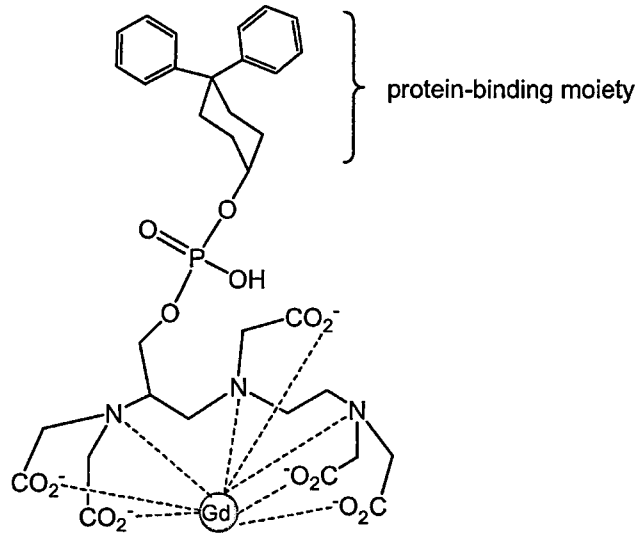

Figure 1.15 Structure of MS-325 (AngioMARK) [39].

MS-325 was developed by Lauffer *et al.* [39] and is currently undergoing human trials. Animal and human studies showed that blood vessels were strongly enhanced for over one hour. The critical positioning of the hydrophobic, diphenylcyclohexyl group next to the hydrophilic phosphodiester is thought to give rise to albumin binding. This diphenylcyclohexyl-substituted DTPA non-covalently binds to human serum albumin (HSA) and reduces the free concentration available for glomerular filtration (Figure 1.16).

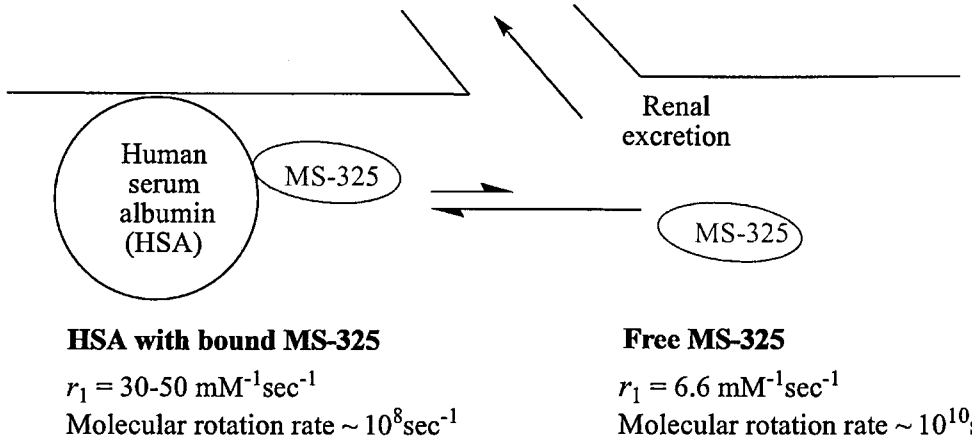

Figure 1.16 Mechanism of action for MS-325 [39]. The bound agent is in equilibrium with a small amount of the free form, which is renally excreted steadily over time. The bound form has greatly increased relaxivity by virtue of its slower molecular tumbling rate.

1.8.2 Targeted contrast agents

A desirable feature of a contrast agent is that it targets a tissue or organ. The basis for designing probes for a given application depends on the location of the target molecule (vascular, extracellular matrix, cell membrane, intracellular, near or at the cell nucleus). Design and synthesis of targeted agents is an active area of research but some compounds are already in clinical use [40]. These include the manganese-based, metalloporphyrin contrast agent (Mn(III)TPPS4) which is used to preferentially enhance contrast of tumours that are iso-intense to surrounding areas on T_1-weighted images [41]. Superparamagnetic iron oxide (SPIO) particles are used clinically to image the lymph nodes [33]. Limitations with targeted agents include the delivery of sufficient quantities of contrast material to the site of the receptor and the biological implications of saturating certain receptors [42].

One challenge that has beset contrast agents for years was their inability to cross cell membranes. This barrier hampered the development of the role of MRI contrast agents in addressing biological questions. In 2003, Allen and Meade found that conjugating Gd(DOTA) to arginine gave a CA (**1.9**) that crossed cell membranes (Figure 1.17) [43].

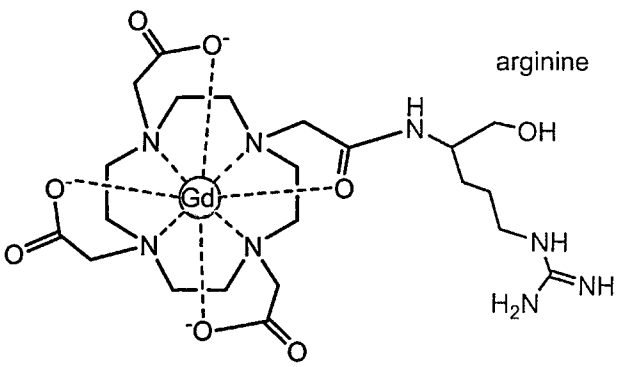

1.9

Figure 1.17 A membrane-permeable contrast agent (**1.9**).

A similar agent (**1.10**) was developed by Aime *et al.*[44]. This conjugate, consisting of glutamine and Gd-DOTA, was found to be actively transported through cell membranes (Figure 1.18).

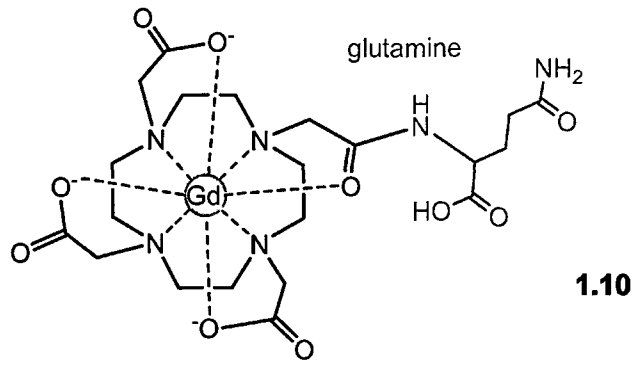

Figure 1.18 A membrane-permeable and tumour-selective contrast agent (**1.10**) [44].

Proliferation of tumour cells require greater amounts of nutrients like the amino acid glutamine and the corresponding membrane-transporters in these cells are up-regulated and/or over expressed. This study found that four times more **1.10** was uptaken by tumour cells than by healthy cells. Clearly, the possibility of targeting cells with low molecular weight, easy to synthesize, gadolinium chelates is highly attractive. The previous examples raise the possibility of diagnosing medical conditions before they become untreatable. For instance, clinical oncology has a need for contrast agents that can identify tumours and metastases at a size of 100,000 cells rather than 1,000,000,000 cells [45].

Amyloid plaques are a characteristic feature in Alzheimer's disease (AD) [46]. Early diagnosis is vital as once the symptoms of the disease become evident, irreversible damage has often occurred. Recently, researchers found that conjugation of the peptide, K6Aβ1–30 (which binds specifically to plaques) to Gd-DPTA enabled earlier detection of the

plaques [47]. As well as detecting symptoms of the disease earlier, this agent may also prove useful for following therapeutic approaches targeting the condition.

Monoclonal antibodies (McAb) have been raised against tumours and covalently attached to DOTA via the ester intermediate (**1.11**; Scheme 1.2) [48]. Complexation of the resultant conjugate with Gd^{3+} gave the highly-specific, contrast agent (**1.13**).

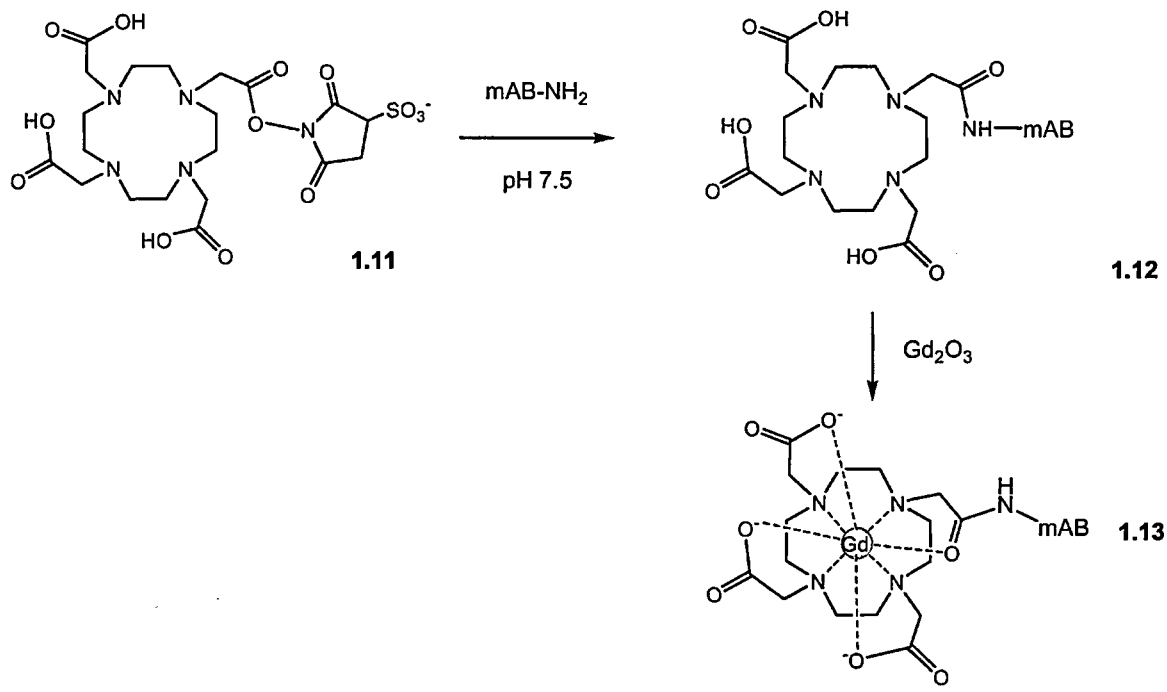

1.11 **1.12** **1.13**

Scheme 1.2 Preparation of a McAb–Gd(DOTA) contrast agent (**1.13**) [48].

One problem with this approach is that the antibody-DOTA agent (**1.13**) delivers only one Gd^{3+} ion to the target which is insufficient to image a tumour. For most biological targets of interest for imaging, multiple Gd^{3+} ions are required to provide the necessary change in relaxation rate. To this end, Lanza *et al.*[49] developed a perfluorocarbon-based nanoparticle loaded with several thousand Gd^{3+} ions. This fibrin-targeted agent (**1.14**) contained ~50,000 paramagnetic gadolinium chelates per 250 nm particle, and could detect clots as small as 500 μm (Figure 1.19) .

1.14

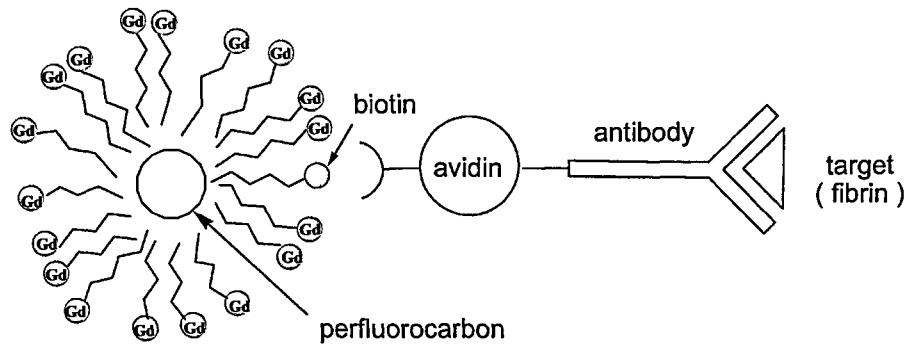

Figure 1.19 Preparation of a fibrin-targeted, fluorocarbon-based nanoparticle (**1.14**) [49].

To construct this nanoparticle, lipids containing biotin were incorporated into the fluorocarbon micelle. Avidin, which has a strong affinity for biotin, was then derivatized with an antibody raised against fibrin (which is found in clots). In this manner, a nanoparticular, contrast agent targeted to fibrin was prepared.

The nanoparticle approach may be more sensitive than the small-molecule approach, as each particle brings tens of thousands of gadolinium atoms to the target site, as compared to a single one. The major drawback of the nanoparticle approach is that not all biochemically-interesting sites can be reached. The average size of this type of nanoparticle is 250 nm which limits intracellular access. Clinical trials of targeted paramagnetic, nanoparticles are expected within a few years [50].

1.8.3 Activatable or "smart" contrast agents

Many new contrast agents are being developed that are capable of reporting on the physiological status and metabolic activity of cells or organisms [51, 52]. These 'Procontrast' agents have been designed to exploit three fundamental physical properties of paramagnetic complexes that function as the switch or trigger to make them detectable by MRI. These properties are: first, q, the number of water molecules coordinated to the

paramagnetic ion; second, τ_m, the lifetime of a water molecule bound to the paramagnetic ion; and third, τ_R, the rotational correlation time of the complex. If motion, hydration number, or water exchange can be altered by an ion, metabolite, enzyme, or a change in pH, then this change may be detected by a change in relaxivity. Since the relaxivity of activatable CAs can be modified by different physiological states, they are predicted to have a crucial role in the imaging field [27, 35].

The first example of a responsive or smart agent is EGad (**1.15**), which was developed by Meade *et al.* (Figure 1.20) [53].

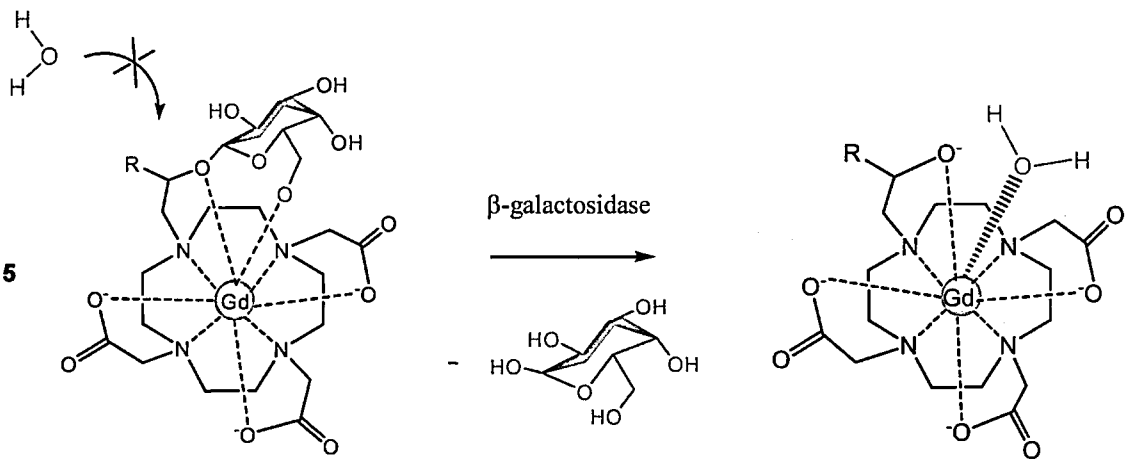

Figure 1.20 Activation of EGad (**1.15**) by the enzyme, β-galactosidase (where R is H or Me).

1.15 is an galactosidase-responsive agent and is essentially DOTA with a galactopyranosyl moiety attached. In **1.15**, all 9 coordination sites of the metal ion are occupied and there is no water molecule in the first coordination sphere. When β-galactosidase cleaves the galactopyranosyl moiety enzymatically, a free coordination site appears which is quickly occupied by a water molecule. Consequently, a 20 % increase in relaxivity is observed in the presence of the enzyme. EGad is used as a research tool to determine if gene delivery has been successful; the enzyme β-galactosidase is not expressed naturally in all human

cells [54, 55]. **1.15** is a prototype agent which demonstrates the potential of MRI for determining the level and location of an enzyme within biological tissues. Egad also demonstrates that MRI is capable of detecting an enzyme that is present at very low (nanomolar) concentrations.

Other research has focused on agents that may enable the observation of cellular processes as they turn off and on. To accomplish this, CAs like **1.16** are being developed whose cage doors are not removed but instead are being opened and closed in a reversible process (Figure 1.21).

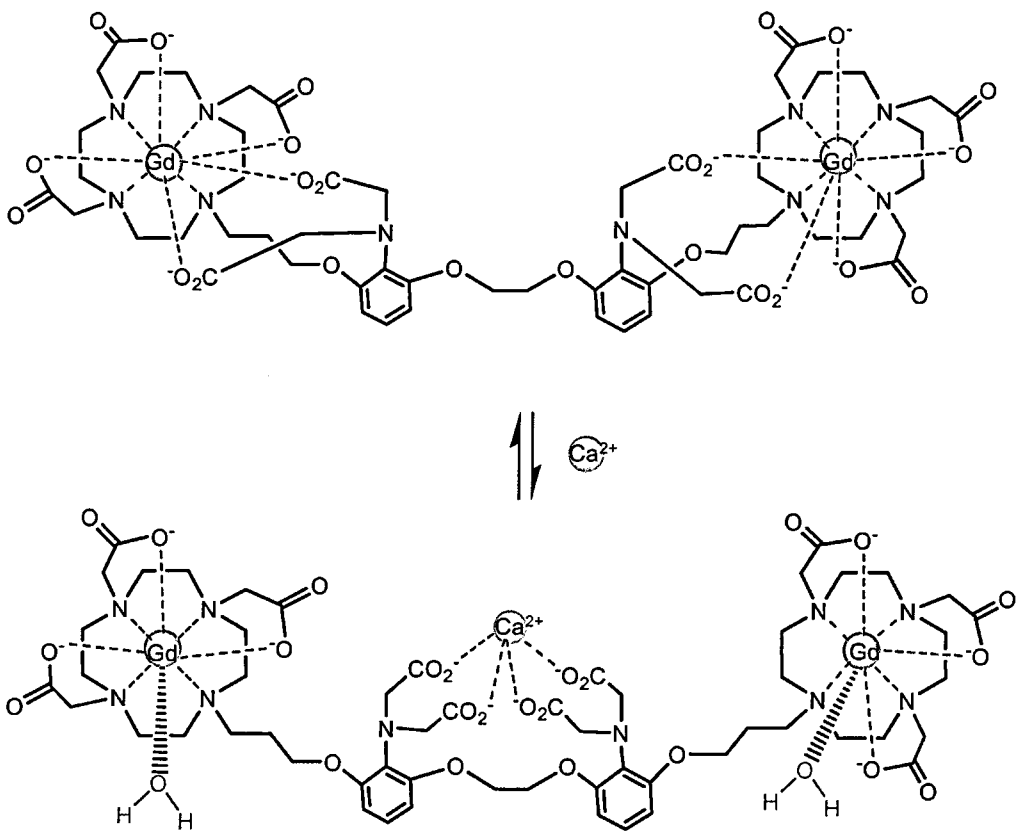

1.16

Figure 1.21 A contrast agent (**1.16**) that is sensitive to Ca^{2+} ions [56].

In **1.16** changes occur in response to the concentration of calcium, an intracellular ion that plays an important role in cell signalling, regulation and metabolism [56]. The $RCOO^-$ groups have a higher selectivity for Ca^{2+} than Gd^{3+}. As the concentration of Ca^{2+} increases, the

$RCOO^-$ groups preferentially bind to Ca^{2+} and expose the Gd^{3+} to water molecules. As a result, water can come into contact with gadolinium resulting in a detectable increase in T_1 relaxivity.

The measurement of pH *in vivo* is an important goal in the diagnosis of kidney disease and cancer [57-59]. Although tissue pH can be measured using microelectrodes, electrodes are invasive and cannot provide good resolution beween different tissues. Therefore, MRI contrast agents have been investigated as possible non-invasive reporters of extracellular pH [60, 61]. One promising pH-sensitive contrast agent is GdDOTA-4Amp (**1.17**) shown in Figure 1.22 [62].

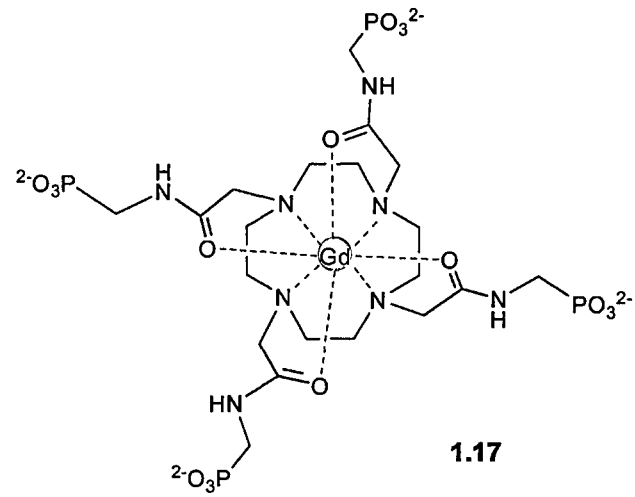

1.17

Figure 1.22 Structure of GdDOTA-4Amp (**1.17**); a CA that can sense tissue pH.

Between pH 2 and 4, **1.17** displays a 25 % increase in relaxivity whereas between pH 6 and 9, an 84 % enhancement of relaxivity is obtained. It is thought the phosphonate side-chains enable rapid prototropic exchange between the single bound water molecule of the complex with the bulk water giving the complex a unique pH-dependent relaxivity.

1.9 Synthesis of macrocyclic ligands based on cyclen

The macrocyclic ligands, DOTA and DO3A, are prepared from cyclen (1,4,7,10-tetraazacyclododecane). Cyclen, shown in Figure 1.23, is a tetraazamacrocycle with 12 atoms and is an aza analogue of crown ether [34, 63].

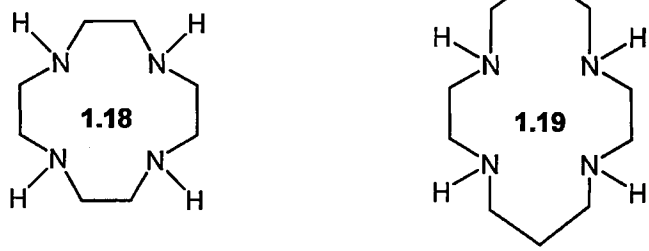

Figure 1.23 Structure of cyclen (**1.18**: [12]aneN$_4$)[f] and cyclam (**1.19**: [14]aneN$_4$) [64].

Cyclen and cyclam are often viewed as models of natural macrocyclic tetra-amine ligands such as porphyrins and corrins which are widespread in nature. The development of synthetic macrocyclic chemistry has resulted in an increased understanding of these important biological macrocycles. Like crown ethers, cyclen derivatives are capable of selectively binding cations like Zn^{2+} as shown in Figure 1.24 [65].

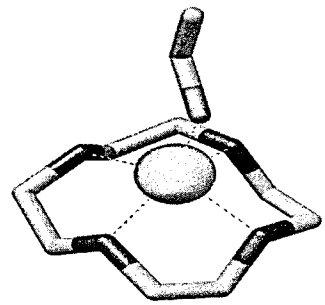

Figure 1.24 Zn^{2+} coordinated to cyclen and an ethanol molecule [65].

One of the biggest drawbacks of macrocyclic ligands lies in their synthesis [2, 34]. The commercial synthesis of cyclen itself is long and tedious (Scheme 1.3) [66]. Richman and

[f] This notation indicates the size of the ring, the number and type of donor atoms, and any substituents that are present [35].

Atkins' protocol involves the condensation of tosylated diethanolamine with the sodium salt of tosylated diethylenetriamine under conditions of high dilution. Unless the reactants are very dilute, ordinary polymerization and not cyclization will take place. The lack of an efficient, commercially-available synthesis of cyclen probably contributes to its high cost (5 g of cyclen from Strem Chemicals, USA costs £83, 2008).

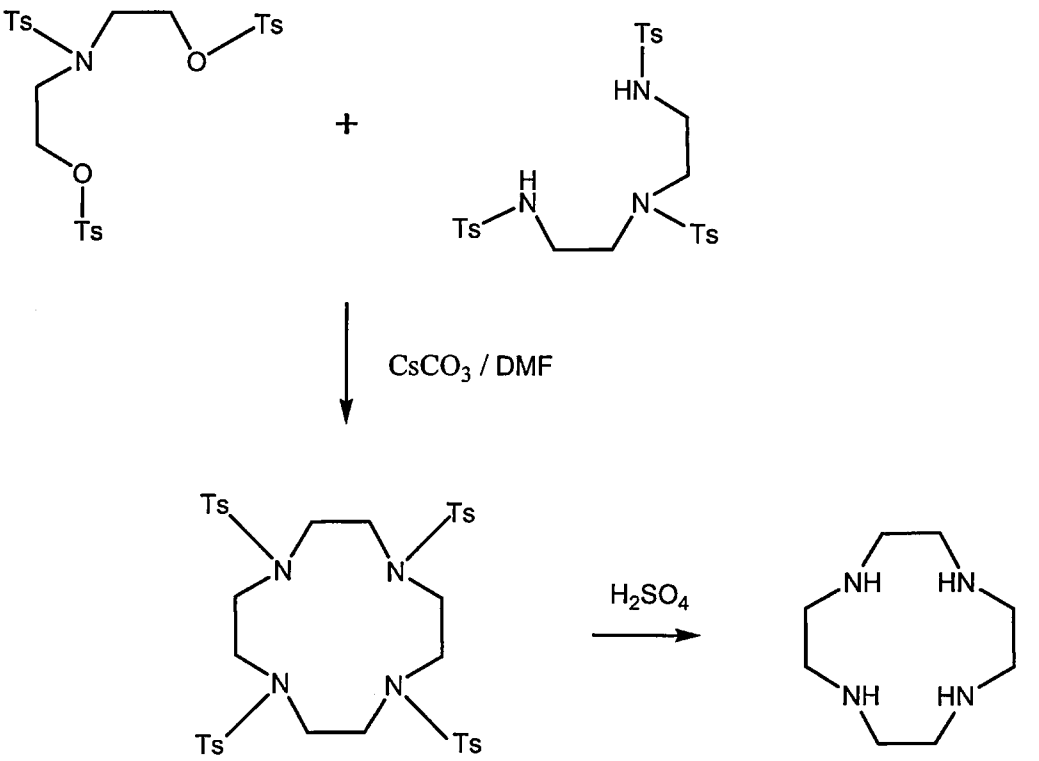

Scheme 1.3 Richman and Atkins synthesis of cyclen [66].

1.9.1 Functionalization of cyclen

Figure 1.25 shows one energy-minimised conformation of cyclen. It can be seen that the methylene groups adopt a staggered conformation. Since hydrogen atoms occupy more space than lone pairs, the lone pairs tend to point towards the centre of the ring [67-69]. Three lone pairs point towards the centre of the ring (endocyclic) and one lone pair points away (exocyclic). This preference is consolidated as the size of the *N*-substituent increases.

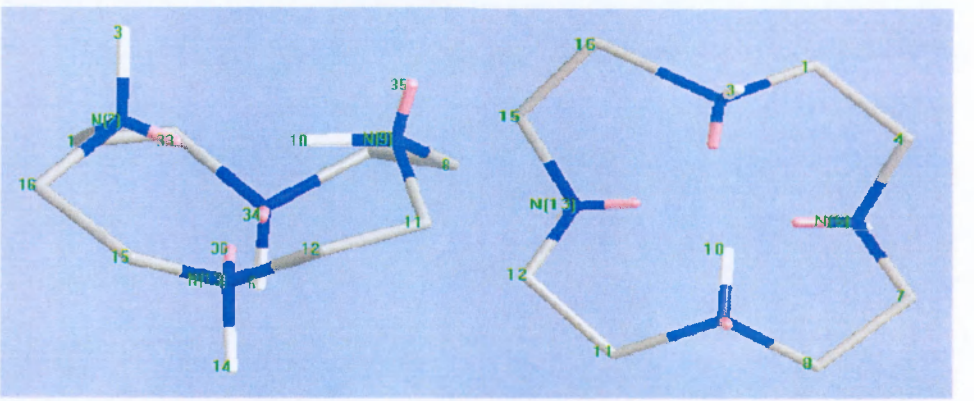

Figure 1.25 3D view of cyclen base in one energy-minimised conformation.
(generated in Chem 3d Ultra 8.0, nitrogen H = white, nitrogen lone pair = pink)

Tertiary (NRR'R") and secondary (NHRR') amines are chiral, the nitrogen atom bears four distinct substituents counting the lone pair [70]. Most chiral amines cannot be resolved into separate enantiomers because the two enantiomeric forms rapidly interconvert by pyramidal inversion (Scheme 1.4). The energy barrier for the inversion of the stereocentre is relatively low, e.g. ~25 kJ/mol for a trialkylamine.

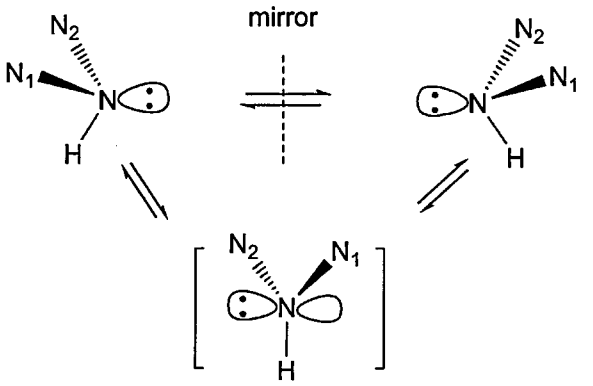

Scheme 1.4 Pyramidal inversion of amines interconverts the two mirror-image forms [70].

When cyclen is *N*-substituted, inversion of the remaining nitrogens is less likely as the increased angle strain in the macrocycle raises the barrier for inversion. In effect, the macrocycle becomes more rigid after each successive substitution. This restriction of conformational mobility may cause the remaining lone pairs to point towards the centre of the ring making them unavailable for reaction.

Tetraazamacrocycles generally follow the trend that two of the pK_a values are high, whereas the other two are significantly lower. This is thought to be due to electrostatic effects [71, 72] (Scheme 1.5). The second proton can bind to a nitrogen atom *trans* to the first one whereas the third and fourth protons must bind *cis* to the positively charged ammonium group.

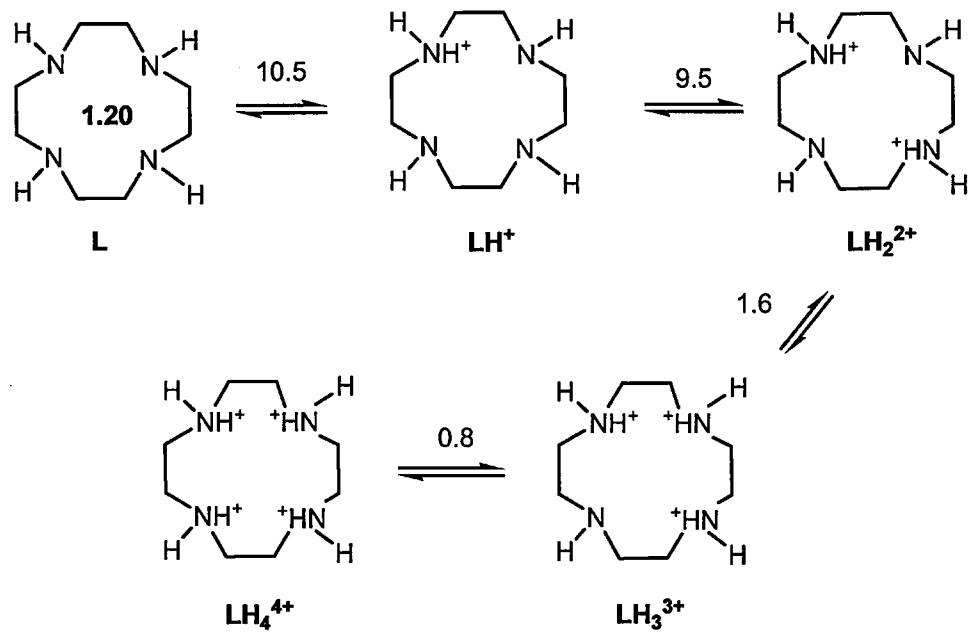

Scheme 1.5 pK_a values of cyclen (**1.20**) [72].

Since the nitrogen atom is nucleophilic, it can be alkylated or acylated. Cyclen has been substituted with a wide variety of side chains containing donor groups capable of binding a metal atom [24]. These include $-CH_2COOH$, $-(CH_2)_2NH_2$, $-CH_2CN$, $-(CH_2)_2OH$ and $-(CH_2)_2PO_3H_2$. In general, these side chains are introduced onto preformed cyclen using halogenated derivatives [2]. Selective substitution of cyclen is more difficult than substitution of all the ring nitrogens. This may be due to two factors; the pK_a values of the cyclen amines and the size of the substituent groups. The pK_a of the amine groups on cyclen can be divided into 2 sets (Scheme 1.5); those with higher pK_a values (10.5, 9.5) and those with lower pK_a values (0.8, 1.6). These groupings of pK_a values make the asymmetric substitution of cyclen difficult as the conditions needed to alkylate one amine in each pK_a pair can also lead to the alkylation of the second amine within the pair. Consequently, attempted mono-*N*-substitution of cyclen can lead to significant amounts of the di-*N*-substituted product. Similarly, attempted tri-*N*-substitution of cyclen can lead to

significant amounts of the tetra-*N*-substituted product. Strategies to prevent over-alkylation include the use of protecting groups and high dilution techniques.

Mono-*N*-substituted cyclen has been prepared by a procedure which employs a statistical effect [2]. This involves the reaction of a large excess of cyclen with the alkylating agent (10:1) in order to minimise the formation of polysubstituted products. This method works well if a carboxylate side chain is introduced onto the cyclen ring as separation of products from starting material is straightforward. A second method as outlined in Scheme 1.6, involves the protection of three amino groups leaving one available for further alkylation. In Scheme 1.6, cyclen is temporarily tri-protected with Boc. This tri-protected species (**1.21**) is then alkylated with a halogenated substrate (RCl) to give a tetra-substituted intermediate (**1.22**). Deprotection of this intermediate yields the mono-*N*-substituted cyclen (**1.23**).

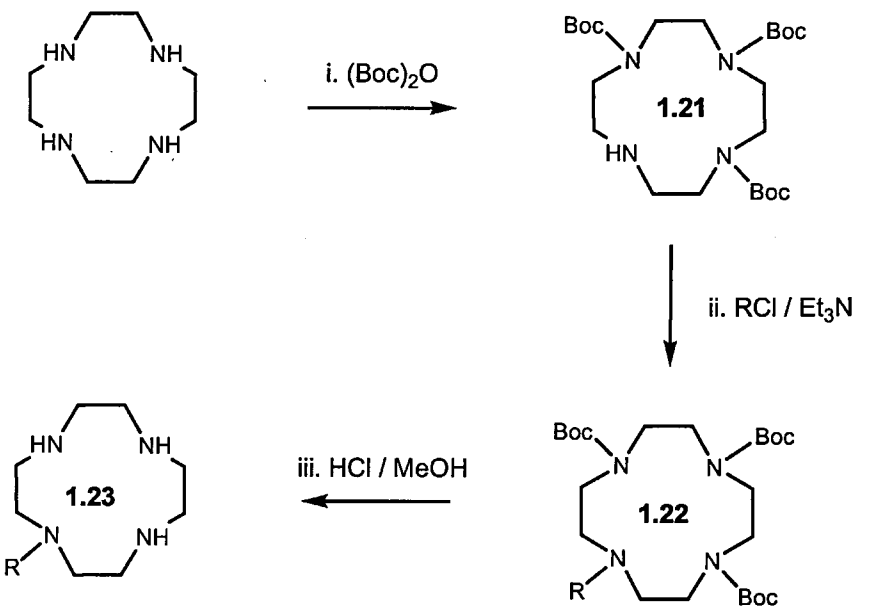

Scheme 1.6 Mono-*N*-substitution of cyclen (**1.23**) via tri-Boc cyclen (**1.21**) [61].

1.9.2 Synthesis of Gd(DO3MA)

The synthesis of Gd(DO3MA) (**1.28**) illustrates several important aspects of the synthesis of a contrast agent (Scheme 1.7) [29, 69, 73].

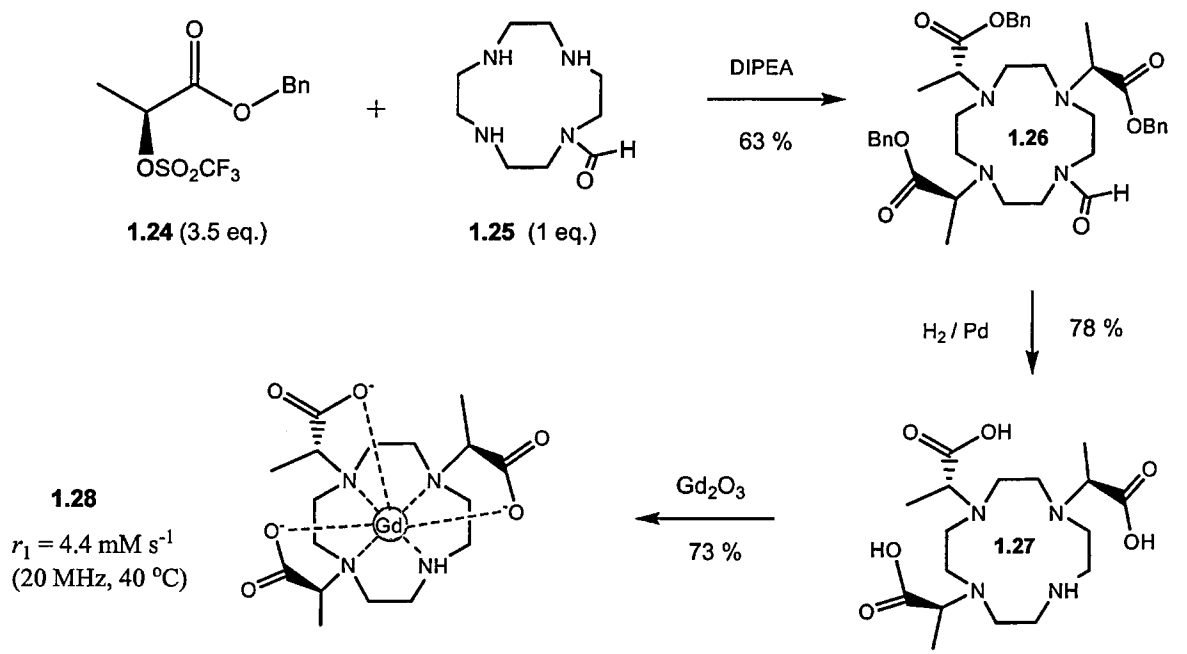

Scheme 1.7 Synthesis of the contrast agent Gd(DO3MA), **1.28** [29].

As tri-substituted cyclen was required, cyclen was mono-*N*-protected with a formyl group to give **1.25**. To avoid the formation of a mixture of diastereomers [g] (which may exhibit different coordination chemistry with Gd^{3+}), chiral L-benzyl lactate was used as starting material. In order to facilitate the alkylation reaction, the lactate alcohol was converted into a triflate leaving group rather than a chloride or bromide. It was thought that the use of a better leaving group like triflate would avoid forcing conditions such as high temperature which may have resulted in extensive racemization

[g] Diastereoisomers have opposite configurations at one or more stereogenic (asymmetric) centres, but the same configuration at others. For example, 1R,4R,7R DO3MA is enantiomeric with 1S,4S,7S DO3MA and diastereomeric with 1R,4S,7R DO3MA [70].

Treatment of *N*-formylcyclen (**1.25**) with 3.5 eq. electrophile (**1.24**) and 3.5 eq. of the hindered base, di*iso*propylethylamine (DIPEA) in acetonitrile at ambient temperature afforded **1.26** in a yield of 63 %. Simultaneous deformylation and debenzylation of **1.26** were achieved in aqueous methanolic HCl in the presence of a palladium catalyst at ambient temperature. The crude product was purification by ion exchange chromatography. Treatment of the free acid of DO3MA (**1.27**) with gadolinium oxide resulted in pure Gd(DO3MA) (**1.28**) in a 73 % yield. X-ray structure analysis of crystallized DO3MA revealed that the three asymmetric carbons bearing α-methyl groups all had (*R*)-configurations. In addition, the chelate was found to be optically active in solution. These facts, together with the synthetic methods chosen, suggest that significant racemization did not occur during the synthesis of Gd(DO3MA).

1.10 Aims of this project

The current generation of MRI contrast agents are non-targeted, hydrophilic compounds with low molecular masses [27]. Since their masses are less than 500 Da, they are rapidly cleared from the intravascular space through the capillaries into the interstitial space, and therefore their biodistribution is non-specific. The search for a new generation of contrast agents is strongly orientated towards CAs that display high tissue and/or organ specificity [36, 73-76]. The non-invasive nature of MRI, its near-cellular resolution, and the ability to acquire images at different time points, all make contrast-enhanced MR imaging a unique and powerful tool to study biological processes at the molecular and cellular level. In this context, the aim of this project is to synthesise a core, bifunctional ligand (**1.29**) that can be derivatised for use as either a targeted or an activatable contrast agent (Figure 1.26).

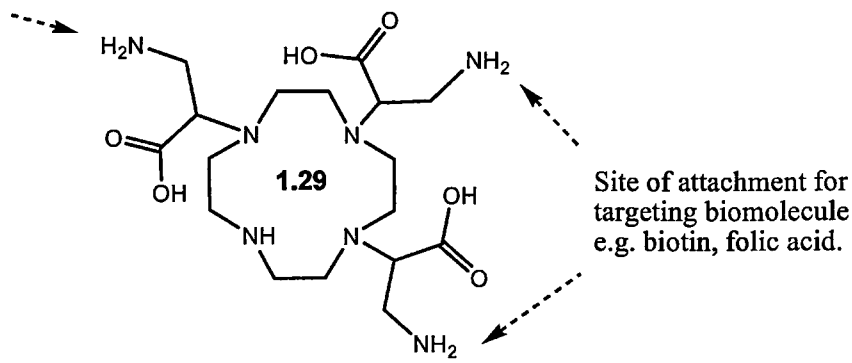

Figure 1.26 Structure of the bifunctional target ligand (**1.29**).

A bifunctional chelating agent (BFCA) contains a reactive group for coupling to proteins or other molecules and a strong metal chelating group such as those in DOTA [77]. The target ligand (**1.29**) is bifunctional as it possesses 7 donor groups to complex the Gd^{3+} ion and keep it in place as well as possessing free amino groups for conjugation to targeting biomolecules.

The presence of an amino group in the side chain of **1.29** allows for conversion into various functional groups (e.g. aminocarboxylates, aminophosponates, etc) or for amide coupling to compounds with free carboxyl groups such as peptides or folic acid. Attaching a contrast agent to a targeting biomolecule that accesses a specific catalysed-transport mechanism creates a Trojan-Horse like deception that tricks the membrane into welcoming the contrast agent through its gates [78-80]. Covalently linking **1.29** to a monoclonal antibody (McAb), for example, should impart biological specificity to the metal chelate complex; the resultant CA should concentrate at the McAb target site e.g. a tumour [48].

The use of a cyclen-based macrocyclic ligand instead of an acyclic DTPA ligand should improve the safety profile of the resultant complex, minimising any dechelation *in vivo*. Substitution of the pendant arms in **1.29** should enhance its stability. For example, α-methyl substitution of the arms on DO3MA (Scheme 1.8) is believed to contribute to the high stability of the corresponding gadolinium complex; Gd(DO3MA) has a thermodynamic stability constant nearly as high as $Gd(DOTA)^-$ even though it is heptadentate [29].

In addition to containing 4 secondary amines, the target ligand (**1.29**) possesses 3 carboxyl groups for coordination to the Gd^{3+} metal. Since Gd^{3+} has 3 positive charges, the overall complex will be charge-neutral. This is important as neutral, non-ionic complexes are better tolerated *in vivo* and thus allow the administration of higher doses [33]. Once complexed with Gd^{3+}, the resulting complex will be heptadentate. This will allow the eight and ninth coordination sites of gadolinium to be occupied by water molecules, that is, the complex will have a q value (hydration number) of two. An increase in the hydration state should translate into an increase in relaxivity (see Section 1.6.1).

Currently, targeted contrast agents (**1.32**) are generally prepared by the the 1+3 route (Scheme 1.8).

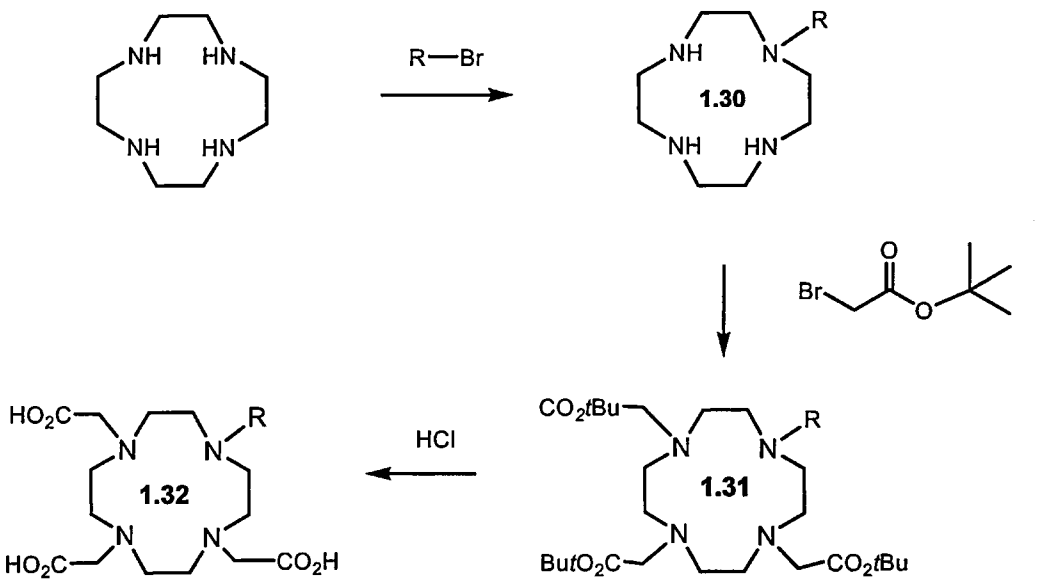

Scheme 1.8 The commonly-used 1+3 protocol for the preparation of a targeted MRI contrast agent (**1.32**).

One reason for the popularity of the 1+3 route to targeted CAs is its relative simplicity. After cyclen is mono-*N*-alkylated with a targeting molecule, it can then be reacted with *tert*-butyl 2-bromoacetate to give the fully-substituted cyclen (**1.31**). Hydrolysis of the *t*-butoxylcarbonyl ester groups then yields **1.32**. A drawback of this method is that targeting biomolecules like antibodies may be sensitive to the basic conditions used to introduce the acetate groups onto cyclen or the acidic conditions required to remove the *t*-butoxylcarbonyl groups.

Chapters 2 and 3 of this thesis will describe attempts to synthesise the bifunctional, core ligand (**1.29**). The synthesised ligands will then be complexed with the paramagnetic, lanthanide metal, gadolinium (Chapter 4). The ability of the complexes to increase the relaxation rate of water protons, that is, their T_1-relaxivity will be determined. The values obtained should indicate the suitability of the complexes for use as MRI contrast agents.

Chapter 2

Functionalization of cyclen via alkylation

2.0 Introduction

This chapter consists of two parts; both of which are concerned with the alkylation of cyclen using halogenated derivatives. Part A of this chapter describes the alkylation of cyclen using amino acid derivatives in pursuit of a generic target ligand. This ligand can be potentially coupled to a variety of targeting biomolecules and can be considered to be bifunctional (see Section 1.10, Chapter 1). Part B of the chapter deals with the synthesis of a cholic acid-cyclen conjugate which, after complexation with gadolinium, could be used as a blood-pool imaging agent. It is an example of a targeted contrast agent.

As discussed in Chapter 1 (Section 1.9.1), alkylation is the primary method used to functionalize cyclen. For example, the core ligand DO3A can be prepared by the alkylation of the commercially available unprotected cyclen (1,4,7,10-tetraazacyclododecane) with chloroacetic acid to give a final yield of 26 % [69]. As a result of over-alkylation, DOTA is also produced in the reaction but it can be readily separated from DO3A by anion exchange chromatography (Scheme 2.1).

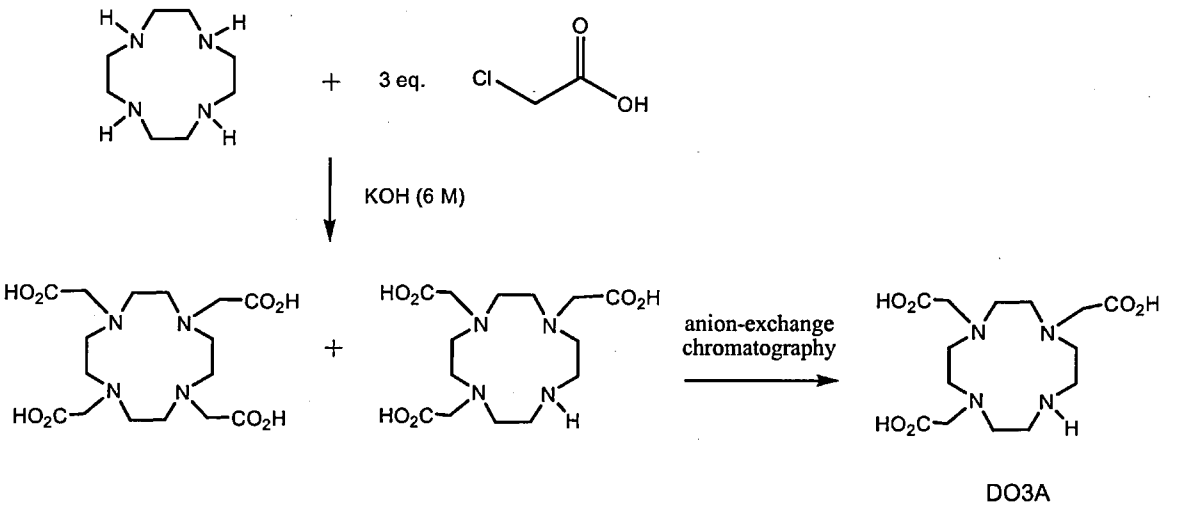

Scheme 2.1 Synthesis of DO3A via alkylation of cyclen [69].

In an effort to improve the yield of DO3A, cyclen was mono-*N*-protected with a formyl group and then reacted with *tert*-butyl-bromoacetate (4 eq.) to give a tetra-substituted intermediate [69]. Hydrolysis of this intermediate gave DO3A in a yield of 69 % (Scheme 2.2).

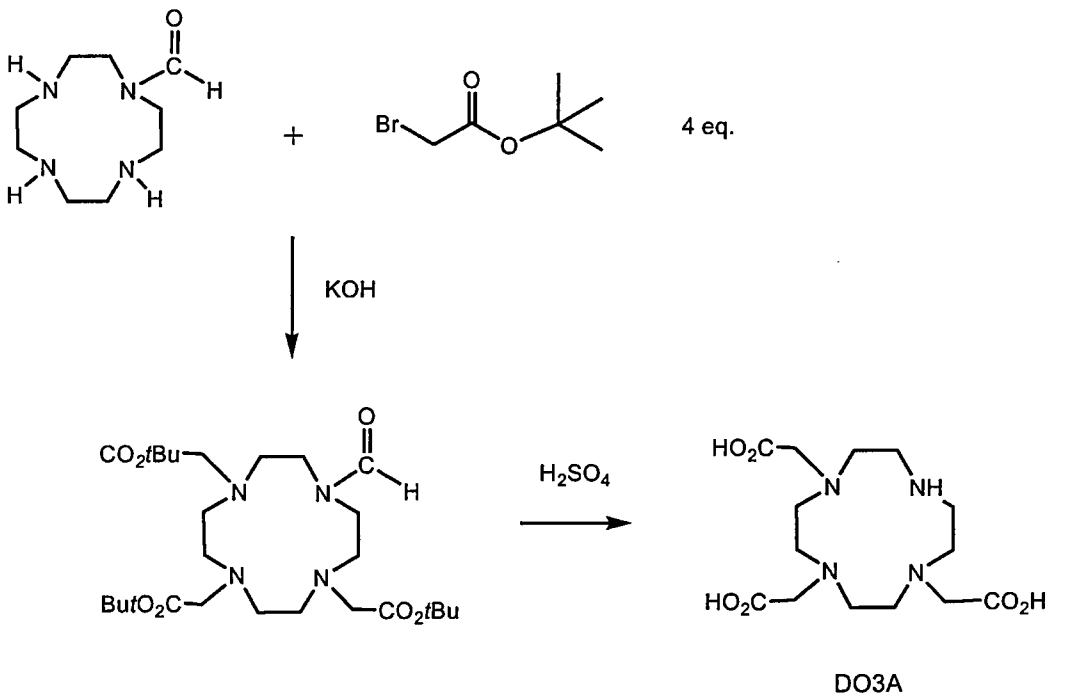

Scheme 2.2 Synthesis of DO3A via alkylation of mono-*N*-formyl cyclen [69].

Part A Alkylation of cyclen using amino acid derivatives

2.1 Alkylation of cyclen with derivatised 4-amino-3-hydroxybutyric acid

In Scheme 2.3, disconnection of the target molecule **2.1** next to the cyclen ring (**2.4**) leads to **2.3** as the electrophilic synthon. The synthetic equivalent of **2.3** is 4-amino-3-mesylbutanoic acid (**2.5**) which can be conveniently prepared from commercially-available, 4-amino-3-hydroxybutyric acid (**2.6**). In essence, replacement of the hydroxyl group in **2.6** allows nucleophilic substitution reactions to be performed at the C-3 atom. The nucleophilic synthon cyclen is also commercially available.

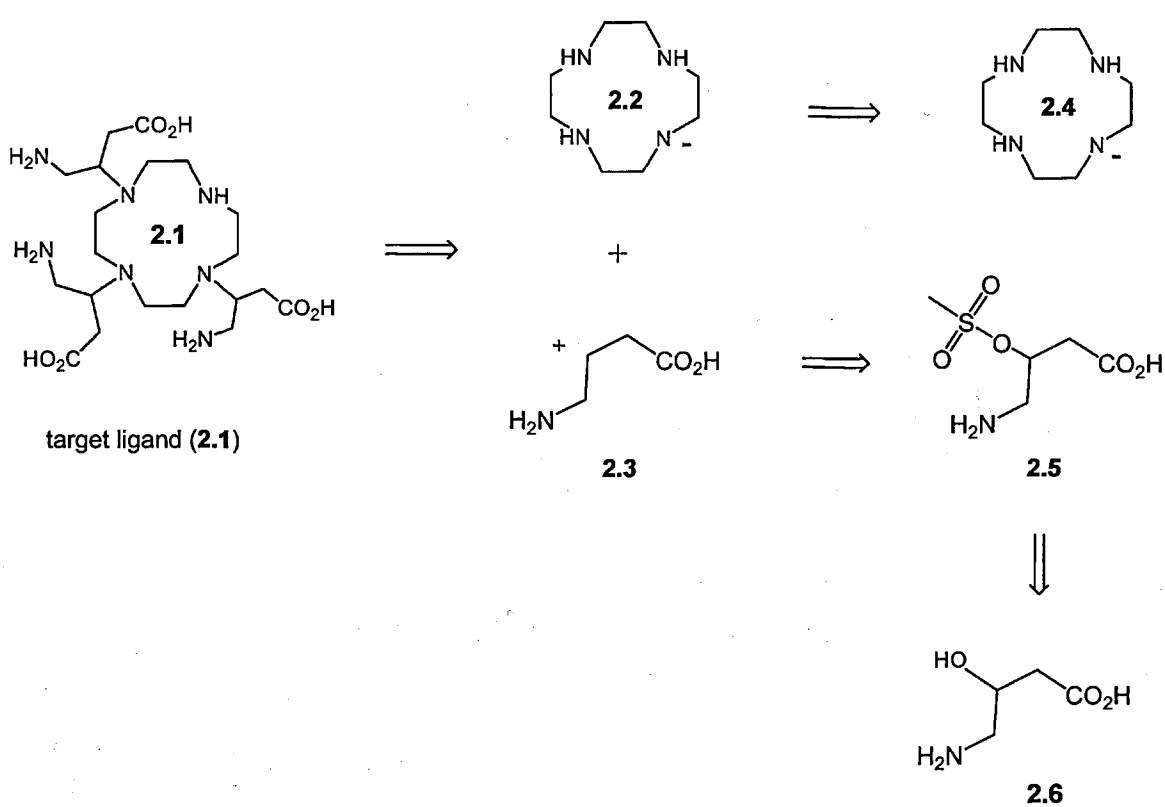

Scheme 2.3 Proposed route to the target ligand (**2.1**).

2.1.1 Derivatisation of 4-amino-3-hydroxybutyric acid

The first substrate investigated as a starting material in the route to the target ligand was 4-amino-3-hydroxybutyric acid (**2.6**). Since the amine and carboxyl groups are nucleophilic, protection is required. A protecting group (PG) must suppress this nucleophilic reactivity by delocalising its electron density into a suitable substituent or by shielding its reactivity behind a sterically-hindered group [81]. After these protection steps, the alcohol group requires conversion into a good leaving group such as a mesylate group in preparation for the subsequent reaction with cyclen.

The first synthetic step involved the protection of the carboxylic acid group with an ethyl ester. This was achieved by refluxing **2.6** in absolute ethanol containing *p*-toluenesulfonic acid as an acid catalyst (Scheme 2.4).

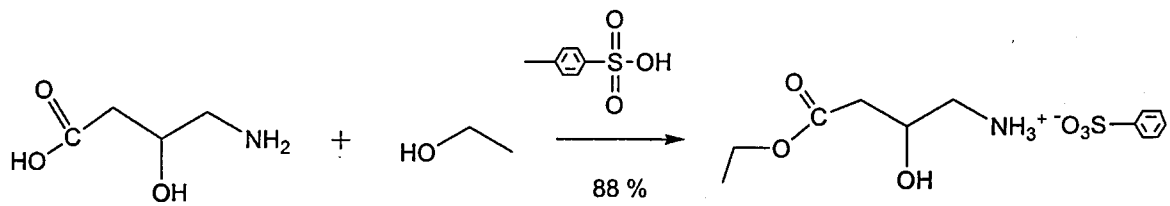

2.6 **2.7**

Scheme 2.4 Esterification of 4-amino-3-hydroxybutyric acid.

The method used was a modification of a procedure described by Bodansky in the textbook *The Practice of Peptide Synthesis* [82]. In the published procedure, 2 eq. *p*-toluenesulfonic acid (*p*TSA) were employed but it was found here that 1.1 eq. were sufficient for the conversion. Since the *p*TSA protonates the basic amino nitrogen group as well as the carbonyl oxygen atom of **2.6**, greater than 1 eq. of acid catalyst is necessary (see the reaction mechanism in Scheme 2.5). Also, washing with diethyl ether, as outlined in the original method, did not remove all the *p*-TSA if the stated 2 eq. were used.

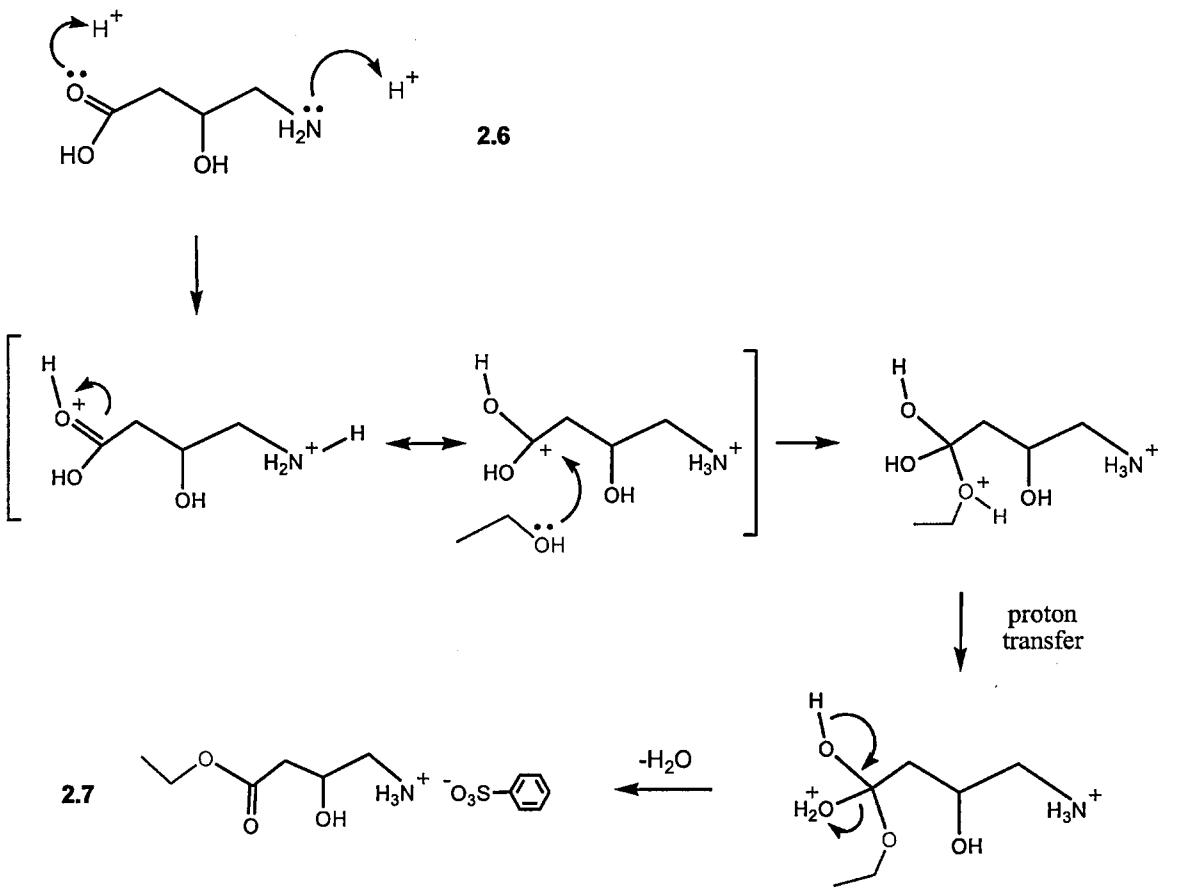

Scheme 2.5 Esterification of **2.6** – the reaction mechanism [83].

The amino group of **2.7** was then protected with the acid-labile, *N-tert*-butyloxycarbonyl group which is commonly known as *t*-Boc. *t*-Boc serves as a protective group in solid phase peptide synthesis and it is stable to most bases and nucleophiles [81]. Amino acids protected with alkoxycarbonylamino PGs such as *t*-Boc tend not to undergo racemization, which can be described as the conversion of an enantiomer to a mixture of enantiomers. The procedure used for the introduction of the *t*-Boc group was also described by Bodansky [82] (Scheme 2.6). Reaction of **2.7** with di-*tert*-butyl dicarbonate (1.1 eq.) and TEA (2.2 eq.) produced **2.8** as a colourless oil. A characteristic Boc singlet at δ 1.45 ppm, which integrated for 9 protons, was observed in the ^{1}H NMR spectrum of the product.

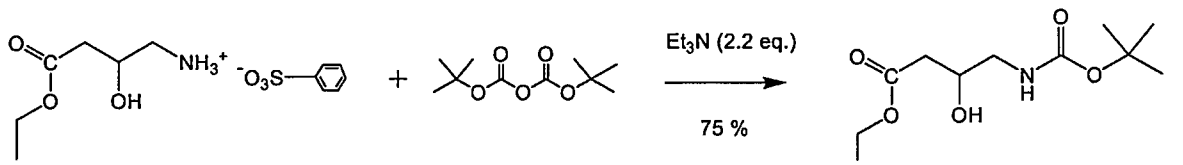

2.7 (1 eq.) 1.1 eq. **2.8**

Scheme 2.6 Protection of amino group of **2.7** with *t*-butyl (Boc).

The OH group of **2.8** was converted to a mesylate (Scheme 2.7) rather than a halide as sulfonic ester groups such as mesylates are regarded as better leaving groups [3]. Primary and secondary alcohols react with methanesulfonyl chloride in base at room temperature to give mesylates, usually in good yield [84]. **2.8** was reacted with methanesulfonyl chloride and triethylamine in DCM to give a high yield (69 %) of the mesylate (**2.9**). Trituration of the mesylate oil with acetone produced a white solid which was subsequently crystallised from toluene-hexane.

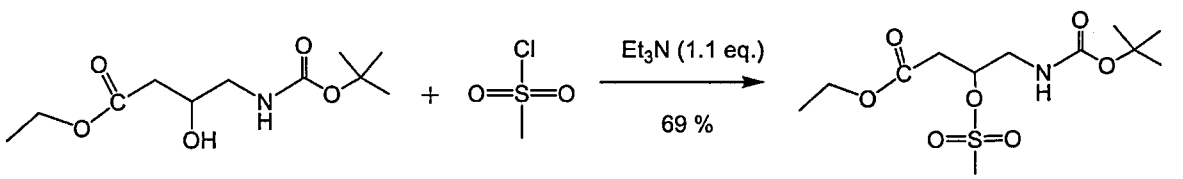

2.8 1.1 eq. **2.9**

Scheme 2.7 Transformation of the alcohol group of **2.8** into the mesylate (**2.9**).

The full synthetic sequence is outlined in Scheme 2.8 oveleaf. The overall yield of **2.9** was 45 %.

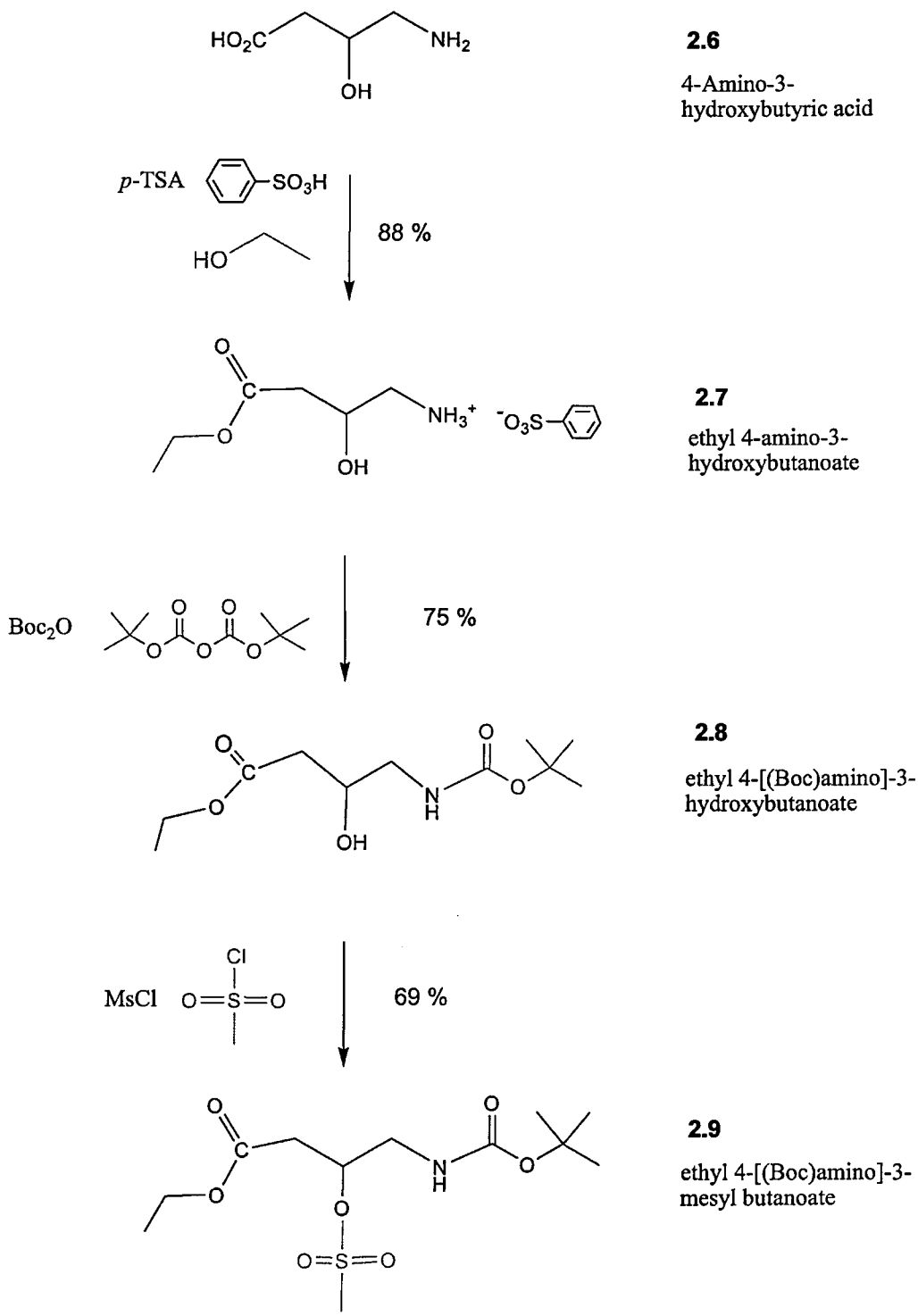

Scheme 2.8 Synthesis of ethyl-4-[(Boc)amino]-3-mesyl butanoate (**2.9**).

2.1.2 Alkylation of cyclen with derivatised 4-amino-3-hydroxybutyric acid.

Cyclen (1 eq.) was stirred with 3.1 eq. of ethyl-4-[(Boc)amino]-3-mesyl butanoate (**2.9**) and 3.1 eq. K_2CO_3 base in dry acetonitrile under argon. Initially, the reaction was carried out at room temperature as both S_N1 and S_N2 reactions are favoured by low temperatures. When electrospray mass spectroscopy (ES-MS) detected only mono-*N*-substituted cyclen after 12 hours, the temperature was increased to 60 °C for a further 12 hours. Purification of the reaction mixture via silica gel column chromatography yielded the alkene **2.10**. This revealed that **2.9** underwent mostly elimination as shown in Scheme 2.9. A coupling constant between the protons of 15.6 Hz showed the alkene to have a *trans* configuration.

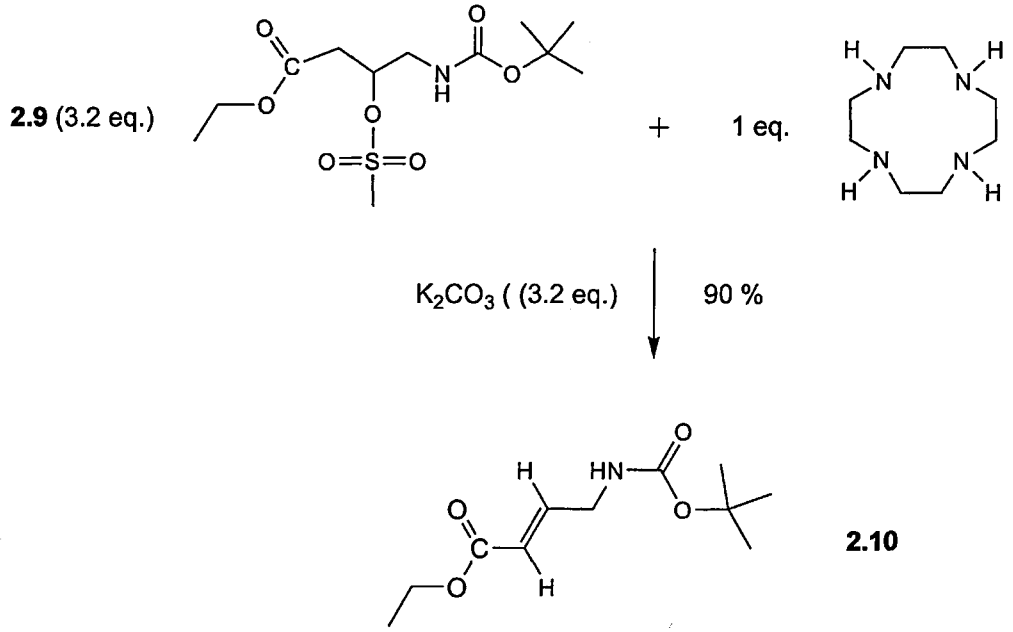

Scheme 2.9 Alkylation of cyclen with **2.9** to give **2.10**.

Primary and secondary substrates normally react by the S_N2 mechanism [70]. S_N2 reactions can only occur at relatively unhindered sites and are normally only useful with primary halides and a few simple secondary halides. In secondary substrates, the S_N2 mechanism

occurs in competition with the E2 mechanism which explains why most of the product, even at room temperature, is an alkene. Also, the mesylate (**2.9**) can eliminate in either of two directions to give either the conjugated alkene (**2.10**) or the non-conjugated alkene (**2.11**) as demonstrated in Scheme 2.10.

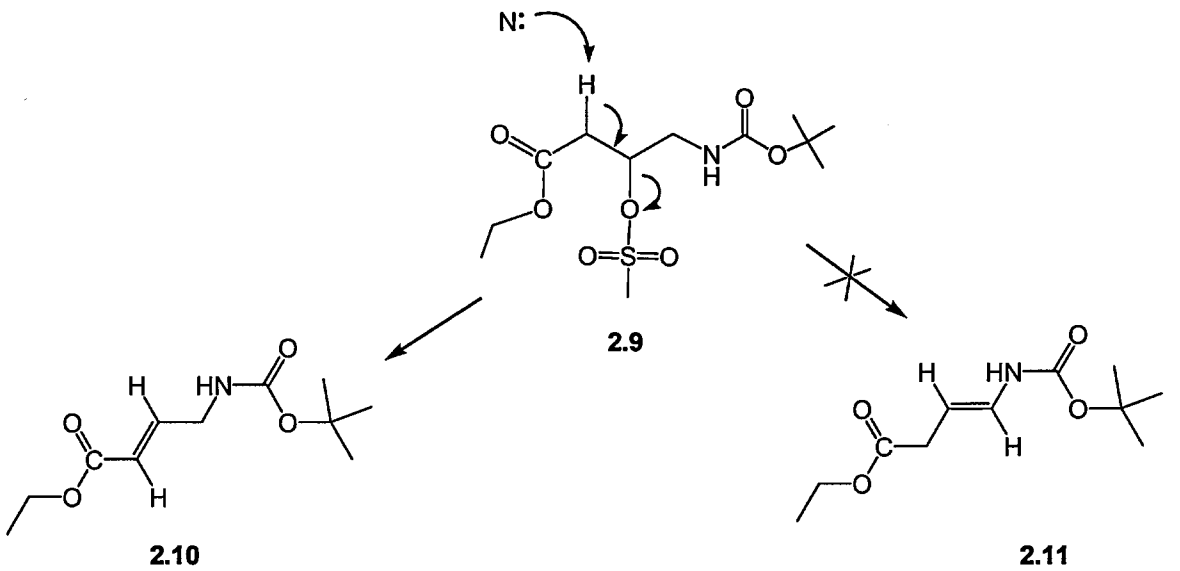

Scheme 2.10 Elimination of **2.9** to give the conjugated alkene (**2.10**).

The FT-IR and ^{1}H NMR spectra of the product confirmed that the more stable conjugated alkene (**2.10**) was produced. In the FT-IR spectrum, the ester C=O of **2.10** absorbs at 1728 cm^{-1} whereas the product absorption was located at 1700 cm^{-1}. Conjugation of C=O with an alkene normally lowers the wavenumber of the absorption by 10-20 cm^{-1}. This downward shift in the C=O absorption provided good evidence that the product alkene was conjugated.

The chemical shift values obtained for H' and H'' in both the ^{1}H NMR and ^{13}C NMR (not shown) spectra correlate with the δ values expected for a conjugated alkene, **2.10** (see Figure 2.1) [85].

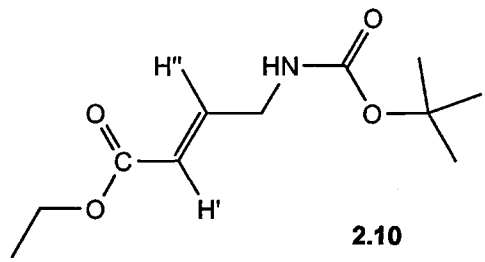

2.10

H' δ expected = 5.95 ppm, observed = 5.93 ppm

H'' δ expected = 7.01 ppm, observed = 6.91 ppm

Figure 2.1 ^{1}H NMR values expected (and observed) for the conjugated alkene (**2.10**).

2.2 Alkylation of cyclen with derivatised L-serine methyl ester hydrochloride (LSME).

In the previous section, the problem of elimination when a secondary substrate was reacted with cyclen was described. Therefore, a primary substrate which should favour the S_N2 reaction and promote substitution was investigated next. Commercially available L-serine methyl ester hydrochloride (LSME; see **2.12** in Scheme 2.11) was employed to investigate if the use of a primary substrate would promote the desired substitution over elimination.

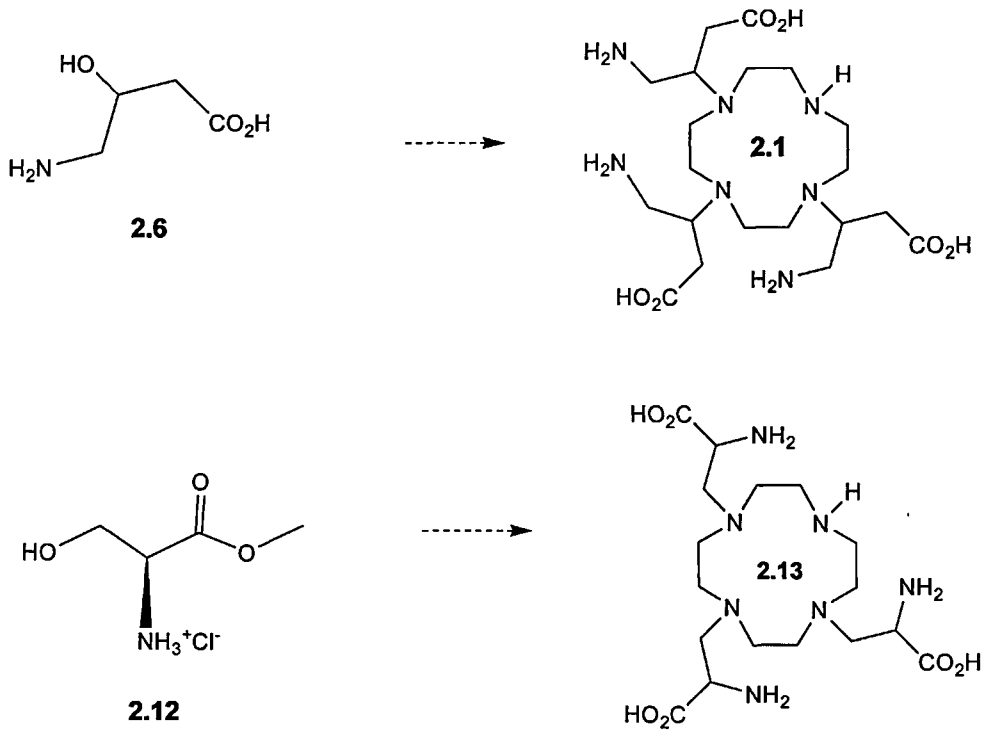

Scheme 2.11 Structure of the new target molecule (**2.13**).

Substituting L-serine methyl ester (**2.12**) for 4-amino-3-hydroxy-butyric acid (**2.6**) changes the structure of the target molecule from **2.1** to **2.13**. The new target ligand (**2.13**) contains three amino acid-bearing pendant arms. Like the ligand (**2.1**), **2.13** also provides three carboxyl groups for coordination to a Gd^{3+} ion and three amino groups for potential conjugation to targeting molecules. However, one area of concern regarding the structure

of **2.13** is the close proximity of the amino group to the carboxyl group. As the amino group is α to the carboxyl group, this configuration could pose steric crowding issues if independent manipulation of either of these functional groups is required.

2.2.1 Derivatisation of L-serine methyl ester hydrochlorlde

2.12 has its carboxyl group conveniently protected as a methyl ester. For substitution, the amino group requires protection and the alcohol once again needs to be transformed into a good leaving group. The amine was protected with the Boc (or *t*-butyl) group to give a yield of 84 % (Scheme 2.12).

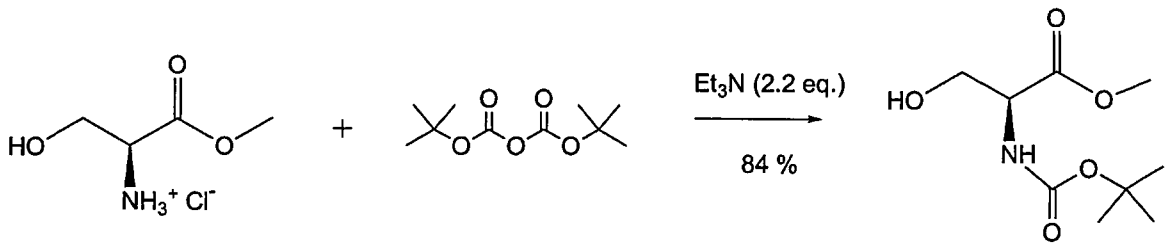

2.12 1.1 eq. **2.14**

Scheme 2.12 *N*-Boc protection of the amino group of **2.12**.

It was decided to replace the sterically-hindered mesylate group with the smaller bromide leaving group. However, the standard reagent for brominating alcohols, HBr-acetic acid, could not be used as the acidic conditions could hydrolyse the methyl ester. *N*-Boc-L-serine methyl ester (**2.14**) was brominated using 1,2-bis(diphenylphosphino)ethane (DPPE) and 1,2-dibromotetrachloroethane (1,2-DB) as shown in Scheme 2.13. These two reagents have previously been utilised to brominate alcohols under mild, non-acidic conditions [86].

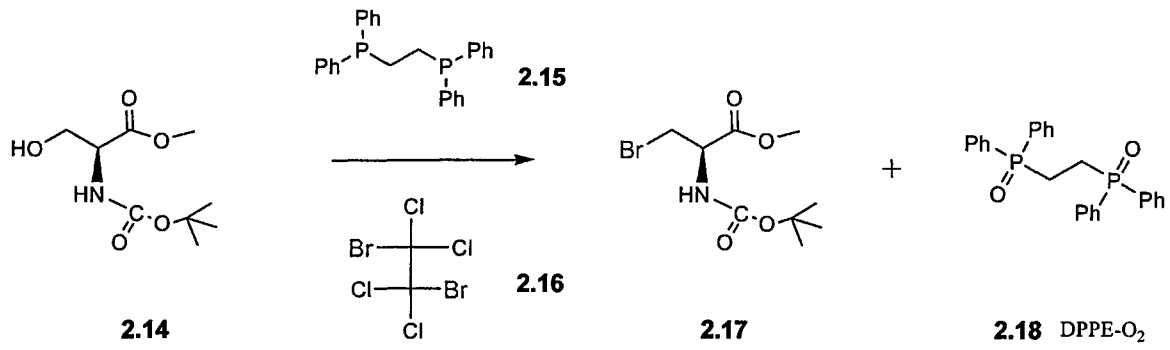

Scheme 2.13 Bromination of **2.14** using DPPE (**2.15**) and 1,2-DB (**2.16**) [86]

DPPE, which is shown in Figure 2.2, was originally investigated as an alternative phosphine source to triphenylphosphine (TPP) in the Mitsunobu reaction [87]. Unlike phosphine oxide, DPPE oxide can be more easily removed at the end of the reaction.

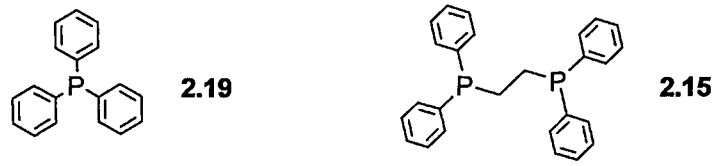

Figure 2.2 Structures of TPP (**2.19**) and DPPE (**2.15**).

Since the structures of TPP and DPPE are similar, it seems reasonable to assume that the mechanism of the bromination reaction, as outlined in Scheme 2.13, would be similar to the mechanism of the halogenation of alcohols using TPP-CCl_4. A possible pathway for the bromination reaction is illustrated in Scheme 2.14 overleaf. The nucleophilicity of trivalent phosphorus in compounds such as DPPE should result in the formation of a phosphonium salt **2.20** when they are treated with reactive alkyl halides (TPP combines with most alkyl halides to give phosphonium salts). Also, triphenylphosphine has previously been shown to induce the 1,2-debromination of 1,2-dibromides [88] and this is thought to proceed via an E2-type elimination [89]. The electrophilic phosphonium salt (**2.20**) is then attacked by the OH of the alcohol substrate. Displacement of DPPE-O_2 by bromide in **2.22** occurs in an

irreversible S_N2 step. The formation of the strong P=O bond provides a thermodynamic driving force in favour of halogenation. Evidence to support this mechanism came from mass spectral analysis of the reaction mixture before it was chromatographed. Peaks at m/z 163 and a more prominent one at m/z 182 correspond to [**2.21**+H^+] and [**2.21**+NH_4^+], respectively.

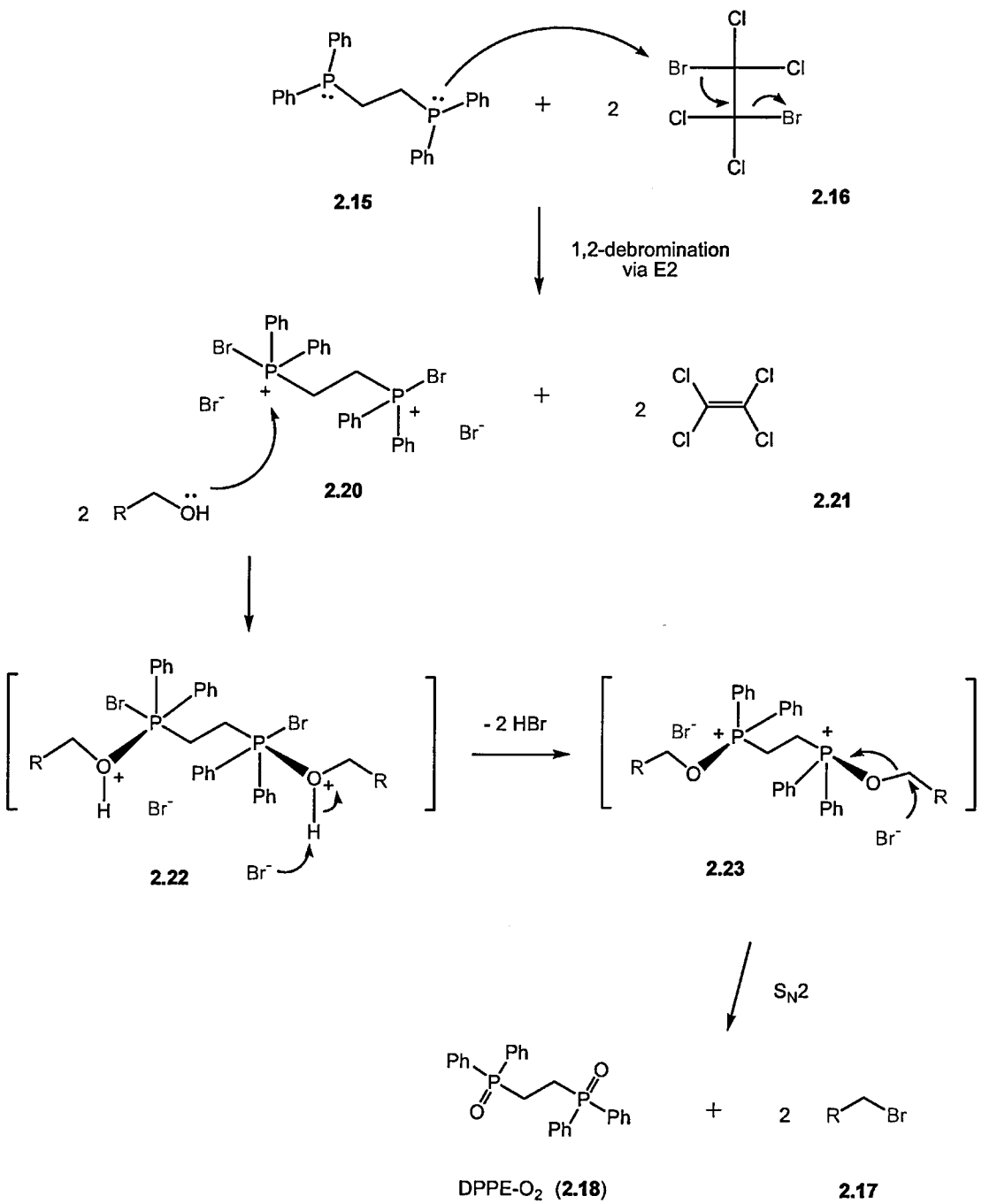

Scheme 2.14 Bromination of alcohols using **2.15** (DPPE) and **2.16** (1,2 DB): a possible reaction mechanism.

The published procedure involves the addition of DPPE (1 eq.) and dibromotetrachloroethane (1,2-DB, 1.7 eq.) to the alcohol (1 eq.) in THF and stirring the mixture overnight. Work-up consisted of simply filtering the suspension through a plug of celite. However, it was found here that the crude product required a more rigorous purification by column chromatography as unreacted **2.16** eluted before the product. The optimisation of the reaction conditions was aided by the use of a fluoroscein-hydrogen peroxide TLC spray (see Appendix A) [90]. The components of this spray react with brominated compounds to give intense pink spots on a yellow background. This spray was found to be especially useful for analysing reaction mixtures as the pseudo-molecular ions[h] of brominated compounds are not always observable on electrospray mass spectrometry. This is due to displacement of the bromide ion by other ions in the MS [91]. Due to the requirement for brominated substrates in this project, several reaction conditions were investigated in order to optimise yields (see Table 2.1).

Table 2.1 Bromination of *N*-Boc-L-serine methyl ester (**2.14**).

N-Boc-LSME (eq.)	DPPE (eq.)	1,2-DB (eq.)	Solvent	Reaction conditions	Yield (%)
0.5	1	1	toluene	RT / 24 h	0
1	0.5	1	toluene	RT / 72 h	< 10 mg
1	0.5	1	DCM	RT / 24 h	9.6
1	0.5	1	THF	RT / 24 h	21.2
1	0.6	1.7	THF	RT / 24 h	33.6
1	1	1.7	THF	RT / 24 h	53.8

It was found that using toluene as the reaction solvent resulted in only a trace of product and less than 10 mg was isolated. DCM gave good conversion but the solvent also

[h] $[M+H]^+$ in positive ion mode, $[M-H]^-$ in negative ion mode

dissolved considerable amounts of unwanted DPPE-O_2 by-product. The best solvent for the reaction was THF as it afforded good yields but did not dissolve excessive oxide by-product.

These results can be rationalised in terms of what we know about the reaction mechanism. Since the reaction is believed to proceed by an S_N2 mechanism, a non-polar solvent like toluene[i] would not be expected to stabilise the phosphorane intermediate [92]. This may explain the lack of reaction when toluene was used as solvent (see Table 2.1). According to the mechanism proposed in Scheme 2.14, 2 eq. of dibromotetrachloroethane react with one equivalent of phosphine. Therefore, the use of the recommended 1.7 eq. 1,2-DB appears to be sub-optimal. This may account for the rather modest yield of brominated product (i.e. 54 %). Since the kinetics of S_N2 reactions are second-order, the rate of the reaction is dependent on the concentration of the two reactants.

[i] On a scale of relative polarity for different solvents where cyclohexane is 0.006 and H_2O is 1.000, toluene is 0.099, THF is 0.207, DCM is 0.309 [92].

2.2.2 Alkylation of cyclen with derivatised L-serine methyl ester

Scheme 2.15 has two potential advantages over Scheme 2.9 described in Section 2.1.2 above. In addition to the use of a primary substrate, the protection of one NH group on cyclen with a Boc group (**2.24**) avoids tetra-alkylation. By employing this strategy, the potentially troublesome separation of tri- and tetra-substituted products can be conveniently avoided. The fully substituted cyclen with one group protected with Boc should elute from a column first as it would be less polar than di- and tri-substituted compounds. The Boc groups on the cyclen and on the serine side arms can be simultaneously deprotected by neat trifluoroacetic acid.

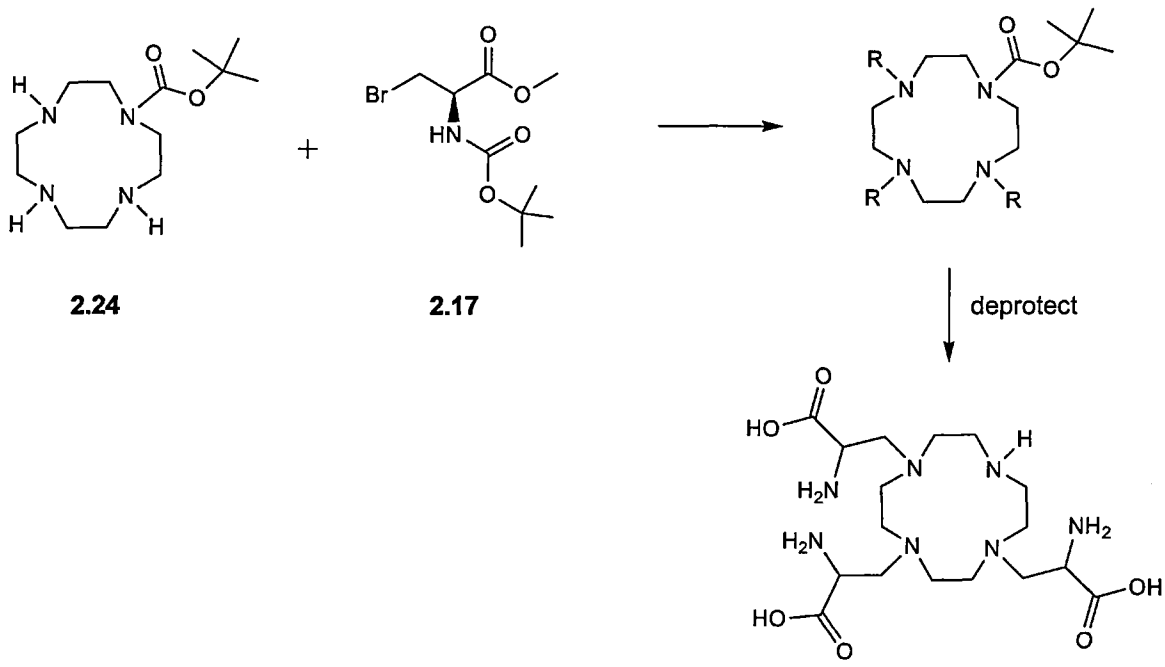

Scheme 2.15 Alternative scheme for the synthesis of target ligand.

Mono-*N*-Boc cyclen (**2.24**) was prepared according to Scheme 2.16 by reacting cyclen, di-*tert*-butyl carbonate and Et_3N in DCM. Some di-*N*-Boc cyclen was also produced in the reaction but this could be readily separated from the mono-*N*-Boc cyclen on an alumina

column. Analysis of mono-*N*-Boc cyclen by ^{1}H NMR showed that the protons of C2 / C2' adjacent to the *t*-butoxycarbonyl (Boc) group are non-equivalent at room temperature (Figure 2.3). The presence of two absorptions indicates a restricted rotation of the N-$CO_2C(CH_3)$ bond.

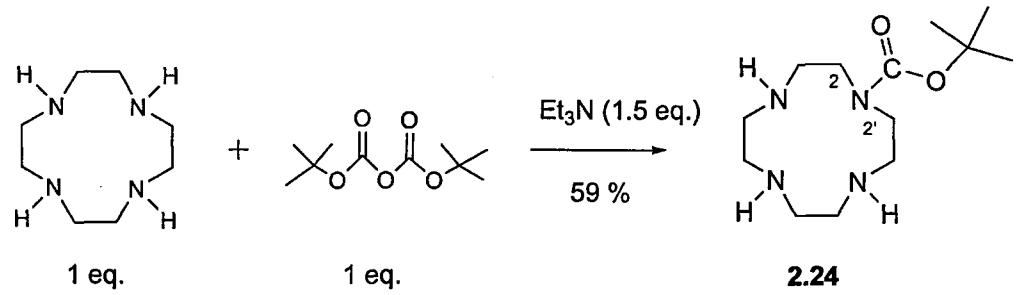

Scheme 2.16 Mono-*N*-protection of cyclen with Boc.

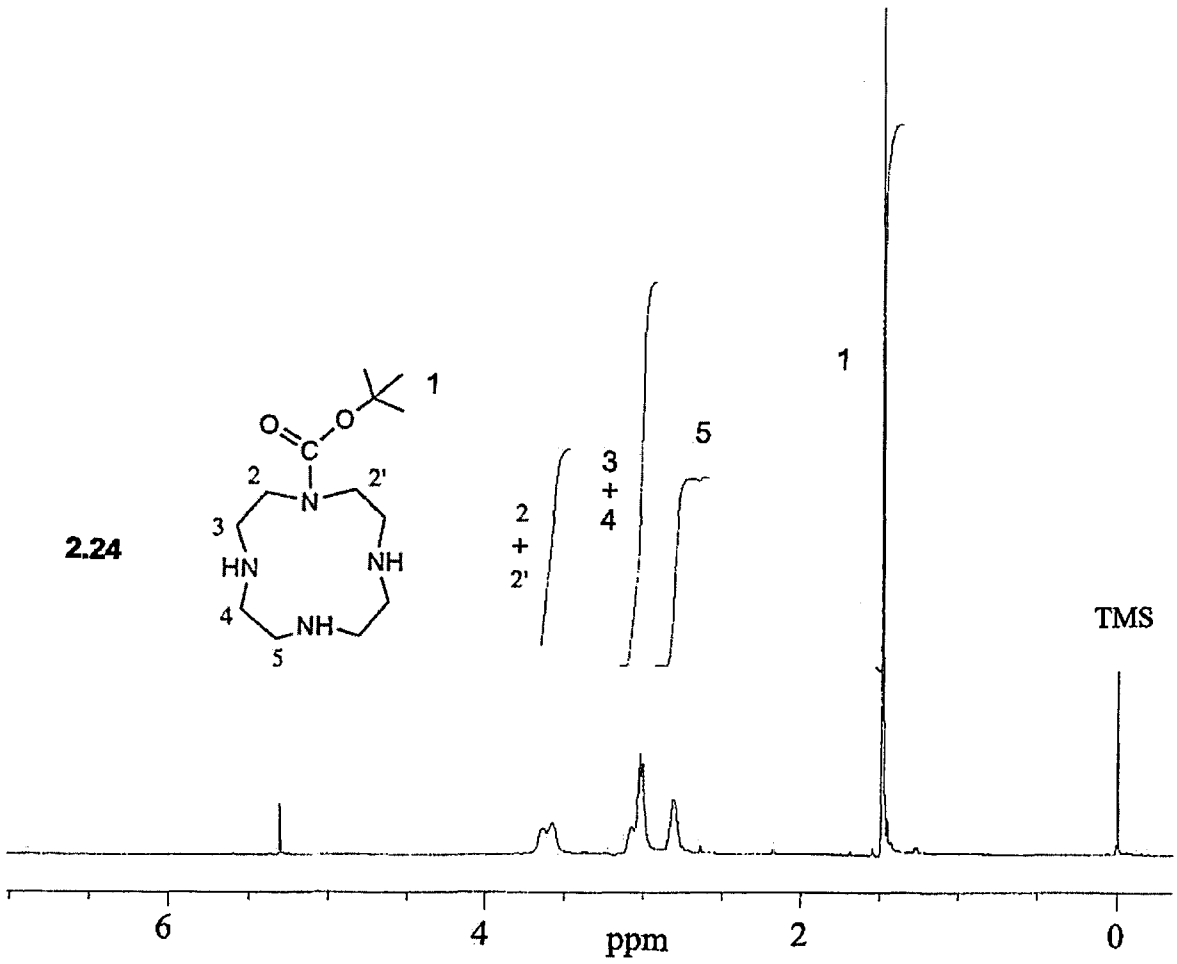

Figure 2.3 ^{1}H NMR of mono-*N*-Boc cyclen (**2.24**) in $CDCl_3$ (300 MHz).

Mono-*N*-Boc-cyclen was then alkylated with **2.17** (3.2 eq.) in the presence of triethylamine (3.2 eq.). The reaction was carried out in dry acetonitrile at 80 °C (Scheme 2.17).

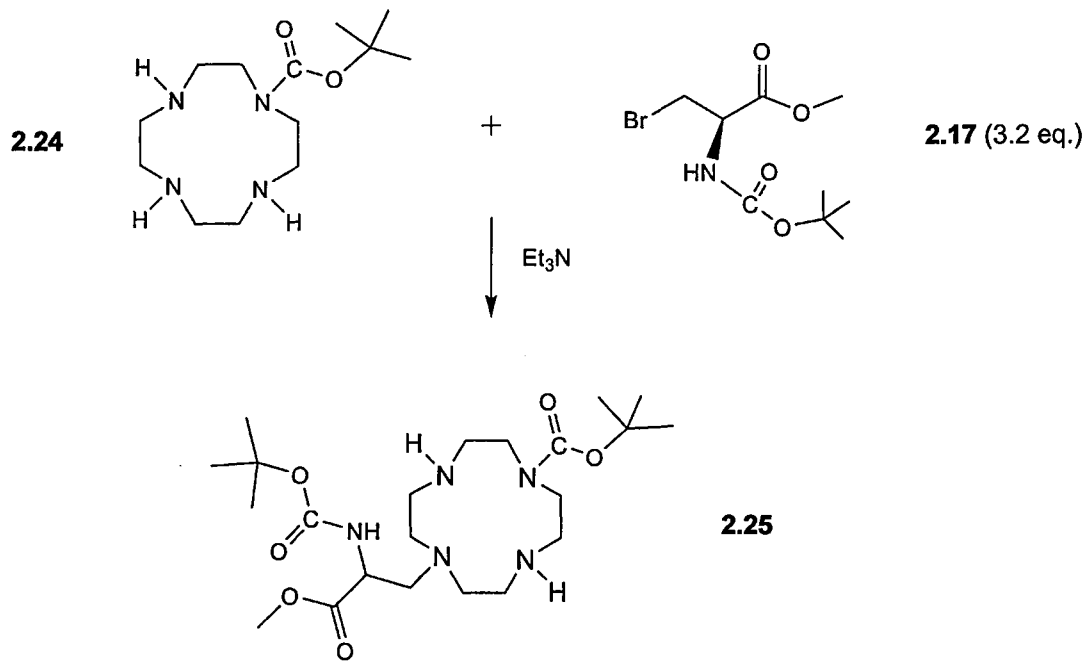

Scheme 2.17 Alkylation of **2.24** to give the 1,7-disubstituted regioisomer (**2.25**).

Purification of the reaction mixture afforded **2.25** in a yield of 60 %. The formation of the 1,7-disubstituted regioisomer as opposed to the 1,4-disubstituted regioisomer was confirmed by ^{13}C NMR spectroscopy. The ^{13}C NMR spectrum showed 5 distinct CH_2 signals which is consistent with the 1,7-isomer. If the product was the 1,4-disubstituted regioisomer, extra CH_2 resonances would be expected as a result of the 8 non-equivalent methylenes in the cyclen ring. The formation of the less-hindered 1,7-diadduct as the major product is in good agreement with the greater reactivity of the two *trans* nitrogen atoms deduced from their pK_a values [93]. The results for this reaction when carried out under different experimental conditions are listed in Table 2.2.

Table 2.2 Alkylation of mono-*N*-Boc cyclen with **2.17**

mono-*N*-Boc cyclen (eq. 2.27)	**2.17** (eq.)	Reaction conditions	LC-MS analysis
1.0	3.2	MeCN / RT Et_3N (3.2 eq.)	di-substituted cyclen (**2.25**) yield = 60 %
1.0	4	THF/H_2O (30:1) [94] Na_2CO_3, RT for 6 days	di-substituted cyclen (**2.25**) yield alcohol (**2.14**) = 30 %
1.0	4	DMF / 72 h (80 °C) Et_3N (4 eq.)	di-substituted cyclen (**2.25**) unreacted halide (**2.17**)
1.0	4	MeCN / 72h (80 °C) [95] K_2CO_3 (5 eq.)	di-substituted cyclen (**2.25**) unreacted halide (**2.17**)
cyclen (1 eq.)	6	MeCN / 72 h (80 °C) K_2CO_3 (5 eq.)	di-substituted cyclen unreacted halide (**2.17**)

Several alkylating conditions described in the literature were employed and the reaction progress in each case was followed by LC-MS. In all cases, only a peak with an *m/z* corresponding to di-*N*-substituted cyclen (**2.25**) was observable ($[M+H]^+ = 475$). No peak corresponding to unreacted halide (**2.17**) was observable when 50 % aqueous THF was used as solvent. Purification of the reaction mixture revealed **2.17** was hydrolysed back to the alcohol (**2.14**) by water in the solvent. Although a peak with an *m/z* corresponding to di-*N*-substituted cyclen (**2.25**) was observed, none was isolated via column chromatography. Significantly, when cyclen was substituted for mono-*N*-Boc cyclen, a peak corresponding to only the di-*N*-substituted cyclen product ($[M+H]^+ = 575$) was evident (entry 5 in Table 2.2).

As no tri- or tetra-substitution of cyclen was observed, it was speculated that the bulky Boc group may have hindered substitution by locking the cyclen ring into a specific conformation, and preventing nucleophilic attack. Support for this view came from the work of Griffin *et al.* [71] who found that when cyclen was protected in the 1,7 positions with

Boc groups, they produced no tri-*N*-substituted cyclen. They attributed this result to a conformational change which rendered one of the nitrogens inaccessible either before or after the first substitution.

To determine if the sterically-hindered Boc group was inhibiting the substitution reaction, an alternative group to mono-protect cyclen was required. It was thought that the use of a less-hindered protecting group may keep cyclen conformationally mobile and as a consequence, nucleophilic. Additionally, it was considered a smaller protecting group on the electrophile (i.e. **2.12**) would facilitate nucleophilic attack by the macrocycle. The effects on substitution of using alternative protecting groups, both on cyclen and **2.12**, are investigated in the following sections.

2.3 Synthesis of mono-*N*-acetyl cyclen (2.26): a novel mono-*N*-protected cyclen intermediate.

In the previous section, it was proposed that the sterically-hindered Boc group on cyclen may be hindering substitution by locking the macrocycle into a specific conformation. Therefore, an alternative to mono-*N*-Boc cyclen as a precursor to tri-substituted cyclen was required if this hypothesis was to be tested. The acetyl group is one of the smallest protecting groups available and would not be expected to restrict conformational movement of the macrocycle significantly [96]. Since *N*-acetyl amides require harsh deprotection conditions (such as refluxing 12M HCl), the acetyl moiety is unsurprisingly rarely used as a protecting group. Mono-*N*-acetyl cyclen was prepared by the dropwise addition of acetyl chloride (1 eq.) in $CHCl_3$ to a solution of cyclen in $CHCl_3$ as outlined in Scheme 2.18.

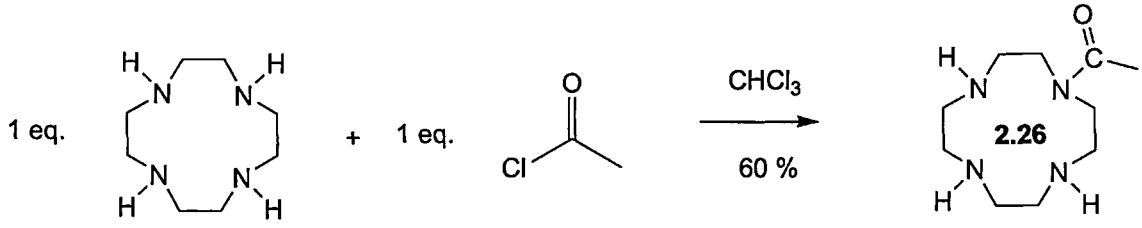

Scheme 2.18 Synthesis of mono-*N*-acetyl cyclen (**2.26**).

Mass spectrometry of the reaction mixture revealed that di-*N*-acetyl substituted cyclen was also formed ($[M+H]^+ = 256.6$). Initial attempts to separate the mono-*N*-acetyl cyclen from the di-*N*-acetyl cyclen via silica or alumina column chromatography proved futile. However, it was found that basification of the product residue prior to column chromatography facilitated their separation. Presumably, conversion of the quaternary salts into free bases alters their polarities and enables them to be separated by chromatography. Mono-*N*-acetyl cyclen was hygroscopic and stored in a dessicator.

2.4 Alkylation of cyclen with *N*-acetyl-1-bromo-L-serine methyl ester and *N*-Z-1-bromo-L-serine methyl ester

2.4.1 Preparation of *N*-acetyl-1-bromo-L-serine methyl ester (**2.27**) and *N*-Z-1-bromo-L-serine methyl ester (**2.28**)

To avoid steric hindrance to the attacking nucleophile (i.e. cyclen) and enable substitution, the protecting group on the amino group of **2.12** must be relatively unhindered. The two protecting groups chosen were the acetyl and the benzyloxycarbonyl (abbreviated to CBz or Z) groups (see Schemes 2.19 and 2.20). Since cyclen was already mono-*N*-protected with an acetyl group, using an acetyl group to protect the amino group on **2.12** seemed an obvious choice. This would permit the simultaneous deprotection of both the acetyl group on the side-arm and the acetyl group on the cyclen ring. **2.27** was prepared in two steps according to Scheme 2.19.

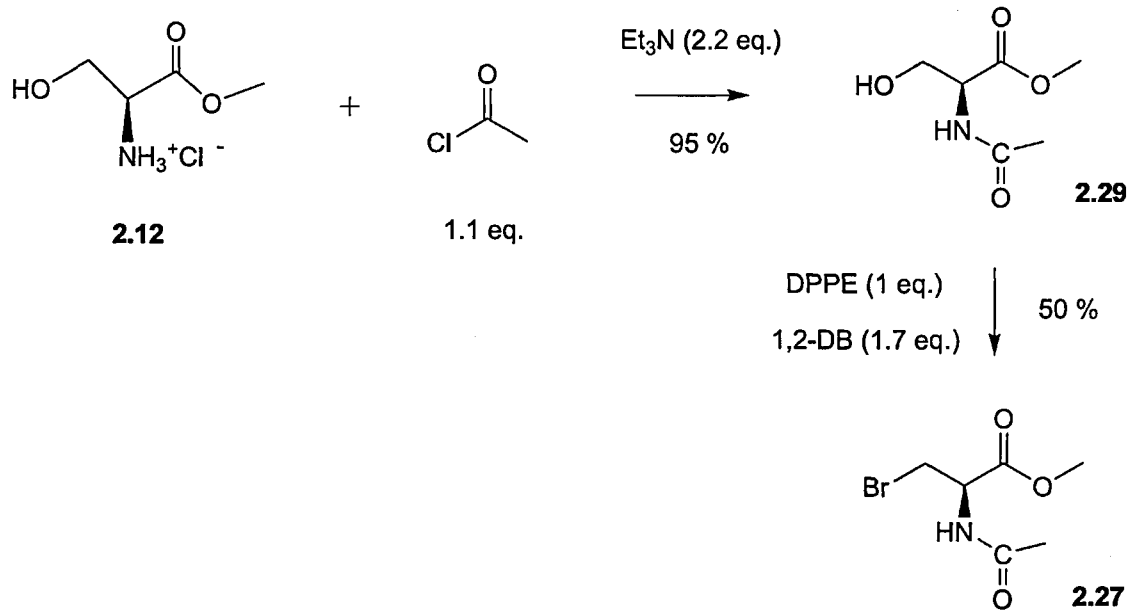

Scheme 2.19 Synthesis of *N*-acetyl-1-bromo L-serine methyl ester (**2.27**).

Acetylation of **2.12** was achieved by the slow addition of acetyl chloride to L-serine methyl ester hydrochloride and triethylamine (all 1 eq.) in chloroform. Acetylation of the

amino group made the product (**2.29**) water-soluble which precluded a simple organic solvent extraction purification procedure. It was found that the addition of acetone precipitated the bulk of the triethylammonium chloride by-product which formed in the reaction but column chromatography was required to remove final traces. The spectral data obtained for **2.27** agreed well with literature values [97]. Bromination of **2.29** was then achieved by reaction with DPPE (1 eq.) and 1,2 DB (1.7 eq.) in THF to give **2.27** as a white solid.

The second protecting group chosen was the benzyloxycarbonyl group which can be abbreviated to CbZ or Z. It is an acid-resistant PG commonly used in peptide synthesis and usually forms stable, crystalline derivatives [96]. It can be easily cleaved by catalytic hydrogenation over Pd/C at room temperature and pressure. Whilst the Z protecting group is not significantly smaller than the *t*-butyl group, it contains a phenyl ring which is a planar ring of sp^2 hybridized carbons. As a result, it occupies less space in the vicinity of the electrophilic carbon than the *t*-butoxylcarbonyl group which hinders nucleophile attack from all directions. **2.28** was prepared in two steps according to Scheme 2.20.

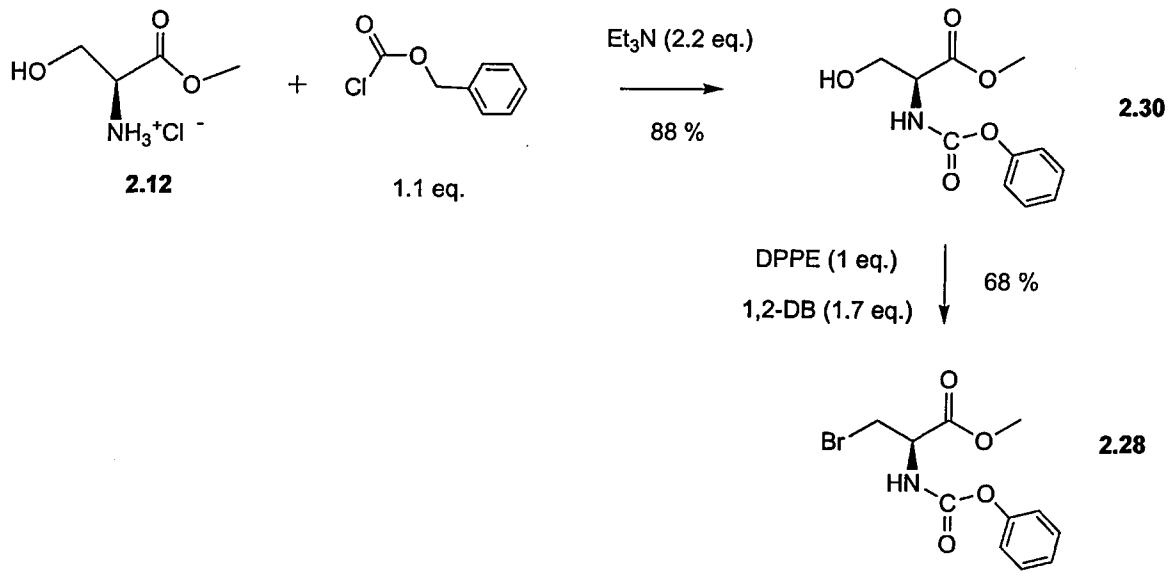

Scheme 2.20 Synthesis of *N*-Z-1-bromo L-serine methyl ester (**2.28**).

2.28 was synthesised by reacting **2.12** with benzyl chloroformate (1 eq.) and triethylamine (2.2 eq.) in $CHCl_3$. After washing the reaction mixture with dilute HCl to remove unreacted starting materials, the solvent was evaporated to give an oil. Analysis of this oil by ^1H NMR revealed the characteristic 5H multiplet of the phenyl group at δ 7.4 ppm indicating the amine had been successfully protected. This oil was then brominated without further purification to give **2.28** as a white solid.

2.4.2 Alkylation of cyclen with *N*-acetyl-1-bromo-L-serine methyl ester (**2.27**) and *N*-Z-1-bromo-L-serine methyl ester (**2.28**)

2.27 (3.2 eq.) in acetonitrile was added dropwise to a stirred solution of mono-*N*-acetyl cyclen (**2.26**, 1 eq.) and triethylamine (4 eq.) (Scheme 2.21).

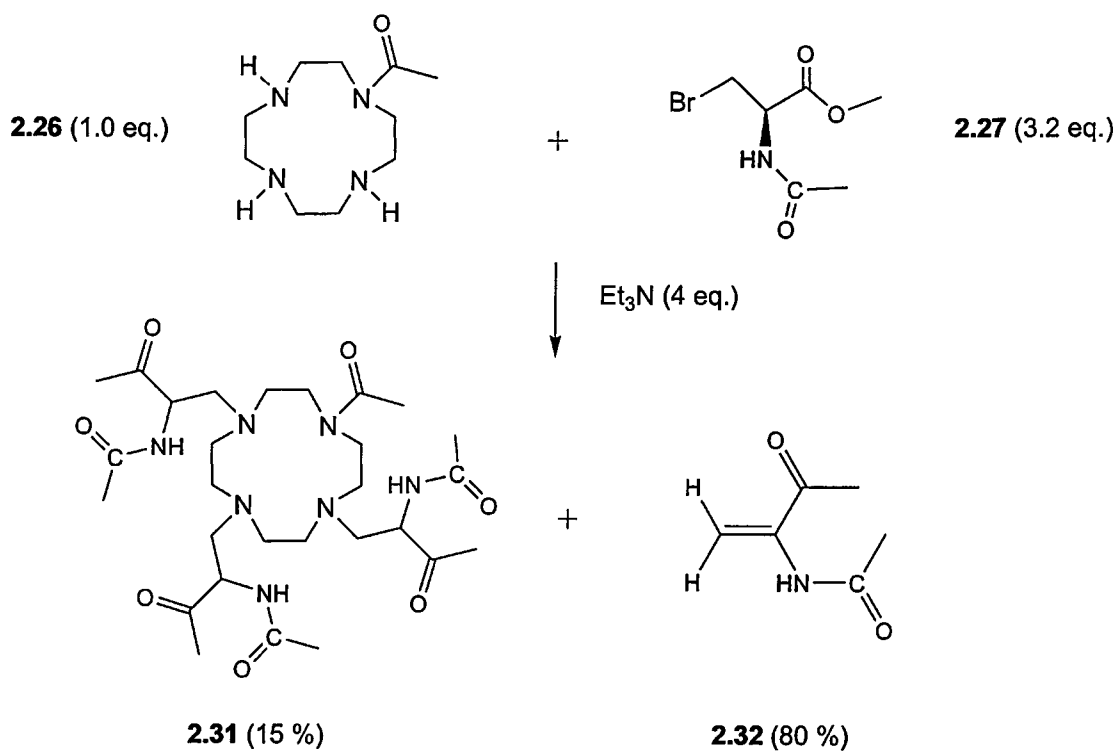

Scheme 2.21 Alkylation of mono-*N*-acetyl cyclen with **2.27**.

The reaction was then stirred at room temperature for 48 h under argon. Removal of the solvent gave an orange oil which was purified on an alumina column to afford the tetra-*N*-

substituted cyclen (**2.31**) in a yield of 15 %. Analysis of the column fractions via LC-MS and NMR revealed that a competing reaction was taking place, namely the elimination of bromide from **2.27** to give the corresponding alkene, **2.32**. The two alkene hydrogens of **2.32** gave peaks at 5.8 and 6.5 ppm in the ^{1}H NMR. In fact, most of the alkyl halide underwent elimination rather than substitution (approx. 80 : 15 % respectively). Therefore, the substitution reaction was competing with a dominant elimination reaction. Although the pendant arms of **2.31** contain 3 asymmetric carbons, their configurations could not be determined by ^{1}H NMR as the CH groups absorbed in the same region of the spectrum as the methylene groups of the cyclen ring.

A similar pattern of substitution versus elimination was found when unprotected cyclen was alkylated with *N*-Z-1-bromo-L-serine methyl ester (**2.28**) as shown in Scheme 2.22.

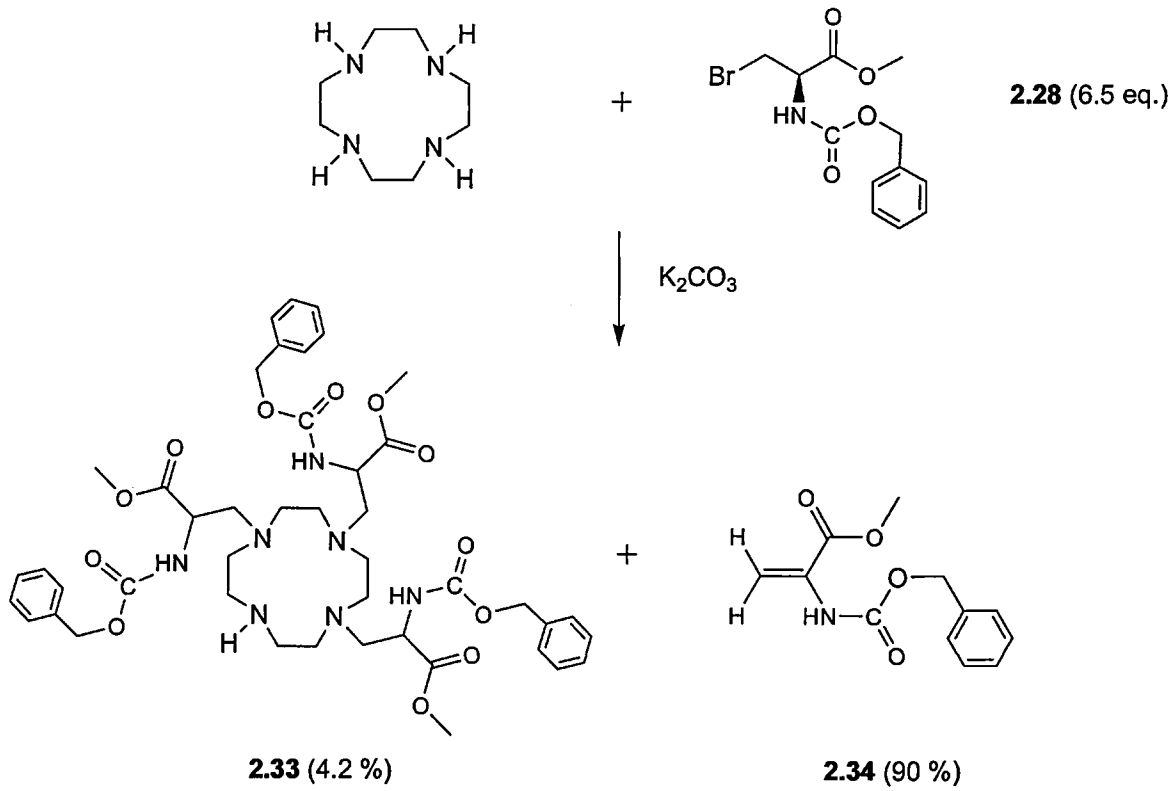

Scheme 2.22 Alkylation of cyclen with **2.28** to give the tri-substituted cyclen (**2.33**) and the alkene (**2.34**).

The reaction was carried out by stirring cyclen and 3.5 eq. **2.28** in dry acetonitrile under argon. After 48 h, LC-MS analysis indicated formation of mono- and di-*N*-substituted cyclen. To promote substitution, another 3 eq. electrophile (**2.28**) was added and the mixture stirred for a further 24 h. LC-MS monitoring indicated formation of **2.33** so the reaction was stopped. The organic layer was then evaporated to give a viscous, orange oil which was purified on a silica gel column to give the elimination alkene (**2.34**) as a colourless oil (90.8 %) and the tri-substituted cyclen (**2.33**) as a yellow, semi-solid (4.2 %). The tri-*N*-substituted product (**2.33**) formed at room temperature but no tetra-*N*-substitution was observed. This result was fortuitous as the tri-*N*-substituted product (**2.33**) was the desired product. As in the previous reaction (Scheme 2.21), substitution was accompanied by elimination of the halide and the alkene (**2.34**) was the major product isolated (90 %). The yield of the tri-*N*-substituted cyclen (**2.33**) was low (approx. 4.2 %) but purification was relatively straightforward as **2.33** eluted first from a silica column. Column chromatography of the non-polar, Z-protected (**2.33**) proved an easier task than the chromatographic purification of the hydrophilic, acetyl-protected (**2.31**). **2.33** was successfully purified on a standard silica gel column whereas **2.31** required chromatographic purification on neutral alumina as it adsorbed strongly to silica gel.

These findings support the hypothesis proposed earlier; that is, the size and/or shape of the amine protecting group on the L-serine methyl ester influences the substitution pattern on the cyclen ring. When Boc was used to protect LSME, only di-*N*-substitution on the cyclen ring was observed whereas the use of an acetyl or Z group resulted in tri-*N*-substitution. It is possible that the alkylation of unprotected cyclen with *N*-acetyl-protected LSME (**2.27**) may have resulted in tetra-substitution but this reaction was not carried out.

The yield of substituted cyclen was significantly higher when the amino group of LSME was *N*-acetyl-protected (15 %) rather than *N*-Z-protected (4.2 %). The *N*-acetyl-protected substrate (**2.27**) may be able to adopt a less sterically-hindered transition state leading to a faster reaction rate. In S_N2 reactions, a planar arrangement of the non-reactive groups in the transition state which has a lower energy, is an essential feature (Figure 2.4) [98]. If it is not possible, the reaction is not observed.

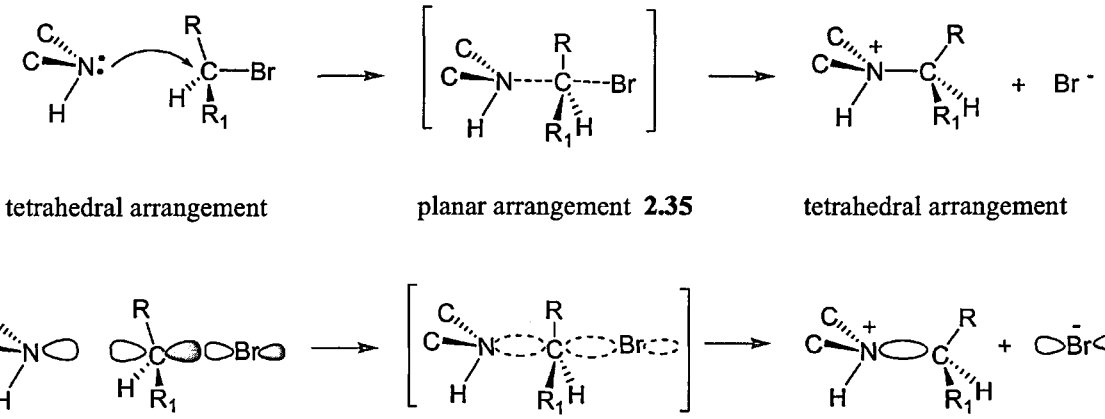

Figure 2.4 The planar transition state (**2.35**) of an S_N2 reaction [98].

In Figure 2.4, a planar planar arrangement of the non-reactive groups in the transition state (**2.35**) is preferred because it permits maximum overlap of the two orbitals, that is the HOMO (highest occupied molecular orbital) on the nucleophile and the LUMO (lowest occupied molecular orbital) on the alkyl halide. The actual configuration of **2.35** is trigonal bipyramidal. Any structural feature which stabilises this trigonal bipyramidal arrangement will lower the energy of the transition state and favour the S_N2 reaction.

To determine what effect K_2CO_3 had on the reaction, **2.27** was reacted with cyclen in the absence of base and elimination was still found to predominate. This result is not so surprising when one considers that cyclen is itself quite basic and the pK_as related to two of

its protonation steps are of the same order of magnitude as triethylamine (pK_a = 10.7). Normally, primary substrates tend to undergo substitution but the location of an acidic H' between two electron-withdrawing groups makes it liable to react with base. This gives the alkene **2.36** (Scheme 2.23).

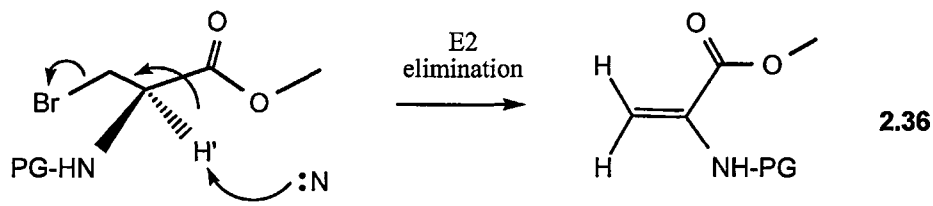

2.36

Scheme 2.23 Proposed E2 elimination mechanism from serine derivatives.

In fact, a survey of the literature revealed that *O*-tosylated serine derivatives rapidly undergo β-elimination under the action of bases. Photaki found that when *N*-benzloxycarbonyl-*O*-tosyl-L-serine methyl ester (**2.37**) was treated with 0.1 M NaOH at room temperature, over 90 % underwent elimination within 15 minutes (Scheme 2.24) [99].

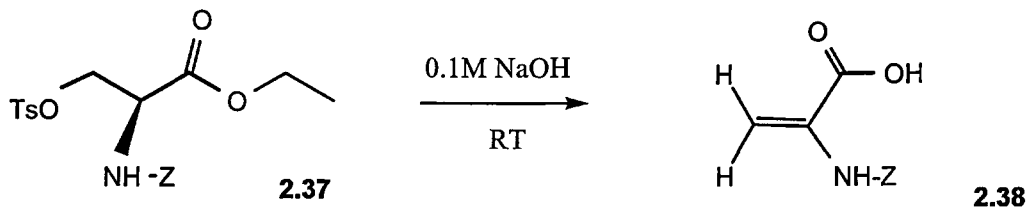

2.37 **2.38**

Scheme 2.24 Elimination from the *O*-tosylated serine derivative (**2.37**) [99].

2.5 Summary of cyclen alkylation reactions using amino acid derivatives (Chapter 2: Part A)

Elimination from both primary and secondary amino acid derivatives was found to be a major problem leading to a low yield (15 %) of tetra-substituted cyclen (**2.31**). These findings are schematically summarised in Scheme 2.25.

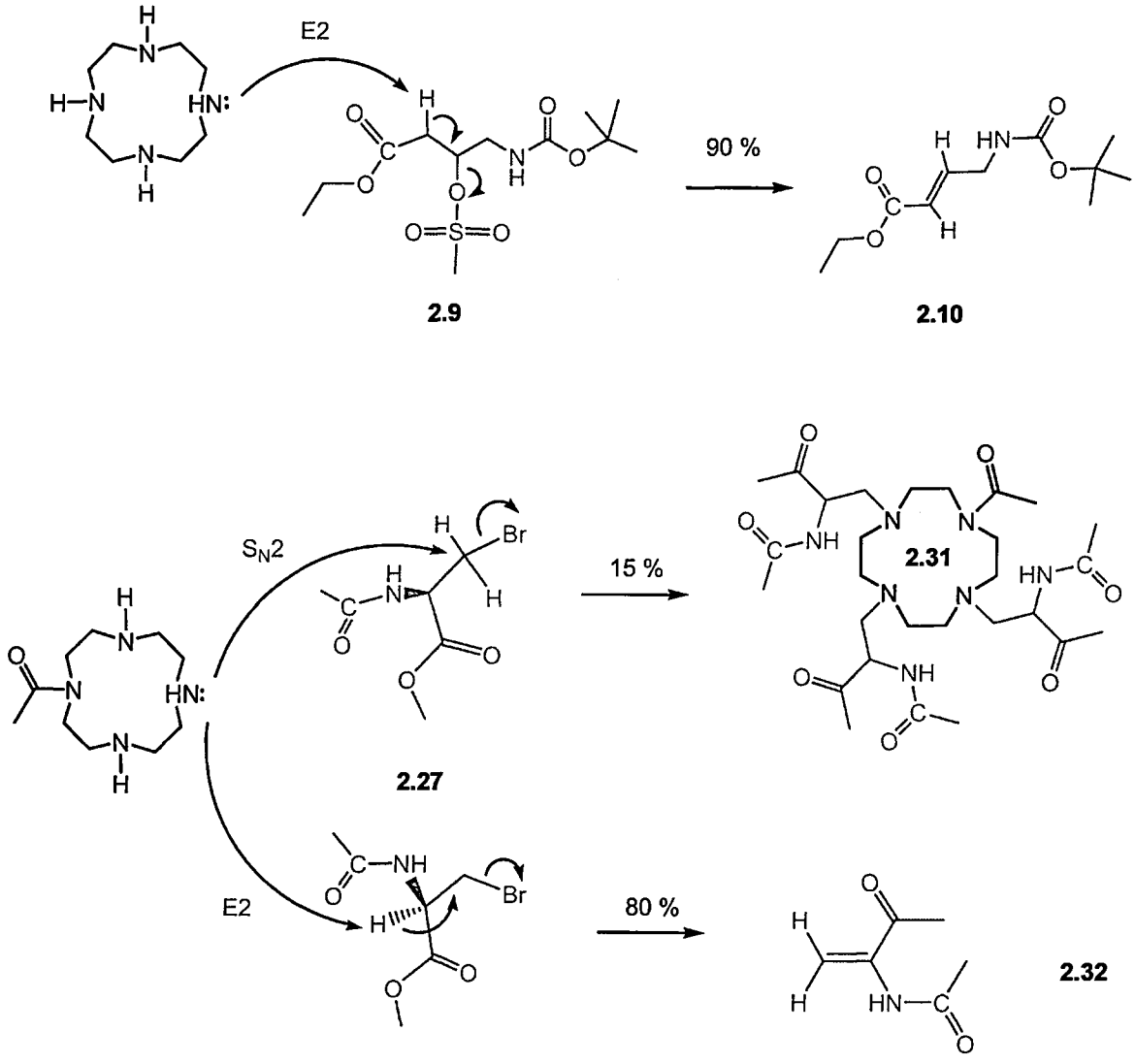

Scheme 2.25 Alkylation of cyclen with secondary (**2.9**) and primary (**2.27**) amino acid derivatives.

It may be possible to promote substitution over elimination by changing the amine and carboxyl protecting groups. For example, the carboxyl could be protected with a benzyloxycarbonyl group as well. This may provide better protection of any acidic protons from base. Dugave and Menez [100] had some success using *N*-trityl (triphenylmethyl) as a protecting group to prevent α-proton abstraction in serine derivatives but only with non-nucleophilic bases. Since cyclen is a nucleophilic base, there is always the possibilty of elimination. For these reasons, an alternative route to our target ligand is investigated in the next chapter.

Part B Synthesis of a cholic acid-cyclen conjugate

2.6 Introduction

Gadolinium complexes with amphiphilic properties have previously been synthesised and evaluated as blood-pool and liver-imaging agents [101]. Generally, these are prepared by coupling a hydrophilic Gd complex to a lipophilic molecule such as a long-chained fatty acid [102]. In an aqueous environment, these complexes are able to form supramolecular systems such as micelles. The formation of these systems increases the T_1-relaxivity of the contrast agent due to an increase in the rotational correlation time (τ_R) of the Gd complex. One example of a lipophilic Gd complex is **2.39** which is shown in Figure 2.5. Lattuada *et al.*[101] conjugated cholesterol to DPTA and after complexation with gadolinium, they obtained the agent **2.39** which displayed a high relaxivity (r_1 = 27.2 mM^{-1} s^{-1}). **2.39** can aggregate to form the micelle (**2.40**) once it's concentration reaches a certain level, that is, it's critical micelle concentration (CMC).

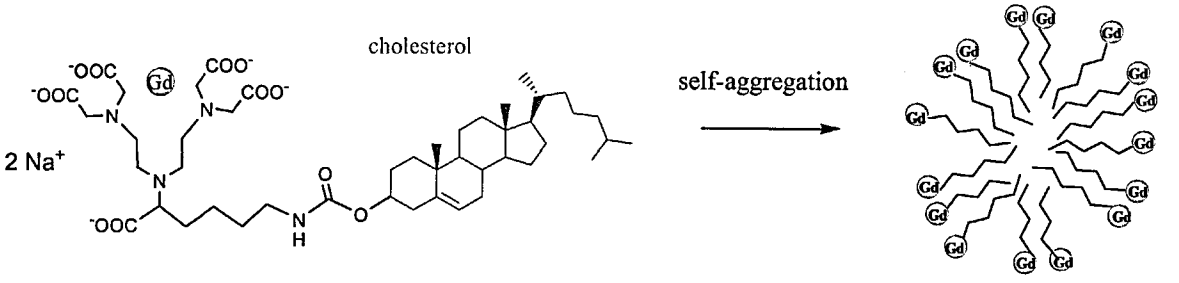

2.39 **2.40** micelle, $r_1 = 27.2\ mM^{-1}\ s^{-1}$

Figure 2.5 Gd-DPTA-cholesterol (**2.39**) and a micelle (**2.40**) formed from self-aggregation of **2.39**.

The aim of the present work was to synthesise a cholic acid-cyclen conjugate (**2.41**), which after complexation with gadolinium, could have potential as a blood-pool imaging agent (Figure 2.6).

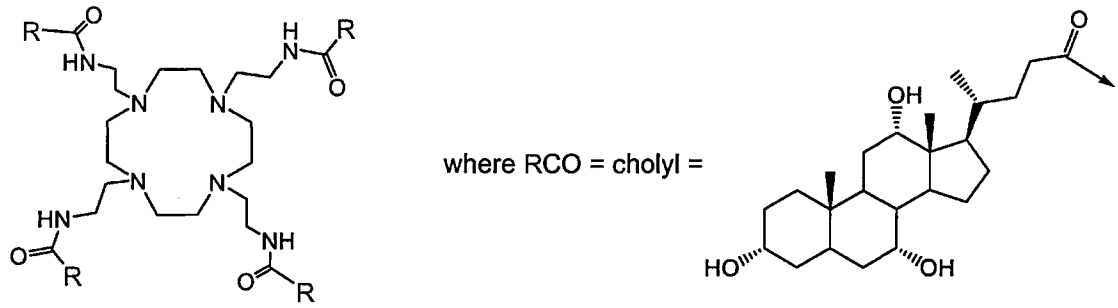

2.41 **2.42**

Figure 2.6 Structure of target ligand (**2.41**) where RCO refers to the cholyl moiety **2.42**.

Cholic acid, or 3α,7α,12α-trihydroxy-5β-cholan-24-oic acid, is a major steroidal constituent of human bile and is produced in the liver [103]. The liver effectively removes excess cholesterol from the body by converting it into bile acids via a fifteen step enzymatic process. Like other bile acids, cholic acid forms micelles with water-insoluble fats allowing their uptake into the bloodstream. The presence of a hydrophobic face on one side and a hydrophilic face on the other give cholic acid its unique amphiphilic properties (Figure 2.7).

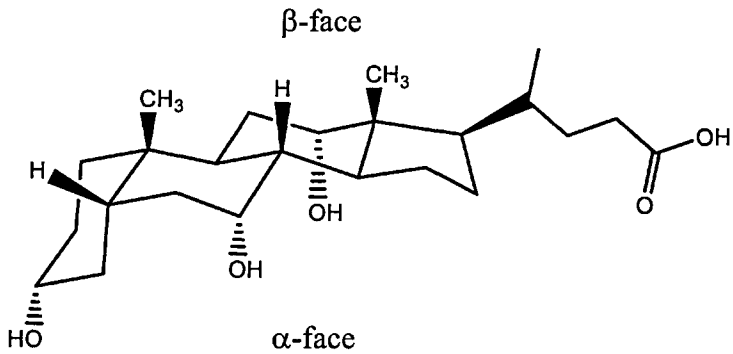

Figure 2.7 Structure of cholic acid showing the hydrophilic α-face and the hydrophobic β-face.

Cholic acid can form bilayered structures made up of repeating hydrophilic and hydrophobic layers, with channels [103]. Prior to secretion by the liver, cholic acid is conjugated with either the amino acid glycine or taurine [103] (Figure 2.8). Conjugation increases the water solubility of cholic acid. As a result, the concentration of bile acids in the small intestine can stay high enough to form micelles and solubilize lipids.

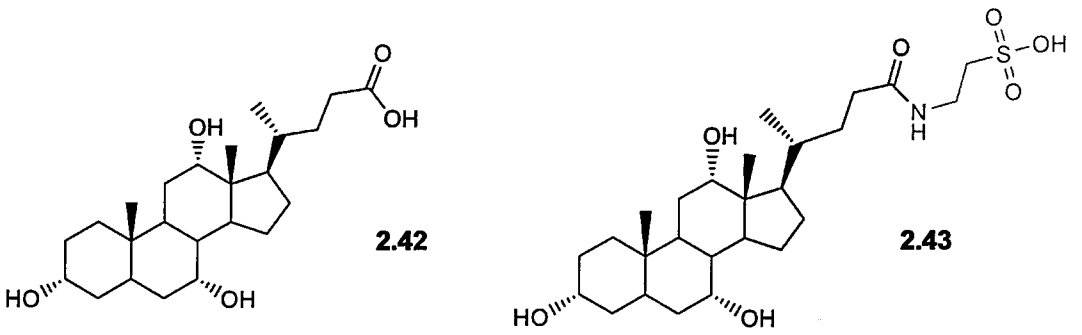

Figure 2.8 Structures of cholic acid (**2.42**) and taurocholic acid (**2.43**).

Based on Lattuada's work, it was envisonaged that conjugation of amphiphilic cholic acid to hydrophilic cyclen may produce a conjugate that has affinity for both aqueous and lipophilic media. In effect, it may have properties similar to **2.39** and taurocholic acid (**2.43**). After complexation with gadolinium, the resultant amphiphilic complex would be expected to form micelles once its concentration reached its CMC.

2.7 Synthetic strategy

Scheme 2.26 overleaf shows the two routes that were considered for the synthesis of the cholic acid-cyclen conjugate (**2.41**). In both Route A and Route B, 2-bromoethylamine (**2.44**) serves as a linker molecule.

Route A involves the formation of an amide bond between cholic acid (**2.42**) and 2-bromoethylamine to give the brominated intermediate (**2.45**). This can be accomplished with dicyclohexylcarbodiimide (DCC) which generates amide bonds between carboxyl and amine groups. Alkylation of cyclen with **2.45** should then afford the desired ligand **2.41**.

Route B is lengthier involving both amine protection and deprotection steps. Once the amino group on 2-bromoethylamine is protected with a suitable protecting group such as *t*-Boc, the product (**2.46**) can be used to alkylate cyclen. Deprotection of the substituted cyclen product (**2.47**) makes the amine groups available for coupling to the carboxyl group of cholic acid. As in Route A above, the cholic acid-cyclen conjugate (**2.41**) is the final product.

Route A

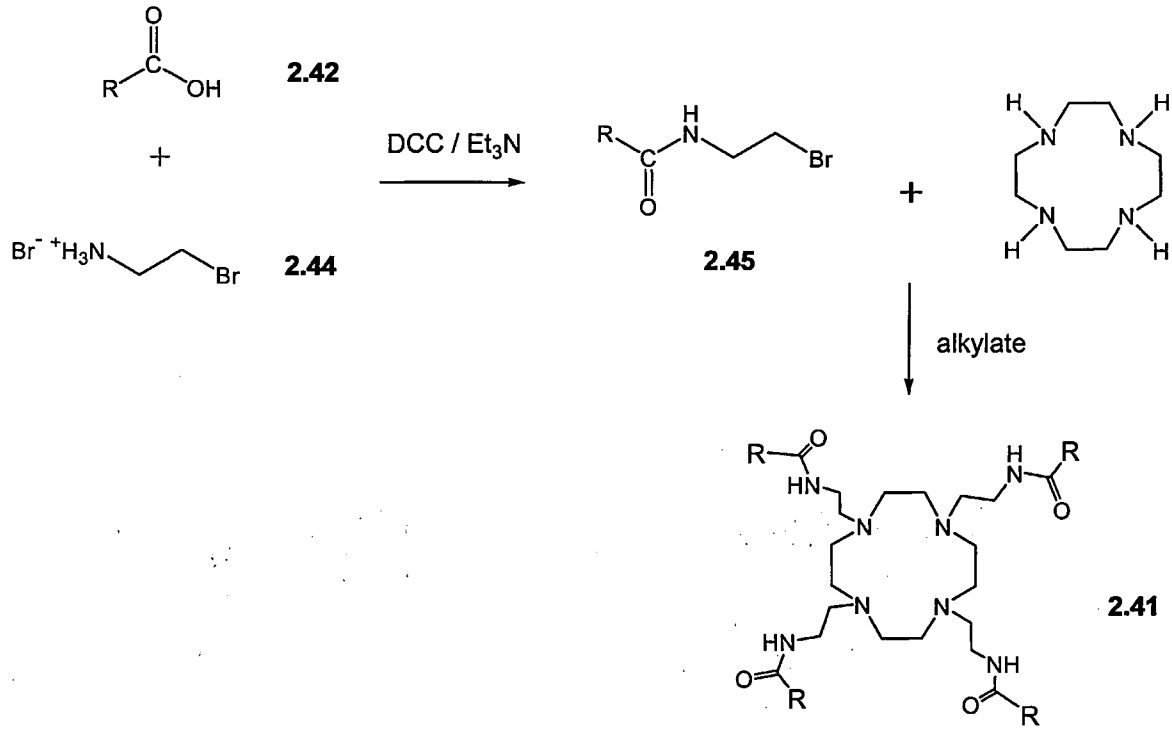

Route B

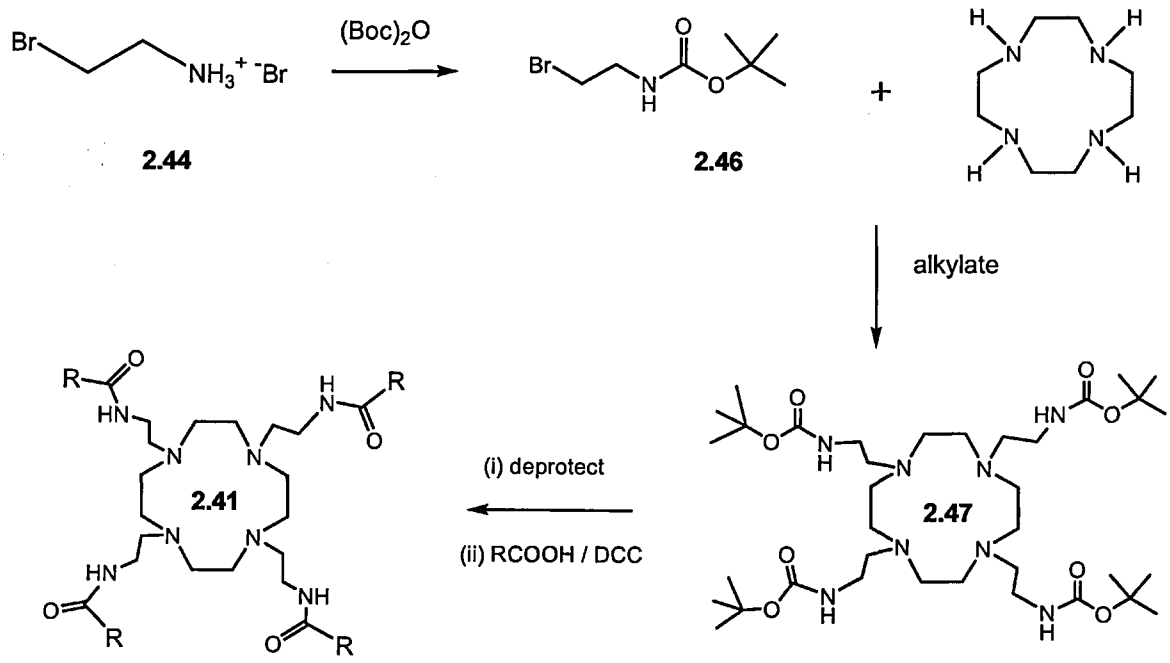

Scheme 2.26 Synthetic Routes A and B to **2.41**
(where RCO and RCOOH refer to the cholyl moiety).

2.7.1 Synthetic Route A

2.7.1.1 *Coupling 2-bromoethylamine to cholic acid using DCC (dicyclohexylcarbodiimide)*

The first step of Route A was the formation of an amide bond between 2-bromoethylamine (**2.44**) and cholic acid (**2.42**) (Scheme 2.27).

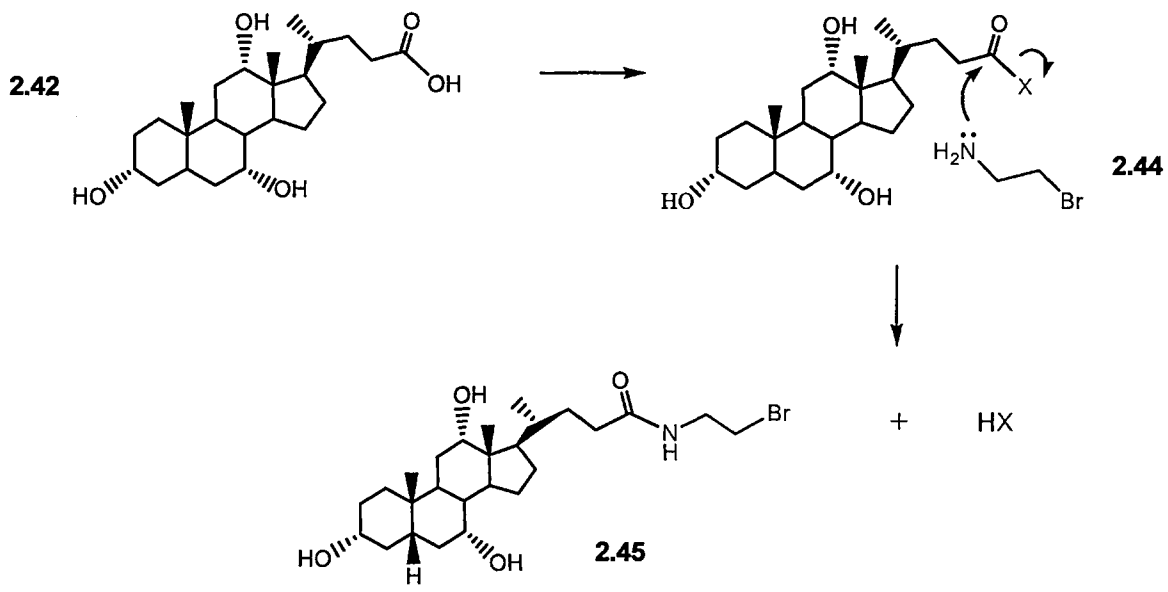

Scheme 2.27 Amide bond formation between cholic acid and 2-bromoethylamine.

DCC was the coupling reagent chosen to effect this transformation (Figure 2.9). Since its introduction in 1955, DCC has been one of the most important reagents for activating carboxy groups in peptide synthesis [84].

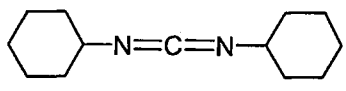

Figure 2.9 Structure of DCC.

A peptide coupling reagent transforms the hydroxyl function into an activated ester which is a better leaving group. Nucleophilic attack of this ester by an amine *in situ* results in the

formation of an amide bond. For the reaction, 2-bromoethylamine (HBr salt), triethylamine and cholic acid (all at 1 eq.) were dissolved in a DCM/DMF (20:2 ml) solution (see Scheme 2.28). Triethylamine base was added to convert the hydrobromide salt to the free amine. After cooling the mixture on an ice bath, DCC (1 eq.) was added in small portions. The reaction was then stirred under argon for 24 hours at ambient temperature.

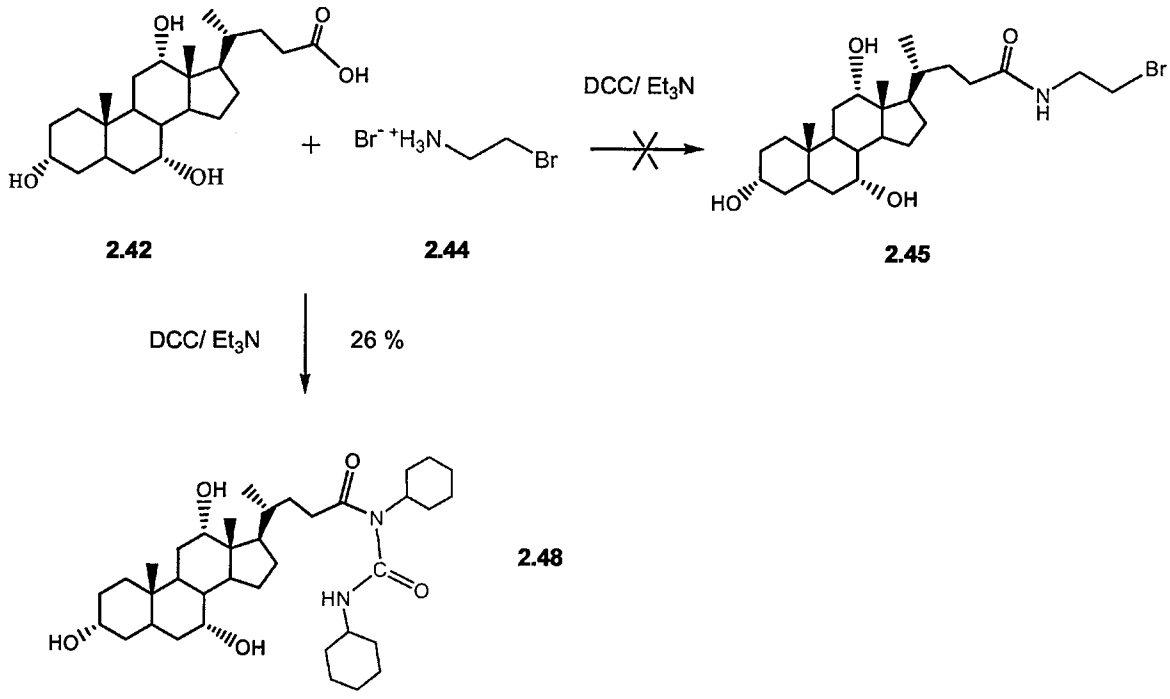

Scheme 2.28 DCC-promoted coupling reaction between cholic acid and **2.44**.

After precipitated dicyclohexylurea (DCU) was filtered off and the solvent was evaporated. TLC of the reaction residue indicated it consisted of unreacted cholic acid and a less polar compound suggestive of an ester or amide. Isolation of this compound by silica gel column chromatography yielded **2.48** whose spectral data was consistent with the structure of the *N*-acylurea derivative of cholic acid (Scheme 2.29). The assignment of individual carbon and proton resonances in **2.48** was aided by comparison with reference spectra [104] and by cross-referencing with data from a ^{1}H-^{13}C COSY spectrum. No bromoethylamine-cholic acid conjugate (**2.45**) was isolated from the reaction mixture.

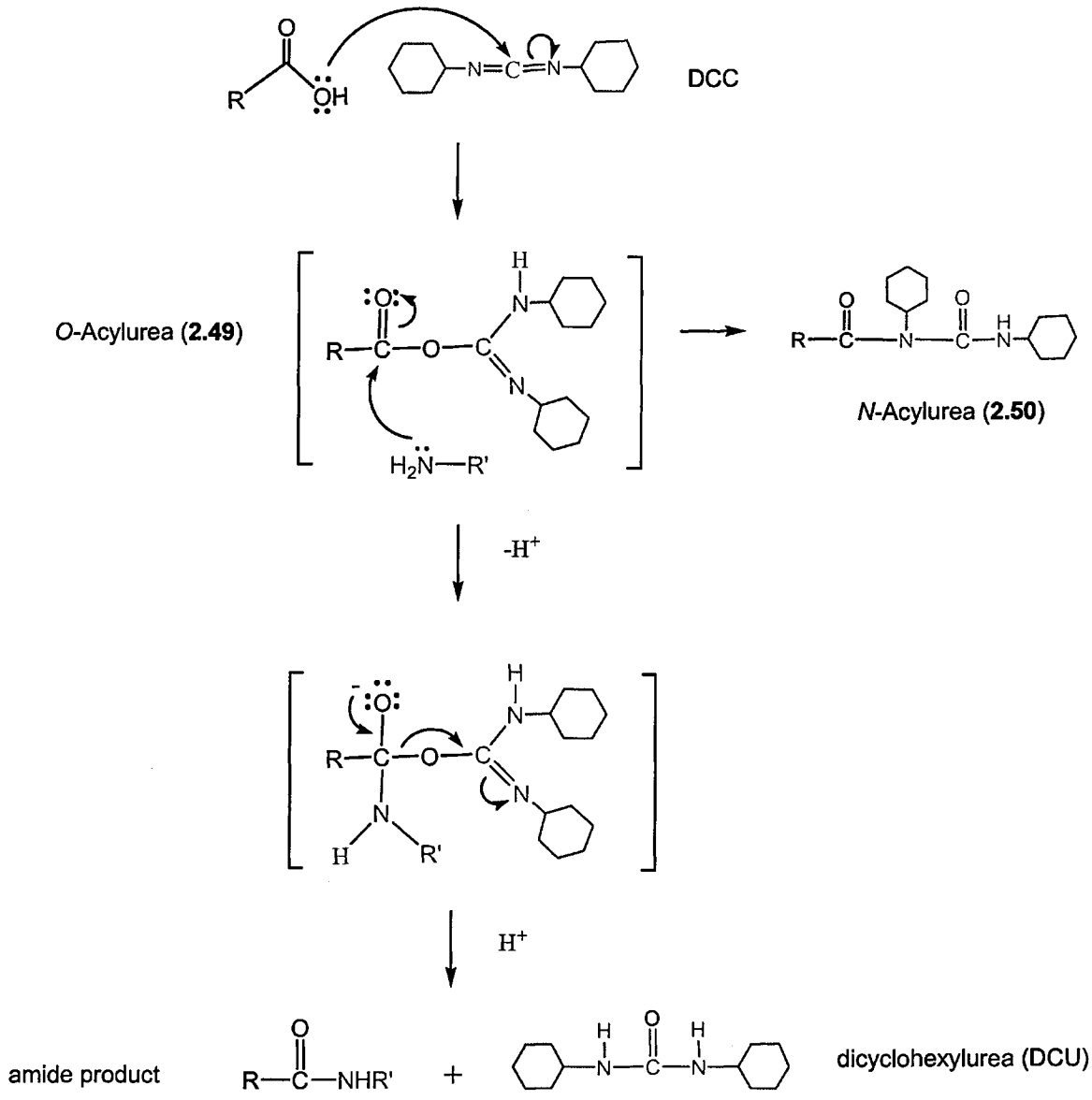

Scheme 2.29 The mechanism of amide formation by reaction of a carboxylic acid and an amine with DCC [70].

Direct coupling with DCC to form an amide is in theory uncomplicated, involving the mixing of the amino and carboxy components in an organic solvent at room temperature [81]. The formation of *O*-acylurea (**2.49**) results in amide formation via nucleophilic attack with the concomitant production of insoluble *N,N*-dicyclohexylurea (DCU). *O*-acylurea is very reactive and if a good nucleophile is not at hand, intramolecular acyl transfer can occur to

form the less reactive *N*-acylurea (**2.50**). As *O*-acylurea isomerised to *N*-acylisourea in the above reaction, 2-bromoethylamine probably reacted sluggishly with *O*-acylurea.

2.7.1.2 *Coupling 2-bromoethylamine to cholic acid using EDCI*

EDCI or EDC (1-Ethyl-3-(3-dimethylaminopropyl)carbodiimide) has a similar mode of action to DCC (Figure 2.10) [81]. However, unlike DCC, excess carbodiimide and derived urea can be washed out with dilute acid.

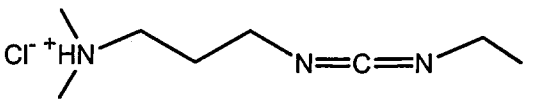

Figure 2.10 Structure of EDCI.

Hirayama *et al.* [105] used EDCI to form amide conjugates between cholic acid and various amino-containing substrates (yields > 90 %). When coupling using this established procedure failed to produce any conjugate, it was suspected the problem may lie with the 2-bromoethylamine starting material. 2-bromoethylamine is supplied as a hydrobromide salt and for the coupling reaction, it is necessary to add base to free the amine group. However, C-2 of 2-bromoethylamine is electron deficient due to bromine substitution and could potentially be attacked by the freed amine group of another 2-bromoethylamine molecule as depicted in Scheme 2.30.

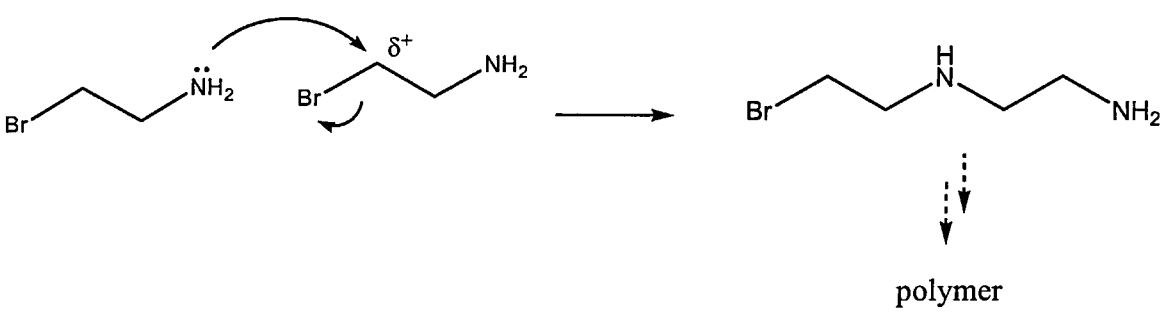

Scheme 2.30 Potential polymerization of 2-bromoethylamine.

This self–condensation or polymerisation reaction may have consumed the 2-bromoethylamine before the carboxyl group was converted to an ester. In an attempt to circumvent this potential side-reaction, cholic acid was pre-converted to an active ester before the condensation reaction with 2-bromoethylamine. It was anticipated this pre-activation strategy would maximise the possibility of 2-bromoethylamine reacting with the cholate ester and reduce the risk of polymerization taking place. The synthesis of activated cholic acid and its subsequent reaction with cyclen are described in the next section.

2.7.1.3 *Reaction of 2-bromoethylamine with the p-nitrophenyl ester of cholic acid*

In peptide bond formation, amidation with an isolated activated ester is often preferred to direct coupling [81]. With this method, side reactions like racemization are generally less of a problem. The isolated *p*-nitrophenyl [106] and *N*-succinimido esters of cholic acid [107] have previously been employed to form amide bonds between cholic acid and the amino group of various compounds (Figure 2.11).

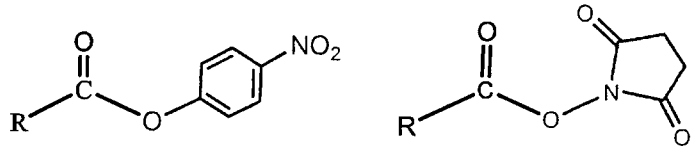

Figure 2.11 *p*-nitrophenyl ester and *N*-succinimido ester.

The *p*-nitrophenyl ester of cholic acid (**2.51**) was prepared using DCC to couple the phenol to the carboxylic acid group of cholic acid (Scheme 2.31) [106].

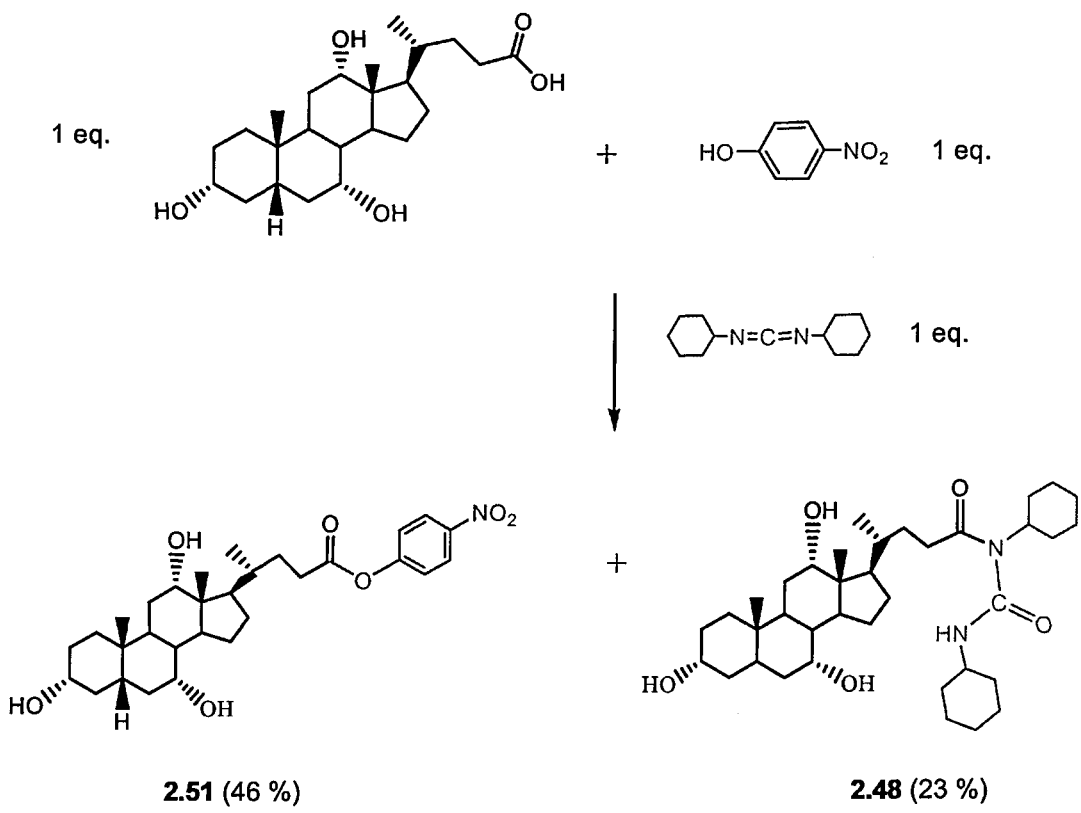

2.51 (46 %) **2.48** (23 %)

Scheme 2.31 Synthesis of cholyl *p*-nitrophenyl ester (**2.51**).

The reaction was performed by adding DCC to a cooled solution of cholic acid and *p*-nitrophenol (all 1 eq.) in an ethyl acetate-DMF solution. After 20 hours, the precipitated dicyclohexylurea was filtered off. The organic phase was then washed with a 5 % sodium bicarbonate solution and evaporated to dryness *in vacuo*. TLC of the reaction product indicated that two compounds were formed, one that was UV-active (R_f 0.36) and one that was UV-inactive (R_f 0.28). Although both compounds had similar R_f values, they were successfully separated on a silica gel column. The crude product yielded 46 % of cholyl *p*-nitrophenyl ester (**2.51**) and 23 % of what appeared to be the *N*-acylurea derivative of cholic acid (**2.48**) **2.48** was also a by-product in the coupling reaction involving DCC (see Section 2.7.1.1).

It is worth noting here that *p*-nitrophenol was successfully coupled to cholic acid using DCC. Significantly, attempted conjugation of 2-bromoethylamine to cholic acid using a

similar DCC procedure above failed to give any product. In contrast to *p*-nitrophenol which can only react with the activated ester intermediate (**2.51**), 2-bromoethylamine can also undergo polymerisation. This explains the difference in reactivity between both substrates.

The next step of Route A involved the condensation reaction between 2-bromoethylamine and cholyl *p*-nitrophenyl ester (**2.51**) in the presence of triethylamine (TEA) base. TEA (1.7 eq.) in THF was added dropwise to a cooled solution of cholyl *p*-nitrophenyl ester (1 eq.) and 2-bromoethylamine (1.5 eq.) in dry THF according to Scheme 2.32.

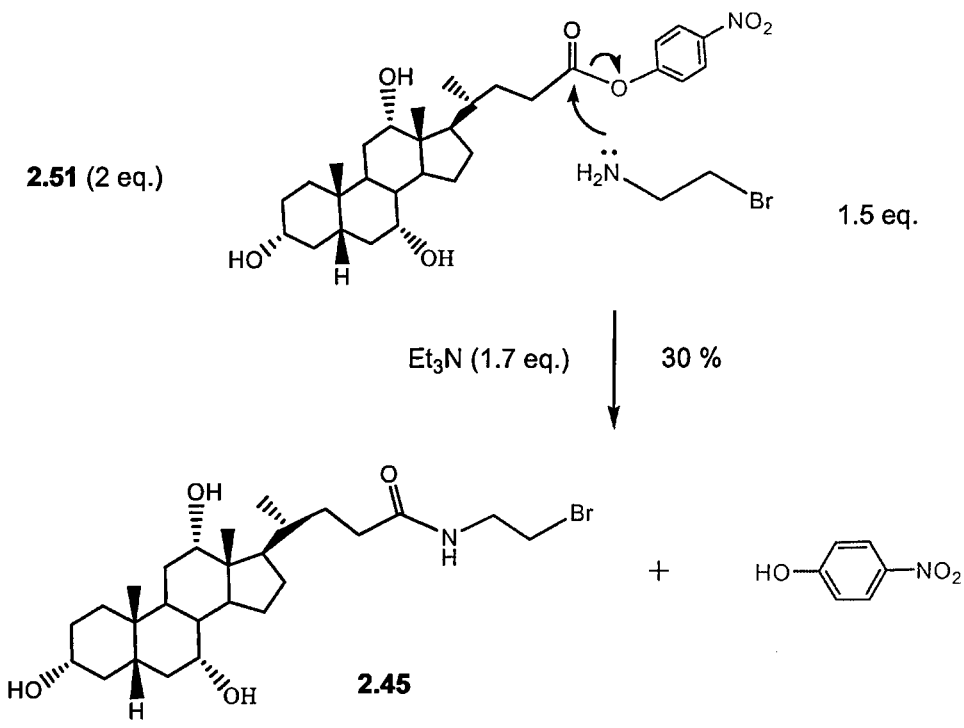

Scheme 2.32 Synthesis of **2.45** via cholyl *p*-nitrophenyl ester (**2.51**).

The triethylamine solution was added slowly to ensure the cholyl *p*-nitrophenyl ester concentration would exceed the concentration of 2-bromoethylamine at the start of the reaction. Accordingly, it was anticipated that 2-bromoethylamine would preferentially react with **2.51** and amide bond formation would be thus promoted. After stirring the

reaction for 12 h at RT, the organic layer was washed with 5 % NaH_2CO_3 and then with water to remove *p*-nitrophenol (yellow colour). After evaporation of the solvent, the residue was purified on a silica gel column using 10 % MeOH in $CHCl_3$ to give **2.45** as an off-white solid (30 % yield).

An absorbance at 1634 cm^{-1} in the IR indicated that **2.45** contained an amide group. In addition, proton signals arising from the amidic linkage were found to be particularly useful for the characterisation of **2.45**. Two pairs of triplets resonating at 3.80 and 4.21 ppm (^3J = 9.52 Hz) were assigned to the methylene protons at C-25 and C-26. A peak at *m/z* 512.4, which may correspond to $[M-H]^-$, was observable on LC-MS in negative ion mode (Figure 2.12). The presence of bromine was indicated by peaks at *m/z* 79 and 81 in a ratio of 1:1, corresponding to the two different isotopes of bromine. However, the synthesis of **2.45** was time-consuming and the yield was poor. Therefore, attention was redirected towards the alternative Route B as a means of preparation of the target ligand **2.41** (see Scheme 2.26).

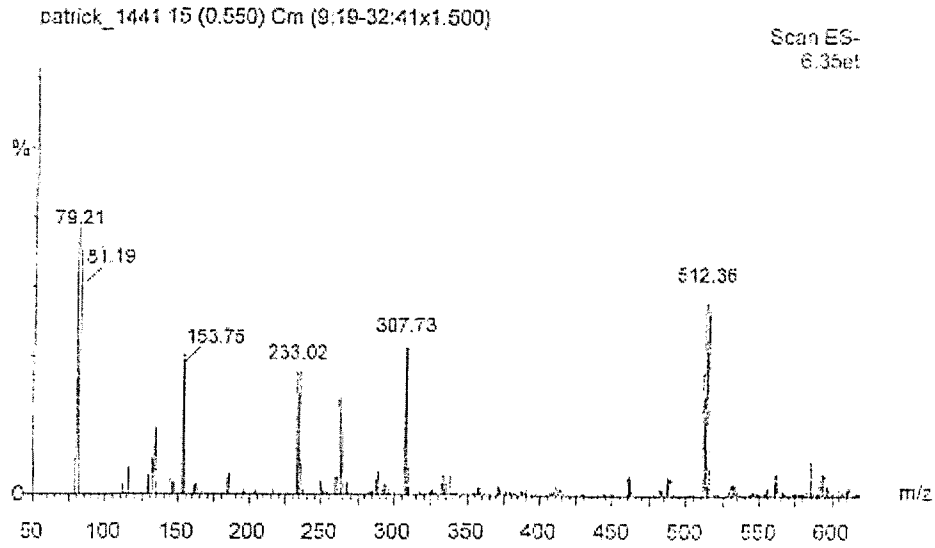

Figure 2.12 The ES-MS spectrum of **2.45** (negative ion mode, cone voltage = 10 eV)

2.7.2 Synthetic Route B

The first step of Route B necessitated the protection of the amine group of 2-bromoethylamine. Reaction of 2-bromoethylamine with di-*tert*-butyl dicarbonate and triethylamine gave *N*-Boc-2-bromoethylamine **2.46** as a colourless oil (Scheme 2.33). The spectral data for **2.46** agreed well with literature values [108].

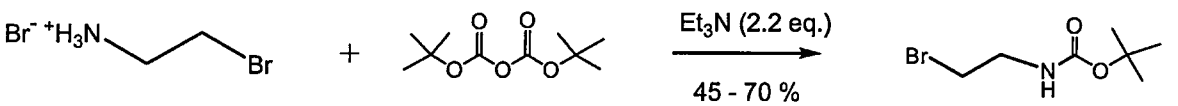

2.44 (1 eq.) 1.2 eq. **2.46**

Scheme 2.33 Synthesis of *N*-Boc-2-bromoethylamine.

In contrast to the coupling reactions involving 2-bromoethylamine and non-activated cholic acid above, the *N*-Boc protection of 2-bromoethylamine was relatively straightforward. Since *N*-Boc product (**2.46**) was obtained, the amine group of 2-bromoethylamine most probably reacts with di-*tert*-butyl dicarbonate, which is an an anhydride, before polymerisation can take place. Therefore, it can be assumed that this protection reaction with the moderately reactive anhydride occurs at a faster rate than the unsuccessful DCC coupling reaction described above which proceeds via an ester intermediate. Although the reaction was performed several times under similar conditions, the yields of **2.46** were highly variable ranging from 45 - 70 %. The inconsistent nature of the yields obtained lends further support to the idea that 2-bromoethylamine undergoes polymerization.

The next step of Route B was the alkylation of cyclen with *N*-Boc-bromoethylamine (**2.46**). Cyclen was refluxed with **2.46** (5 eq.) in acetonitrile in the presence of K_2CO_3 (5 eq.) for 12 hours according to Scheme 2.34.

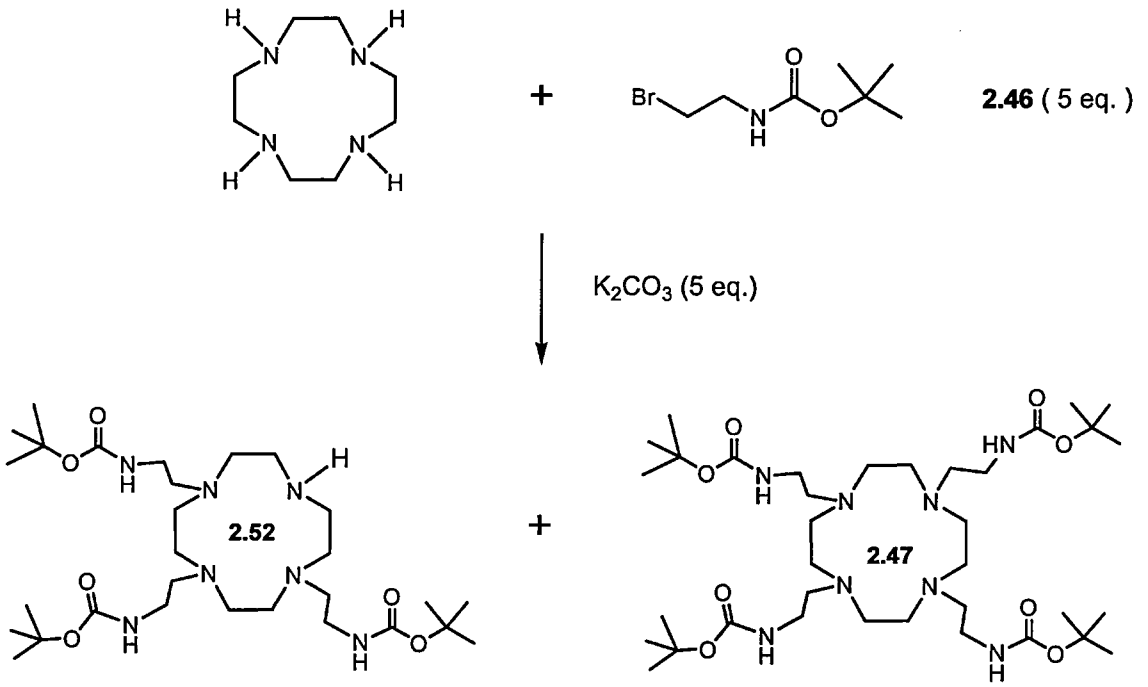

Scheme 2.34 Alkylation of cyclen with *N*-Boc-2-bromoethylamine.

Both TLC and ES-MS of the product residue indicated that a mixture of tri-substituted cyclen (**2.52**) and tetra-substituted cyclen (**2.47**) were formed. Attempted purification of the product residue on a silica gel column using a gradient of 0 - 15 % methanol in chloroform resulted in poor separation between **2.52** and **2.47**. This result ruled out Route B as a viable method for the preparation of the cholic acid-cyclen conjugate (**2.41**).

2.8 Summary of Chapter 2: Part B

Two synthetic routes (A and B) to **2.41** were attempted and each one was found to be problematic. Difficulties with Route A were attributed to the use of 2-bromoethylamine as a linker molecule. As discussed above, polymerization of 2-bromoethylamine can occur if the amine group of one molecule attacks the electron-deficient C-2 of another molecule. This problem was partially solved by pre-converting cholic acid to the *p*-nitrophenyl ester before the condensation reaction with 2-bromoethylamine. This modification enabled successful amide formation between cholic acid and 2-bromoethylamine to furnish the conjugate **2.45**. However, a low yield of **2.45** (30 %) coupled with a laborious synthesis discouraged further work on this route. Therefore, attention was directed towards the alternative Route B proposed in Scheme 2.26.

In Route B, *N*-Boc-bromoethylamine was prepared and reacted with cyclen. A mixture of tri-substituted (**2.52**) and tetra-substituted cyclen (**2.47**) was produced which proved to be inseparable by silica gel column chromatography. This result highlights the difficulties that can arise when cyclen is functionalized with halogenated substrates using conventional base-promoted alkylation techniques. These reactions routinely suffer from poor regioselectivity due to poly-alkylation [109]. A mixture of substituted cyclens is often obtained, imposing a difficult and sometimes impossible purification process as was discovered above. Consequently, functionalization of cyclen by alkylation has generally been addressed indirectly by using various protecting groups in multi-step sequences [110]. The use of mono-*N*-Boc cyclen (**2.24**) and mono-*N*-acetyl cyclen (**2.26**) as precursors to tri-substituted cyclen derivatives in Part A of this chapter illustrate this protecting group methodology. As an alternative to alkylation, Chapter 3 investigates the Michael addition of cyclen to conjugated alkenes as a means of the preparation of functionalized cyclen ligands.

Chapter 3

Functionalization of cyclen via the Michael addition reaction

3.1 Introduction

Currently, cyclen is primarily functionalized by reaction with alkyl halides [111, 112]. However, functionalization of cyclen via alkylation tends to be inefficient as the complete range of substitution products (i.e. mono-, di-, tri- and tetra-substituted cyclens) is often produced. Additionally, substituted cyclens often have similar polarities and cannot always be separated by column chromatography [111-113]. To avoid poly-alkylation and the waste of expensive cyclen, regioselective functionalization of cyclen generally requires pre-protection of the cyclen ring to ensure only the desired amines react. The use of mono-*N*-Boc-cyclen **(2.24)** and mono-*N*-acetyl cyclen (**2.26**) as precursors to tri-substituted cyclen derivatives in Chapter 2 illustrate this protecting group methodology.

Additional difficulties encountered with the alkylation approach were described in Part A of Chapter 2. These include steric hindrance to the attacking nucleophile (i.e. cyclen) and the elimination of the halide substrate. This chapter investigates the Michael addition of cyclen to activated alkenes as an alternative route to functionalized macrocycles.

3.2 The aza-Michael reaction

The Michael addition reaction is a valuable synthetic method in which a nucleophile adds across the carbon–carbon double bond of an activated alkene [114]. The Michael addition reaction is a specific example of a conjugate addition where an enolate nucleophile adds to a conjugated carbonyl [115]. Although nucleophiles do not normally react with simple alkenes, they do so if the double bond is conjugated to an electron-withdrawing group and resonance stabilizing activating group. Then, the anion formed by addition, and the preceding transition state, is stabilized sufficiently by charge delocalization so that addition occurs at a reasonable rate.

Scheme 3.1 shows the addition of dimethylamine to ethyl acrylate. The carbonyl of the acrylate stabilizes the resulting anion until proton transfer occurs. The overall driving force for the conjugate addition is the enthalpic change that accompanies replacement of a π-bond with a σ-bond [116]. The reaction tends to follow second-order kinetics based on the concentration of the alkene acceptor and the amine.

Although the Michael addition reaction originally referred to the addition of enolate nucleophiles to activated alkenes, a wide range of functional groups such as amines, thiols, and phosphines possess sufficient nucleophilicity to perform as Michael donors. The nitrogen-donor version of the Michael addition is often referred to as the aza-Michael reaction. Since amines can act as both nucleophiles and bases, no additional base is typically needed in these reactions. The ability of the aza-Michael reaction to generate β-amino carbonyl compounds has become increasingly important to the natural product and pharmaceutical areas [116, 117]. The following section looks at some of the Michael-type reactions that have previously been used to functionalize nitrogen-containing macrocycles.

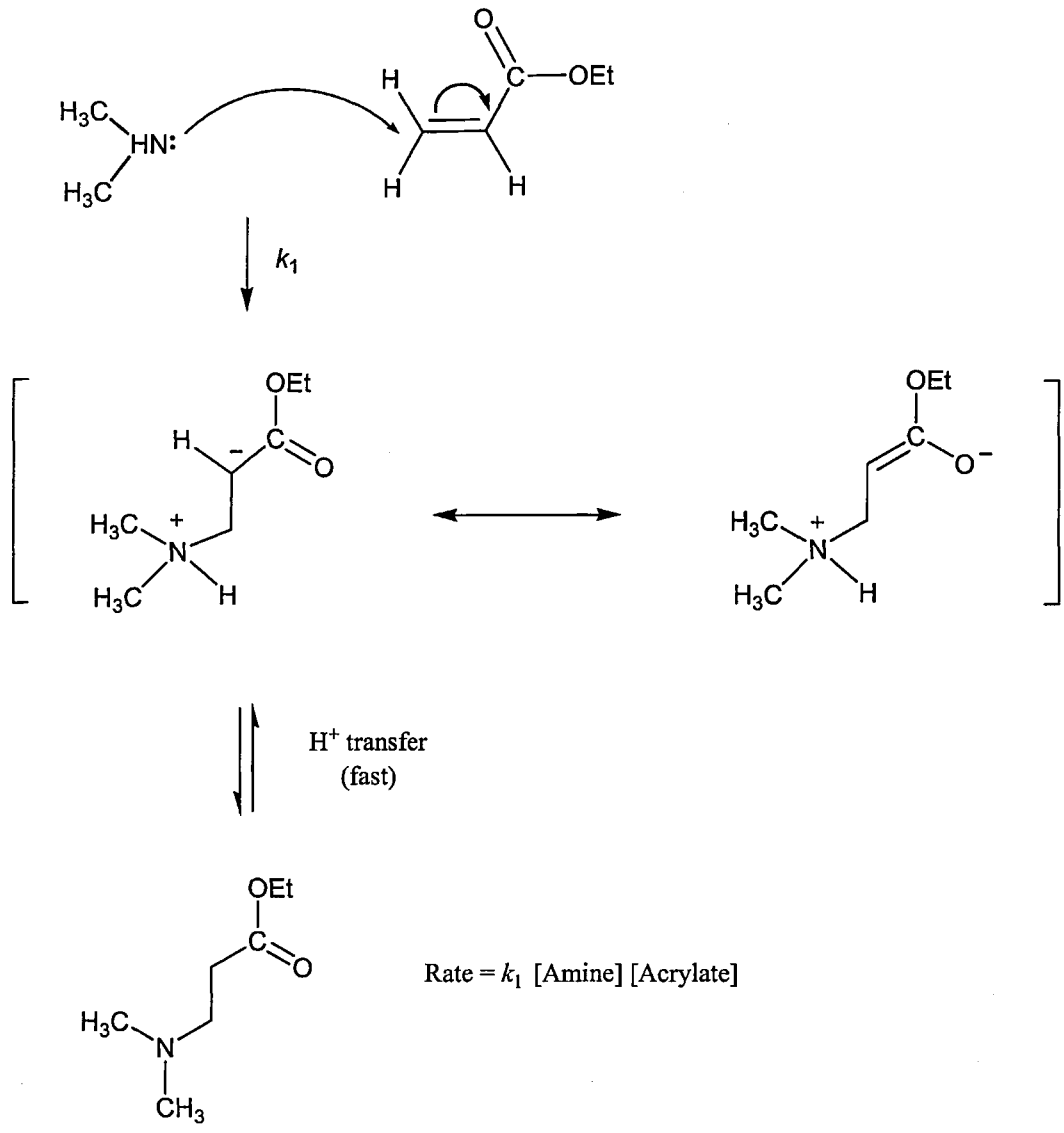

Scheme 3.1 Aza-Michael addition of dimethylamine to ethyl acrylate [116].

3.3 Functionalization of azamacrocycles using the aza-Michael reaction

As discussed in Section 1.9.1 of Chapter 1, cyclen has primarily been functionalized by alkylation. However, some examples which have used the Michael reaction to functionalize cyclen are described in the literature. Notable examples include the synthesis of 1,4,710-tetra-(2-carboxyethyl)-1,4,7,10-tetraazacyclododecane by Cocolios *et al.*[118]. In

this reaction, cyclen was reacted with a large excess of acrylic acid to give the tetra-substituted product **3.1** in a yield of 55 % (Scheme 3.2).

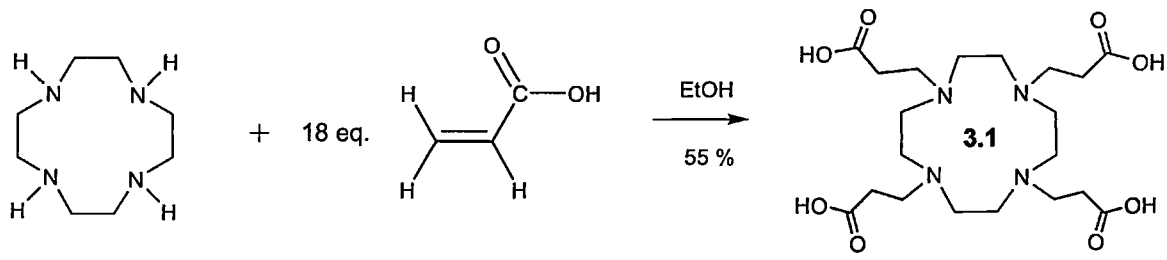

Scheme 3.2 Michael addition of cyclen to acrylic acid to give **3.1** [118].

The same authors successfully produced the tri-*N*-substituted macrocycle **3.4** by reacting mono-protected, *N*-benzylcyclam (**3.2**) with a large excess of acrylic acid. Cleavage of the benzylic nitrogen bond in **3.3** was then accomplished by hydrogenation over palladium on charcoal to give 1,4,8-tris(carboxyethyl)-1,4,8,11-tetraazacyclotetradecane, **3.4** (Scheme 3.3).

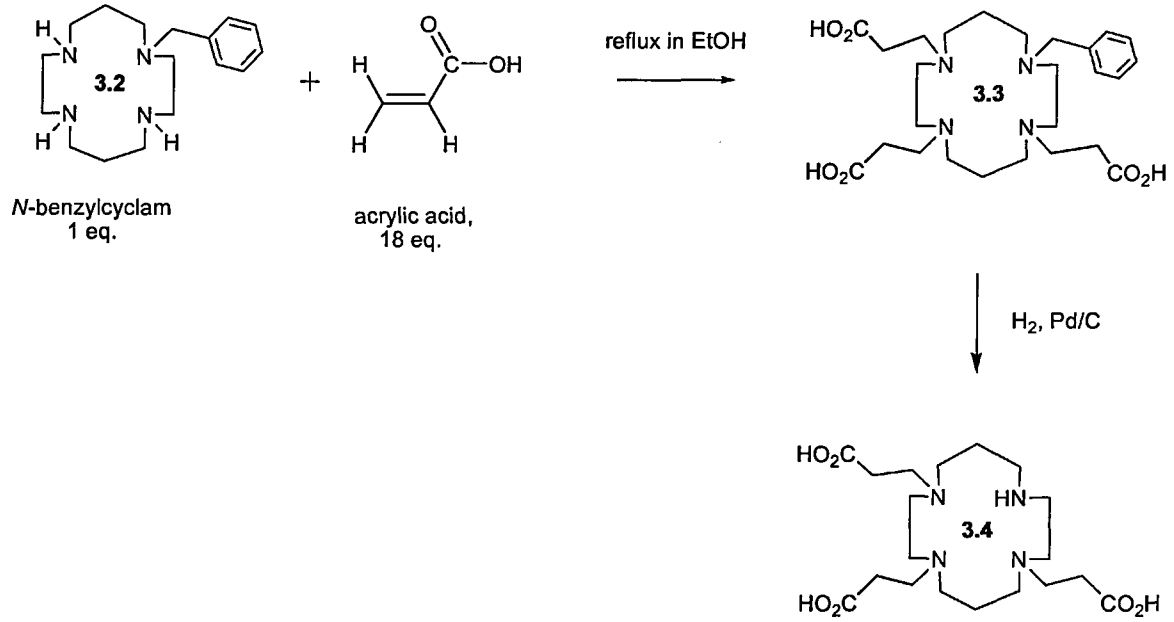

Scheme 3.3 Synthesis of the tri-substituted cyclam derivative (**3.4**) via the Michael addition of *N*-benzylcyclam to acrylic acid [118].

Fensterbank *et al.*[119] carried out the selective mono-functionalization of cyclam using a Michael addition (Scheme 3.4). By using one equivalent of a Michael acceptor in chloroform in the presence of one equivalent of *p*-toluene sulfonic acid (*p*-TSA), they obtained moderate to good yields of mono-alkylated cyclam (**3.5**). They attributed this selectivity to the protonation of the azamacrocycle that occurs in the presence of one equivalent of acid. Since two nitrogens on cyclen have very different pK_as from the other two, the addition of 1 eq. acid should leave one amine nucleophilic.

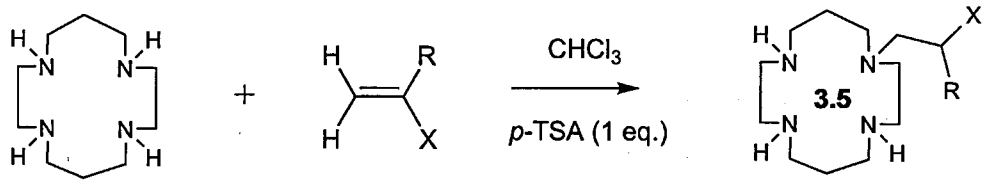

Scheme 3.4 Selective mono-*N*-alkylation of cyclam via Michael addition [119].

Wainwright prepared the tetra-substituted cyclam product (**3.6**) by reacting cyclam with an excess of acrylonitrile [120]. This reaction is an example of cyanoethylation which is often used to describe the conjugate addition of nucleophiles to acrylonitrile. Reduction of the terminal nitrile residues in **3.6** added functionality to **3.7** as these exocyclic amines could bind metal ions (Scheme 3.5).

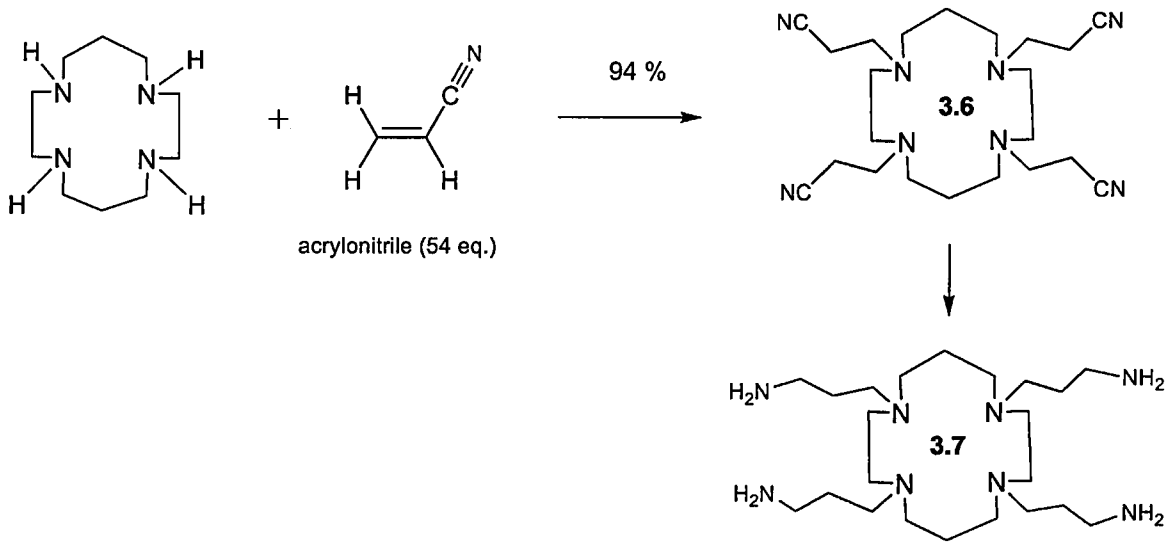

Scheme 3.5 Tetra-alkylation of cyclam via Michael addition [120].

3.4 Reaction of cyclen with acrylamide

In 1984, the Michael addition of cyclam to acrylamide to give the tetra-substituted product (**3.8**) was described by Freeman *et al.*[121]. For such a simple synthesis, a high yield of 92 % was reported (Scheme 3.6).

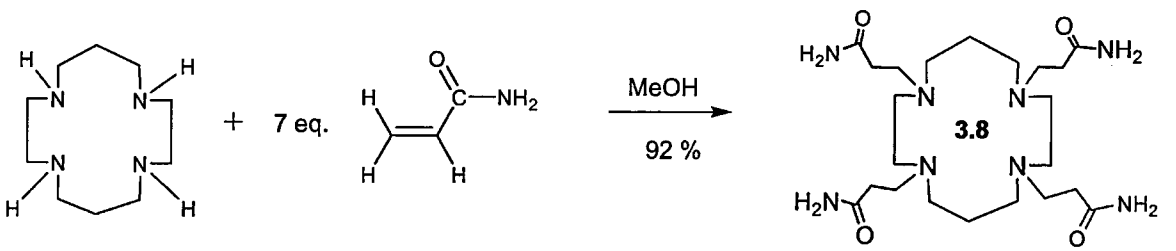

Scheme 3.6 Reaction of cyclam with acrylamide to give **3.8** [121].

To ascertain whether this facile, high-yielding, one-step reaction would work similarly for cyclen, the experiment was repeated here with cyclen being substituted for cyclam. Cyclen has two carbons less in its ring than cyclam. Apart from the fourth amine, both macrocycles have similar protonation constants (Table 3.1).

Table 3.1 Protonation constants for cyclen and cyclam [93].

Ligand	pK_a	pK_a	pK_a	pK_a
Cyclen	10.6	9.6	1.5	0.5
Cyclam	11.3	10.2	1.6	1.9

For the reaction, cyclen (1 eq.) was refluxed with acrylamide (7 eq.) in methanol for 24 hours (Scheme 3.7). After most of the solvent was removed, diethyl ether was added until a white solid formed. The resultant white solid was filtered, washed with ether and dried under vacuum. The mass spectrum of the product presented peaks at *m/z* 385.1 and 457.4 corresponding to the tri-amide (**3.9**) and the tetra-amide (**3.10**) species respectively. The peak corresponding to the tri-amide (**3.9**) was significantly higher than that of **3.10**. TLC analysis showed that the product consisted of two compounds with similar R_f values (R_f **3.9**, **3.10** = 0.57, 0.62 respectively). In addition, TLC showed that the product contained no acrylamide (R_f= 0.78). 0.2 % ninhydrin in ethanol, which stains cyclen ligands purple, was used as to detect spots.

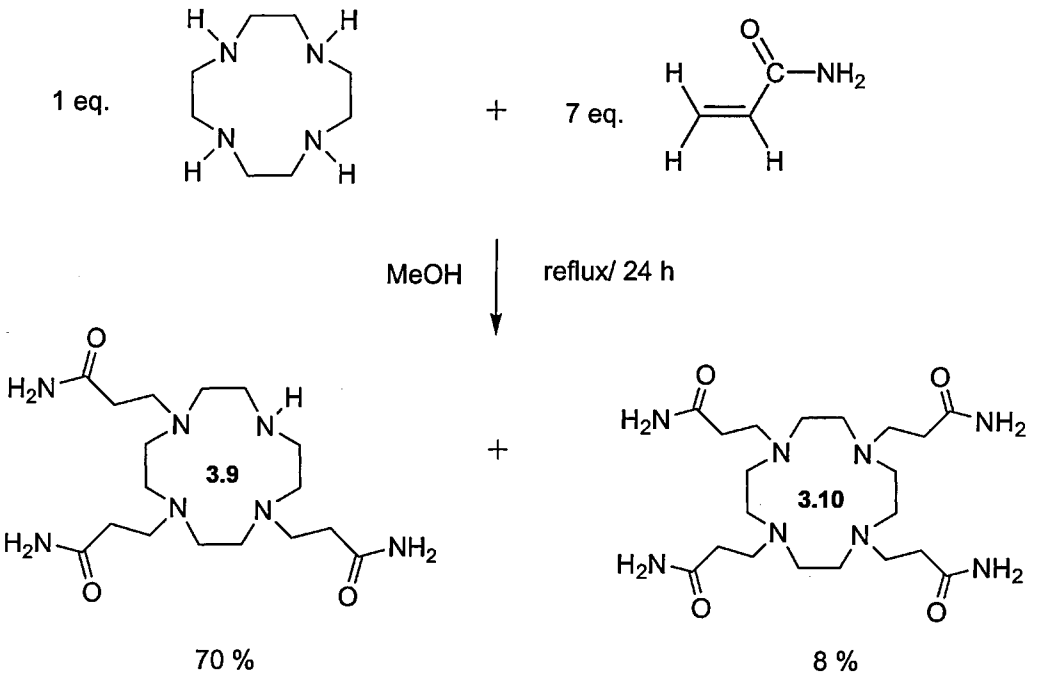

Scheme 3.7 Reaction of cyclen with acrylamide to give **3.9** and **3.10**.

Separation of **3.9** from **3.10** was achieved on a silica gel column using 5 % ethanol in dichloromethane as eluent. **3.9** was obtained as an hygroscopic, white solid (70 %) whereas **3.10** was obtained as a colourless, solid in a yield of 8 %. An X-ray crystallographic

analysis of **3.10** (1,4,7,10-tetrazacyclododecane-4,7,10-tetrapropanamide) is presented in the following section.

A high ratio of the triamide (**3.9**) to the tetramide (**3.10**) ligand was produced (approx. 8.75 :1, respectively) even though an excess of Michael acceptor was employed in the reaction. Since cyclen has two carbons less in its ring than cyclam, steric crowding close to the fourth nitrogen atom may be the key to this regioselectivity. An alternative explanation may be an intra-annular H-bond from the unalkylated nitrogen to the nitrogen on the opposite side of the ring. In partially-substituted cyclen derivatives, intra-annular hydrogen bonding has been observed by various groups [112, 122]. When Li and Wong [122] reacted cyclen (1 eq.) with triethylamine (10 eq.) and *tert*-butyl bromoacetate (3.5 eq.) in anhydrous chloroform, they obtained the tris *N*-alkylated product in a 77 % yield (Figure 3.1). Significantly, no tetra *N*-alkylated product was isolated. An intra-annular hydrogen bonding effect was invoked to explain this selective alkylation; a hydrogen bond from an unalkylated, protonated nitrogen to the nitrogen on the opposite side of the ring (N_1-H···N_3, 3.032 Å) was deemed to have caused the lone pairs on the remaining nitrogens to reorient towards the cavity. Consequently, these lone pairs would be unavailable for substitution reactions. Since the reaction was carried out in a non-polar, aprotic solvent, the authors argued that the hydrogen-bonded proton would be tightly held within the macrocycle even in the presence of base.

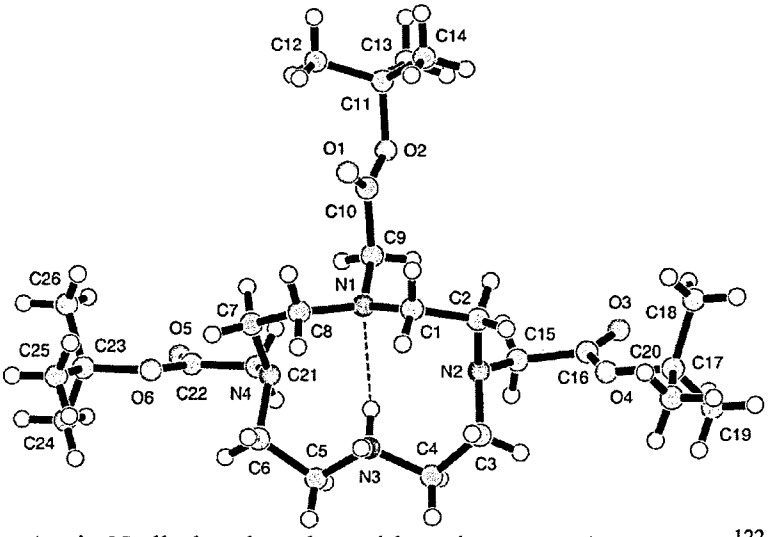

Figure 3.1 A tris *N*-alkylated cyclen with an intra-annular H-bond [122].

For **3.9**, the number and type of resonances in both the ^{13}C and ^{1}H NMR spectra indicated tri-*N* substitution of the cyclen ring. Individual carbon and proton resonances were assigned by data from a ^{1}H - ^{13}C COSY experiment and by comparison with the spectra of structurally-similar ligands [123]. The ^{13}C NMR spectrum of **3.9** in D_2O showed two signals at 178.6 ppm (C5) and 179.1 ppm (C6) for the amide carbonyls in an approximate ratio of 2:1 indicating that the ligand was tri-substituted (Figure 3.2).

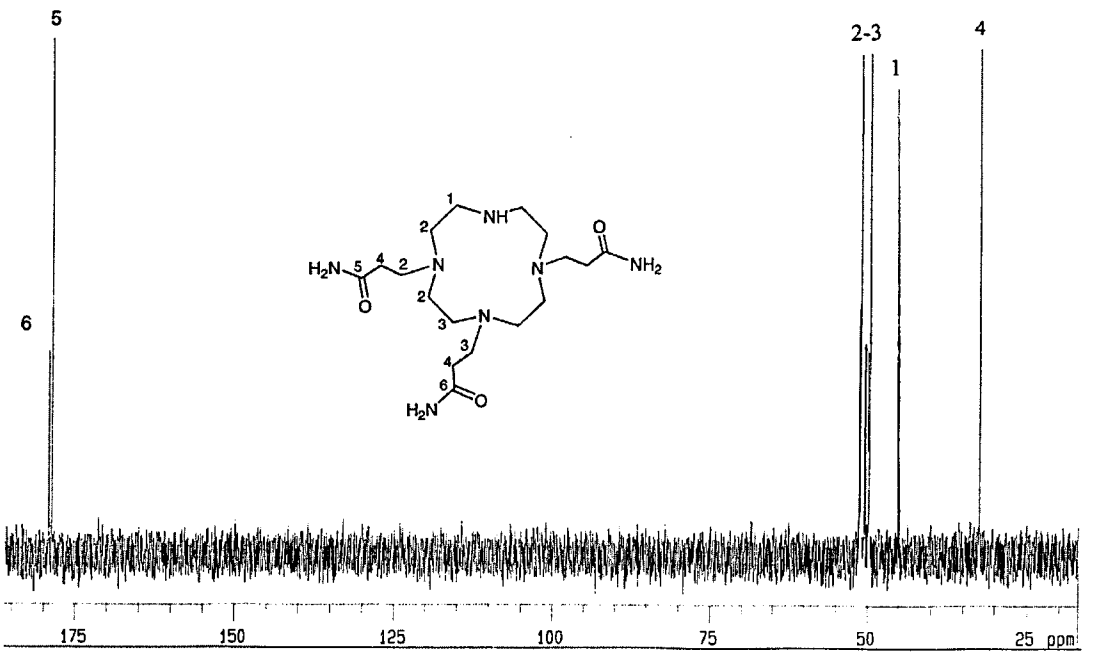

Figure 3.2 ^{13}C NMR spectrum of the ligand **3.9** (in D_2O, 300 MHz).

A possible mechanism for the Michael addition of cyclen to acrylamide is shown in Scheme 3.8. Addition of cyclen to acrylamide is followed by proton transfer either from cyclen (i.e. intramolecular) or from the solvent methanol (i.e. intermolecular). The use of a polar, protic solvent like methanol served to stabilise any charged intermediates and ensured any anionic intermediates were protonated rapidly. In the absence of acidic or basic catalysts, the high electrophile to nucleophile ratio (that is, 7 eq. acrylamide to 1 eq. cyclen, respectively) should have promoted addition [116].

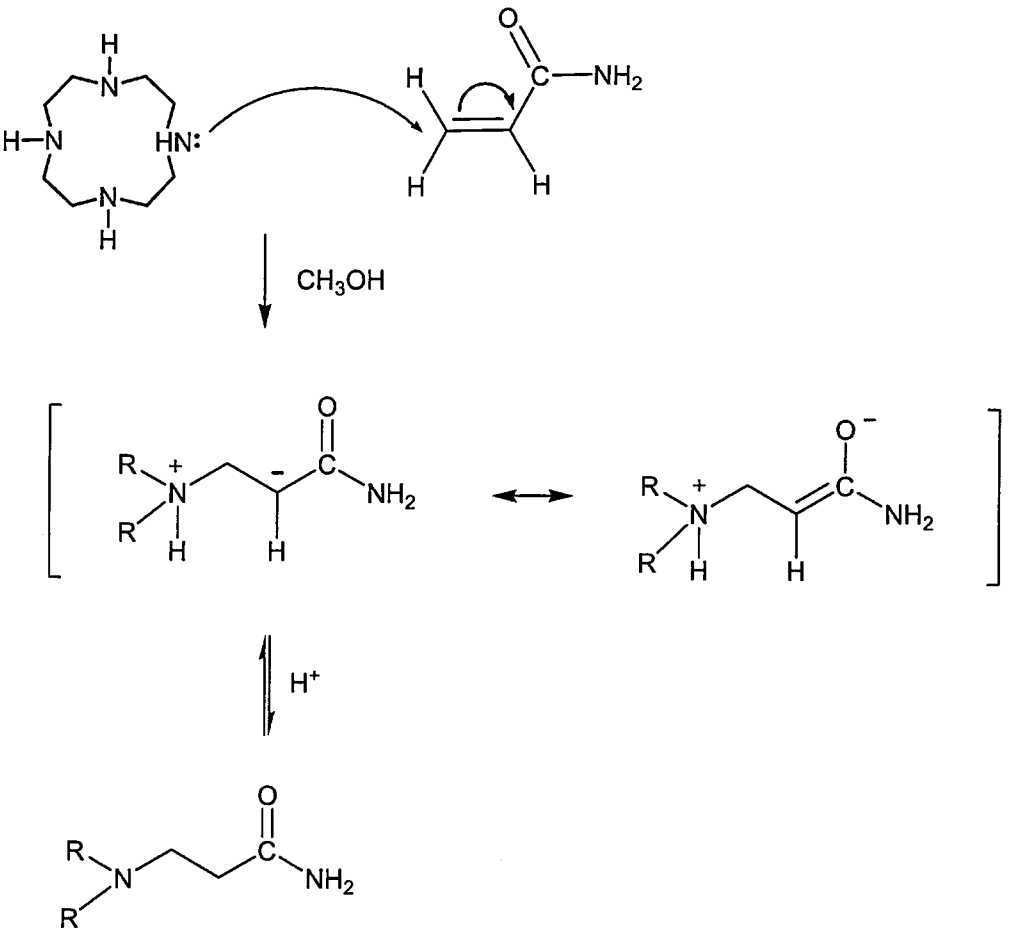

Scheme 3.8 A possible mechanism for the addition of cyclen to acrylamide.

A simple functional group interconversion was next employed to convert the pendant amide groups on **3.9** into carboxylic acid acid groups which are known to have stronger

coordinating ability with Gd^{3+}. Hydrolysis of the triamide (**3.9**) was accomplished by refluxing with 12 M HCl to give the triacid (**3.11**) in a 90 % yield (Scheme 3.9) [124].

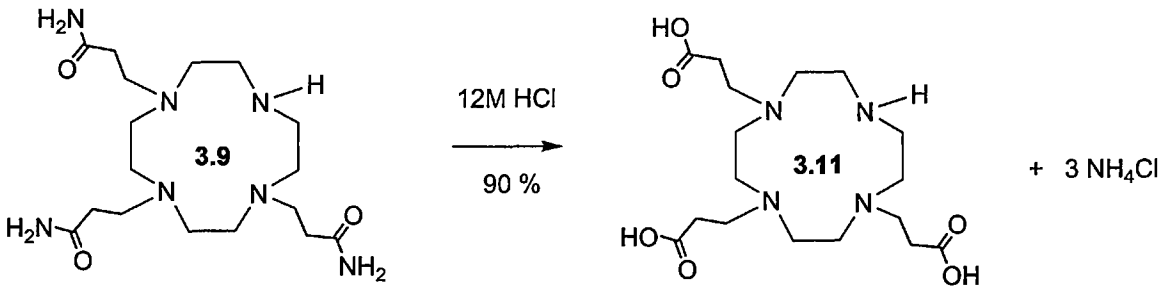

Scheme 3.9 Hydrolysis of **3.9** with 12 M aqueous HCl to give **3.11**.

The arms on both the triamide (**3.9**) and triacid (**3.11**) were found to be stable to the harsh hydrolytic conditions used to hydrolyse the amide bonds. A difference of approximately two mass units was observed between the starting material ($[M+H]^+$ = 387.0) and the product ($[M+H]^+$ = 388.9). Since ammonium chloride was also formed during this reaction, the product required purification. This was achieved by two recrystallizations from aqueous methanol.

3.9 and **3.11**, which have one more methylene group in their pendant arms, are analogues of the ligands **3.12** and **3.13** respectively (Figure 3.3). **3.12** is known as DO3AM [125] (1,4,7,10-tetrazacyclododecane-4,7,10-triacetamide) and **3.13** is known as DO3A (1,4,7,10-tetrazacyclododecane-4,7,10-triacetate). Indeed, the system of nomenclature used to name DO3AM and DO3A was employed here to name **3.9** and **3.11** as DO3PAM (1,4,7,10-tetrazacyclododecane-4,7,10-tripropanamide) and DO3P (1,4,7,10-tetrazacyclododecane-4,7,10-tripropanoate), respectively.

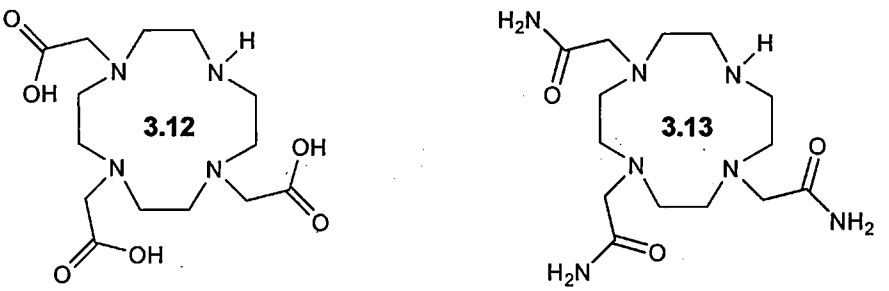

Figure 3.3 Structures of the ligands DO3AM (**3.12**) and DO3A (**3.13**).

3.4.1 X-ray crystallographic analysis of 1,4,7,10-tetrazacyclododecane-4,7,10-tetrapropanamide (**3.10**)

Colourless, amorphous crystals of **3.10** were grown by slow diffusion of acetone into a saturated, aqueous solution of the compound. Ortep plots showing an overhead and side view of **3.10** are given in Figure 3.4.

(a) Overhead view

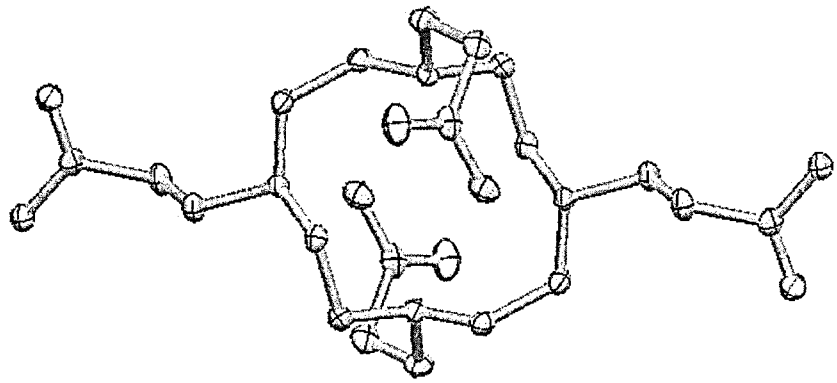

(b) Side view

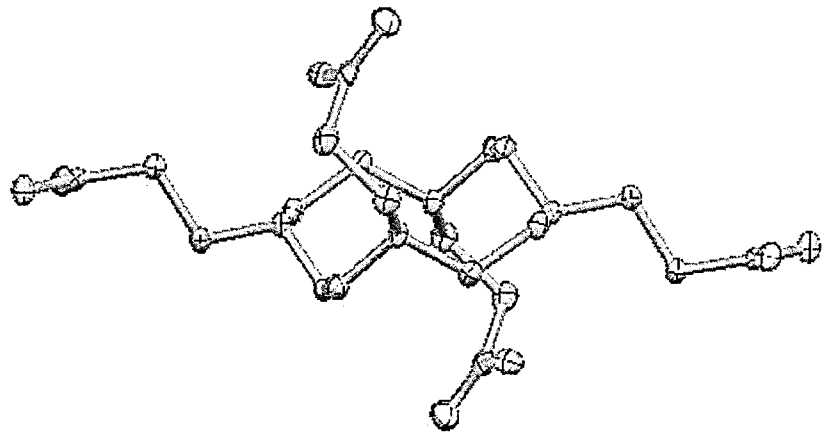

Figure 3.4 Ortep plots of **3.10**

Displacement ellipsoids are shown at a 50 % probability level. Hydrogens are omitted for clarity. See Appendix B for bond lengths and bond angles.

Examination of Figure 3.4 reveals that **3.10** possesses a twofold rotation symmetry, the axis of which passes through the centre of the 12-membered ring. Like other cyclen ligands, **3.10** has a [3333] square conformation with carbon atoms occupying corner positions [126]. The conformation, which is schematically shown in Figure 3.5, is considered important in the preorganisation of 1,4,7,10-tetrazacyclododecane and its derivatives prior to complexation to metal ions [93].

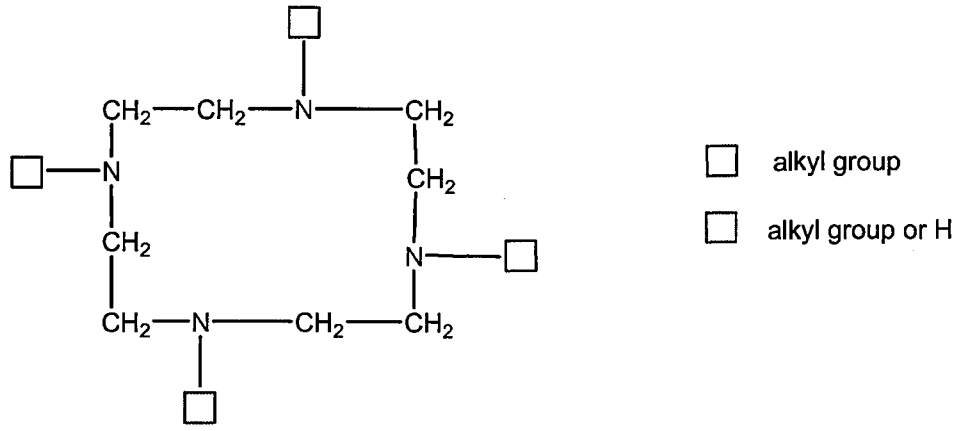

Figure 3.5 [3333] square conformation of 12-membered cyclen ring [122].

Visualisation of **3.10** from a side perspective (Figure 3.4b) reveals that the methylene groups of the cyclen ring have adopted a low-energy, staggered conformation. This conformation reduces non-bonded interactions, particularly those of C-H eclipsed bonds that would add to the torsional strain of the ring. Torsional strain in a molecule is caused by electron repulsion between eclipsed bonds [67]. Figure 3.4 also shows that two of the propanamide arms extend outside the macrocyclic ring, whereas the other two are folded above and below the cavity.

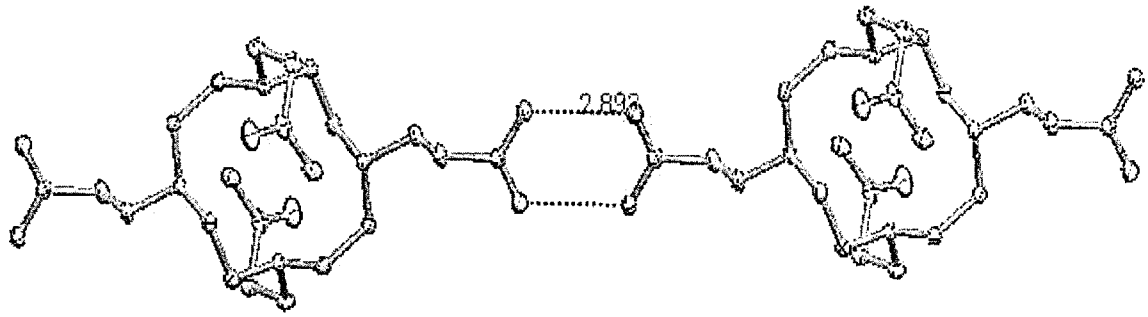

Figure 3.6 View of two molecules of **3.10**
(H-bonds are indicated by dashed lines)

In Figure 3.6, two molecules of **3.10** are shown. A short distance of 2.893 Ångstroms[j] between the amide oxygen of one **3.10** molecule and the amide nitrogen of the adjacent molecule indicates the presence of a hydrogen bond [127]. No intramolecular hydrogen-bonds were found between the tertiary amines of the cyclen ring in **3.10** as they are fully-substituted.

3.5 Reaction of cyclen with 1-cyanovinylacetate

The Michael addition reaction is ubiquitous in classical polymer chemistry, such as the anionic polymerization of alkyl methacrylates and cyanoacrylates [116]. Cyanoacrylates like ethyl-2-cyanoacrylate (**3.14**) are initiated with very poor nucleophiles, such as water, due to the electron poor alkene and strong resonance contributions of the adjacent cyano and ester groups (Figure 3.7).

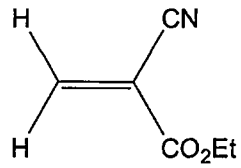

3.14

Figure 3.7 Ethyl-2-cyanoacrylate (**3.14**).

[j] A distance larger than 2.7 Å is considered a weak H-bond, 2.5 - 2.7 Å charcterizes a strong H-bond and < 2.5 Å (down to 2.39 Å at ambient conditions) defines a very strong H-bond [126].

Holton originally used **3.14** to construct quaternary carbon centres via the Michael reaction [128]. More recently, Klemarczyk studied the reactivity of ethyl-2-cyanoacrylate with various amines [129]. He found that polymerization was much slower with primary and secondary amines than with tertiary amines due to proton transfer after the first addition of monomer (Scheme 3.10). In fact, he discovered that polymerisation was not inevitable and intramolecular proton transfer could be the preferred reaction to form the neutral, less reactive aminocyanopropionate ester (**3.15**).

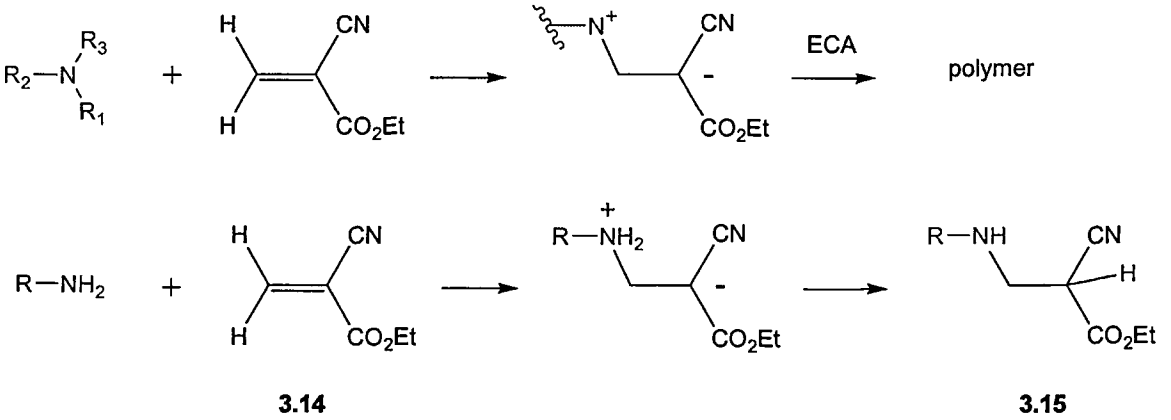

3.14 **3.15**

Scheme 3.10 Reaction of ethyl-2-cyanoacrylate with secondary and tertiary amines [129].

To establish if an analogous reaction would work with cyclen, 1-cyanovinylacetate (**3.16**) which has a similar reactivity to ethyl-2-cyanoacrylate, was added to cyclen in dry acetonitrile (Scheme 3.11). After the addition, an off-white solid began to precipitate out of solution within minutes. This precipitate was formed irrespective of whether three or five equivalents of 1-cyanovinylacetate was used in the reaction. The analytical data obtained for this solid suggests **3.21** as a possible structure which can tautomerize to **3.17** in D_2O (Scheme 3.11).

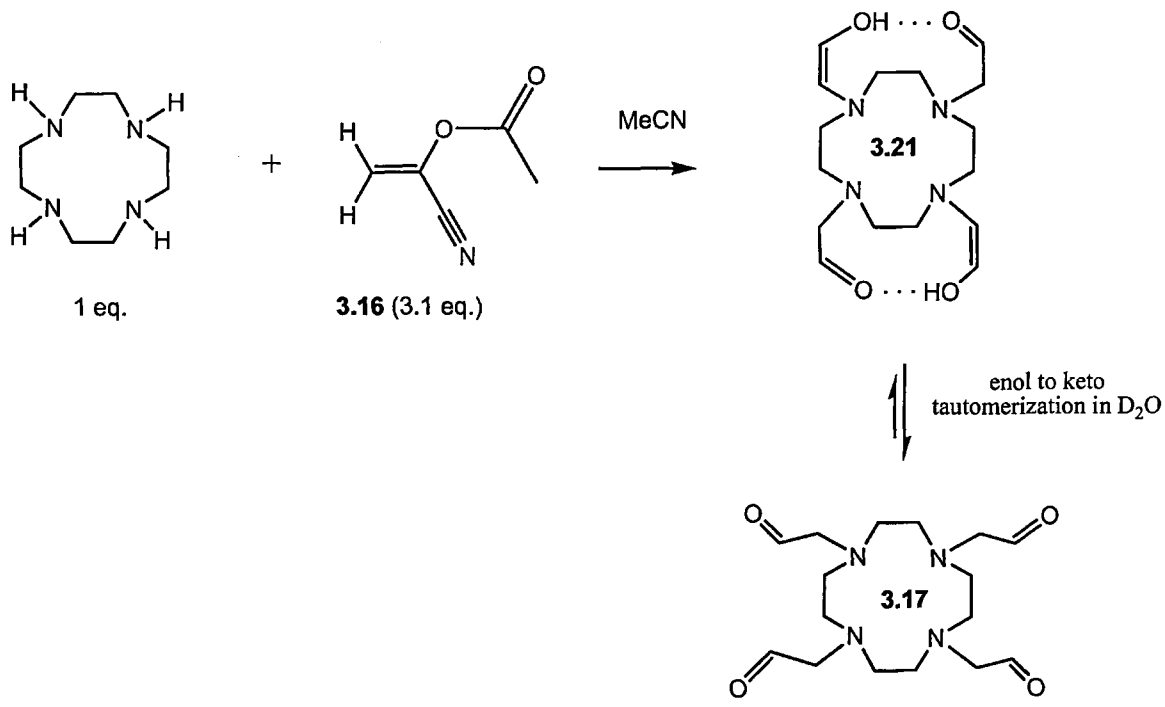

Scheme 3.11 Reaction of cyclen with 1-cyanovinylacetate to give **3.17**.

High resolution mass spectrometry (*m/z* = 340.2104) and combustion analysis for **3.17** showed the molecular formula to be $C_{16}H_{28}N_4O_4$ which is consistent with the two isomeric compounds **3.21** and **3.17**. Analysis by FT-IR indicates **3.21** exists primarily as an enol in the solid state as there is a strong enol (C=C-OH) absorption at 1635 cm^{-1} (Figure 3.8). The C=O absorption at 1779 cm^{-1} of the unchelated ester starting material has dissappeared. Moreover, an OH band at 3400 cm^{-1} (and possibly one at 2982 cm^{-1}) also suggest the presence of an enol. Enolization of **3.17** may be stabilised by intra-molecular H-bonding between the C=O groups on the pendant arms. This serves to reduce dipole-dipole repulsion between carbonyl groups which can be quite strong in cyclic compounds because of their fixed geometry [130]. When an ^1H NMR of **3.17** was run in D_2O, no evidence of an enol was observed. Instead, a resonance at 9.7 ppm indicative of an aldehyde group was visible. This suggests that the more polar D_2O solvent favours the keto tautomer by disrupting the H-bonding of the enol.

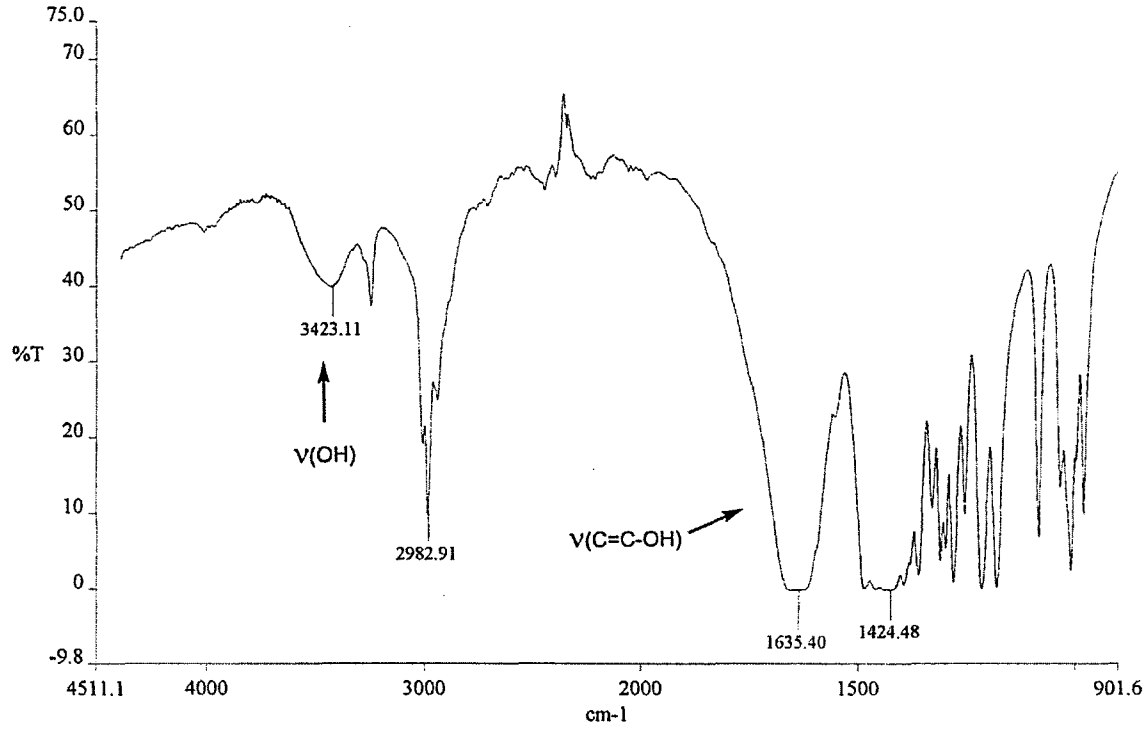

Figure 3.8 FT-IR of **3.21** (KBr disc).

A possible mechanism for the formation of **3.17** is outlined in Scheme 3.12. Addition of cyclen to 1-cyanovinylacetate is followed by intramolecular proton transfer. Abstraction of the proton on C1 of the pendant arm by another molecule of cyclen results in elimination of cyanide to form the ester intermediate (**3.20**). This ester intermediate spontaneously hydrolyses to the enol (**3.21**). Attack of the C=O group of **3.20** by the eliminated cyanide anion may have been the trigger for this cleavage. The resultant enol (**3.21**) may then rearrange to the keto tautomer (**3.17**) in D_2O.

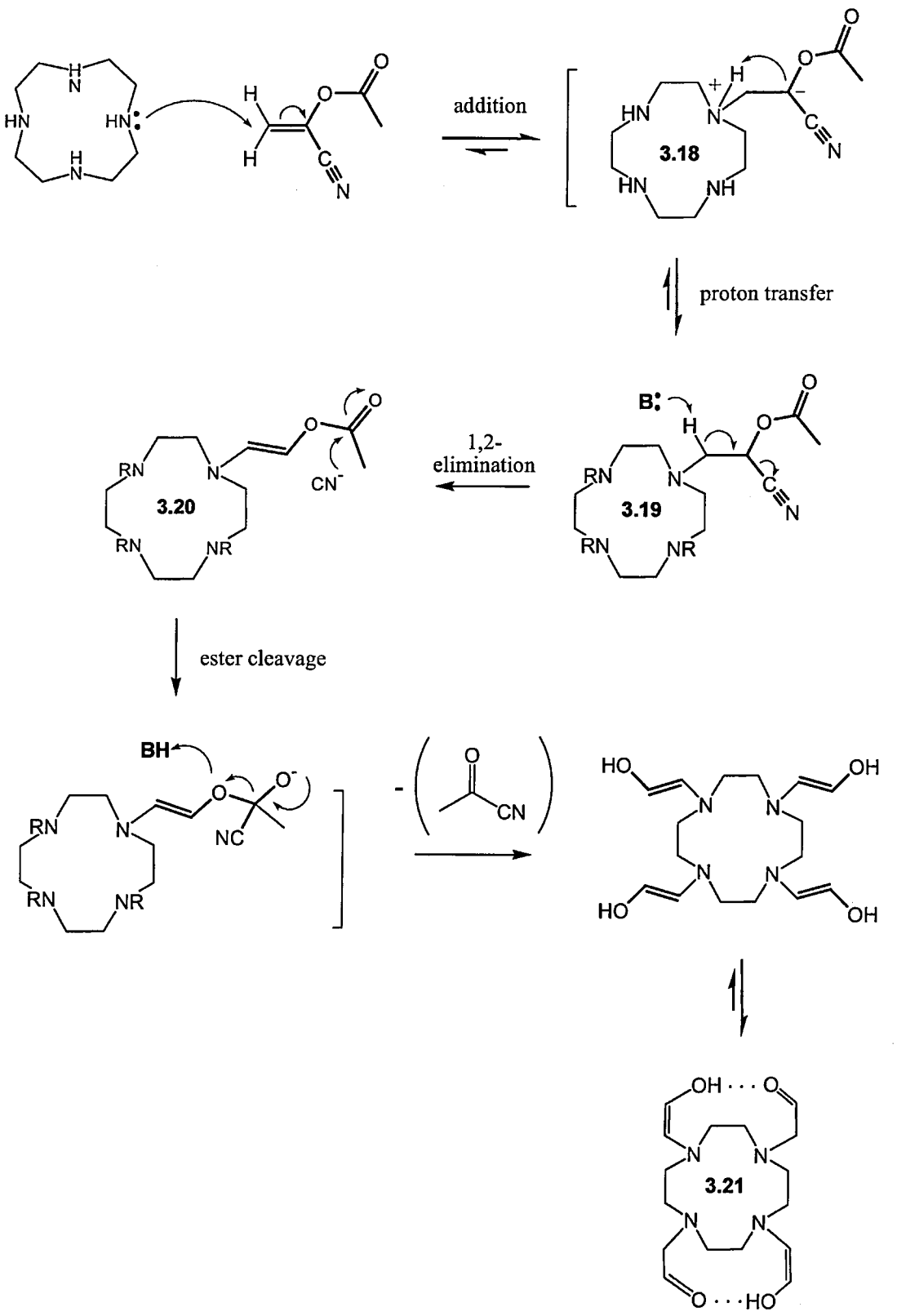

Scheme 3.12 A possible mechanism to explain the formation of **3.21**.

3.6 Reaction of cyclen with ethyl 3-hydroxy-2-nitropropanoate

Like ethyl-2-cyanoacrylate (**3.14**) in the preceeding section, ethyl 2-nitroacrylate (**3.22**) offers a route to the bifunctional ligand, **3.23** (Scheme 3.13).

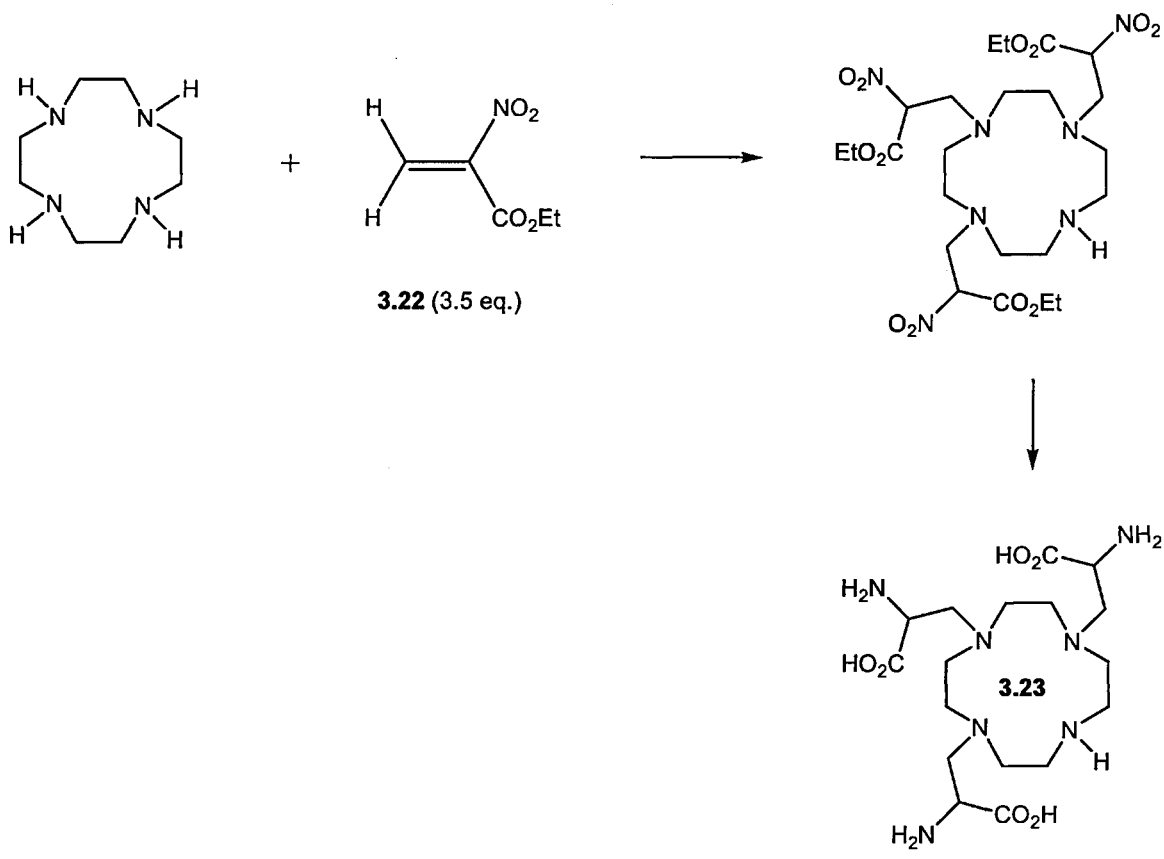

Scheme 3.13 A possible route to the bifunctional ligand (**3.23**).

However, **3.22** is not commercially-available. Babievskii *et al.* [131] showed that **3.22** could be formed *in situ* from ethyl 3-hydroxy-2-nitropropanoate (**3.24**). **3.24** was found to dehydrate at high temperatures to form **3.22** which then reacted with cyclopentadiene in a Diels-Alder cycloaddition reaction (Scheme 3.14).

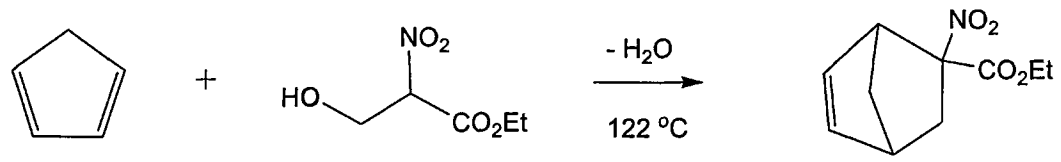

cyclopentadiene **3.24** **3.25**

Scheme 3.14 Reaction of cyclopentadiene with **3.24** at high temperature [131].

Ethyl 3-hydroxy-2-nitropropanoate (**3.24**) was synthesised by condensing formaldehyde with ethyl 2-nitroacetate according to the method described by Babievskii *et al.*[131] (Scheme 3.15).

Ethyl 2-nitroacetate (1 eq.) 33 % aq. formaldehyde (1.8 eq.) **3.24**

Scheme 3.15 Synthesis of ethyl 3-hydroxy-2-nitropropanoate (**3.24**) [131].

The reaction was performed by stirring ethyl 2-nitroacetate (1 eq.) and sodium acetate (1 eq.) in 33 % aqueous formaldehyde (1.8 eq.) at -15 °C for 3 hours. Addition of HCl to the reaction mixture caused an oil to separate which was extracted with ether. After evaporation of the ether, the oil was distilled in a short-path distillation apparatus at 0.3 mm Hg. TLC analysis of the fraction which distilled between 80-105 °C revealed it contained unreacted ethyl 2-nitroacetate, the title compound **3.24** and one other unknown. These compounds were successfully separated on a silica gel column using 10 % ethyl acetate in DCM as eluent. In contrast, the original method used only distillation to purify **3.24**. The reaction mechanism is given in Scheme 3.16.

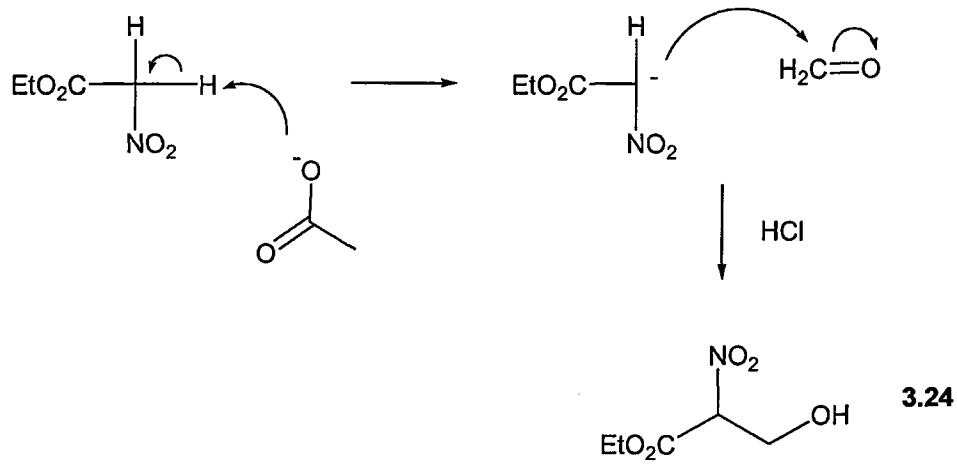

Scheme 3.16 Reaction mechanism for the synthesis of **3.24**.

The reaction between 3-hydroxy-2-nitropropanoate (**3.24**) and cyclen was unsuccessful with only a polymeric material being produced (Scheme 3.17).

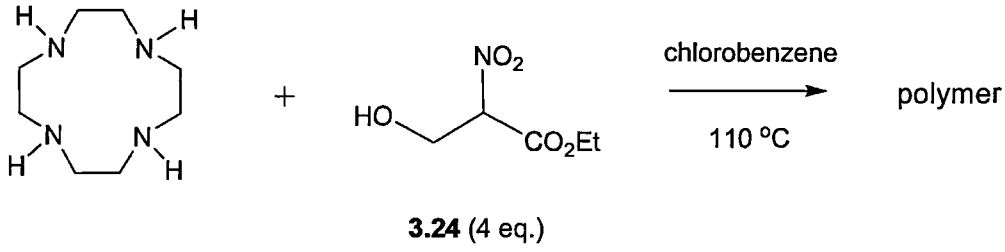

3.24 (4 eq.)

Scheme 3.17 Reaction of cyclen with ethyl 3-hydroxy-2-nitropropanoate (**3.24**).

For the reaction, 4 eq. **3.24** and 1 eq. cyclen were heated in dry chlorobenzene (b.p. 131 °C) at 110 °C. Within minutes, the reaction developed a deep red colour and a precipitate formed. After 1 hour, the reaction was stopped and the precipitate which had formed was filtered off. All attempts to dissolve the precipitate in a variety of solvents were unsuccessful indicating a polymer had been formed. The alkene which is formed during the reaction, ethyl 2-nitroacrylate (**3.22**), is likely to be highly reactive as it has both an ester and a nitro electron-withdrawing group. At the high temperatures required to dehydrate **3.24**, polymerisation instead of addition was likely to occur.

3.7 Reaction of cyclen with methyl 2-acetamidoacrylate

In Scheme 3.18, a simple retrosynthetic analysis of the target molecule (**3.23**) identifies methyl-2-acetamidoacrylate (**3.25**) as the electrophilic reagent. Therefore, reaction of cyclen with the commercially-available alkene, methyl-2-acetamidoacrylate (**3.25**) should theoretically furnish the bifunctional ligand (**3.23**).

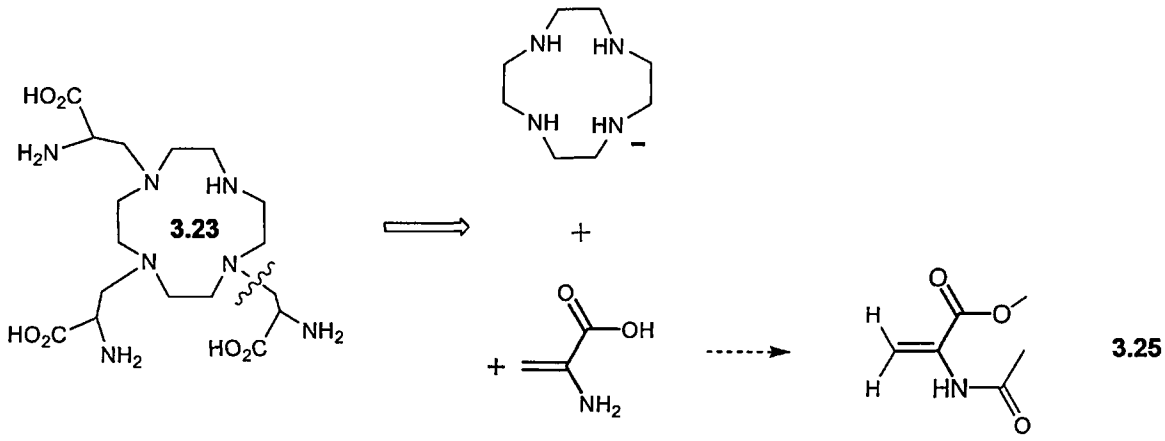

Scheme 3.18 Retrosynthetic analysis of the bifunctional ligand (**3.23**).

The reaction was performed by stirring 3.5 eq. methyl-2-acetamidoacrylate (**3.25**) with cyclen (1 eq.) in dry acetonitrile under argon overnight. Analysis by LC-MS indicated that only di-substitution ($M+H^+$ = 459) was occuring so an extra 1.5 eq. methyl-2-acetamidoacrylate was added to the reaction which was then heated to reflux for a further 12 hours (Scheme 3.19).

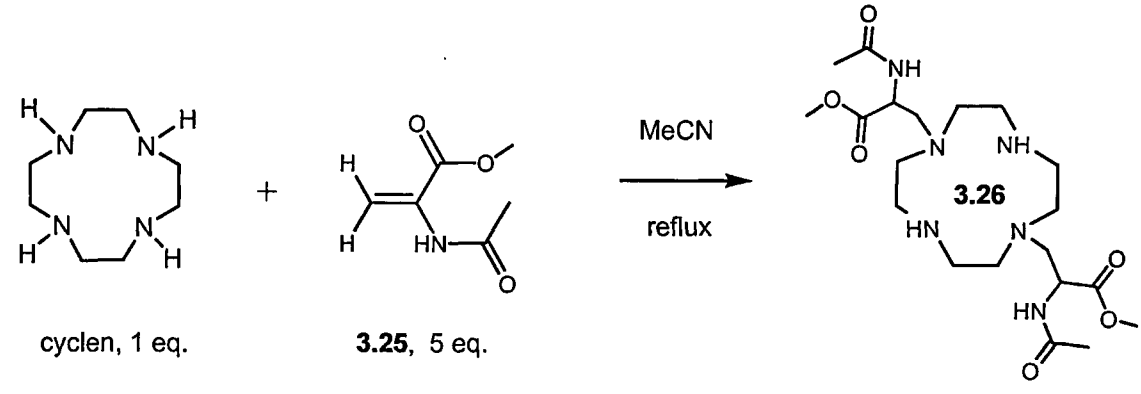

cyclen, 1 eq. **3.25**, 5 eq.

Scheme 3.19 Reaction of cyclen with **3.25** under forcing conditions.

Despite these forcing conditions, only di-substituted cyclen (**3.26**) was formed. A more sterically-hindered substrate with less electron-deficient withdrawing groups attached to the double bond may explain this lack of reactivity.

Over recent years, catalysts such as iron(III) chloride [132], bismuth nitrate [133] and sodium dodecyl sulfate (SDS) [134] have been employed to catalyse the addition of amines to Michael acceptors. More recently, Wabnitz and Spencer [135] found that strong Brønsted acids like trifluoromethanesulfonic acid could catalyse the hetero-Michael addition of weakly basic nucleophiles like carbamates (NHCOOR) to α,β-unsaturated carbonyl compounds (Scheme 3.20).

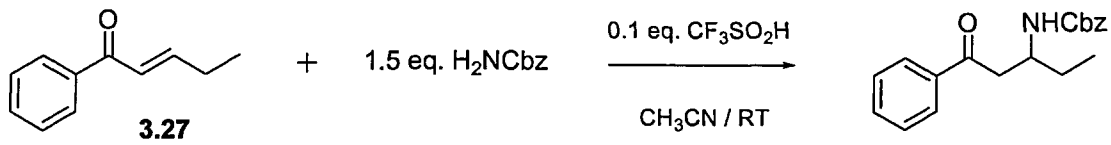

Scheme 3.20 Acid-catalysed addition of benzyl carbamate to **3.27** [135].

The authors reasoned that activation of Michael acceptors by protonation of the carbonyl group (pK_a -5 for α, β-unsaturated ketones) was possible with strong acids. One of the acids they used to catalyse this reaction was trifluoromethanesulfonic acid. Trifluoromethanesulfonic acid (CF_3SO_3H), which is also known as triflic acid, is one of the strongest Brønsted acids, with a pK_a of -13.6. It is one of a small group of acids commonly known as 'super acids', being stronger than 100 % sulfuric acid. Amongst the super acids, triflic acid has several important advantages. It is non-oxidizing, has a high thermal stability, is resistant to both oxidation and reduction, and does not yield fluoride ions, even in the presence of strong nucleophiles.

In a test reaction, 0.7 eq. triflic acid was carefully added to a solution of cyclen and methyl-2-acetamidoacrylate (**3.25**) in acetonitrile. The reaction was allowed to stir at room temperature under argon. LC-MS monitoring of the reaction after 12 hours indicated both tri- and tetra-substitution of the cyclen ring had occurred. Since the tri-*N*-substituted product was our desired target, mono-*N*-protection of the cyclen ring was required.

3.7.1 Mono-*N*-protection of cyclen with a benzyloxycarbonyl (Z) group

The cyclen macrocycle was mono-*N*-protected with the aromatic benzyloxycarbonyl (Z) group as it was considered the hydrophobic character of this group would ease purification. Furthermore, compounds containing the Z moiety have another advantage in that they tend to crystallize readily [136]. Mono-Z-cyclen (**3.28**) was synthesised using a procedure similar to the one that was used to prepare mono-*N*-acetyl cyclen (see Section 2.3, Chapter 2). The synthesis consisted of the dropwise addition of benzylchloroformate in chloroform to a solution of cyclen in chloroform (Scheme 3.21).

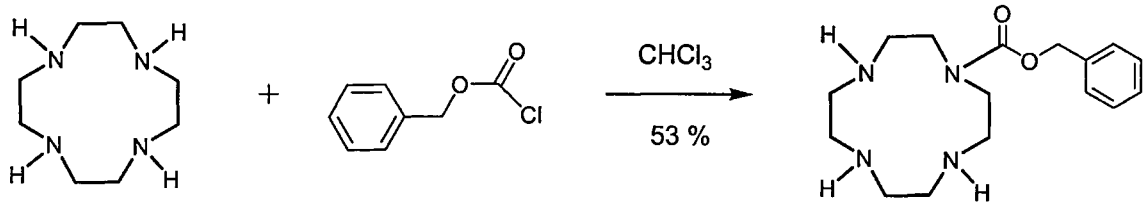

Scheme 3.21 Synthesis of mono-Z-protected cyclen (**3.28**)

After the reaction was stirred overnight, it was washed with dilute sodium hydroxide to convert the products into free bases. The organic solvent was then separated and evaporated to give an oil. This oil was purified by silica gel column chromatography using 5 % methanol in chloroform containing 0.1 % iPrNH$_2$. A small amount of di-Z-cyclen

eluted from the column first. Mono-Z-cyclen (**3.28**), which eluted from the column as an oil, was crystallized by the addition of acetonitrile. The yield of **3.28** was 53 %. Although Woods *et al.* [61] prepared the hydrochloride form of **3.28** in an overall yield of 82 %, their synthesis involved three separate steps (Scheme 3.22).

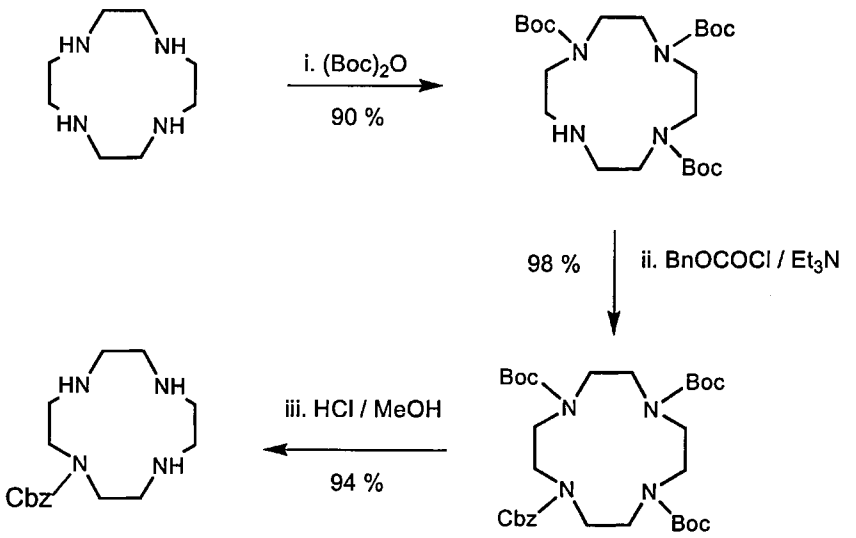

Scheme 3.22 Synthesis of mono-Z-protected cyclen by an indirect method [61].

3.7.2 Triflic acid-catalysed addition of mono-Z-cyclen to methyl-2-acetamidoacrylate

Scheme 3.23 outlines the triflic acid-catalysed addition of mono-Z-cyclen (**3.28**) to methyl-2-acetamidoacrylate (**3.25**).

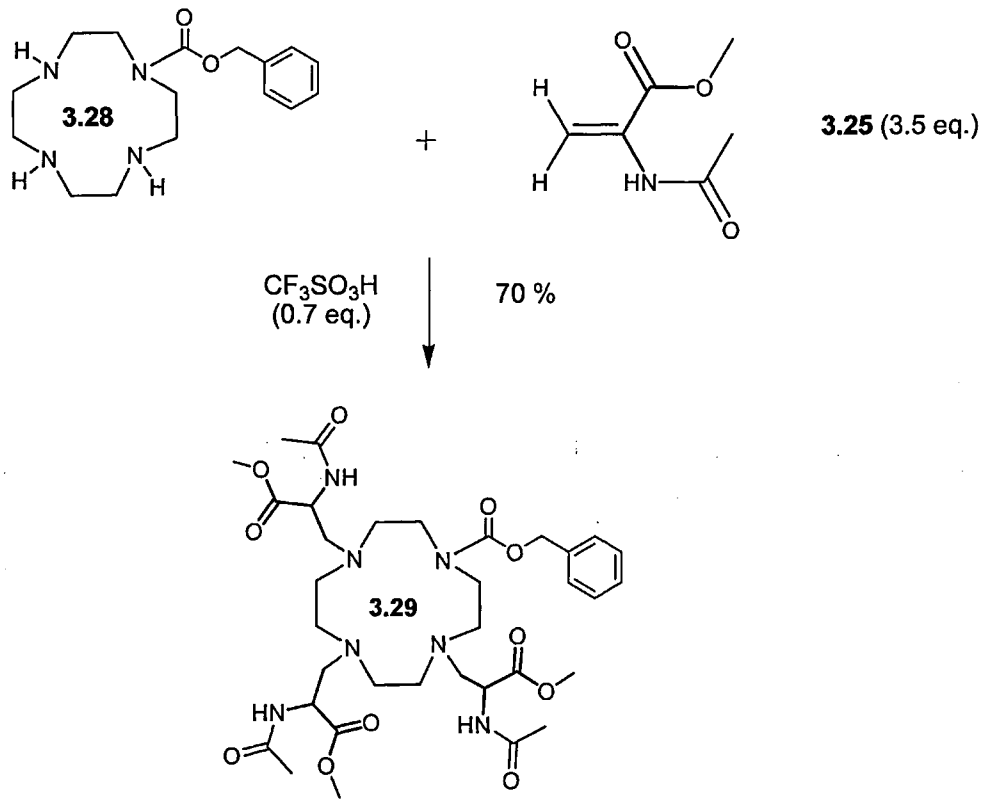

Scheme 3.23 Addition of mono-Z-cyclen to **3.25** catalysed by triflic acid.

Mono-*N*-Z-cyclen and methyl-2-acetamidoacrylate were suspended in dry acetonitrile. Quick but careful addition of the strong acid, triflic acid, caused the suspended reactants to become soluble. Triflic acid was added with an automatic pipette to ensure the correct amount was added. The reaction was allowed to stir at room temperature under argon overnight. After the solvent was removed *in vacuo*, the residue was partitioned between 1M ammonia (10 ml) and chloroform (20 ml). The aqueous layer was washed with another 10 ml chloroform and the pooled organic extracts were evaporated to give a pale yellow,

viscous oil. The resulting oil was dissolved in a small amount of $CHCl_3$ and Et_2O was added to induce crystallisation. The yield of the fully-substituted Michael adduct (**3.29**) was 70 %.

To avoid complete protonation of the amines and the nitrogens of cyclen becoming non-nucleophilic, the concentration of acid in the reaction was kept below the concentration of cyclen (i.e. 0.7 eq. acid to 1 eq. cyclen). Despite the use of a strong acid, no evidence of ester or amide hydrolysis was observed, presumably because of the non-aqueous conditions used. Michael additions often result in poor yields when the acceptor is a di-substituted *trans* alkene, presumably because of steric hindrance to the attacking nucleophile [137]. The protonation of methyl-2-acetamidoacrylate by triflic acid most likely enhances its activity as a Michael acceptor (Figure 3.9).

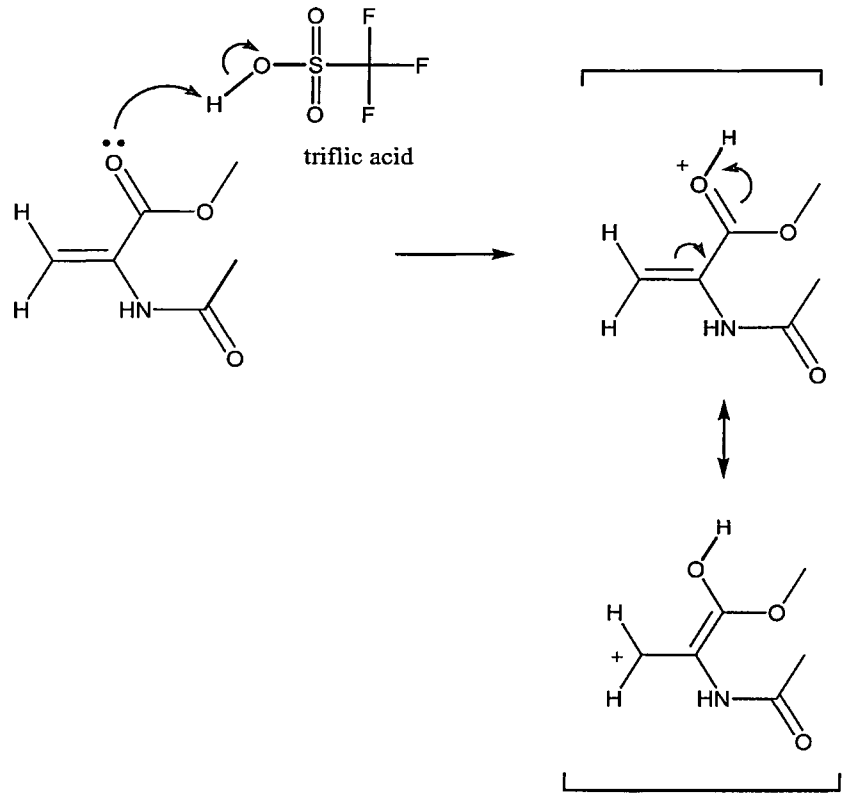

Figure 3.9 Protonation of methyl-2-acetamidoacrylate by CF_3SO_3H.

The synthesis of **3.29** demonstates that strong acids can activate poor acceptors to such an extent that steric effects are overcome and all four amines of the cyclen ring can react. It is possible that triflic acid is having a dual catalytic effect on the reaction. Once the carbonyl group of the acceptor alkene is protonated, the triflate anion could engage in hydrogen-bonding to the N-H of cyclen and effect a conformational change in its structure (Figure 3.10). This conformational change may cause the nitrogen lone pair to point away from the centre of the ring and become nucleophilic. This switch from an *endo* to an *exo* conformation would enable cyclen to attack the electron-deficient alkene acceptor.

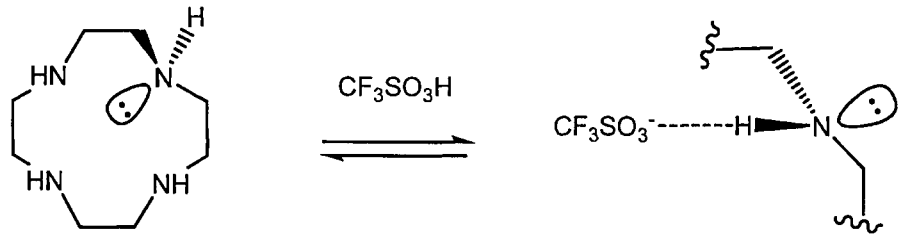

Figure 3.10 An acid-catalysed conformational change in cyclen.

Some clues to the effect acid has on the conformation of cyclen in solution can be obtained from crystallographic data [138]. In its hydrochloride salt form, cyclen adopts a square conformation in which its nitrogen atoms and lone pairs point outwards in an exocyclic mode. In contrast, the free base form of cyclen has two exocyclic and two endocyclic amines. In this conformation, the two endocyclic amines are less available for nucleophilic attack as their lone pairs are oriented into the cavity of the macrocycle.

3.7.3 Deprotection of 1-Benzyloxycarbonyl-4,7,10-tris-(methyl-2-acetamidopropanoate)-1,4,7,10-tetraazacyclododecane (**3.29**)

Cleavage of the benzylic nitrogen bond in **3.29** was accomplished by hydrogenation over 10 % palladium on charcoal to give **3.30** (Scheme 3.24) [139]. The reaction was performed by bubbling a slow stream of H_2 through an ethanolic suspension of Pd/C and **3.29** in a fume cupboard overnight. After the catalyst was precipitated by centrifugation, the supernatant was decolorised with activated charcoal. After filtration through celite and evapoartion under reduced presure, the resultant residue was dried under high vacuum to remove traces of toluene which is a by-product of the reaction. **3.30** was obtained in a yield of 90 % as a viscous, yellow oil. ^{1}H NMR of the product confirmed that the benzyloxycarbonyl group had been removed. Furthermore, LC-MS showed that the compound had the expected $[M+H]^+$ of 603.

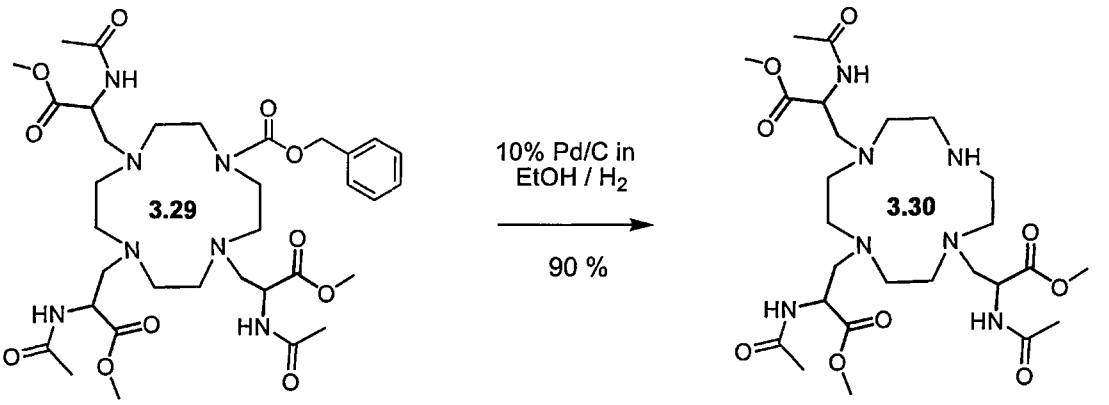

Scheme 3.24 Deprotection of **3.29** to give **3.30**

The second deprotection step involved the hydrolysis of the methyl esters and *N*-acetyl amides in **3.30**. Simultaneous deprotection of both protecting groups was achieved by heating **3.30** in 12M aqueous HCl at 60 °C for 6 hours. The product (**3.31**) was a hygroscopic, white solid and essentially consists of cyclen with three pendant amino acid arms. However, analysis of the product by LC-MS indicated cyclen with two amino acid

arms (**3.32**) was also present (Scheme 3.25). The peak ratio of **3.32** to **3.31** was found to increase in solution after 24 hours.

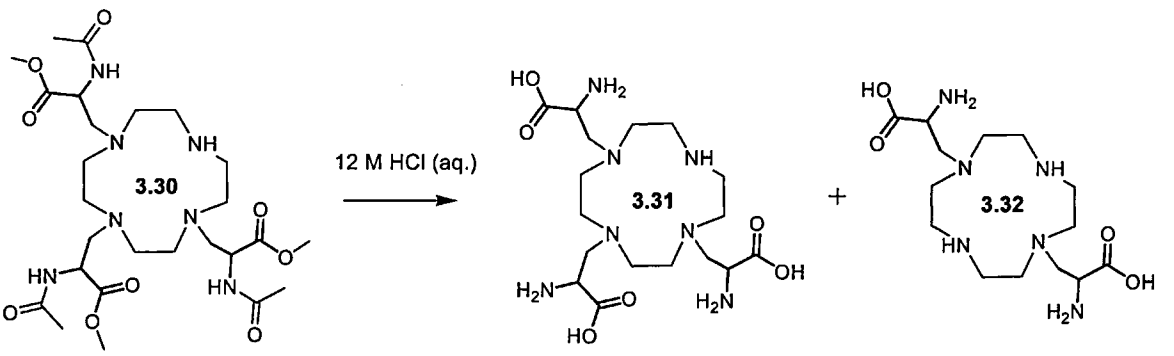

Scheme 3.25 Hydrolysis of **3.30** with 12M HCl (aq.).

Since hydrolysis using aqueous HCl has previously been used to cleave *N*-acetyl amides and methyl esters without problems [140], it seems the loss of an arm from N-10 is cyclen-related. An acid-catalysed decarboxylation as outlined in Scheme 3.26 is one possibility.

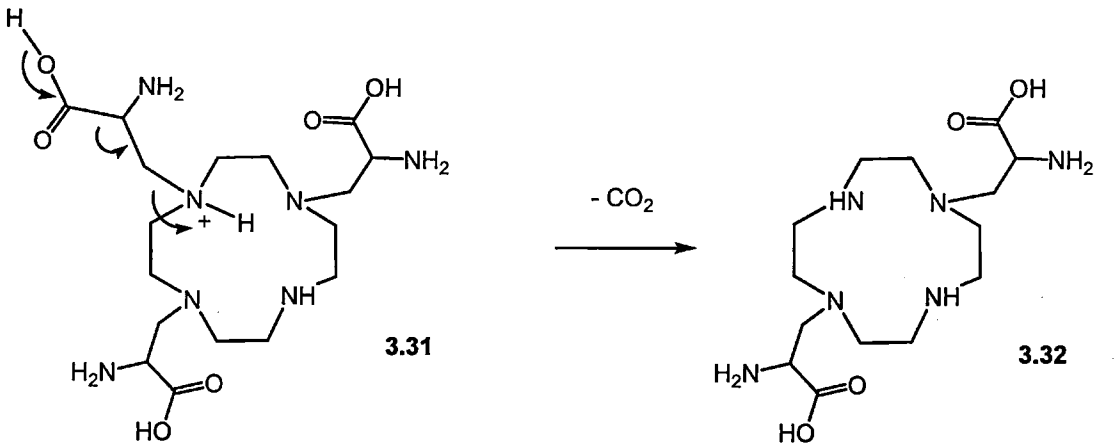

Scheme 3.26 Acid-catalysed decomposition of **3.31**.

3.8 Reaction of cyclen with ethyl-cis-β-cyanoacrylate

The final Michael acceptor investigated was the di-substituted, *cis* alkene, ethyl-*cis*-β-cyanoacrylate (**3.33**) which is commercially-available. The reaction was carried out by stirring cyclen with ethyl-*cis*-β-cyanoacrylate (3.1 eq.) in acetonitrile at room temperature (Scheme 3.27). LC-MS monitoring of the reaction mixture after 24 hours indicated that the tri-substituted product (**3.34**) was formed ($[M+Na]^+$ = 569.2). Tetra-substituted product was also detected ($[M+Na]^+$ = 692.9) but **3.34** was the dominant species. Once the solvent was evaporated, the resulting residue was purified on a silica gel column to afford the tri-substituted product (**3.34**) as a viscous, yellow oil. A low yield of product (i.e. 20 %) suggests that some decomposition of **3.34** may have occurred on the silica gel during column chromatography.

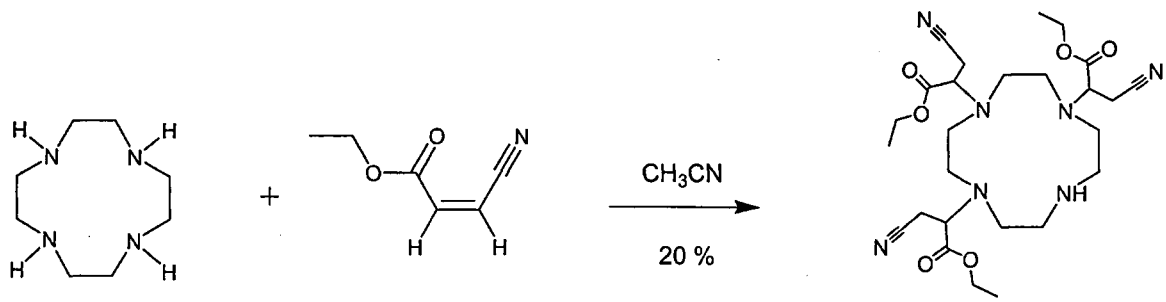

Scheme 3.27 Reaction of cyclen with ethyl-*cis*-β-cyanoacrylate.

Analysis of **3.34** by ^{13}C NMR revealed that the methine carbon in the pendant arm resonated at δ 49.41. This indicates that addition of cyclen took place at the carbon opposite the nitrile group. Addition opposite the ester group is predicted to give rise to a signal with a more upfield chemical shift because of deshielding by the neighbouring nitrile group. This regioselectivity was expected as the nitrile moiety has stronger electron-withdrawing ability than the ester group. Therfore, the use of two different electron-

withdrawing groups on the alkene acceptor provides a subtle means of introducing regioselectivity into the reaction.

Unlike the previous additions with acrylamide and methyl-2-acetamidoacrylate, addition of cyclen to the double bond of **3.33** took place without heating or the use of an acid catalyst. Also, the nitrile group offers synthetic versatility as it can potentially be reduced to an amine or hydrolysed to a carboxylic acid. For example, reduction of the nitrile groups in **3.34** followed by hydrolysis of the ethyl esters offers a route to the bifunctional ligand, **3.35** (Scheme 3.28).

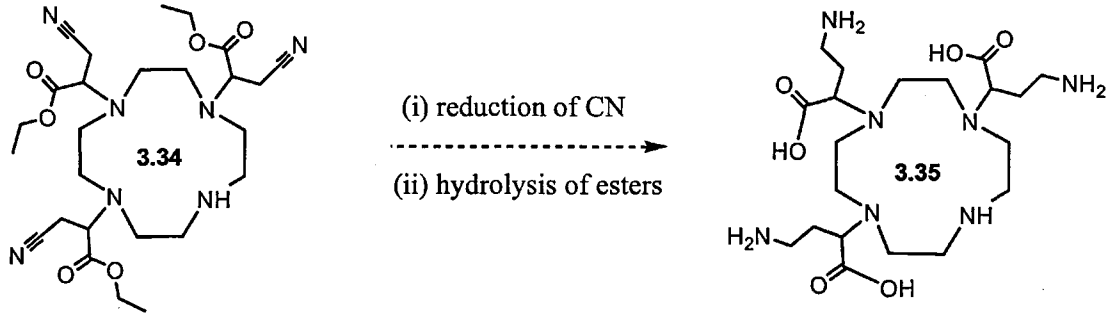

Scheme 3.28 A possible transformation of **3.34** into the ligand **3.35**.

3.35 has pendant arms which are substituted at C1 with COOH groups (for coordination to Gd^{3+}) and substituted at C-3 with primary amino groups. These amino groups can be used in coupling reactions to various targeting molecules. As both the amino and carboxyl groups in **3.35** are separated by two methylenes, independent manipulation of either group should be possible. Additionally, the carboxyl groups in **3.35** are situated closer to the cyclen ring than the amino groups and should preferentially coordinate to the Gd^{3+} ion.

3.9 Summary of Chapter 3

In combination with alkylations and condensations, the Michael reaction has traditionally been used to construct a wide variety of complex molecules from relatively simple starting materials [116]. The Michael reaction benefits from mild reaction conditions, high functional group tolerance, a large host of reactive alkenes as well as high conversions and good reaction rates. In the reactions investigated, the Michael addition of cyclen to activated alkenes proved to be a valuable reaction for functionalizing the cyclen macrocycle.

Reaction of the commonly-available monomer, acrylamide, with cyclen furnished two new, potentially-useful, tri-substituted cyclen ligands (Figure 3.11). These were named DO3PAM (**3.9**) and DO3P (**3.11**). The syntheses of these two macrocycles were both high-yielding and facile. Both ligands were characterised using ^{1}H and ^{13}C NMR spectroscopy and high resolution mass spectrometry.

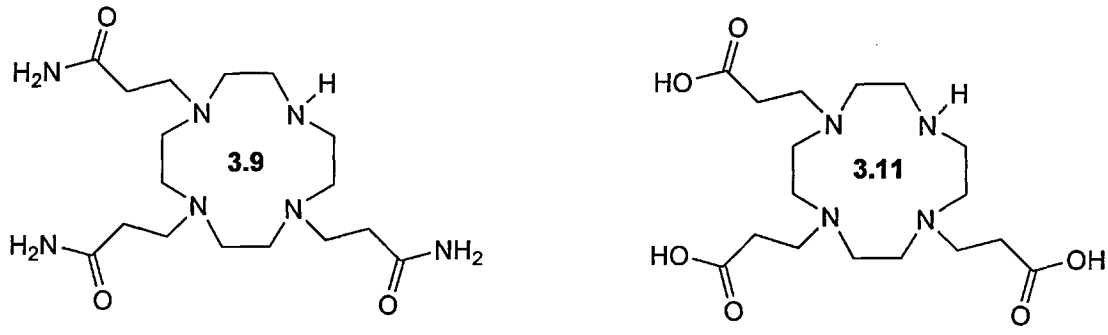

Figure 3.11 Structures of DO3PAM (**3.9**) and DO3P (**3.11**)

The triflic acid-catalysed addition of mono-Z-cyclen (**3.28**) to activated alkenes offers a new and versatile methodology for the tri-*N*-substitution of cyclen (Scheme 3.29). Even a relatively poor Michael acceptor, like methyl-2-acetamidoacrylate, was found to react with cyclen in the presence of the strong Brønsted acid, triflic acid. Since the conditions used to remove the benzyloxycarbonyl group are mild, most substituents that are introduced onto the macrocycle should remain unaffected during this deprotection step.

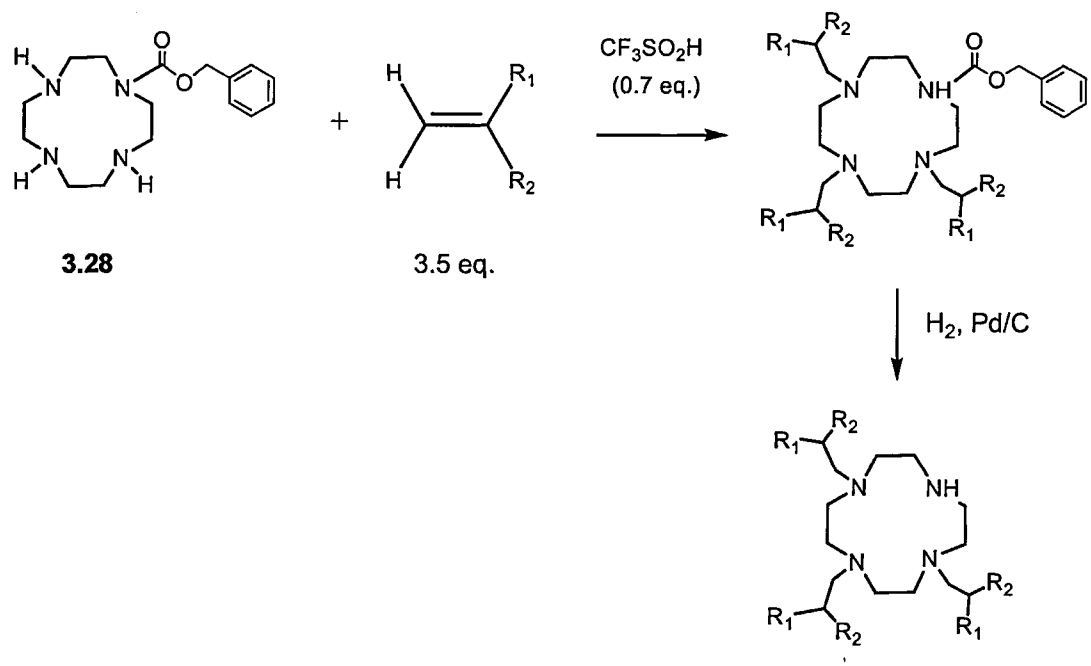

Scheme 3.29 General procedure for the tri-*N*-substitution of cyclen via Michael addition.

Reaction of cyclen with 3.1 eq. ethyl-*cis*-β-cyanoacrylate gave the tri-*N*-substituted ligand (**3.34**) (Scheme 3.30).

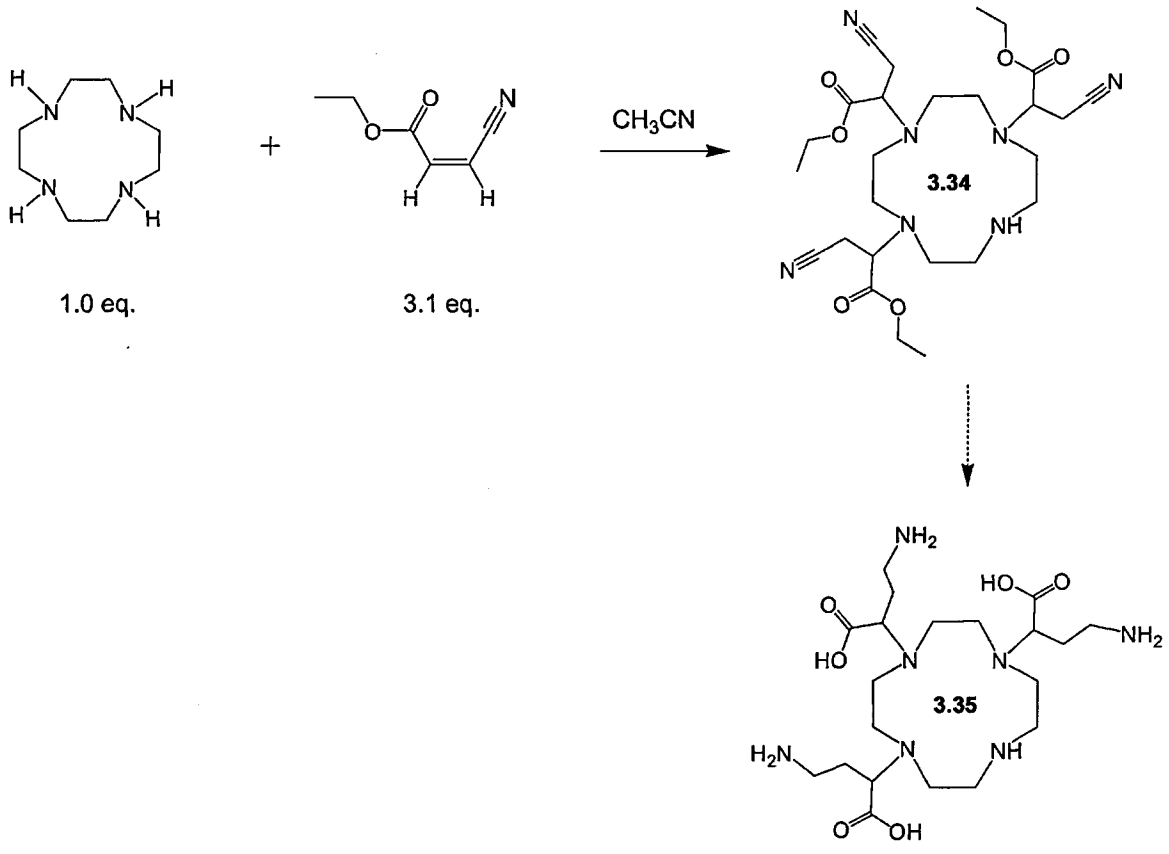

Scheme 3.30 Reaction of cyclen with ethyl-*cis*-β-cyanoacrylate to give **3.34**.

Interestingly, the addition was regioselective with cyclen attacking the alkene at the side opposite to the nitrile group. Once **3.34** is transformed into **3.35**, it should have good potential as a bifunctional ligand because of the favourable spatial arrangement of its carboxyl and amino groups. **3.35** has three carboxyl groups positioned α to the cyclen ring for coordination to Gd^{3+}. The terminal amino groups located on C3 of the pendant arms are available for coupling to vector molecules. As the amino groups are distant from the macrocycle, it is expected they should not coordinate to the central Gd^{3+} ion.

The choice of solvent used in the Michael reaction strongly depends on the solubility of the catalyst, donor, and acceptor as well as sensitivity to side reactions. Solvents with weakly basic functionalities like THF, ether, or acetone could interfere with protonation equilibriation and were not used. Reactions involving strong acids or reactive Michael acceptors like 1-cyanovinylacetate could not be carried out in alcoholic solvents as they could potentially react with the medium. Non-protic solvents such as acetonitrile, chloroform or a combination of both were the solvents of choice for these reactions. In these non-protic solvents, the proton transferred to neutralise the carbanionic intermediate should have originated from cyclen; in other words, the proton transfer was intramolecular. However, the addition of cyclen to acrylamide was performed in methanol. As a result, the transferred proton could have originated either from methanol (i.e. intermolecular) or from cyclen (i.e. intramolecular).

In common with the alkylation reactions described in Chapter 2, reaction of 1 eq. cyclen with 3 eq. Michael acceptor invariably produced unwanted tetra-substituted product in addition to the desired tri-substituted cyclen. It was found that mono-protection of cyclen with the benzoyloxycarbonyl group conveniently prevented this over-alkylation. Additionally, the use of this hydrophobic protecting group facilitated the purification of the product via simple extraction with chloroform. In contrast, a difficult column chromatography was required to separate the tri- and tetra-substituted products when substrate was reacted with unprotected cyclen.

Chapter 4

Synthesis of gadolinium complexes and relaxivity measurements

4.0 Introduction

This chapter is concerned with the preparation, purification and characterisation of gadolinium complexes. Complexes were prepared from the ligands synthesised by the Michael addition reactions described in Chapter 3. The alkylation reactions described in Chapter 2 yielded insufficient products for complexation. Ligands normally require purification with ion-exchange chromatography before complexation as extraneous cations and anions can interfere with the reaction. Therefore, at least 0.25 g of crude ligand is required because of the mechanical losses that occur during the ion-exchange process. Cations such as Ca^{2+} and Na^{+} compete with the Gd^{3+} ion for the ligand and a number of other anions (e.g. Cl^{-}, CO_3^{2-}, OH^{-}) compete with the ligand for the Gd^{3+} ion.

As the donor atoms in macrocyclic ligands are pre-organised for coordination, there is a less dramatic ordering effect upon coordination to a metal than their open-chain analogues [138]. However, the coordination reaction rate of a macrocycle to a metal can be slow and often requires heating the ligand and metal salt for many hours. This ensures the ligand can attain the higher energy conformations which are often necessary for reaction to occur. Conversely, the rate of dissociation of macrocyclic complexes is also slow which explains why their use is preferred over acyclic complexes.

Water-soluble gadolinium complexes are usually prepared in water by using either gadolinium chloride ($GdCl_3.6H_2O$) or gadolinium oxide (Gd_2O_3) as the source of the Gd^{3+} ion. When using a salt such as chloride, the addition of base (e.g. NaOH) is then required to neutralise the hydrochloric acid produced during the complexation reaction. This means that the aqueous solution of the desired complex also contains variable amounts of a NaCl by-product. The presence of these inpurity salts can be avoided by using Gd_2O_3 or

gadolinium acetate ($Gd(CH_3CO_2)_3$) as the source of the Gd^{3+} ion. The pH can be adjusted with volatile ammonium hydroxide base or acetic acid to precipitate any excess Gd^{3+}.

Following complex prepararation, the chapter then describes the method employed for measuring T_1 spin-lattice relaxation times of the complexes on a Minispec mq60 NMR analyser. The Minispec provides a 1.4 Tesla (or 60 MHz ^1H frequency) magnetic field which is the same field strength as that used by many MRI instruments. From the measured relaxation times, the r_1 values of the Gd^{3+} complexes were calculated and compared to published values for complexes of a similar nature. For method validation, the relaxivities of a clinical preparation of Magnevist (i.e. $Gd(DTPA)^{2-}$) and $Gd(DOTA)^-$ were determined and compared to literature values.

4.1 Synthesis of Gd(DO3P)

The ligand DO3P (**3.11**), which is shown in Scheme 4.1, was obtained as the hydrochloride salt from the hydrolytic reaction described in Chapter 3 (See Section 3.4). For complexation, **3.11** required conversion to the free base as chloride anions could compete with the ligand for Gd^{3+}. This was achieved using anion exchange chromatography.

4.1.1 Deionization of DO3P hydrochloride using anion-exchange chromatography

DO3P hydrochloride was converted to the free base by anion exchange chromatography on Amberlite IRA-400 (Scheme 4.1). Amberlite IRA-400 is a strongly basic anion exchange gel-type resin with a quaternary ammonium functionality. Applications of this resin include the deionization of water and the removal of amino acids at high pH [141].

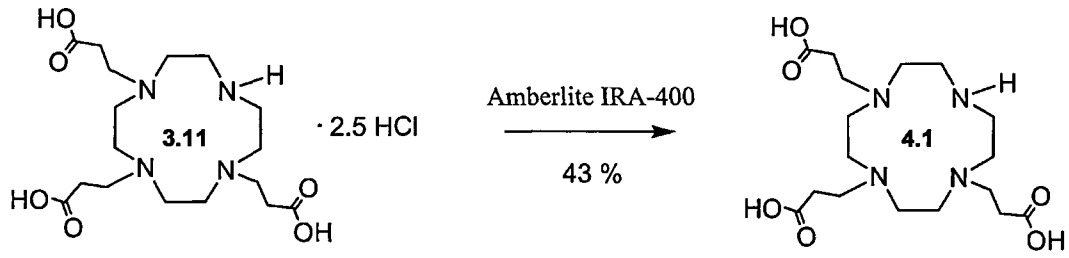

Scheme 4.1 Deionization of DO3P hydrochloride.

3.11 was dissolved in a small amount of water and the pH was adjusted to approximately 10 using dilute sodium hydroxide. This ensured deprotonation of the carboxyl group and enabled adsorption of the negatively-charged ligand onto the positively-charged resin (see Figure 4.1). The resin was then washed with deionized H_2O to remove unbound Na^+ and Cl^- ions. The presence or absence of Cl^- ions in the eluate was conveniently determined by spot-testing with a dilute solution of silver nitrate.

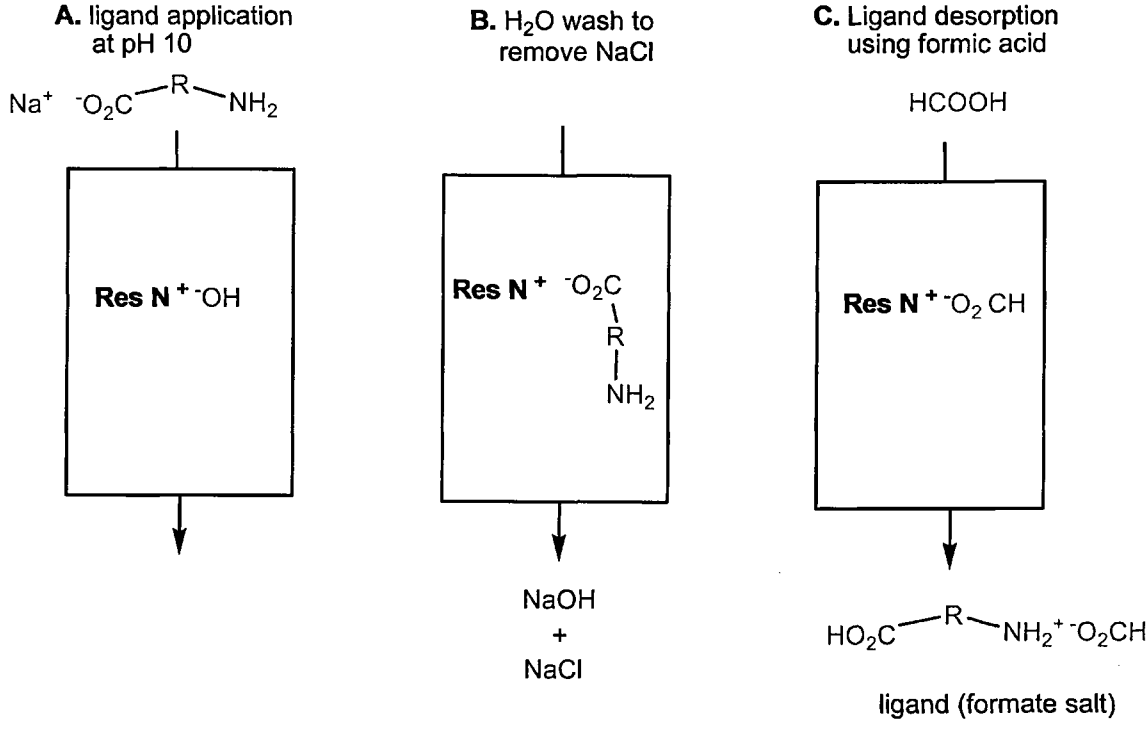

Figure 4.1 Deionization of DO3P hydrochloride on Amberlite IRA-400.

Desorption of the ligand from the column was then accomplished by the stepwise addition of increasing concentrations of formic acid i.e. 0.1, 0.25, 0.5, 0.75 and 1.0 M. The ligand eluted at 0.5 M formic acid. Removal of the formic acid *in vacuo* at 30 °C gave a waxy residue which was the formate salt of the ligand. This formate salt residue was dissolved in deionized H_2O and the solvent evaporated under reduced pressure at 40 °C. This procedure of dissolution in H_2O and evaporation was repeated three times in order to ensure removal of the volatile formic acid from the ligand. The free base form of DO3P (**4.1**) was obtained as a white, mobile powder.

4.1.2 Complexation of DO3P

Scheme 4.2 depicts the complexation of deionized DO3P (1,4,7,10-tetrazacyclododecane-4,7,10-tripropanoate) with gadolinium oxide to give the complex, Gd(DO3P). The method used was analogous to that employed by Dischino *et al.* to synthesise Gd(DO3A) [69].

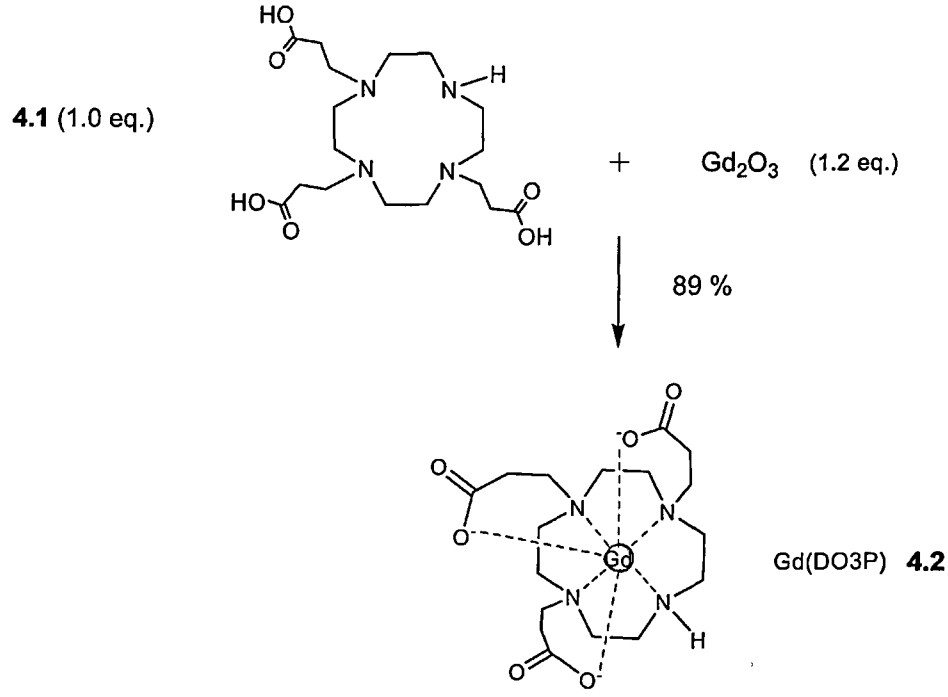

Scheme 4.2 Synthesis of Gd(DO3P), **4.2**

DO3P free base (**4.1**) was refluxed with a slight excess of Gd_2O_3 in a small amount of deionized H_2O for 16 hours. After passing the cooled suspension through a 0.2 micron polypropylene filter, the filtrate was freeze-dryed. In addition to confirming Gd(DO3P) had one Gd^{3+} ion, microanalytical data indicated that the complex was monohydrate. The high resolution mass spectrum of the product (Figure 4.2) gave the appropriate isotopic distribution pattern for the charge-neutral, mono-gadolinium salt (**4.2**). The ^1H NMR of the complex showed several broad resonances indicating the presence of paramagnetic Gd^{3+}. From IR spectroscopy, the carbonyl stretching frequency at 1753 cm^{-1} in **4.1** was shifted to 1560 cm^{-1}, an indication that the pendant arms were bound to the metal centre [142].

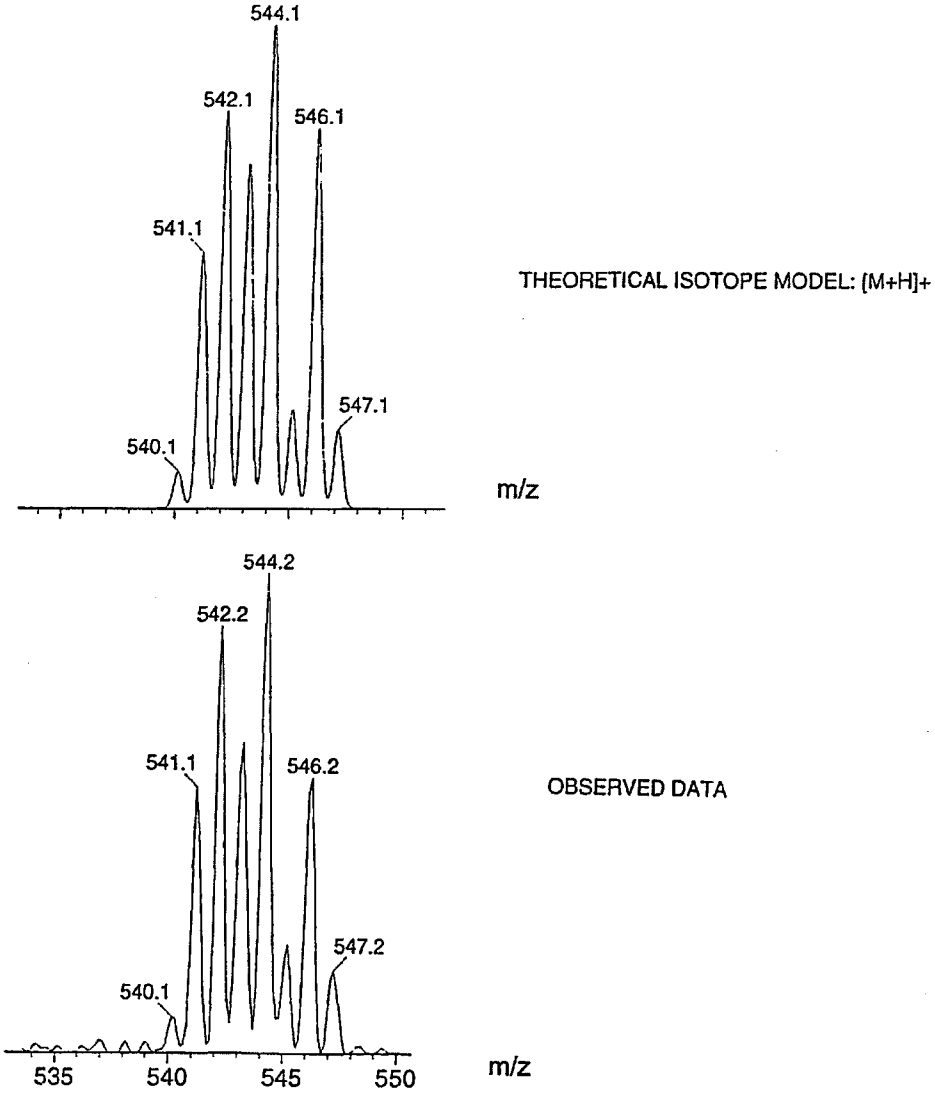

Figure 4.2 High resolution mass spectrum of Gd(DO3P).

4.2 Synthesis of Gd(DO3PAM)

Gd(DO3PAM) was prepared by reacting DO3PAM (**3.9**) with gadolinium chloride (Scheme 4.3). The method consisted of heating DO3PAM with 1 eq. of $GdCl_3$ in anhydrous MeOH at 60 °C for 16 hours [61]. After the solvent was removed, the residue was recrystallised from methanol and diethyl ether.

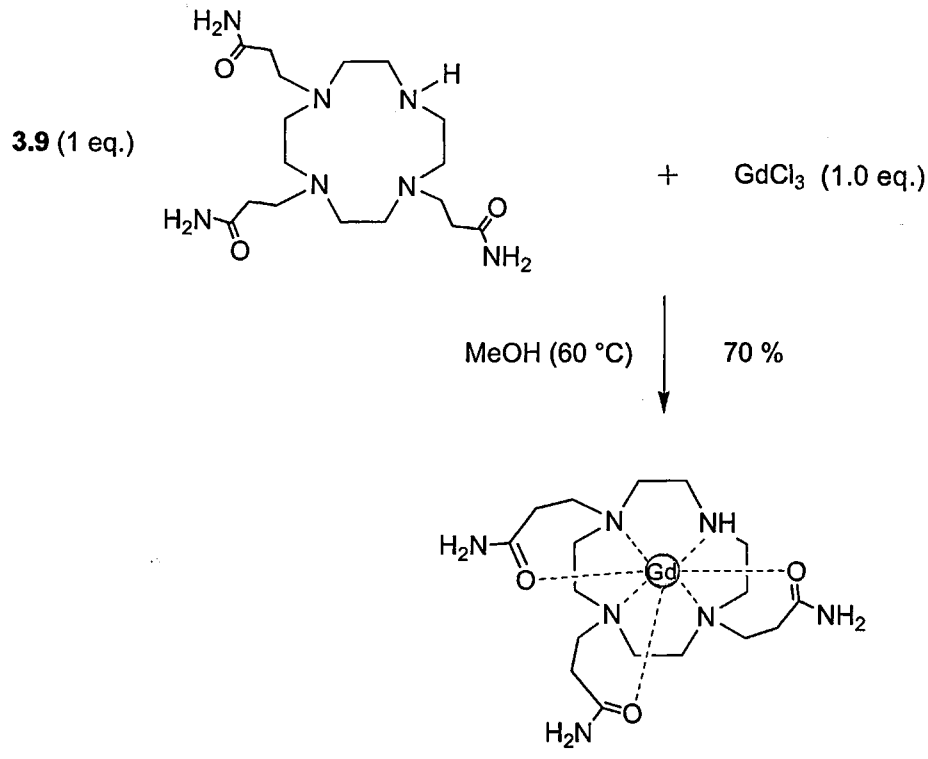

Scheme 4.3 Synthesis of Gd(DO3PAM), **4.3**.

In addition to confirming Gd(DO3PAM) had one Gd^{3+} ion, elemental analysis data showed that the complex was dihydrate and contained three chloride counter-ions. This indicates the complex has an overall formal charge of 3+. The HR-MS of the product ($[LGd+2(NH_4Cl)+HCl]^+$) is shown in Figure 4.3. It is possible that the NH_4Cl and HCl adduct ions were formed in the ion-source of the mass spectrometer. The Cl^- anions of the complex could have formed clusters with NH_4^+ and H^+, which commonly occur with

electrospray ionisation (ES+) [91]. In the HR-MS, the presence of the two expected metal-bonded water molecules was not observed.

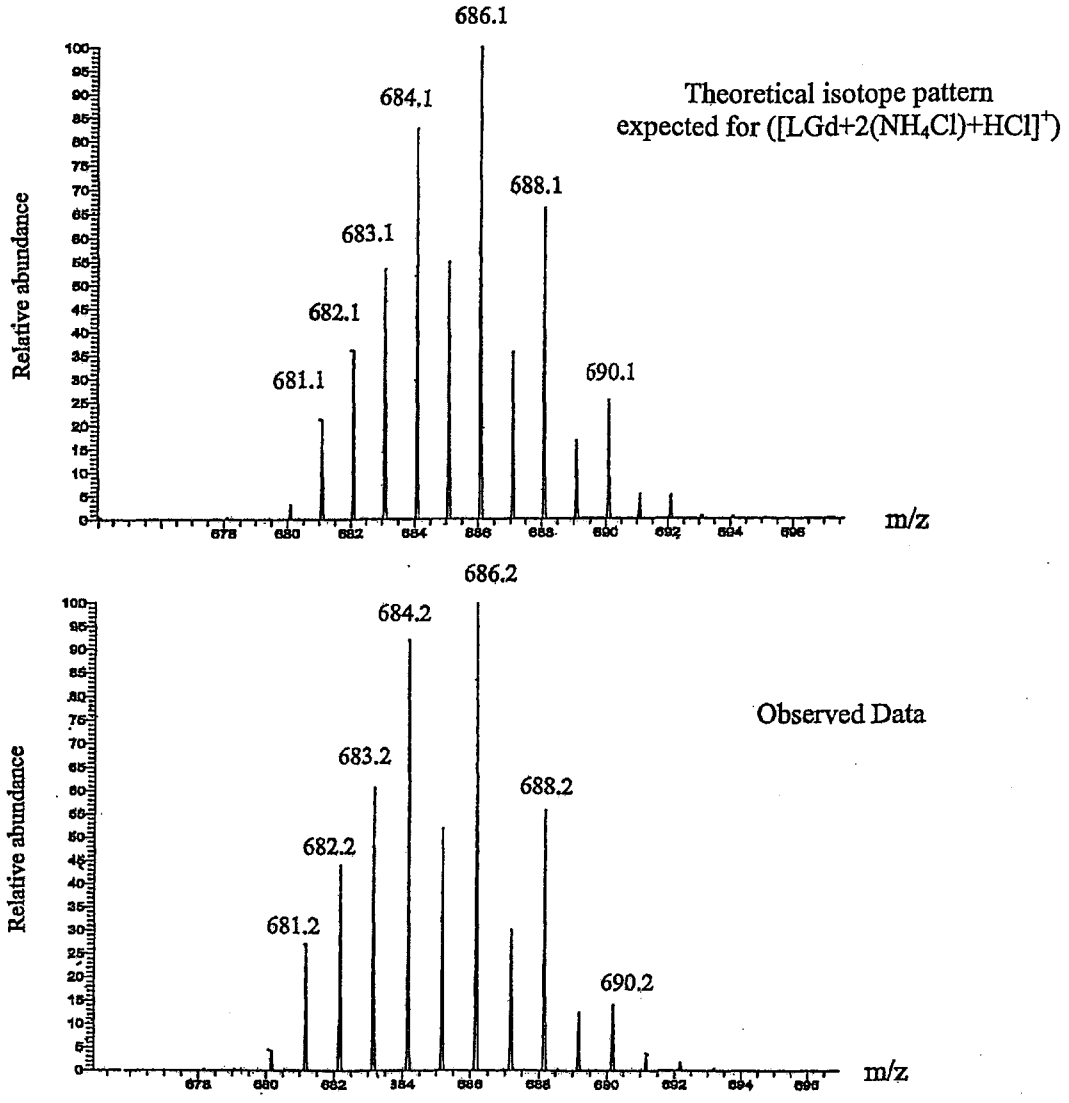

Figure 4.3 High resolution isotope pattern observed for Gd(DO3PAM).

From IR spectroscopy, the carbonyl stretching frequency occurring at 1673 cm^{-1} in **3.9** was shifted to 1652 cm^{-1}, an indication that the pendant arms were indeed bound to the metal centre.

4.3 Synthesis of Gd(DO3-2AP)

4.3.1 Deionization of DO3-2AP hydrochloride using cation-exchange chromatography

DO3-2AP hydrochloride was converted to its ammonium salt form by cation exchange chromatography on Amberlyst IR-120 (Scheme 4.4).

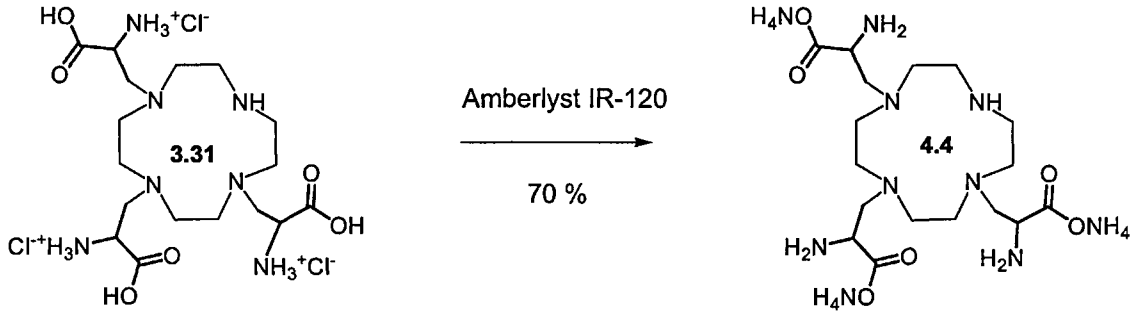

Scheme 4.4 Deionization of DO3-2AP hydrochloride using Amberlyst IR-120.

Amberlyst IR-120 is a strongly acidic cation exchange resin (H^+ or Na^+) with a sulfonic acid functionality [141]. DO3-2AP hydrochloride was dissolved in a small amount of water and its pH was measured (pH = 1.3). At this acidic pH, the amino groups of **3.31** are protonated which ensures adsorption onto the negatively-charged resin (see Figure 4.4). The resin was then washed with deionized H_2O to remove Cl^- ions. Desorption of the ammonium form of the ligand (**4.4**) from the resin was then accomplished by the addition of aqueous ammonium hydroxide (7.5 %). The yellow residue which remained was triturated with ethanol and acetone to give an off-white solid.

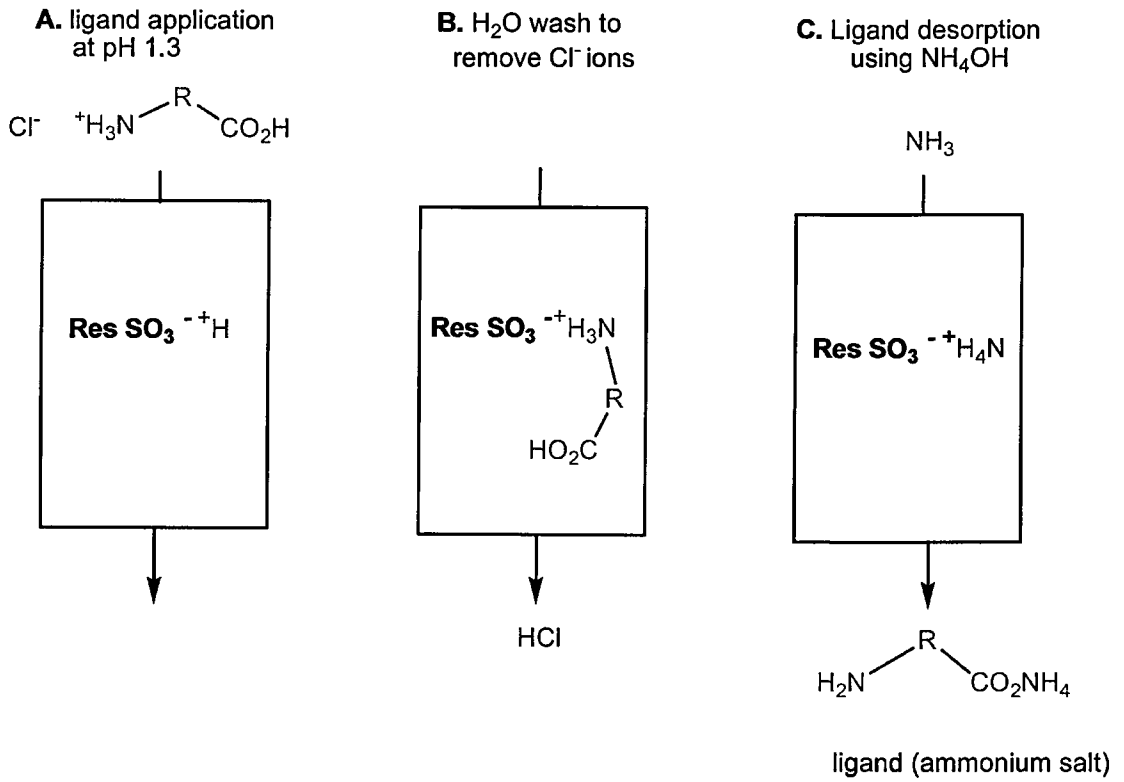

Figure 4.4 Deionization of DO3-2AP hydrochloride on Amberlyst IR-120.

4.3.2 Complexation of DO3-2AP

Scheme 4.5 depicts the complexation of DO3-2AP with gadolinium oxide to form the complex Gd(DO3-2AP), **4.5**.

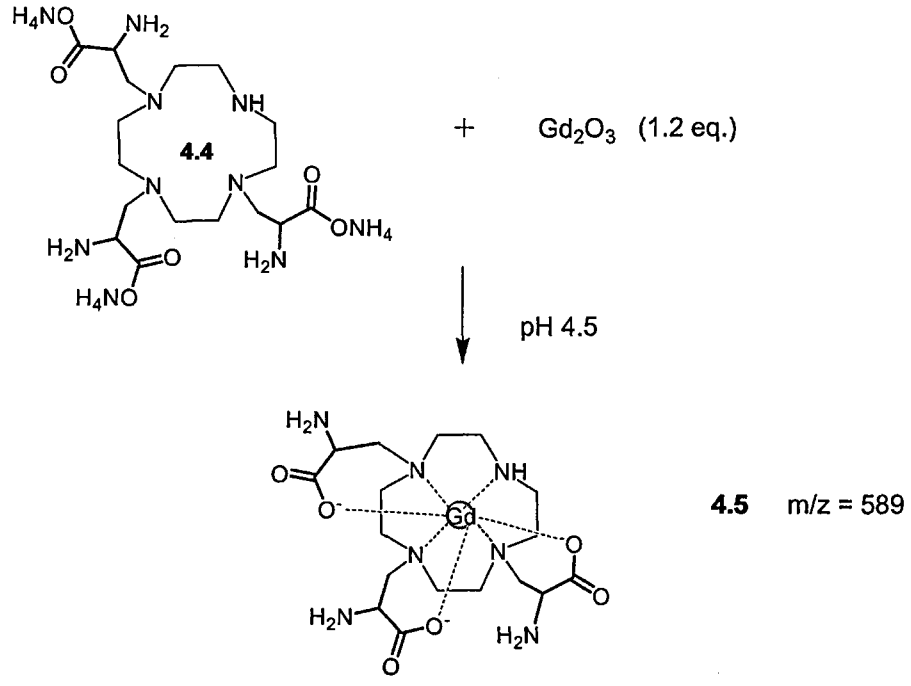

4.5 m/z = 589

Scheme 4.5 Synthesis of Gd(DO3-2AP), **4.5**.

The ammonium salt of **4.4** was reacted with gadolinium oxide at pH 4.5 (the pH was adjusted with dilute acetic acid). After 1 hour, the pH had risen to 4.8. The reaction was allowed to stir overnight and the pH was readjusted to 7.0 with dilute ammonia. After the solvent was removed *in vacuo*, the residue was resuspended in ethanol and acetone was added until a white turbidity appeared. The suspension was then put in the freezer overnight and the filtered precipitate dried under a high vacuum for 24 hours. Low resolution mass spectrometry revealed that Gd(DO3-2AP) had been formed but a peak corresponding to the Gd^{3+} complex of the di-substituted ligand (**4.6**) was also present (see Figure 4.5).

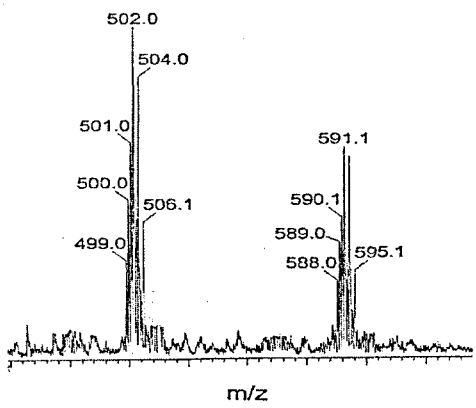

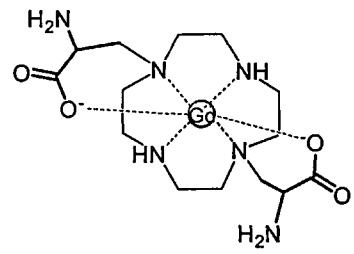

4.6 $[M+H]^+ = 502$

Figure 4.5 LR-MS of Gd(DO3-2AP) showing the impurity complex **4.6**.

In Section 3.7.3 of Chapter 3, deprotection of the tri-substituted ligand (**3.31**) with acid resulted in the loss of a pendant arm to form a ligand with only two arms (**3.32**). This decomposition explains the presence of a peak corresponding to the complex **4.6** in the MS spectrum. Since the desired complex (**4.5**) contained **4.6** as an impurity, a high resolution mass spectrum was not obtainable.

4.4 Synthesis of Gd(DOTA)$^-$

DOTA (1,4,7,10-Tetraazacyclododecane-1,4,7,10-tetraacetic acid) was purchased from Sigma-Aldrich and complexed with gadolinium oxide according to Scheme 4.6. The complexation technique was analogous to the procedure used to prepare Gd(DO3P) in Section 4.1.2.

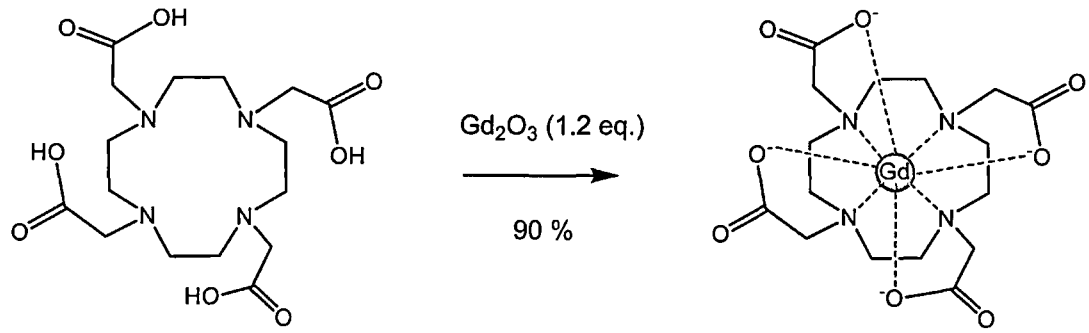

DOTA Gd(DOTA), **4.7**

Scheme 4.6 Complexation of DOTA with Gd^{3+} to give **4.7**.

4.5 Relaxivity measurements of Gd^{3+} complexes

4.5.1 Theory

As discussed in Section 1.6 of Chapter 1, the presence of a Gd^{3+} ion increases the longitudinal and transverse relaxation rates, $1/T_1$ and $1/T_2$, respectively, of water protons. The observed solvent relaxation rate, $(1/T_i)_{obs}$, is the sum of the diamagnetic $(1/T_i)_d$ and paramagnetic $(1/T_i)_p$ relaxation rates (where i = 1 or 2):

$$(1/T_i)_{obs} = (1/T_i)_d + (1/T_i)_p \quad (4.1)$$

The diamagnetic term $1/T_{i,d}$ corresponds to the relaxation rate of the solvent (i.e. water) protons in the absence of paramagnetic Gd^{3+}. The paramagnetic term $1/T_{i,p}$ gives the relaxation rate enhancement caused by the paramagnetic substance, which is linearly proportional to the concentration of the paramagnetic species, $[Gd^{3+}]$:

$$(1/T_i)_{obs} = (1/T_i)_d + r_i [Gd^{3+}] \quad (4.2)$$

According to Equation (4.2), a plot of the observed relaxation rate versus the gadolinium concentration gives a straight line with a slope equal to the relaxivity, r_i. The unit of relaxivity is $mM^{-1} s^{-1}$.

4.5.2 *In vitro* relaxivity measurements

Solutions of gadolinium chloride (0.95, 1.90, 2.85, 3.80, 4.75 mM) were prepared by dissolving the salt in ultra-pure water. For accuracy, the solutions were made to volume in 5 ml volumetric flasks. A 5 mm NMR tube was then filled with solution and the tube placed in a Minispec mq60 pulsed time-domain analyser (Bruker, Massachusetts, USA). The temperature of the sample was maintained at 25 +/- 0.1 °C by an external circulator (Haake Phoenix II P1-C35P). Proton solvent longitudinal relaxation times $(T_1)_{obs}$ were

measured for each sample at 60 MHz and 25 °C by means of the inversion-recovery technique. Three measurements were made for each sample and the average was taken to represent the T_1 relaxation time constant of that sample. A plot of the inverse of this average value versus the Gd^{3+} concentration gives the T_1-relaxivity (r_1) as the slope of the graph (Figure 4.6).

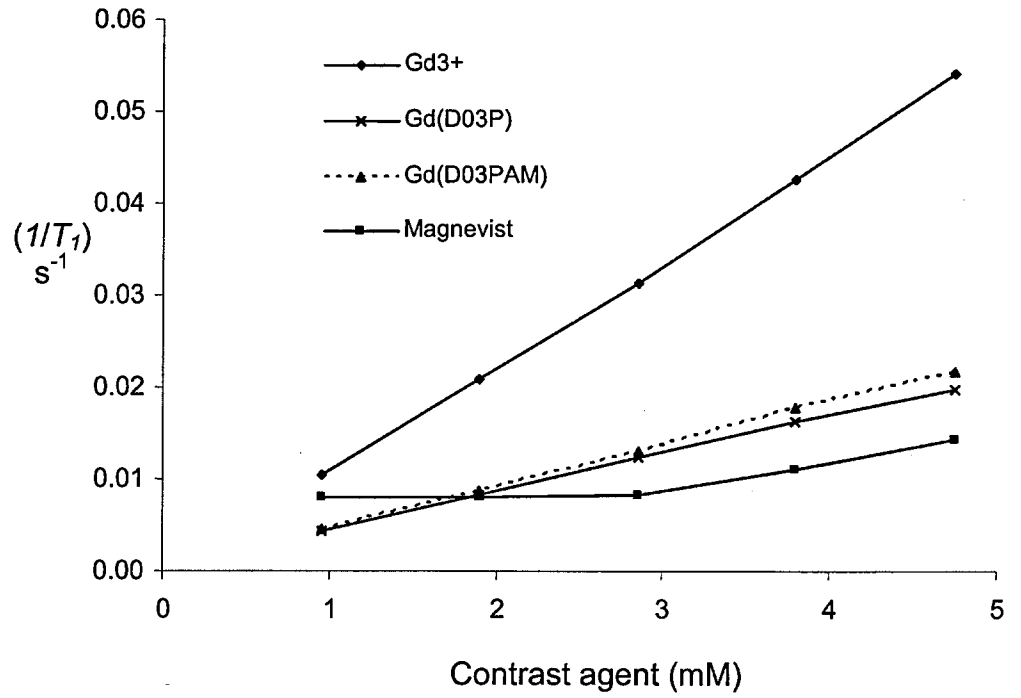

Figure 4.6 Graph of ($1/T_1$) against contrast agent (mM).

The coefficient of regression (R^2) for each line in Figure 4.6 was found to be greater than 0.99. The slope of the Magnevist preparation was only linear between 3-5 mmol. As the vial of Magnevist was a clinical preparation for intravenous use, its formulation may account for this observed behaviour. Since Magnevist, $[Gd(DTPA)H_2O]^{2-}$, is ionic and has an overall charge of -2, two counterions of *N*-methyl-D-glucamine (NMG) are added to the complex to neutralise it. NMG is a sugar-amine derivative, which contains multiple hydroxy groups that hydrogen-bond effectively with water molecules (Figure 4.7).

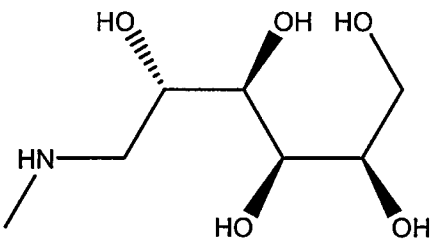

Figure 4.7 *N*-methyl-D-glucamine (NMG).

Van Der Elst *et al.* showed that the addition of NMG to Magnevist increased the rotational correlation time of the complex, presumably because of the increase in size of the adduct formed [143]. Relaxation times were found to be very reproducible and almost identical results were obtained for the $GdCl_3$ solutions when they were re-measured after 7 days.

4.6 Discussion of results

Relaxivity (r_1) describes the effectiveness of the paramagnetic contrast agent in changing the rate of water proton relaxation at 1 mM concentration. It represents the reciprocal of the longitudinal relaxation time constant per unit concentration (mM) of metal. Table 4.1 lists the r_1 relaxivities obtained for the three complexes that were synthesised in this project. It also lists the r_1 of the free Gd^{3+} ion (prepared from $GdCl_3$), Gd(DOTA) and the commercial contrast agent, $[Gd(DTPA)H_2O]^{2-}$, whose trade name is Magnevist.

Table 4.1 T_1-relaxivity (r_1) values of complexes.

Complex	r_1 , $mM^{-1}s^{-1}$, (60 MHz, 25 °C)	r_1, Literature values
Gd^{3+}	11.0	12.2 [118] (20 MHz, 37 °C)
$[Gd(DOTA)(H_2O)]$	3.2	3.5 [24] (20 MHz, 25 °C)
$[Gd(DPTA)H_2O]^{2-}$ Magnevist	2.8	3.1 [24] (20 MHz, 25 °C)
$[Gd(DO3PAM)(H_2O)_2]^{1+}$	4.6	
$[Gd(DO3P)(H_2O)_2]$	4.0	
Gd(DO3-2AP) Impure sample	1.5	

Relaxivity values of 11.0, 3.2 and 2.8 $mM^{-1}s^{-1}$ were determined for free Gd^{3+}, Gd(DOTA) and $[Gd(DPTA)H_2O]^{2-}$ (Magnevist) respectively. These values compare well with the literature values of 12.2 [118], 3.5 [24] and 3.1 [24] $mM^{-1}s^{-1}$, respectively. The similarity of these results to the literature values effectively validates the method used to determine the relaxivity. However, the r_1 values of these reference complexes obtained at 60 MHz are

slightly less than the r_1 values obtained by other studies at 20 MHz [118, 24]. As T_1-relaxivity is both field and temperature-dependent, comparison between data taken at different field strengths or temperatures must be approached with caution. The T_1-relaxivity of small-molecular Gd(III) complexes tends to fall slightly between 20 and 60 MHz (see Figure 4.8). This explains the slightly reduces relaxivity values obtained in this study.

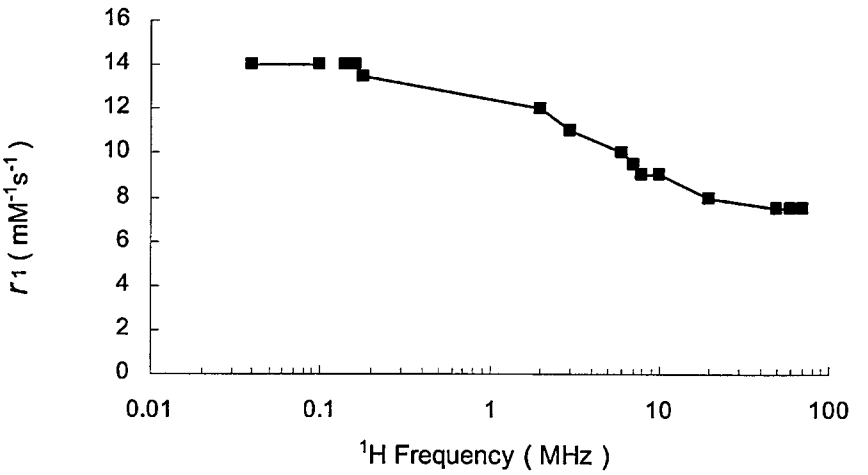

Figure 4.8 r_1 of $[Gd((DOTA(BOM^k)_3)(H_2O)]^-$ versus ^1H frequency [28].

On first inspection, the r_1 values obtained for Gd(DO3P) and Gd(DO3PAM) look quite promising. They show an estimated 50 % increase in relaxivity over the best-selling contrast agent currently on the market, Magnevist, which is shown in Figure 4.9.

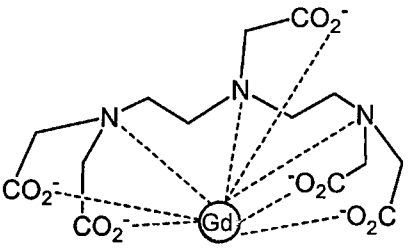

$r_1 = 2.8\ mM^{-1}s^{-1}$
(60 MHz, 25 °C)

Figure 4.9 Magnevist or $[Gd(DTPA)(H_2O)]^{2-}$.

[k] BOM refers to the benzyloxymethylcarbonyl group [25].

However, the DTPA ligand of Magnevist occupies eight binding sites at the metal centre with the ninth coordination site being occupied by a water molecule, i.e. the complex has a q or hydration number of one. Although the hydration numbers of Gd(DO3P) and Gd(DO3PAM) were not determined experimentally, it can be assumed they would approximate a hydration number of two. This assumption is based on the fact that each ligand has only 7 groups available for coordination to gadolinium leaving 2 available for water coordination. Since the hydration number is a strong determinant of relaxivity, a comparison with the r_1 values of other, macrocyclic $q = 2$ complexes carries more validity than a comparison with acyclic, $q = 1$ Gd(DTPA). Two complexes ideally suited for this comparison are the heptadentate complexes Gd(DO3A) and $Gd(DO3AM)^{3+}$ which are shown in Figure 4.10.

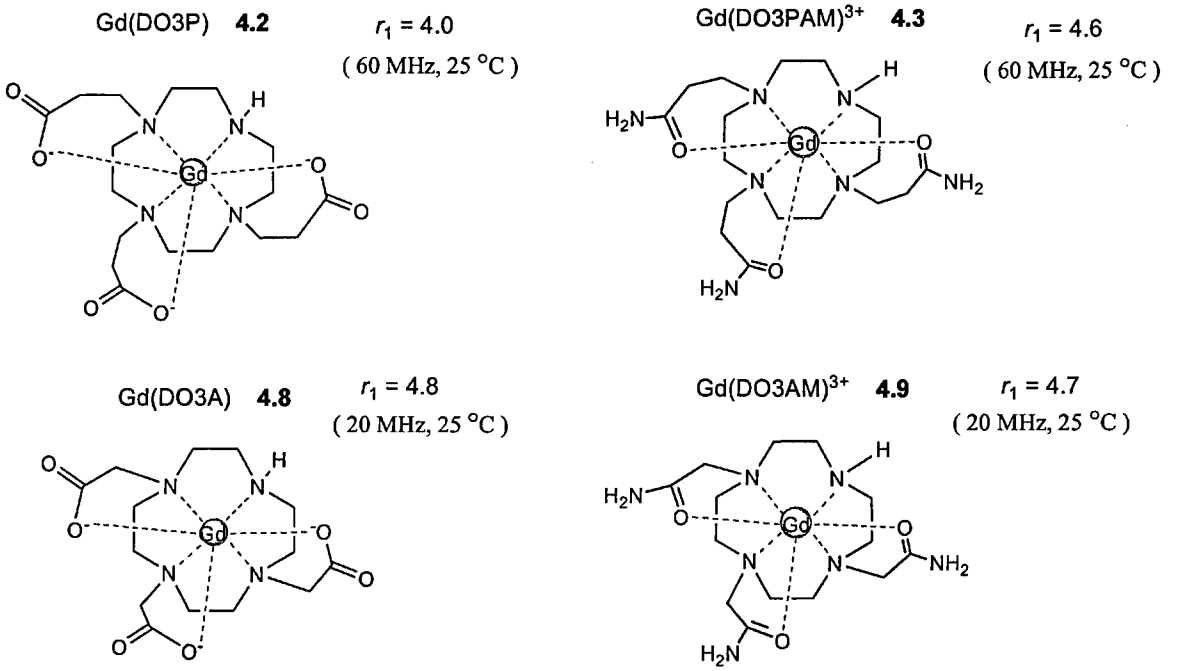

Figure 4.10 Comparison of the T_1-relaxivities of Gd(DO3P) and $Gd(DO3PAM)^{3+}$ to the values of the structurally-similar complexes Gd(DO3A) and $Gd(DO3AM)^{3+}$.

Literature r_1 values of 4.8 and 4.7 $mM^{-1}s^{-1}$ (20 MHz, 25 °C) have been reported for Gd(DO3A) and $Gd(DO3AM)^{3+}$, respectively [144]. These values compare favourably with the r_1 values determined for the structurally-similar, Gd(DO3P) and Gd(DO3PAM). The relatively high relaxivity of Gd(DO3PAM) was unexpected as complexes containing amide donors often suffer from slow water exchange in comparison to their acetate analogues. For example, the replacement of one carboxylate by an amide group has been found to decrease the water exchange rate of a Gd^{3+} complex by a factor of between 3 and 4 [19]. One explanation for the relatively high relaxivity of Gd(DO3PAM) might be the contribution of counterions such as Cl^- in the complex. The nature of the counter-anion has previously been shown to affect the water exchange rate for a series of cationic gadolinium complexes in aqueous solution, as a consequence of the ordering effect that the anion imposes on the structure of the second hydration sphere [145].

In the related triamide complex $(Eu(NP\text{-}DO3AM)(H_2O)(CF_3SO_2^-)_2$, hydrogen-bonding interactions with triflate anions have been observed (see Figure 4.11) [61]. Two triflate anions lie above the coordinated water molecule with each triflate positioned such that a hydrogen bond from one triflate oxygen to one of the protons of the coordinated water molecule is possible. It can also be observed that the oxygen of the water molecule is coordinated directly to the Gd^{3+} ion. Since Gd(amide) complexes have been reported to possess good selectivity for the Gd^{3+} ion *in vivo* [24], Gd(DO3PAM) merits further investigation as a possible contrast agent given its relatively high relaxivity.

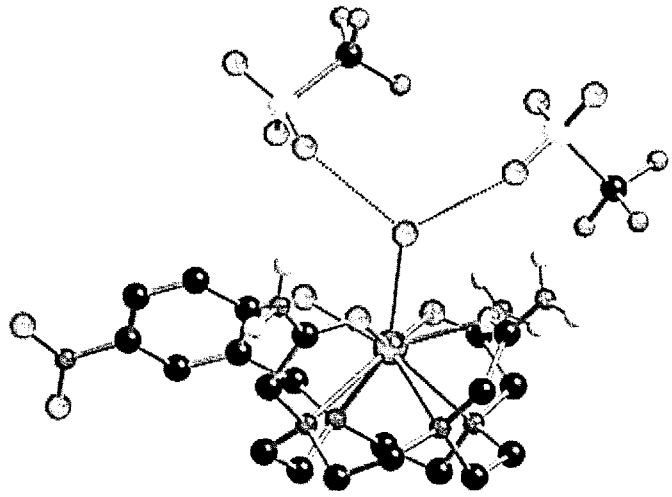

Figure 4.11 Crystal structure of Eu(NP-DO3AM)(H_2O)(CF_3SO_2)$_2$ where dashed lines indicate the hydrogen-bonding interactions of the coordinated water molecule and 2 triflate anions [61].

In Chapter 1, the desirable characteristics of a contrast agent were discussed. Table 4.2 summarises these properties along with the properties of GdDO3P and Gd(DO3PAM).

Table 4.2 Desirable properties of a contrast agent.

Properties	Gd(DO3P)	Gd(DO3PAM)
Adequate relaxivity	✓	✓
Water solubility	✓	✓
Amenable synthesis	✓	✓
In vitro stability	?	?
In vivo stability	?	?

In the investigations conducted to date, both Gd(DO3P) and Gd(DO3PAM) have properties that are considered desirable in a contrast agent. As well as possessing adequate relaxivity, both complexes are highly water-soluble. This allows substantial doses to be

administered in smaller volumes. Additionally, the synthesis of the corresponding ligands was readily accessible. Due to time constraints, no stability or specificity studies were conducted on Gd(DO3P) or Gd(DO3PAM).

Thermodynamic stability ultimately determines the tendency of the Gd^{3+} ion to dissociate from the complex, while the dissociation rate constant (k_f) measures the rate of that process (Equation 4.3).

$$Gd^{3+} + L \underset{k_d}{\overset{k_f}{\rightleftharpoons}} Gd^{3+}(L) \qquad \text{where } K_{eq} = k_f / k_d \tag{4.3}$$

The dissociation rate, which is generally the reverse reaction of Equation (4.4), is only measurable in acidic media. Thermodynamic stability data is especially useful in formulation work, where aqueous preparations of contrast agents are often stored for long periods at room temperature. However, good kinetic stability is a more important property of the complex than good thermodynamic stability. The complex only needs to be stable whilst *in vivo* which is for a few hours at most. Table 4.3 shows that the three clinically-available complexes have large thermodynamic stability constants (For comparison, iron binding by transferrin has log $K_{eq} = 22$). As a result of strong chelation, these complexes should have long shelf lives.

Table 4.3 Equilibrium constants, dissociation kinetics and endogenous ion competition for selected Gd^{3+} complexes [19].

Complex	Log (K_{eq}/ M^{-1})	$t_{1/2}$, dissociation $[H^+] = 0.01$	Reaction with 25 mM Zn(II) / PO_4^{3-}
Gd(HPDO3A)	23.8	1.3 days	< 1 %
$Gd(DOTA)^-$	25.8	95 days	< 1 %
$Gd(DTPA)^{2-}$	22.1	< 2 s	21 %

To assess the effect of endogenous ions upon the relaxivity of a complex, a zinc ion stress test can be performed. This test measures the free Gd^{3+} formed in 15 min after mixing the Gd chelate with zinc cations in a phosphate medium [19]. Table 4.3 shows that the combined stress of phosphate and Zn(II) ion was enough to cause significant dechelatation (21 %) of $Gd(DTPA)^{2-}$ in 15 min, but the macrocyclic complexes remained essentially unaffected. Additionally, $Gd(DTPA)^{2-}$ was found to be very unstable in the presence of acid and dissociated after just 2 sec. Overall, it seems the most important structural feature affecting the relative stability and dissociation of a complex is the presence or absence of the macrocycle.

As both Gd(DO3P) and Gd(DO3PAM) are heptadentate, it is important that they undergo both stability and specificity studies. Lanthanide complexes with 2 water coordination sites are known to bind endogenous anions such as phosphate and bicarbonate. These ions can displace inner sphere water molecules leading to a lowering of relaxivity [59, 146]. Although no heptadentate, $q = 2$ complexes have yet been approved for clinical use, several $q = 2$ have recently been reported with strong safety and relaxivity profiles [4]. A recent entry in this small group of promising, heptadentate ligands is the triaminotetracarboxylic ligand, AAZTA (Figure 4.12) [147].

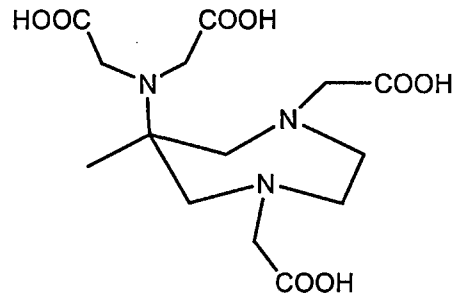

Figure 4.12 Structure of the heptadentate ligand, AAZTA [147].

The corresponding Gd^{3+} complex of AAZTA was found to have adequate stability. The 2 coordinated water molecules of Gd(AAZTA) ensure a high relaxivity (7.1 mM^{-1} s^{-1}, 20 MHz, 25 °C) which was not quenched by bidentate anions such as lactate and phosphate as observed in similar heptadentate complexes. Complexes like Gd(AAZTA) demonstrate that not all heptadentate complexes are adversely affected by the presence of endogenous ions. Since the contrast agents currently available are considered by radiologists as not sensitive enough [148], research and interest will continue into ways of boosting their relaxivity and that includes looking at complexes with higher hydration numbers.

An important factor in the tolerance of contrast agents is the hyperosmolality[1] of their aqueous solutions [9]. The osmolality of blood and extravascular water is 0.3 Osm/kg-H_2O. Intravenous injection of a hyperosmolar contrast medium with an osmolality > 0.7 Osm/kg-H_2O can cause pain to the patient.

[1] An osmole (Osm) is the number of moles of a chemical compound that contribute to a solution's osmotic pressure [10]. Osmolality is a measure of the osmoles of solute per kilogram of solvent. Hyperosmolality is the abnormal increase in the osmolality of a solution, especially a body fluid.

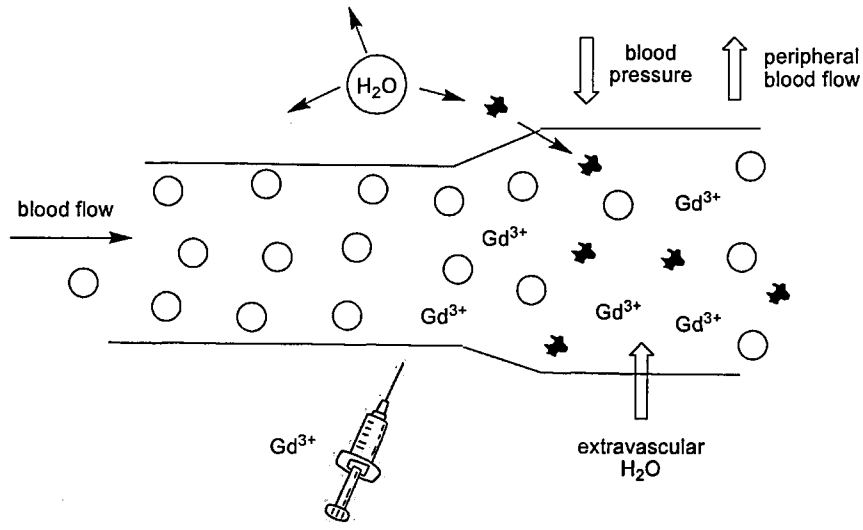

Figure 4.13 Effects from the injection of a hyperosmolar contrast agent [9].

As shown schematically in Figure 4.13, the body responds to an injection of hyperosmolar solutions by transferring water from the surrounding areas to the blood. Loss of water from the cells in these areas cause them to shrivel. Other effects of raised ion concentrations include a reduction in blood pressure and elevation of blood volume which may lead to cellular and circulatory damage. To combat these side-effects, Bracco Research developed the nonionic contrast agent, ProHance [19]. ProHance is Gd(HP-DO3A) and has a high osmotolerance (Figure 4.14).

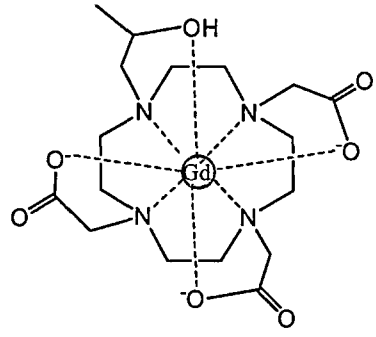

Figure 4.14 Gd(HP-DO3A) or ProHance.

In ProHance, the ligand consists of DO3A with an hydroxyalkyl group on the fourth amine. The uncharged oxygen on the hydroxyalkyl arm coordinates with Gd^{3+} to give an

octadentate, charge-neutral (nonionic) contrast agent. As ProHance is non-ionic and octadentate, it is well-tolerated and stable *in vivo*. Indeed, it is the only example of a commercial MRI agent that is both macrocyclic and nonionic. Table 4.4 shows that the osmolality of a 0.5 M aqueous solutions of non-ionic, ProHance is 2 to 3 times less than that of the ionic complexes, Na[Gd(DOTA)] and NMG_2[Gd(DTPA)].

Table 4.4 Osmolality of selected Gd^{3+} complexes (0.5 M) at 37 °C [19].

Complex	Ion type	Osmolality (Osm/kg-H_2O)
Gd(HP-DO3A)	non-ionic	0.63
Na[Gd(DOTA)]	ionic 1:1	1.35
NMG_2 [Gd(DTPA)]	ionic 2:1	2.0
blood		0.3

Like DO3A, the ligands DO3P and DO3PAM are conveniently tri-*N*-substituted. This allows their properties to be fine-tuned by adding a functional moiety onto the unsubstituted amine group. Using ProHance as an example, DO3P could be alkylated with 1-bromopropan-2-ol and then complexed with gadolinium to give the ProHance analogue **4.10** as outlined in Scheme 4.7. Alternatively, a group which does not coordinate Gd^{3+} could be added at the unsubstituted amine, thus allowing greater relaxivity values.

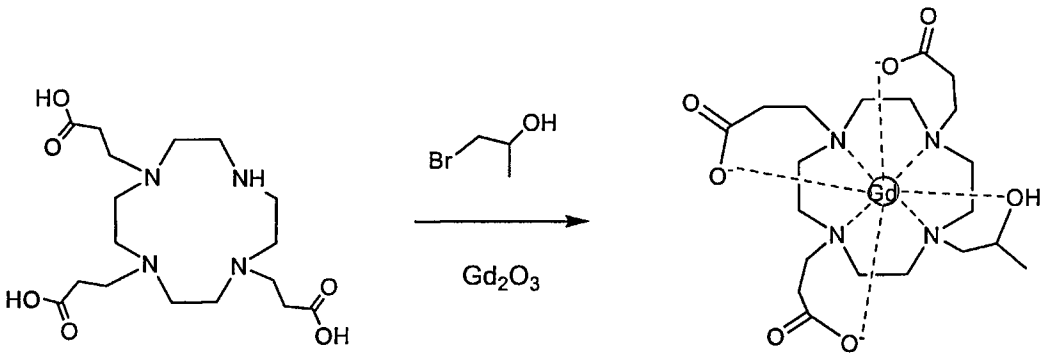

3.11 **4.10** (a ProHance analogue)

Scheme 4.7 Fine-tuning of DO3P to give **4.10**: a possible example.

In summary, Gd^{3+} complexes of the ligands DO3P and DO3PAM were prepared and characterised. Their r_1 values ($mM^{-1}\ s^{-1}$) were found to be in good agreement with literature values for complexes of similar structure and hydration number. Gd(DO3P) possesses three carboxyl groups whereas Gd(DO3PAM) has three amide groups for coordination to Gd^{3+}. In addition, both complexes have a free amine group on the cyclen ring and can be further derivatized. For example, a linker group or a targeting biomolecule could be added at this location.

Chapter 5

Overview

5.1 Summary

Research into targeted contrast agents is currently taking place in all the major imaging techniques [50]. The first generation of MRI contrast agents, currently in clinical use, are small-molecule, extracellular agents such as Gd-DOPA and Gd-DTPA (Figure 5.1).

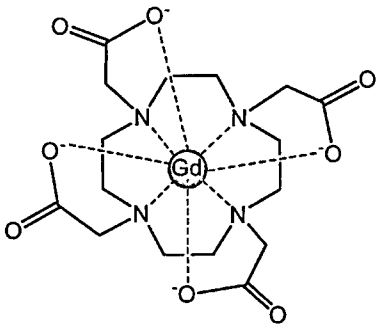

1.1

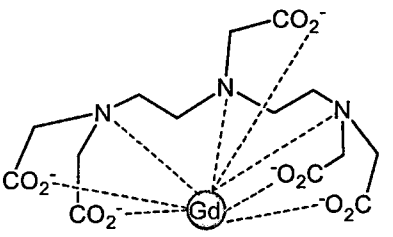

1.2

Figure 5.1 Structures of Gd-DOTA (**1.1**) and Gd-DPTA (**1.2**).

These CAs distribute non-specifically throughout the plasma and are normally excreted within 1.5 hours. Better relaxivity and targeting ability are key requirements for the next generation of contrast agents as more innovative MRI applications are envisonaged. With this in mind, a major goal of this project (see Section 1.10, Chapter 1) was to develop a bifunctional chelating agent (BFCA) with improved targeting ability (Figure 5.2).

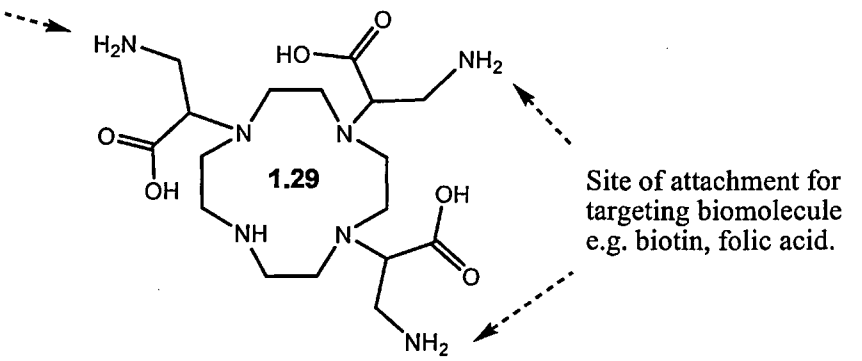

Fi gure 5.2 Structure of the bifunctional chelating ligand (**1.29**).

Based on the cyclen molecule, the ligand (**1.29**) is bifunctional as it possesses 3 carboxyl groups to co-ordinate with Gd^{3+} as well as three conjugation reactive groups (primary

amines). Conjugation of a nucleophilic amino moiety to carrier molecules (e.g. antibodies, peptides, steroids) is a well-assessed method of obtaining pharmaceuticals that display high organ or tissue selectivity [77, 149, 150]. For example, conjugation of the amino acid, folic acid, to a nano-agent enabled uptake of the agent into tumour cells [79].

Initial approaches to the preparation of a bifunctional chelating agent focussed on the alkylation of cyclen with mesylated 4-amino-3-hydroxy-butyric acid (**2.9**). This reaction resulted in elimination of the mesylate from the secondary substrate to give the *trans* alkene (**2.10**) in a high yield (Scheme 5.1).

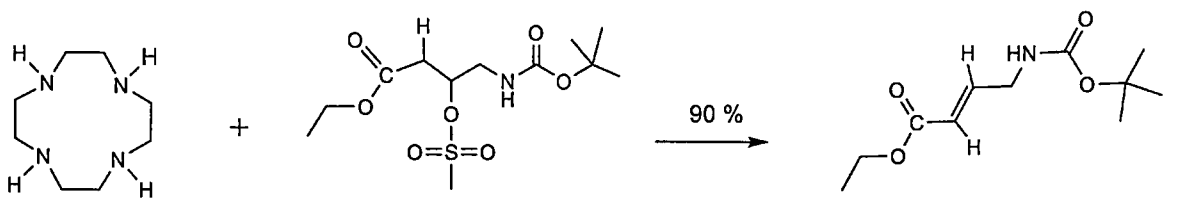

1 eq. **2.9** (3.5 eq.) **2.10**

Scheme 5.1 Alkylation of cyclen with the secondary amino acid derivative (**2.9**).

In an attempt to circumvent elimination, the primary bromide (**2.27**) was prepared and reacted with mono-*N*-acetyl cyclen (**2.26**: Scheme 5.2). Although the alkene (**2.32**) was the main reaction product, some tri-substitution (~ 15 %) of mono-*N*-acetyl-cyclen occurred to give the tetra-substituted product (**2.31**).

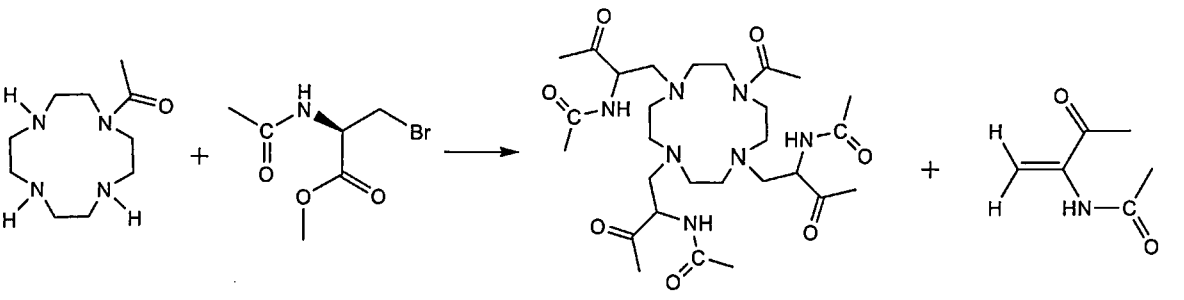

2.26 (1.0 eq.) **2.27** (3.2 eq.) **2.31** (15 %) **2.32** (80%)

Scheme 5.2 Alkylation of cyclen with the primary amino acid derivative (**2.27**)

As the ratio of substitution to elimination in the above alkylation reaction was low, the Michael addition of cyclen to activated alkenes was investigated as an alternative route to functionalised cyclen derivatives. Although a large body of literature concerning the Michael reaction exists for carbon nucleophiles, specific reactions involving azamacrocycles are still quite limited. Reaction of cyclen with acrylamide (7 eq.) in methanol gave the tri-amide cyclen DO3PAM (**3.9**) in a yield of 70 %. Hydrolysis of **3.9** was then achieved with 12 M aqueous HCl to give the triacid, DO3P (**3.11**) in a yield of 90 %.

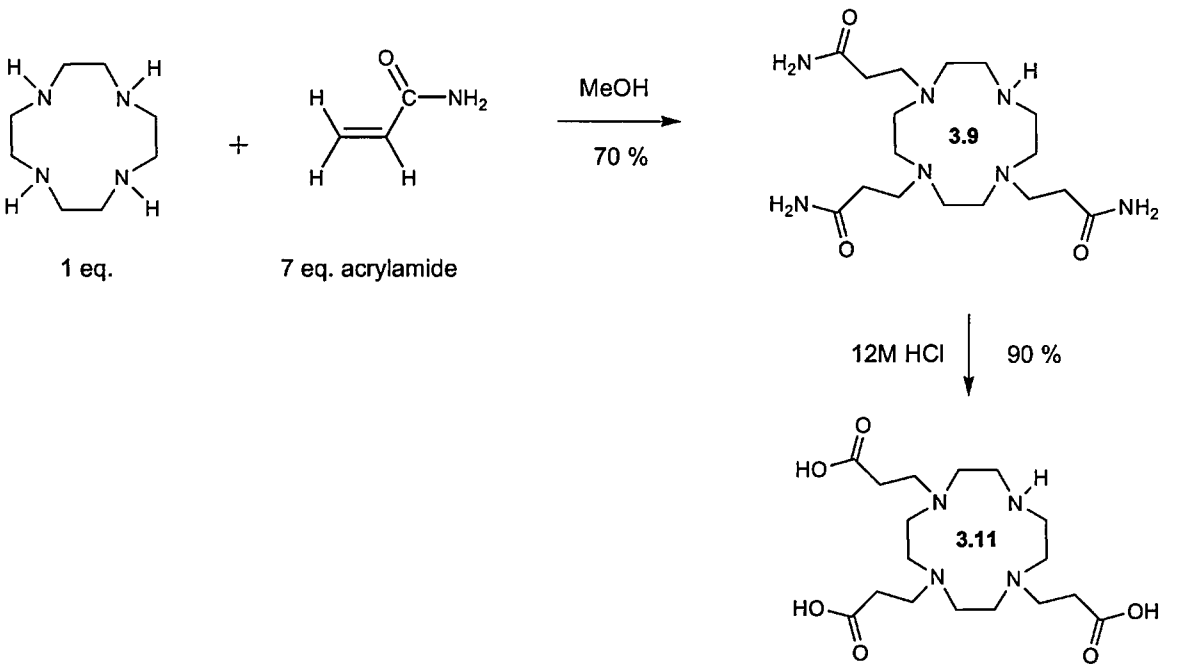

Scheme 5.3 Reaction of cyclen with acrylamide to give the tri-substituted cyclen (**3.9**).

The Michael addition of cyclen to acrylamide was regioselective as the tri-amide substituted cyclen (**3.9**) was the major product. This unexpected result meant that the mono-*N*-protection and deprotection of the cyclen ring after addition were unnecessary. Selective methods for the *N*-substitution of cyclen are central to most syntheses of cyclen-based ligands. Both **3.9** and **3.11** possess free amino groups which are available for further

derivatisation. Encouraged by this result, the addition of cyclen to other Michael acceptors was investigated.

The alkene, methyl-2-acetamidoacrylate (**3.25**), has previously been employed to prepare amino acid derivatives via aza-Michael addition [132]. Reaction of **3.25** with mono-*N*-Z-cyclen (**3.28**) only produced the di-*N*-substituted product. However, it was found that addition of a catalytic amount of triflic acid to the reaction mixture resulted in the formation of the fully-substituted cyclen compound (**3.29**: Scheme 5.4). **3.29** was produced in a yield of 70 % at room temperature.

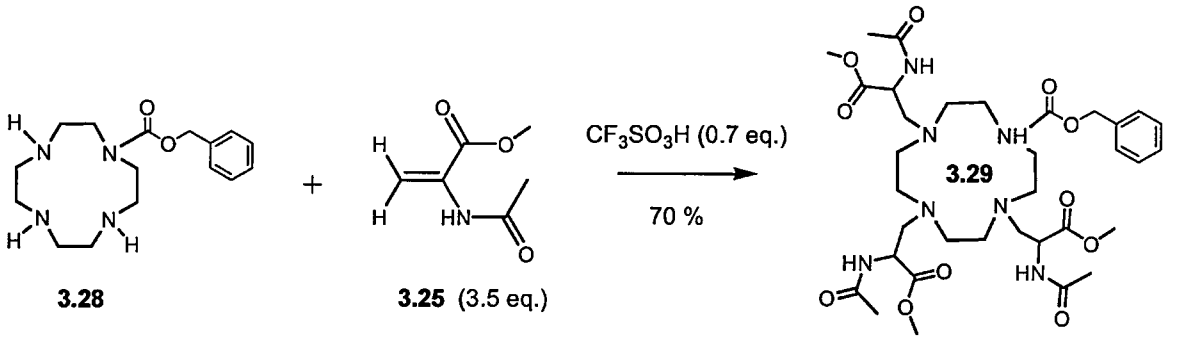

3.28 **3.25** (3.5 eq.)

Scheme 5.4 Triflic acid-catalysed addition of mono-*N*-Z-cyclen to methyl-2-acetamidoacrylate (**3.25**).

Deprotection of **3.29** turned out to be problematic. Once the benzyloxycarbonyl group was removed via catalytic hydrogenation, the product (**3.30**) was heated with 12M HCl at 60 °C (Scheme 5.5). This hydrolytic reaction produced the desired bifunctional ligand (**3.31**) as well as a significant amount of unwanted di-substituted cyclen (**3.32**).

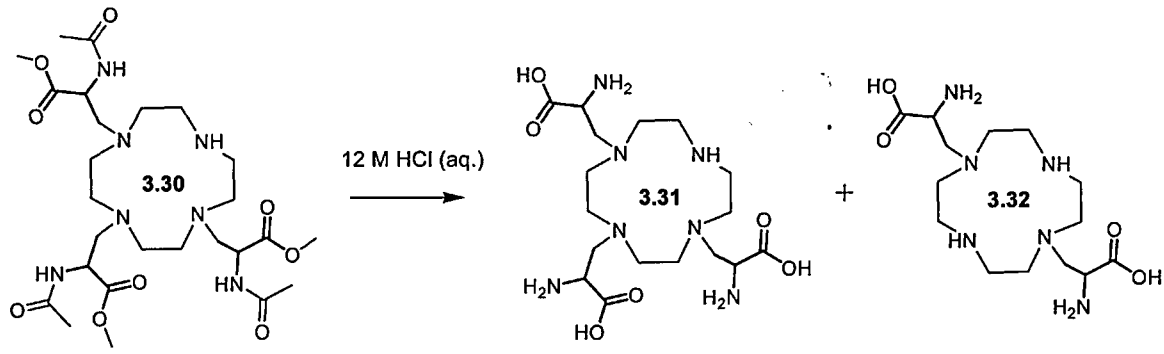

Scheme 5.5 Deprotection of **3.30** with 12 M aqueous HCl.

Reaction of cyclen with 3.5 eq. ethyl-*cis*-β-cyanoacrylate (**3.33**) in dry acetonitrile at room temperature afforded the tri-*N*-substituted ligand, **3.34** (Scheme 5.6). The addition was regioselective with cyclen attacking the side of the alkene opposite to the nitrile group. This regioselectivity can be explained by the stronger electron-withdrawing ability of the nitrile group in comparison to the ester moiety.

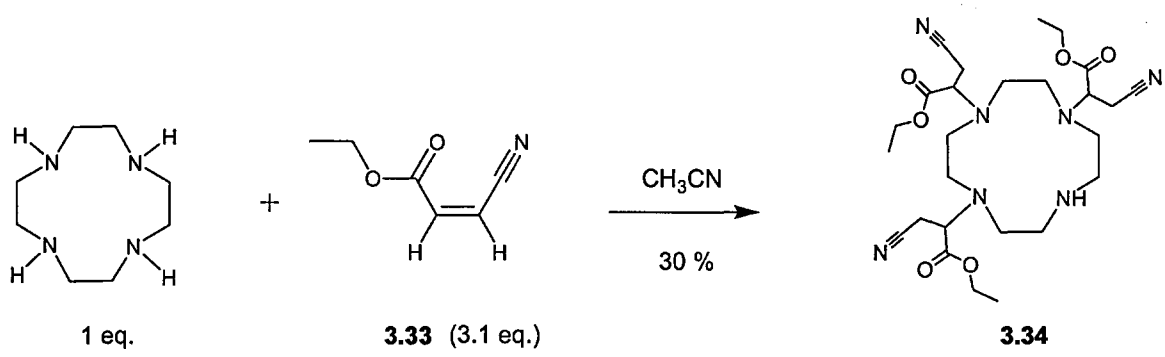

Scheme 5.6 Regioselective addition of cyclen to ethyl-*cis*-β-cyanoacrylate (**3.33**).

Gadolinium complexes of the ligands DO3P (**3.9**) and DO3PAM (**3.11**) were prepared by using Gd_2O_3 and $GdCl_3$ as the source of the Gd^{3+} ion, respectively (Figure 5.2). The T_1 spin-lattice relaxation times of the complexes were measured in H_2O using a Minispec mq60 NMR analyser. The T_1-relaxivity values (r_1) of Gd(DO3P) and Gd(DO3PAM) were determined to be 4.0 and 4.6 $mM^{-1} s^{-1}$ respectively (Table 4.1, Figure 5.2). These values are in good agreement with literature values for complexes of similar structure and hydration number.

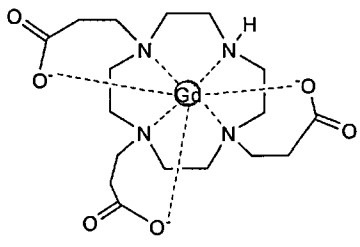

4.2

$r_1 = 4.0\ mM^{-1}s^{-1}$
(60 MHz, 25°C)

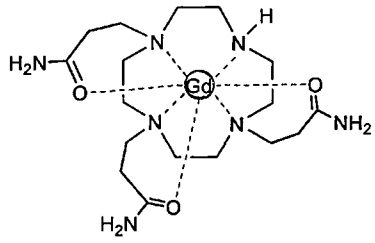

4.3

$r_1 = 4.6\ mM^{-1}s^{-1}$
(60 MHz, 25°C)

Figure 5.2 Structures of Gd(DO3P), **4.2** and Gd(DO3PAM), **4.3**.

Both Gd(DO3P) and Gd(DO3PAM) demonstrated properties which are considered desirable in a contrast agent. As well as possessing adequate relaxivity and good water-solubility, the preparation of both complexes (and their corresponding ligands) were easily achieved.

5.2 Future work

This project has opened up several avenues for further research. More immediate objectives relate to the synthetic transformations of the ligands **3.30** and **3.34**. As regards the ligand **3.30** (Scheme 5.5), a deprotection procedure which prevents the loss of a pendant arm is required (see Section 3.7.3, Chapter 3). It is possible that deprotection of **3.30** with a base such as LiOH may solve this problem. With respect to the ligand **3.34**, reduction of the nitriles to amines followed by hydrolysis of the ethyl ester groups offers a route to the bifunctional ligand, **3.35** (Scheme 5.7).

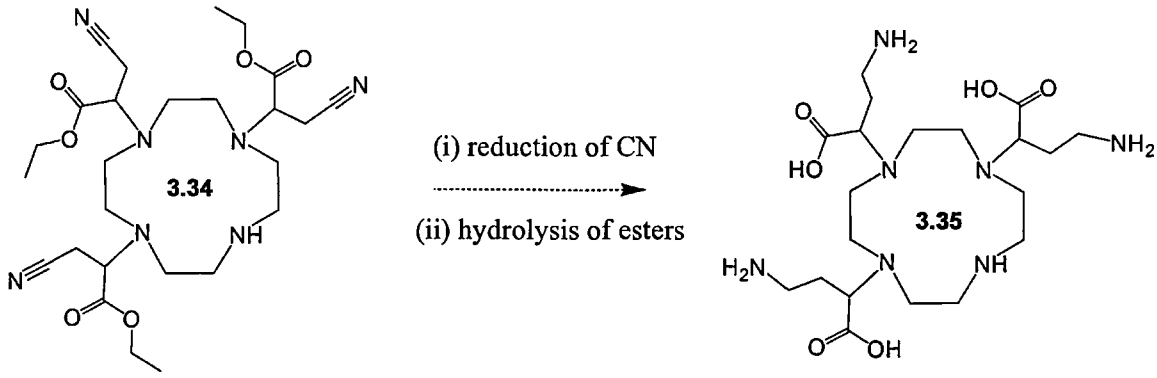

Scheme 5.7 Preparation of the bifunctional ligand **(3.35)**

The first step of this subtle transformation requires the use of a chemoselective reducing agent; this reagent should be able to reduce nitriles to amines in the presence of ester groups. A reagent which may achieve this first step is sodium acetoxyborohydride or $NaBH_3(OCOCF_3)$. Sodium acetoxyborohydride has previously been used to effect the reduction of nitriles to amines whilst leaving ester groups in the same molecule unaffected [151]. It can be conveniently prepared *in situ* from $NaBH_4$ and CF_3CO_2H. Once the hydrolysis of **3.30** and the transformation of **3.34** are achieved, two novel bifunctional macrocyclic ligands, namely **3.31** and **3.35**, will be produced.

The ligands **3.9** and **3.11** (Scheme 5.3) are conveniently tri-*N*-substituted; this allows the fourth unsubstituted amine to be further derivatised. A targeting biomolecule or a linker moiety can be introduced here (Scheme 5.8). In the design of bifunctional chelates, a linker group is often employed to keep the biomolecule distant from the chelate [152,153]. This strategy minimises any possible chelate interference in the binding of the biomolecule to its receptor.

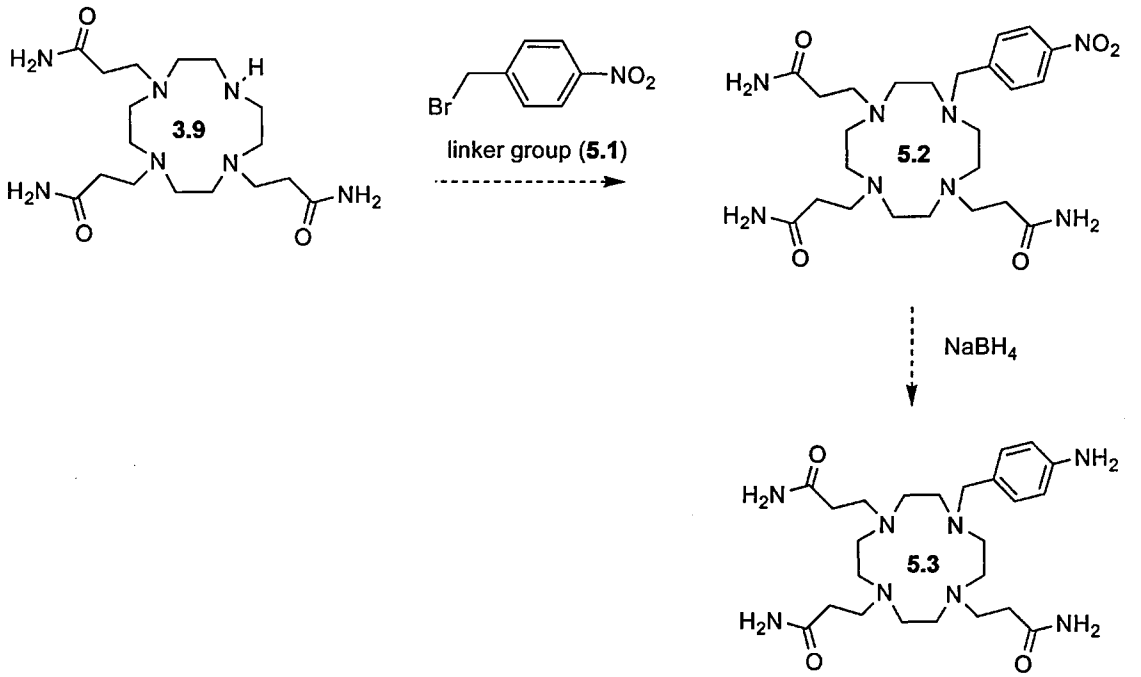

Scheme 5.8 Introduction of a linker group into the ligand (**3.9**)

With regards to the gadolinium complexes, both Gd(DO3P) and Gd(DO3PAM) (Figure 5.2) need to undergo stability studies. Since the stability of these complexes in solution may be compromised by their heptadenticity (see Section 4.6, Chapter 3), preliminary *in vitro* tests should indicate their potential for use as MRI contrast agents.

Macrocyclic ligands based on DOTA are widely employed as radiopharmaceuticals because they form complexes that exhibit high thermodynamic stability and kinetic

inertness [153, 154]. The chemistry developed in this project can, in principle, be exploited to prepare bifunctional chelators for complexing radioactive metal ions for use in other imaging techniques. The choice of radiometal depends on whether the radiopharmaceutical is to be used for diagnostic or therapeutic purposes. For radiopharmaceuticals, ligands that provide higher denticity are preferred as they demonstrate enhanced complex stability. Additionally, radiopharmaceuticals do not need to coordinate water molecules which is a key requirement for MRI contrast agents [155]. Higher denticity can be accomplished by incorporating extra donors into the linker arm. Scheme 5.9 shows one possible derivatisation of the ligand (**3.11**) for use as a bifunctional radiochelator.

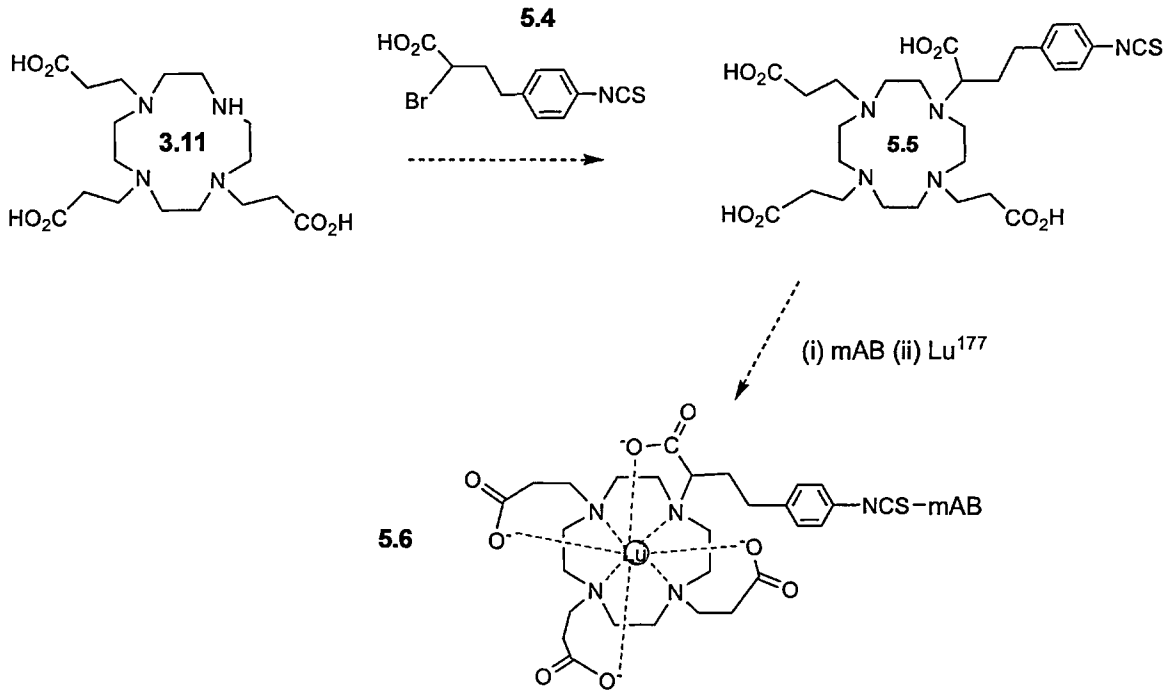

Scheme 5.9 Preparation of the bifunctional chelator (**5.6**) for the radiolabeling of biomolecules.

In summary, the synthetic methods developed in this project have broad applicability and can be applied to the preparation of macrocyclic ligands for use as either MRI contrast agents or radiopharmaceuticals.

Chapter 6

Experimental

6.0 General

Chemicals

Cyclen (1,4,7,10-tetraazacyclododecane) was purchased from Strem Chemicals, USA. DOTA (1,4,7,10-tetraazacyclododecane-1,4,7,10-tetraacetic acid) was purchased from Sigma-Aldrich. Dry DMF was purchased from Fluka. Dry acetonitrile was purchased from Acros. Potassium carbonate was dried at 105 °C for 1 hour before use. 4A and 3A (for alcohols only) molecular sieves were activated in a furnace at 300 °C for 3 hours before use. Tetrahydrofuran was distilled from potassium and benzophenone, dioxane was distilled from lithium aluminium hydride, chloroform and chlorobenzene were distilled from calcium hydride. All solvents were distilled under nitrogen and stored over 4A molecular sieves.

Column chromatography

Column chromatography was performed on silica unless otherwise stated. Alumina (Type 507C, neutral) was purchased from Fluka. Thin layer chromatography was carried out on Fluka silica or alumina plates with fluorescent indicator. TLC Spots were visualised with iodine vapour, UV light or with potassium permanganate spray ($KMnO_4$; water, 0.1 % w/v). Compounds containing cholic acid were visualised with phosphomolybdic acid, brominated compounds were stained with fluoroscein and ninhydrin was found to be particularly useful for detecting cyclen compounds (see Appendix A).

NMR and T_1 relaxivity measurements

^1H NMR and ^{13}C NMR data were obtained using a 300 MHz JEOL instrument. Chemical shift values are recorded in parts per million (ppm) from tetramethylsilane (TMS) as the internal standard for ^1H spectra and from the solvent peaks for ^{13}C spectra. Multiplicities are given as s-singlet, d-doublet, t-triplet, q-quartet, m-multiplet and br-broad signal.

Coupling constants are expressed in Hz. The longitudinal water proton relaxation rates of the complexes were measured at 59.97 MHz and at 25 °C on a Bruker mq 60 NMR analyzer (Bruker Canada, Milton, Ontario, Canada). Gadolinium complexes and $GdCl_3$ were dissolved in ultra-pure water.

Mass spectra

Mass spectra were recorded on a VG Quattro spectrometer, equipped with an electrospray ionization source (ESI). The spectrometer was coupled to a Waters HPLC system. Electrospray was normally used in the positive ion mode (ES+) and the samples were diluted in H_2O: MeOH (50:50). Accurate mass spectrometry was kindly carried out by EPSRC National Mass spectrometry Service Centre, Department of Chemistry, University of Wales Swansea, Swansea, SA2 8PP.

Other analyses

Melting points were measured using an Electrothermal digital melting point apparatus and are uncorrected. Infra-red spectra were recorded as neat films, nujol mulls or KBr discs using a Perkin-Elmer 1710 infrared fourier transform spectrometer. Elemental analyses were performed by Medac LTD, Brunel Science Centre, Cooper's Hill Lane, Englefield Green, Egham, Surrey TW20 0JZ. X-ray structures were kindly determined by EPSRC National Crystallography Service, School of Chemistry, University of Southampton.

New compounds

New compounds are indicated with an asterisk * whereas a new method for preparing a known compound is indicated with a double asterisk **.

6.1 Esterification of 4-amino-3-hydroxybutyric acid to give **2.7**.

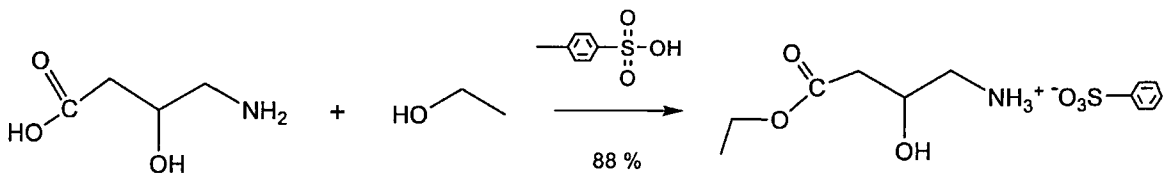

2.6 **2.7**

To a suspension of 4-amino-3-hydroxy-butyric acid (2.5 g, 20.9 mmol) in absolute ethanol (100 ml), *p*-toluenesulfonic acid (4.79 g, 25.18 mmol) was added with stirring. **2.6** was found to dissolve after the addition of *p*-TSA. The resulting solution was heated under reflux for 24 h. After the alcohol was removed under reduced pressure, Et_2O (100 ml) was added to the resultant oil which induced the formation of a white solid. After the solid was stirred with the Et_2O vigorously for 15 min, the solvent was decanted. This procedure was repeated to remove excess *p*-TSA which was found to be soluble in Et_2O. The crystals were washed on a Buchner funnel with a third aliquot of Et_2O (100 ml). As the product was very hygroscopic, it was dried in a dessiccator over P_2O_5 for 24 h. **2.7** was obtained as a white solid. Yield: 5.9 g (88 %). m.p. 72-74 °C. ^{1}H NMR (300 MHz, $CDCl_3$, δ): 1.12 (3H, t, ^3J 6.96 Hz, CH_3,), 2.25 (3H, t, ^3J 7.14 Hz, Arom CH_3,), 2.39 - 2.56 (2H, m, CH_2), 3.02 - 3.07 (2H, dd, ^4J 2.76 Hz and ^2J 13.02 Hz, CH_2), 4.05 (2H, q, ^3J 7.14 Hz, ethyl CH_2), 4.11 - 4.20 (1H, m, CH-OH), 7.20-7.23 (2H, d, ^3J 8.43 Hz, CH x 2-Arom), 7.55 (2H, d, ^3J 8.25 Hz, CH x 2-Arom); ^{13}C NMR (75 MHz, $CDCl_3$, δ); 14.09 (CH_3), 21.28 (CH_3), 40.22 (CH_2), 44.67 (CH_2), 62.89 (ethyl CH_2), 65.20 (CH-OH), 126.15 (Arom), 130.25 (Arom), 140.23 (Arom), 143.28 (Arom), 173.52 (C=O); IR (ν_{max} / (cm^{-1}), KBr): 3076 (broad ammonium -NH_3^+), 1716 (ester C=O), 1600 (arom), 1569 (NH bend), 1500 (arom), 1231 (SO_3), 1038 (CO stretch), 822, 685 (arom), 569 (NH). MS (+ES): 148 $[M+H]^+$, 294 $[2M+H]^+$ (dimer).

6.2 Synthesis of ethyl 4-[(Boc)amino]-3-hydroxybutanoate (**2.8**).

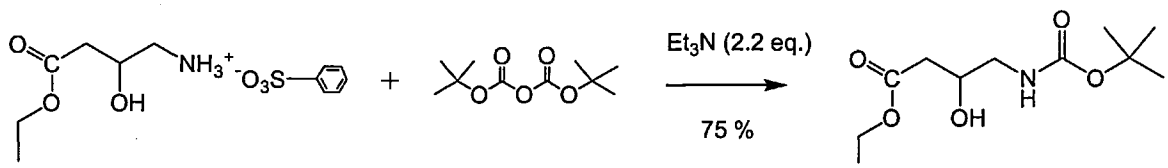

2.7 (1 eq.) 1.1 eq. **2.8**

2.7 (3.19 g, 10 mmol) and Et_3N (2.1 ml, 15 mmol) were stirred in a mixture of dioxane: H_2O (20:20 ml) in an ice-water bath. Di-*tert*-butyldicarbonate (2.4 g, 11 mmol) was added in portions over approximately 10 minutes. The ice-water bath was removed and the mixture was allowed to stir at RT for 24 hours. As the pH of the solution was adjusted from 8.1 to 2.5 using 1M HCl, an evolution of bubbles (CO_2) was observed. The reaction mixture was then extracted with DCM (2 x 50 ml). The extracts were pooled, washed with water, dried over $MgSO_4$ and evaporated under reduced pressure. The residue was dried under high vacuum for 3 hours to remove traces of dioxane. **2.8** was obtained as a clear, colourless, viscous oil. Yield: 1.87 g (75 %). ^{1}H NMR (300 MHz, $CDCl_3$, δ): 1.28 (3H, t, ^3J 7.14 Hz, CH_3), 1.45 (9H, s, Boc), 2.47 (1H, d, CH_2-1, J 3.1 Hz), 2.49 (s, 1H, CH_2-2), 3.07 - 3.17 (1H, m, CH-O), 3.93 (2H, t, CH_2), 4.17 (2H, q, ^3J 7.14 Hz, CH_2), 5.07 (1H, br s, NH); ^{13}C NMR (75 MHz, $CDCl_3$, δ): 14.09 (CH_3), 28.31 (Boc CH_3), 36.71 (CH_2), 45.53 (CH_2), 60.85 (CH_2-O), 67.71 (CH-OH), 79.58 (C_q) 156.20 (CO), 172.49 (CO); IR (ν_{max} / (cm^{-1}) neat, film): 3387 (OH), 2927, 2854, 1723 (C=O), 1530, 1461. MS (+ES): 247 $[M+H]^+$.

Note: DCM could be substituted for dioxane-H_2O but using this aqueous mixture allowed the pH to be adjusted more accurately with a hand-held pH checker. One disadvantage of using dioxane is that it can take several hours under high vacuum to remove it because of its high boiling point. Dioxane removal was confirmed by the absence of a signal at δ 3.71 in the ^{1}H NMR spectrum and δ 67.02 in the ^{13}C NMR spectrum.

6.3 Mesylation of **2.8** to give ethyl 4-[(Boc)amino]-3-mesyl butanoate (**2.9**).

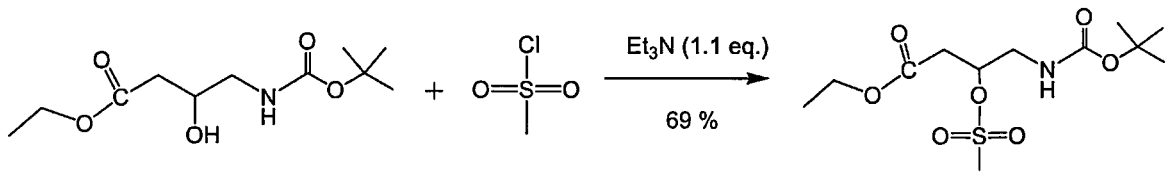

2.8 1.1 eq. **2.9**

Ethyl 4-[(Boc)amino-3-hydroxybutanoate (1.29 g, 5.2 mmol) and Et_3N (0.88 ml, 6.3 mmol) were dissolved in DCM (10 ml) and cooled on an ice bath. Methanesulfonyl chloride (0.66 g, 5.7 mmol) in DCM (10 ml) was added with stirring under N_2 over 20 min. After stirring on the ice bath for 10 min, the mixture was stirred at RT for 3 hours. The reaction mixture was washed with H_2O (3 x 50 ml) and evaporated to give a pale yellow, viscous oil. Crystallisation of the oil was induced by adding acetone and evaporating off the solvent. Recrystallisation from toluene-hexane gave white crystals. Yield: 1.17 g (68.9 %). m.p. 60-63 °C. ^{1}H NMR (300 MHz, $CDCl_3$, δ): 1.27 (3H, t, ^3J 7.14 Hz, CH_3), 1.45 (9H, s, Boc), 2.47 - 2.49 (2H, m, CH_2-N), 3.07 (3H, s, CH_3SO_3), 3.43 - 3.55 (2H, m, CH_2-CO), 4.17 (2H, q, ^3J = 7.14 Hz, ethyl CH_2), 4.98 (1H, br s, NH), 5.05 - 5.12 (1H, m, CH): ^{13}C NMR (75 MHz, $CDCl_3$, δ); 14.06 (CH_3), 28.30 (Boc CH_3), 36.99 (CH_2), 38.21 (CH_3SO_3), 43.95 (CH_2), 61.14 (ethyl CH_2), 78.04 (CH), 156.15 (CO), 169.65 (CO): IR (ν_{max} / (cm^{-1}), KBr): 3398, 2982, 1728, 1520, 1337 (mesyl O-SO_2-CH_3), 1255, 1177, (mesyl O-SO_2-CH_3), 1029, 918, 870, 785, 589, 523, 541, 445. MS (+ES): 325 $[M+H]^+$.

6.4 Alkylation of cyclen with **2.9** to give **2.10***.

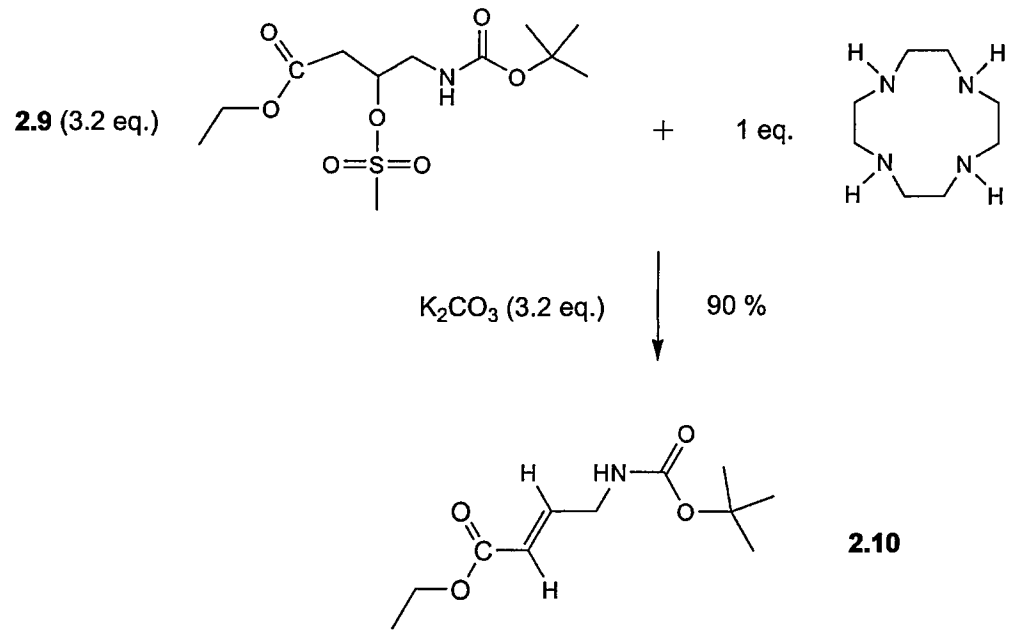

Cyclen (0.16 g, 0.96 mmol), K_2CO_3 (0.42 g, 3.07 mmol) and MeCN (20 ml) were added to a 100 ml round-bottomed flask. **2.9** (1.0 g, 3.1 mmol) was dissolved in MeCN (20 ml) and added dropwise to the reaction over 30 min. After the reaction was allowed to stir at RT under N_2 for 24 hours, the K_2CO_3 was filtered off and the organic solvent evaporated to give a dark orange oil (0.69 g). This residue was purified on a silica gel column using a 0-10 % gradient of MeOH in $CHCl_3$ containing 0.2 % *i*PrNH$_2$. **2.10** eluted at 6-8 % MeOH to give a yellow oil which solidified on standing. Yield: 0.3 g (90 %). R_f 0.42 (I_2, 5 % MeOH in $CHCl_3$ with 0.2 % *i*PrNH$_2$). ^{1}H NMR (300 MHz, $CDCl_3$, δ): 1.23 - 1.31 (3H, m, CH_3), 1.45 (9H, s, Boc), 3.00 (2H, t, ^2J = 6.42 Hz, ^2J = 6.96 Hz, CH_2-CH_3), 3.92 (1H, br s, NH), 4.09 - 4.23 (2H, m, CH_2), 5.94 (1H, dt, ^3J = 15.57, ^4J = 2.0 Hz, HN-*H*C=CH), 6.92 (1H, dt, ^3J = 16.20 Hz, ^3J = 4.9 Hz, CH-*H*C=CH); ^{13}C NMR (75 MHz, $CDCl_3$, δ); 14.10 (ethyl CH_3), 28.28 (Boc CH_3), 31.71 (CH_2), 41.27 (CH_2), 121.26 (HC=CH), 144.73 (HC=CH), 155.56 (CO), 166.07 (CO); IR (ν_{max} / (cm^{-1}), KBr): 3355 (NH), 2980, 1700 (Conj C=O), 1501, 1244, 1165, 1042, 868, 785, 658. MS (+ES): 229 $[M+H]^+$.

6.5 Synthesis of *N*-Boc(*tert*-butoxycarbonyl)-L-Serine methyl ester (**2.14**).

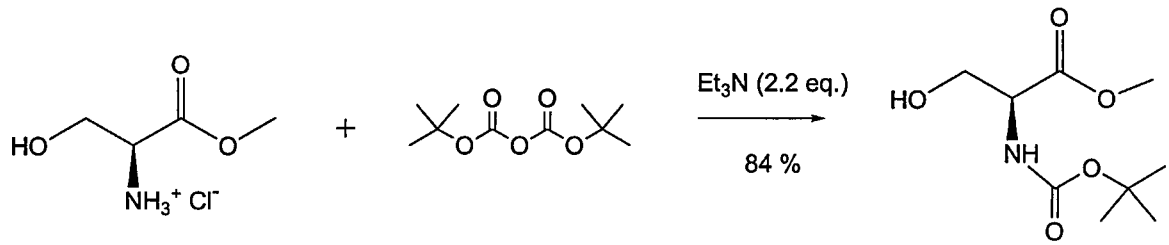

2.12 1.1 eq. **2.14**

L-serine methyl ester hydrochloride (2.0 g, 12.86 mmol) and Et_3N (3.25 g, 32.14 mmol) were dissolved in a mixture of dioxane and H_2O (20 : 20 ml). The solution was cooled on an ice-bath and di-*tert*-butyldicarbonate (3.1 g, 14.14 mmol) was added in small portions over 15 min. The reaction was allowed to stir overnight under N_2. The pH of the reaction mixture was adjusted from 8.6 to 2.5 with 1 M HCl (20 ml) and extracted with $CHCl_3$ (2 x 75 ml). The organic extracts were washed with H_2O (2 x 50 ml) and dried over $MgSO_4$. After the $CHCl_3$ was evaporated under reduced pressure, the dioxane was removed under high vacuum at 40 °C. The residue was subjected to high-vacuum for several hours to give **2.14** as a clear, colourless, viscous oil. Yield: 2.37 g (84 %). ^1H NMR (300 MHz, $CDCl_3$, δ): 1.46 (s, 9H, Boc), 3.79 (s, 3H, OCH_3), 3.94 (dd, J = 3.84 Hz, 2H, CH_2), 4.39 (br t, 1H, CH), 5.48 (br s, 1H, NH); ^{13}C NMR (75 MHz, $CDCl_3$, δ): 28.30 (Boc CH_3), 52.67 (CH_3), 55.73 (CH), 63.59 (CH_2), 157.61 (CO), 171.31 (CO). IR (ν_{max} / (cm^{-1}), Nujol): 3438, 2982 (CH), 1709 (C=O), 1505, 1456, 1439, 1394, 1369, 1164, 1121, 1063 (CO), 1031, 874, 850. MS (+ES): 220 $[M+H]^+$.

6.6 Bromination of **2.14** with DPPE (**2.15**) and 1,2-DB (**2.16**).

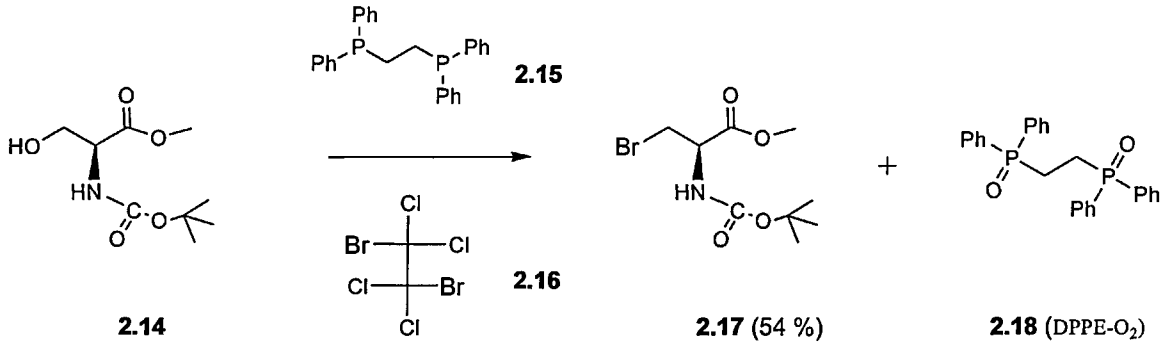

2.14 **2.17** (54 %) **2.18** (DPPE-O_2)

N-Boc-L-Serine methyl ester (2.5 g, 11.40 mmol, 1 eq.) and 1,2-dibromotetrachloroethane (1,2-DB, 6.31 g, 19.39 mmol, 1.7 eq.) were dissolved in 70 ml THF. DPPE (1,2-bis(diphenylphosphino)ethane, 4.54 g, 11.4 mmol, 1 eq.) was added in portions over 10 minutes. The reaction was allowed to stir at RT for 12h. The suspension was then filtered through a 2 cm plug celite on a Buchner funnel. The celite was washed with THF (2 x 10 ml) and the combined filtrates evaporated under reduced pressure to give a yellow oil (9.86 g). The oil was purified on a silica gel column (150 g) by successively eluting the column with DCM (300 ml), DCM with 1 % MeOH (450 ml) and DCM with 2 % MeOH (450 ml). **2.17** eluted at 1 - 2 % MeOH in DCM (R_f = 0.74, fluoroscein spray, 1% MeOH in DCM) whereas unreacted 1,2-DB eluted in neat DCM (R_f = 0.43). Fractions containing **2.17** were evaporated to give white solid. Yield: 1.73 g (54 %). m.p. 200-210 °C. ^{1}H NMR (300 MHz, $CDCl_3$, δ): 1.46 (9H, s, Boc), 3.71, 3.84 (2H, dd, ^3J = 3.69, 3.66, Br-C*H*$_2$-CH), 3.81 (3H, s, OCH_3), 4.76 (1H, dt, J = 3.30 Hz, CH_2-C*H*-NH), 5.41 (1H, d, ^3J= 8.04 Hz, CH-N*H*); ^{13}C NMR (75 MHz, $CDCl_3$, δ); 28.29 (Boc CH_3), 34.10 (CH_2), 52.97 (OCH_3), 53.92 (CH), 154.98 (CO), 169.70 (CO); IR (ν_{max} / (cm^{-1}), Nujol): 3436, 2983 (CH), 1751 (C=O), 1709, 1440, 1369, 1369, 1309, 1164, 1068 (CO), 1012, 852. MS (+ES): 283 $[M+H)^+$.

6.7 Synthesis of mono-*N*-Boc cyclen (**2.24**)*.

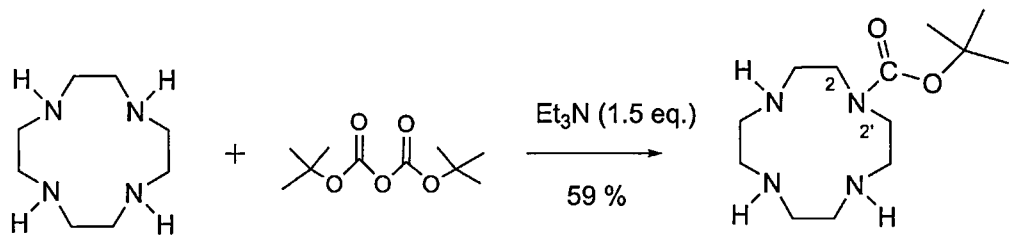

1 eq. 1 eq. **2.24**

A solution of di-*tert*-butyl carbonate (1.9 g, 8.7 mmol) in $CHCl_3$ (20 ml) was added slowly over 1 hour to a solution of cyclen (1.5 g, 8.7 mmol) and Et_3N (0.97 g, 9.6 mmol) in $CHCl_3$ (25 ml). After the reaction was stirred for 24 hours at RT, the organic solvent was removed under reduced pressure. The remaining residue was purified by alumina (neutral) column chromatography using a gradient of 0-15 % MeOH in $CHCl_3$ containing 0.5 % *i*PrNH$_2$.The title product **2.24** was a colourless, glassy, semi-solid. Yield: 1.4 g (59 %). A small amount of di-*N*-Boc-cyclen eluted first from the column. The mono-*N*-Boc cyclen eluted with 5-6 % MeOH in $CHCl_3$ containing 0.5 % *i*PrNH$_2$. R_f **2.24** = 0.62 (I_2, 15 % MeOH in $CHCl_3$ with 0.5 % *i*PrNH$_2$). ^{1}H NMR (300 MHz, $CDCl_3$, δ); 1.48 (s, 9H, $C(CH_3)_3$), 2.8 (s, 4H, CH_2), 3.0 - 3.1 (m, 8H, CH_2), 3.60 (d, ^2J =16.4 Hz, 4H, C2+C2'); ^{13}C NMR (75 MHz, $CDCl_3$, δ); 28.50 (Boc CH_3), 46.85 (CH_2), 48.7 (CH_2, C2/C2'), 48.8 (CH_2, C2/C2'), 50.50 (CH_2), 51.00 (CH_2), 80.71 (C_q), 155.73 (Boc CO); IR (ν_{max} / (cm^{-1}), KBr): 3522, 2976, 2818, 1691 (CO_{Boc}), 1464, 1418, 1366, 1272, 1250, 1171, 1100. MS (+ES): 272 $[M+H]^+$.

6.8 Alkylation of mono-*N*-Boc cyclen with **2.17** to give **2.25***.

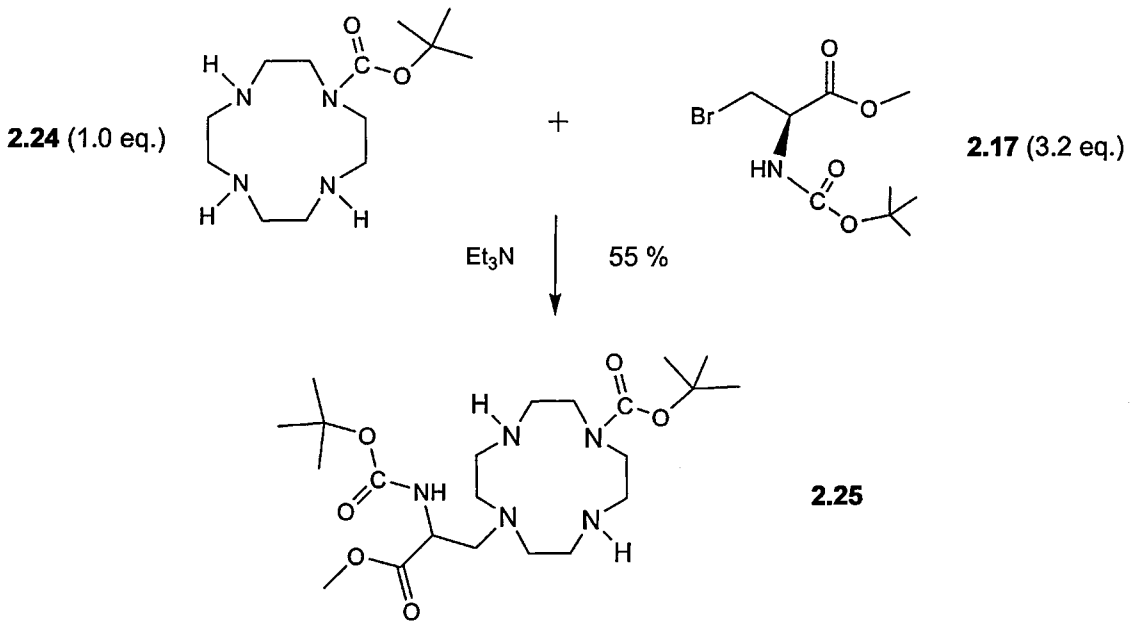

Mono-*N*-Boc-Cyclen (0.17 g, 0.61 mmol) and Et_3N (0.27 ml, 1.95 mmol) were dissolved in MeCN (15 ml) in a 100 ml round-bottomed flask. **2.17** (0.55 g, 1.95 mmol) was dissolved in MeCN (10 ml) and added dropwise to the round-bottomed flask over 15 min. The reaction was allowed to stir under argon at RT for 30 min. and then the temperature was increased to 80 °C. After 24 h, the reaction mixture was evaporated under reduced pressure to give a yellow oil. This residue was purified on an alumina column using a gradient of 0-10 % MeOH in $CHCl_3$. **2.25** was obtained as a viscous, yellow oil. Yield (0.17 g, 55 %). ^{1}H NMR (300 MHz, $CDCl_3$, δ); 1.48 (s, 18H, $C(CH_3)_3$), 2.48 (s, 4H, CH_2), 2.65 (m, 4H, CH_2), 2.81 (m, 4H, CH_2), 2.9 (m, 2H, CH_2), 3.0 (t, 4H, CH_2, ^3J = 4.77 Hz), 3.52 (CH_3), 3.0 - 3.1 (m, 8H, CH_2), 3.4-3.6 (m, 4H, CH_2); ^{13}C NMR (75 MHz, $CDCl_3$, δ); 28.50 (Boc CH_3), 43.3 (CH_2), 43.9 (CH_2), 50.9 (CH_2), 51.9 (CH_2), 54.6 (CH_2), 55.1 (CH_2), 56.2 (CH), 80.4 (C_q), 80.7 (C_q), 155.7 (Boc CO), 156.0 (Boc CO), 171.6 (CO). MS (+ES): 474.6 $[M+H]^+$.

6.9 Alkylation of mono-*N*-Boc cyclen with **2.17** using THF/ H_2O (30:1) as solvent [94].

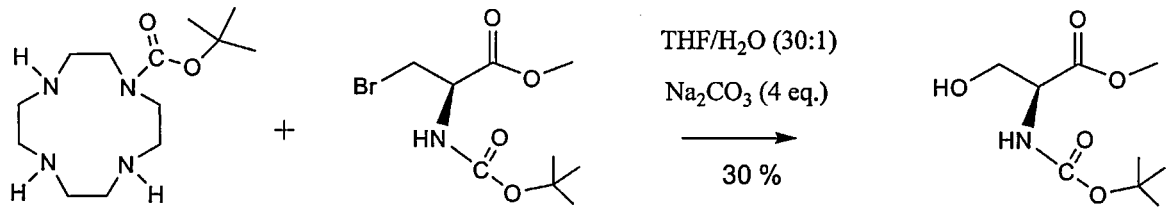

2.24 **2.17** (4 eq.) **2.14**

Mono-*N*-Boc-Cyclen (0.075 g, 0.27 mmol) and $Na_2CO_3.10\ H_2O$ (0.85 g, 1.09 mmol) were dissolved in THF/H_2O (30:1 ml) in a 100 ml round-bottomed flask. **2.17** (0.31 g, 1.1 mmol) was dissolved in THF (20 ml) and added dropwise to the round-bottomed flask over 30 min. After stirring overnight, solid material was collected by filtration and the filtrate was evaporated *in vacuo*. This residue was purified on an alumina column using a gradient of 0-10 % MeOH in $CHCl_3$. **2.14** was obtained as a viscous, oil with a yellow tinge. Yield (0.072 g, 30 %). ^1H NMR (300 MHz, $CDCl_3$, δ): 1.46 (s, 9H, Boc), 3.79 (s, 3H, OCH_3), 3.94 (dd, J = 3.84 Hz, 2H, CH_2), 4.39 (br t, 1H, CH), 5.48 (br s, 1H, NH); MS (+ES): 220 $[M+H]^+$.

Note: Although a peak corresponding to the disubstituted compound (**2.25**) was visible on LC-MS ($[M+H]^+$ = 475), **2.25** was not isolated from the reaction mixture.

6.10 Synthesis of mono-*N*-acetyl cyclen (**2.26**)*.

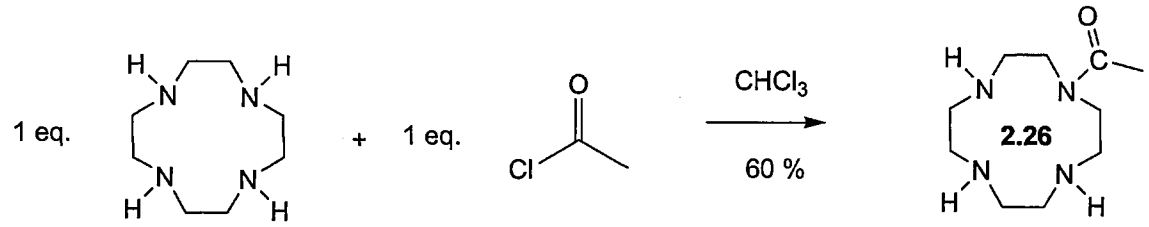

A solution of acetyl chloride (0.69 g, 7.4 mmol) in chloroform (25 ml) was added dropwise over 90 min. to a cooled solution of cyclen (1.5 g, 7.4 mmol) in chloroform (50 ml). The reaction was allowed to reach ambient temperature and stirred for a further 12 hours. The organic solvent was removed under reduced pressure and the residue dissolved in H_2O. The pH of the solution was adjusted to 11.0 with 5 % NaOH and re-extracted with $CHCl_3$ (3 x 50 ml). After drying over $MgSO_4$, the organic extracts were evaporated under reduced pressure to give an oil. The oil was purified on a silica gel column with 5 % MeOH in $CHCl_3$ containing 0.1 % *i*PrNH$_2$. Stirring of the resultant oil with acetone provided **2.26** as a white, crystalline, hygroscopic solid. Yield: 1.04 g (60 %). m.p. 187-190 °C, R_f = 0.25 (SiO_2, 10 % MeOH in $CHCl_3$ with 0.2 % *i*PrNH$_2$); ^{1}H NMR (300 MHz, $CDCl_3$, δ); 2.14 (3H, s, CH_3), 2.69 - 3.05 (12H, m, CH_2), 3.62 (4H, m, CH_2); ^{13}C NMR (75 MHz, $CDCl_3$, δ); 22.39 (CH_3) 44.70 (ring CH_2), 46.45 (ring CH_2), 46.93 (ring CH_2), 48.23 (ring CH_2), 172.15 (C=O); IR (ν_{max} / (cm^{-1}), KBr): 3513, 3362 (NH), 3294, 3200, 2934 (CH), 2783, 2337, 1638 (N-C=O), 1424, 1361, 1267, 1017, 912, 598, 493. HRMS (+ES): found $[M+H]^+$ 215.1868, $C_{10}H_{22}N_4O$ requires 215.1866.

6.11 Synthesis of *N*-acetyl-L-serine methyl ester to give **2.29**[**].

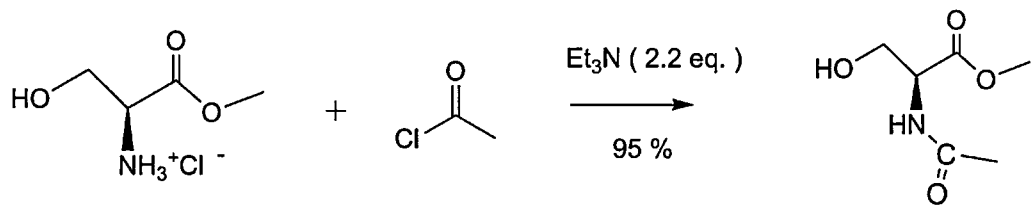

2.12 1 eq. **2.29**

L-serine methyl ester hydrochloride (5.0 g, 31.1 mmol) and triethylamine (7.14 g, 70.6 mmol) were dissolved in $CHCl_3$ (100 ml). Acetyl chloride (2.78 g, 35.3 mmol) in $CHCl_3$ (25 ml) was added dropwise over 30 minutes. The reaction was allowed to stir at RT overnight. The organic solvent was evaporated under reduced pressure and acetone was added to precipitate the bulk of the triethylammonium chloride (**2.29** was found to be soluble in acetone). However, the addition of acetone did not remove all of the triethylammonium chloride so the yellow residue was chromatographed on silica. The column was eluted with 5 % MeOH in DCM and then with 10 % MeOH in DCM. The relevant fractions were collected and evaporated under reduced pressure to give **2.29** as an oil with a slight yellow tinge. The oil was dried *in vacuo* for several hours. Yield: 4.9 g (95 %). R_f = 0.36 ($KmNO_4$; 10 % MeOH in DCM). ^{1}H NMR (300 MHz, CD_3OD, δ): 1.72 (3H, s, CH_3), 3.45 (3H, s OCH_3,), 3.49 (1H, dd, ^3J = 4.23 Hz, 4.20 Hz, HO-CH_2-CH), 3.58 (1H, dd, ^3J = 4.23 Hz, 4.20 Hz, HO-CH_2-CH), 4.22 (1H, t, ^3J = 4.38 Hz, CH), 4.55 (1H, br s, NH); ^{13}C NMR (75 MHz, CD_3OD, δ); 22.68 (CH_3), 49.85 (OCH_3), 56.5 (CH), 63.0 (CH_2), 172.59 (CO), 173.63 (CO). IR (ν_{max} / (cm^{-1}), film): 3277 (OH), 3083 (CH), 1736 (C=O), 1771, 1545, 1438, 1377, 1226, 1149, 1081 (CO), 983, 756. MS (+ES): 162 $[M+H]^+$, 322.7 $[2M+H]^+$. The spectral data agree well with published data for **2.29** [97].

6.12 Bromination of *N*-acetyl-L-Serine methyl ester to give **2.27**.

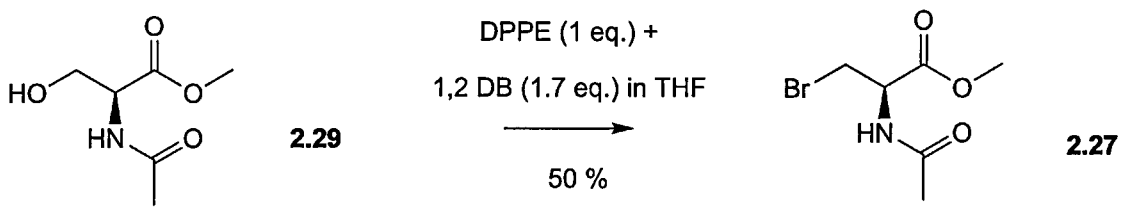

2.29 (2.0 g, 11.04 mmol, 1 eq.) and 1,2 dibromotetrachloroethane (6.31 g, 19.39 mmol, 1.7 eq.) were dissolved in 70 ml THF and 4.54 g DPPE (11.40 mmol, 1 eq.) was added in portions over 10 minutes. The reaction was allowed to stir at RT for 24 h. The suspension was then filtered through a 2.5cm plug of celite on a Buchner funnel. The celite was washed with THF (2 x 10 ml) and the combined filtrates were evaporated at 30 °C to give a yellow oil (9.86 g). This oil was purified on a silica gel column with 2 % MeOH in DCM containing 0.2 % *i*PrNH$_2$ (*i*PrNH$_2$ was added to the eluent as the product tended to adsorb strongly to the silica gel). Fractions containing **2.27** were evaporated under reduced pressure to give an off-white solid. Yield: 1.27 g, (50 %). R_f = 0.48 (fluoroscein spray, 2.5 % MeOH in DCM). m.p. 107-109 °C. ^{1}H NMR (300 MHz, CD3OD, δ): 1.92 (3H, s, CH_3), 3.67 (3H, s, OCH_3), 3.72 (1H, d, J = 4.2 Hz, CH_2), 3.35 (1H, t, J = 4.02 Hz, CH), 3.72 (1H, dd, ^2J = 1.47 Hz, ^3J = 3.84 Hz, CH_2); ^{13}C NMR (75 MHz, CD_3OD, δ); 22.23 (CH_3), 32.56 (CH_2), 53.19 (OCH_3), 54.89 (CH), 170.79 (CO), 173.27. Anal. Calcd (found) for $C_6H_{10}BrNO_3$: C, 32.16 (33.51); H, 4.50 (4.84); N, 6.25 (5.99). IR (ν_{max} / (cm^{-1}), KBr): 3436, 1749 (O-C=O), 1635 (N-C=O), 1521, 1442, 1376, 1242, 1046 (CO), 975, 778, 603. HRMS (+ES): found $[M+H]^+$ 222.9836 $C_6H_{10}NO_3Br$ requires 222.9839.

6.13 Synthesis of *N*-Z-L-Serine methyl ester (**2.30**).

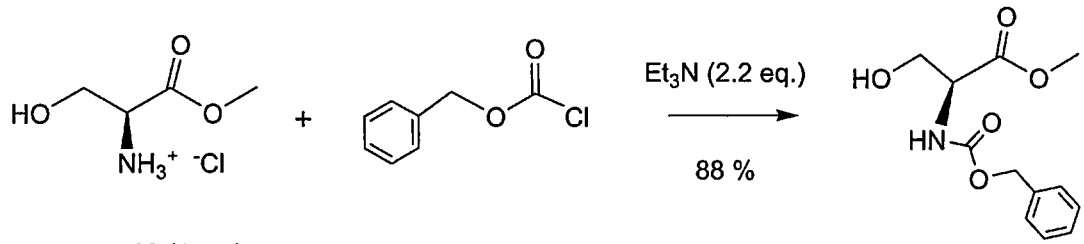

2.12 (1 eq.) 1.1 eq. **2.30**

L-serine methyl ester hydrochloride (3.0 g, 19.28 mmol) and Et_3N (4.29 g, 42.42 mmol) were dissolved in $CHCl_3$ (50 ml). Benzylchloroformate (3.62 g, 21.21 mmol) in $CHCl_3$ (25 ml) was added dropwise over 20 minutes. The reaction was allowed to stir at RT for 3 h. The organic solvent was evaporated under reduced pressure at 40 °C (to remove the bulk of the Et_3N). The residue was redissolved in $CHCl_3$ (50 ml) and washed with 50 ml 1M HCl (to remove traces Et_3N and LSME starting material) and then with H_2O (50 ml). After drying the extracts over $MgSO_4$, the organic solvent was evaporated under reduced pressure. The colourless, viscous oil was dried for 6 h *in vacuo*. Attempted crystallisation of this oil from ethyl acetate-hexane, DCM-hexane and EtOH-H_2O solvent pairs proved unsuccessful. Yield: 4.39 g (87.9 %). $R_f = 0.27$ (UV, 2.5 % MeOH in DCM). ^{1}H NMR (300 MHz, $CDCl_3$, δ): 3.77 (3H, s, OCH_3), 4.15 (2H, dd, ^3J = 4.23 Hz, CH_2), 4.59 (1H, t, ^3J = 4.38 Hz, CH), 5.12 (2H, s, CH_2-Arom), 5.74 (1H, br s, NH), 7.35 (5H, s, Arom CH): ^{13}C NMR (75 MHz, $CDCl_3$, δ); 52.77 (CH_3), 56.04 (CH), 63.29 (CH_2), 67.24 (CH_2), 128.28 (CH Arom), 157.10 (CO), 170.98 (CO). IR (ν_{max} / (cm^{-1}), film): 3374 (OH), 2949 (CH), 1716 (C=O), 1529, 1454, 1343, 1216, 1059 (CO), 981, 912, 743 (arom), 701 (arom), 457. MS (+ES): 254 $[M+H]^+$.

6.14 Synthesis of 1-bromo-*N*-Z-L-Serine methyl ester (**2.28**).

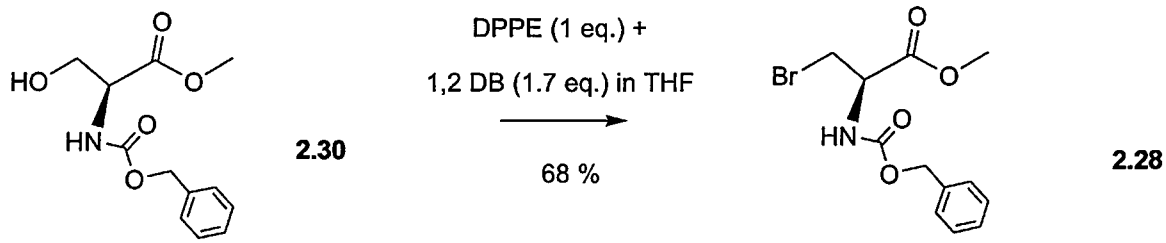

2.30 **2.28**

2.30 (6.0 g, 23.7 mmol) and 1,2 DB (15.43 g, 47.4 mmol) were dissolved in 75 ml THF in a 250 ml conical flask. The mixture was cooled on an ice-bath and DPPE (9.4 g, 23.7 mmol) was added in portions over 10 minutes. The reaction was allowed to stir at RT overnight under argon and then filtered through a 2.5 cm plug of celite on a Buchner funnel. After washing the celite with THF (2 x 10 ml), the combined filtrates were evaporated under reduced pressure at 30 °C to give a yellow oil (19.9 g). The oil was purified on a silica gel column with DCM containing 1 % MeOH to give **2.28** as a white solid. Yield: 5.1 g, (67.8 %). $R_f = 0.54$ (fluoroscein spray, 1 % MeOH in DCM). ^{1}H NMR (300 MHz, $CDCl_3$, δ): 3.74, 3.84 (2H, dd, $^3J = 3.48$ Hz, Br-CH_2-CH), 3.80 (3H, s OCH_3,), 4.82 (1H, dt, $^3J = 3.3$ Hz, CH_2-C*H*-NH), 5.13 (2H, s, CH_2-Arom), 5.63 (1H, d, $^2J = 7.14$ Hz, NH), 7.37 (5H, s, C_6H_5); ^{13}C NMR (75 MHz, $CDCl_3$, δ); 33.69 (CH_2-Br), 53.09 (OCH_3), 54.31 (CH), 67.33 ($\underline{C}H_2$-Arom), 129.32 (benzyl CH), 155.54 (CO), 169.32 (CO). MS (+ES): 316.57 $[M+H]^+$, 338.57 $[M+Na]^+$.

6.15 Alkylation of mono-*N*-acetyl cyclen with **2.27** to give **2.31*** and **2.32**.

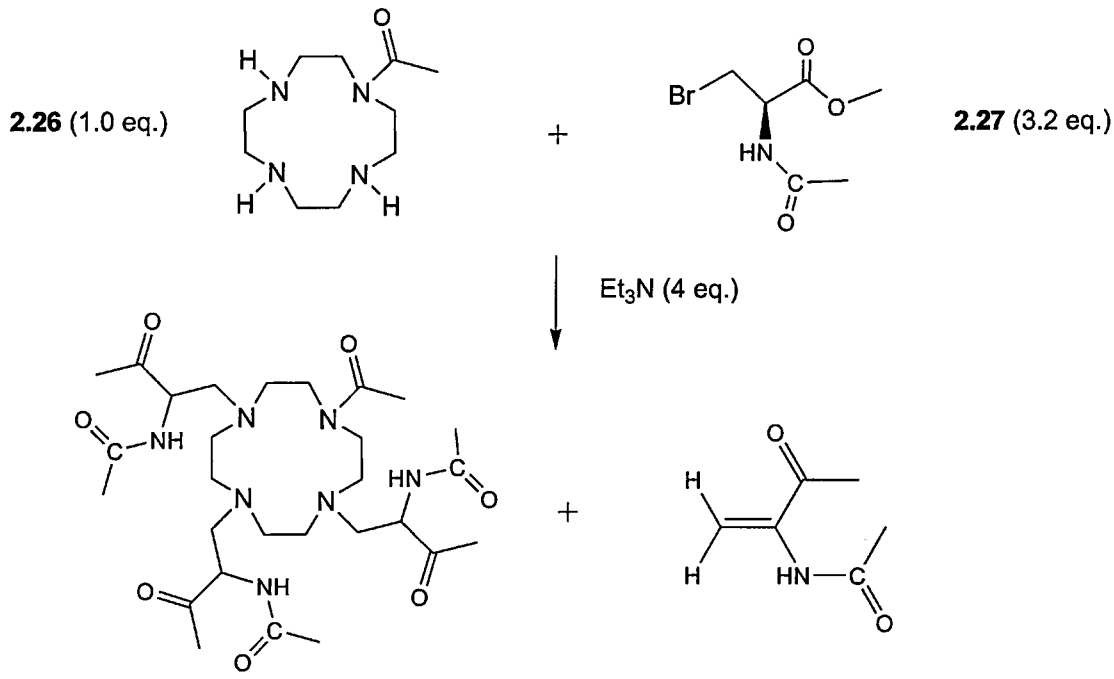

Mono-*N*-acetyl cyclen (168 mg, 0.78 mmol) and Et_3N (0.30 g, 4 eq.) were dissolved in acetonitrile (20 ml) in a twin-necked round-bottomed flask (100 ml). **2.27** (0.7 g, 3.14 mmol) in acetonitrile was added dropwise and the reaction allowed to stir at room temperature overnight under argon. The reaction was then heated at 60 °C for a further 12 hours. Acetonitrile was removed under reduced pressure to give a viscous, orange oil (0.62 g). Purification of the oil was carried out on an alumina column with 5 % MeOH in $CHCl_3$. **2.32** (white solid): ^{1}H NMR (300 MHz, $CDCl_3$, δ): 2.14 (s, 3H, CH_3), 3.85 (s, 3H, CH_3), 3.85 (s, R=CH, CH_2), 5.89 (s, 1H, R=CH), 6.60 (s, 1H, R=CH). MS: 255.1 $[M+H]^+$. The title product (**2.31**) eluted as a viscous, yellow oil. Crystallisation of the oil was achieved by dissolving it in $CHCl_3$ and adding Et_2O dropwise until turbidity. Yield: 0.10 g (15 %) R_f **2.31** = 0.78 (5 % MeOH in $CHCl_3$; $KMnO_4$). ^{1}H NMR (300 MHz, $CDCl_3$, δ): 1.96 (s, 9H, NHCOC*H*$_3$), 2.03 (s, 3H, CH_3), 2.2 - 3.75 (m, 29 H, CH_2 + CH), 3.33 (s, 3H, CH), 3.68 (s, 9H, CO_2CH_3), 4.61 (br s, 3H, NH); ^{13}C NMR (75 MHz, $CDCl_3$, δ): 21.76

(CH$_3$), 23.03 (CH$_3$), 48.35 (CH$_2$), 50.90 (CH$_2$), 51.27 (CH), 52.49 (CH$_3$), 171.20 (CO), 172.65 (CO). HRMS (+ES): found $[M+H]^+$ 644.3624 $C_{28}H_{49}N_7O_{10}$ requires 644.3614.

6.16 Alkylation of cyclen with **2.28** to give **2.33*** and **2.34**

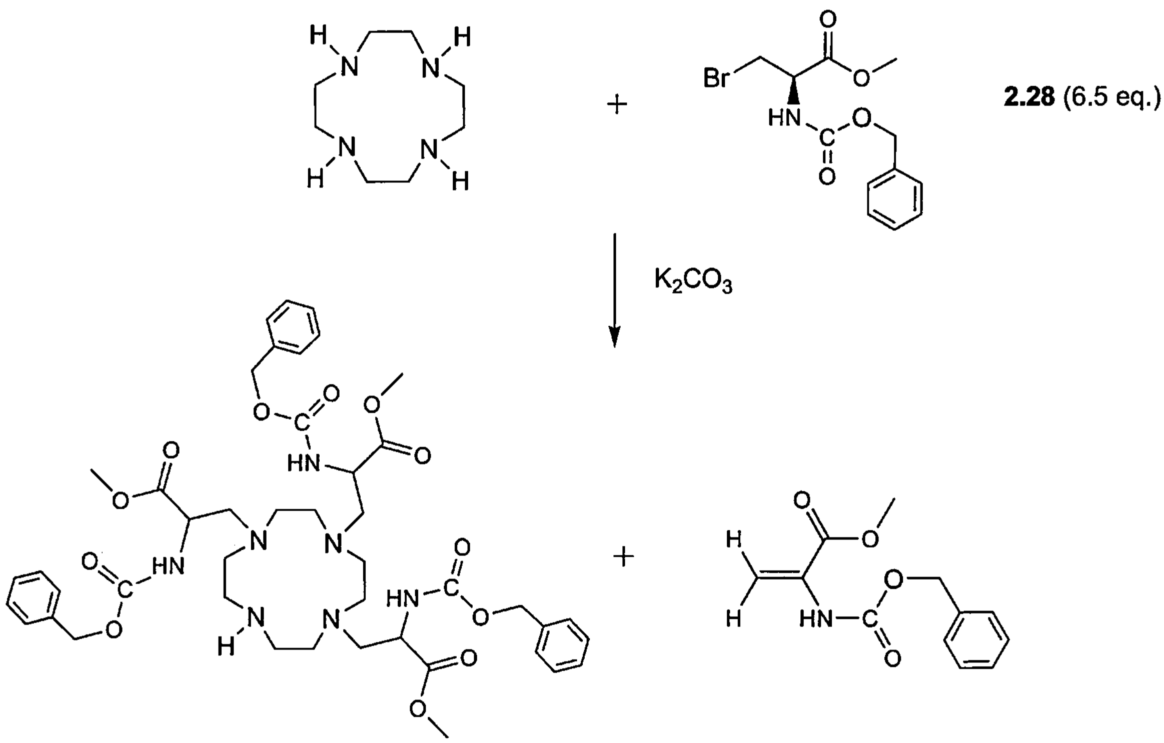

2.33 (4.2 %) **2.34** (90 %)

To a suspension of cyclen (0.39 g, 2.3 mmol) and K_2CO_3 (1.09 g, 3.5 eq.) in MeCN (25 mL) was added **2.28** (2.5 g, 7.9 mmol, 3.5 eq.) in MeCN (25 mL) dropwise. The reaction mixture was stirred for 24 h at RT. LC-MS analysis indicated formation of mono- and di-substituted cyclens. To promote substitution, an extra 3 eq. **2.28** (2.14 g, 6.8 mmol) was added and the mixture stirred for a further 48 h. LC-MS indicated **2.33** had formed so the reaction was stopped. The K_2CO_3 was filtered off and the organic layer evaporated to give a yellow oil (3.32 g). Partitoning of this oil between water (50 ml) and $CHCl_3$ (50 ml) successfully separated the mono-substituted cyclen (aqueous layer) from the di- and tri-substituted cyclen products (organic layer). The organic layer was then dried over

magnesium sulfate, filtered and evaporated to give a viscous, orange oil (2.74 g). The resulting oil was purified by chromatography using 5 % MeOH in DCM to give **2.34** as a colourless oil. Yield: 1.69 g (90.8 %). R_f = 0.84 (UV, CH_2Cl_2-MeOH, 9 : 1). ^1H NMR (300 MHz, $CDCl_3$): 3.75 (s, 3H, CH_3), 5.09 (s, 2H, CH_2), 5.65 (s, R=CH, CH_2), 6.17 (s, 1H, CH=R), 7.29 (m, 1H, CH=R). MS (+ES): 257.5 $[M+Na]^+$. **2.33** was obtained as a yellow, semi-solid. (R_f = 0.56, CH_2Cl_2-MeOH, 9 : 1). Yield: 0.29 g (4.2 %). ^1H NMR (300 MHz, $CDCl_3$): 2.63-2.86 (16H, m, cyclen CH_2), 3.62 (9H, s, 3 x CH_3), 5.03 (6H, s, O-CH_2-Ph), 7.19-7.29 (15H, m, 3 x phenyl), 9.67 (3H, br s, 3 x NH); ^{13}C NMR (75 MHz, $CDCl_3$, δ): 52.67 (CH_2), 66.85 (OCH_2), 128.0 (Ph), 136.17 (Ph), 156 (NH-CO), 171.63 (C=O-O). HRMS (+ES): found $[M+H]^+$ 878.4294 $C_{44}H_{59}N_7O_{12}$ requires 878.4302.

6.17 DCC-mediated coupling of 2-bromoethylamine to cholic acid.

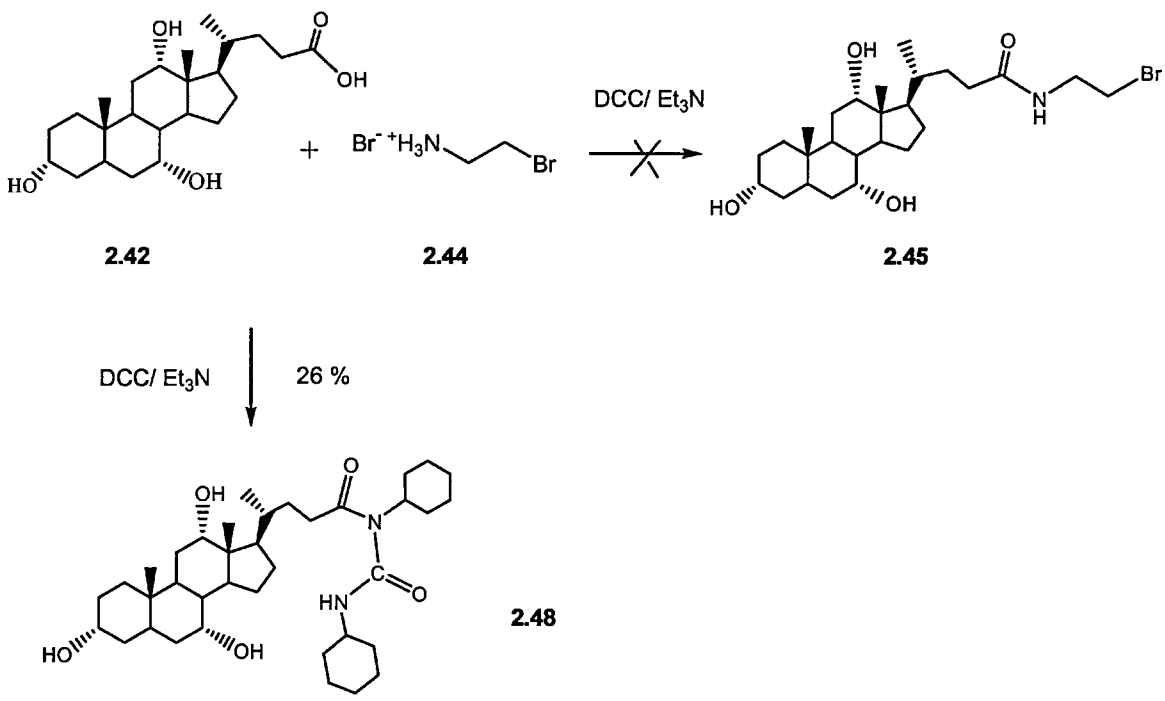

2-bromoethylamine hydrobromide (0.2 g, 1 mmol), Et_3N (0.16 ml, 1.1 mmol) and cholic acid (0.41 g, 1 mmol) were dissolved in DCM (20 ml). DCC (0.23 g, 1.1 mmol) was added in small portions over 10 min. As cholic acid was not fully-soluble, 2 ml DMF (dry) was added to the reaction mixture. The reaction was allowed to stir at RT overnight. The white dicyclohexylurea precipitate which developed was filtered off. The filtrate was washed with H_2O (25 ml) and evaporated under reduced pressure. TLC of the residue on silica gel using 10 % MeOH in DCM showed up two spots, one with an R_f identical to cholic acid (0.16) and the second spot had an $R_f = 0.26$. The residue was applied on to a silica column and chromatographed with 0 - 12 % MeOH in DCM. **2.48** eluted at 9 % MeOH in DCM. Evaporation of the solvent gave a white solid. Yield: 1.1 g (26.3 % based on 10 mmol cholic acid).

N-acylurea derivative of cholic acid (**2.48**)*.

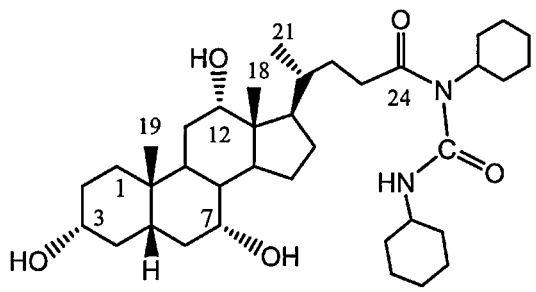

2.48

m.p. 130-137 °C, R_f = 0.24 (PMA, UV active; 10 % MeOH in $CHCl_3$); ^1H NMR (300 MHz, $CDCl_3$, δ): 0.68 (3H, s, 18-CH_3), 0.89 (3H, s, 19-CH_3), 0.99 (3H, d, J = 6.1 Hz, 21-CH_3), 1.08 - 2.52 (44H, m, aliph), 2.76 (1H, br s, NH), 3.45 (1H, m, CH), 3.68 (1H, m, CH), 3.85 (1H, d, J = 2.55 Hz, 7β-H), 3.97 (1H, s, 12β-H): 12.48 (CH_3-18), 17.53 (21-CH_3), 22.46 (19-CH_3), 24.72 (CH_2), 25.32 (CH_2), 25.47 (CH_2), 26.30 (CH), 26.46 (CH_2), 30.90 (CH_2), 31.45 (CH_2), 32.69 (CH_2), 34.58 (CH_2), 34.72 (CH_2), 35.42 (CH_2), 39.54 (CH_2), 41.44 (CH), 41.74 (CH), 46.51 (CH), 46.83 (CH), 49.81 (CH), 68.45 (C^3H-OH), 71.94 (C^7H-OH), 72.99 (C^{12}H-OH), 77.43 (CH), 154.17 (CO), 172.3 (C^{24}O): IR (ν_{max} / (cm^{-1}), KBr): 3347 (OH), 2932 (CH stretch), 1689 (amide I), 1610 (amide II, CO), 1527, 1451, 1380, 1078 (CO stretch), 612. HRMS (+ES): found $[M+H]^+$ 615.4730. $C_{17}H_{36}N_7O_3$ requires 615.4731.

Note: The assignment of individual carbon and proton resonances was aided by comparison with reference spectra [104] and by cross-referencing with data from a ^1H - ^{13}C COSY spectrum.

6.18 Esterification of cholic acid with *p*-nitrophenol to give **2.51** and **2.48**.

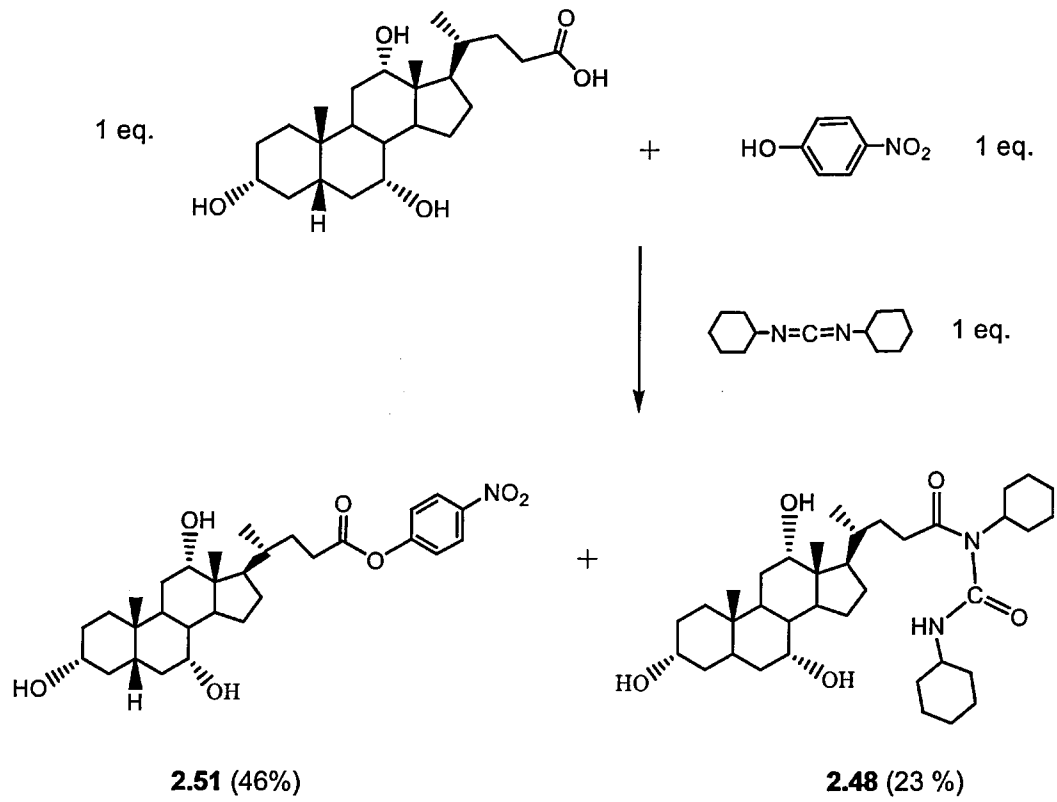

2.51 (46%) **2.48** (23 %)

To a solution of cholic acid (4.1 g, 10 mmol) in 80 ml ethyl acetate and DMF (15 ml), *p*-nitrophenol (1.39 g, 10 mmol) was added. The reaction mixture was cooled on an ice bath and dicyclohexylcarbodiimide (DCC, 2.1 g, 10 mmol) was added with stirring. After 20 h stirring at RT, the dicyclohexylurea (DCU) which precipitated was filtered off. The organic phase was washed with a 5 % sodium carbonate solution (100 ml), 4 x 50 ml water (to remove the yellow colour of *p*-nitrophenol). Evaporation of the solvent gave an orange, crystalline material. TLC of the product on silica using 10 % MeOH in $CHCl_3$ showed two spots, R_f **2.51** = 0.36 (uv-active, *p*-np ester), R_f **2.48** = 0.28 (R_f cholic acid = 0.14). Both spots were detected with phosphomolybdic acid spray reagent. Although the R_f values of both compounds were similar, 1.7 g crude product was successfully purified on a silica gel column (52 g) using a gradient of 0 - 11 % MeOH in chloroform.

p-nitrophenyl ester of cholic acid (**2.51**).

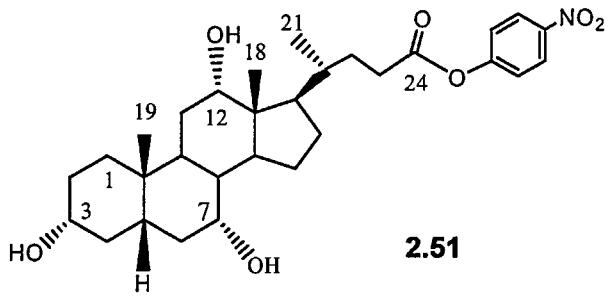

2.51

Off-white crystals. Yield: 1.9 g (43.5 % based on 10 mmol cholic acid). R_f = 0.31 (PMA, UV active; 10 % MeOH in $CHCl_3$). m.p. 122-125 °C (Lit. [106], 123-125 °C). ^{1}H NMR (300 MHz, $CDCl_3$): δ 0.71 (3H, s, CH_3, 18-CH_3), 0.89 (3H, s, CH_3, 19-CH_3), 1.06 (3H, d, J = 6.1 Hz, 21-CH_3), 1.28 - 2.72 (27H, m, aliph H), 3.50 (1H, m, 3β-H), 3.86 (1H, d, J = 2.58, 7β-H), 3.99 (1H, s, 12β-H), 7.27 (2H, d, J = 10.8 Hz, arom CH), 8.27 (2H, d, J = 10.8 Hz, arom CH); ^{13}C NMR (75 MHz, $CDCl_3$): δ 12.55 (CH_3-18), 17.36 (CH_3-21), 22.49 (CH_3-19), 23.21 CH_2), 26.52 (CH), 27.55 (CH_2), 28.33 (CH_2), 30.46 (CH_2), 30.68 (CH_2), 31.30 (CH_2), 34.68 (CH_2), 34.74 (CH), 35.19 (CH_2), 39.52 (CH_2), 41.42 (CH), 41.83 (CH), 46.50 (CH), 46.96 (C), 68.47 (C^3H-OH), 71.94 (C^7H-OH), 73.04 (C^{12}H-OH), 122.43 (arom CH), 125.21 (arom CH), 145.2 (arom-NO_2), 155.53 (O-C-arom), 171.79 (C^{24}=O); IR (ν_{max} KBr/cm^{-1}): 3392 (OH), 2928 (CH stretch), 2862, 2108, 1764 (C=O), 1692, 1641, 1517 (conjugated NO_2), 1448, 1343 (conjugated NO_2), 1204, 1074, 1038, 984, 918, 858, 610. MS (+ES) 530 (MH^+), 547 (MNH_4^+).

6.19 Synthesis of **2.45*** via cholyl *p*-nitrophenyl ester (**2.51**).

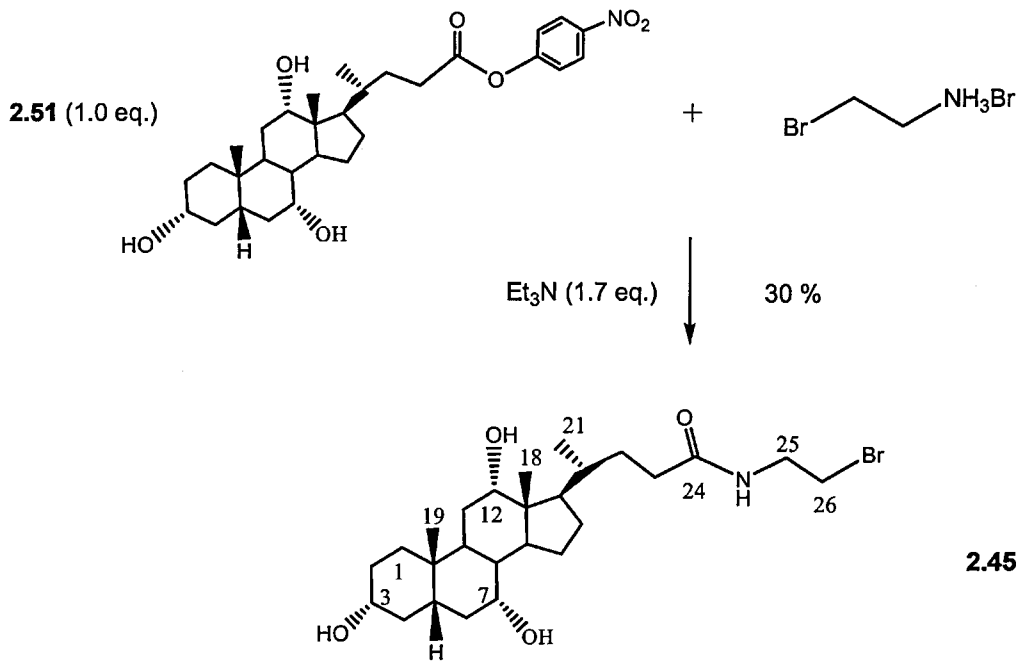

2.45

To a cooled solution of cholyl *p*-nitrophenyl ester (0.33 g, 0.64 mmol) and 2-bromoethylamine (0.198 g, 0.964 mmol, 1.5 eq.) in THF (60 ml, dry), Et_3N (0.16 ml, 1.1 mmol, 1.7 eq.) in THF (20 mL) was added dropwise over 30 min. After stirring the reaction for 12 h at RT, the organic layer was washed with 5 % NaH_2CO_3 and then with water to remove free *p*-nitrophenol (yellow colour). After evaporation of the solvent, the residue was purified on a silica gel column using 10 % MeOH in $CHCl_3$ to give **2.45** as an off-white solid. Yield: 0.15 g (30 %). R_f = 0.35 (fluoroscein-peroxide; 10 % MeOH in $CHCl_3$); m.p. 66 - 70 °C. ^{1}H NMR (300 MHz, $CDCl_3$): δ 0.67 (3H, s, CH_3, 18-CH_3), 0.88 (3H, s, CH_3, 19-CH_3), 1.01 (3H, d, J = 5.49 Hz, 21-CH_3), 1.23 - 1.98 (19H, m, aliph H), 2.2 (3H, s, OH), 2.96 (2H, s, CH_2), 3.45 (2H, m, CH), 3.79 (2H, t, J = 9.54 Hz, $C^{25}H_2$), 3.95 (1H, s, CH), 4.22 (2H, t, J = 9.51 Hz, $C^{26}H_2$), 8.02 (1H, br s, NH); ^{13}C NMR (75 MHz, $CDCl_3$):): δ 12.48 (CH_3-18), 17.45 (CH_3-21), 22.52 (CH_3-19), 24.98 CH_2), 25.32 (CH_2), 26.52 (CH), 27.62 (CH_2), 28.33 (CH_2), 30.46 (CH_2), 30.68 (CH_2), 31.01 (CH_2), 34.68 (CH_2), 35.30 (CH), 35.73 (CH), 36.49 (CH_2), 68.31 (C^3H-OH), 71.84 (C^7H-OH),

72.93 ($C^{12}H$-OH), 169.59 (C=O-N); IR (ν_{max} KBr/cm^{-1}): 3328 (OH), 2933 (C-H str), 1660 (amide I, CO), 1643 (amide II, CO), 1533, 1451, 1369, 1078 (C-O str), 981, 914, 690. MS (+ES): 434 $[M\text{-}Br+H]^+$. MS (-ES): 512.4 $[M\text{-}H]^-$.

6.20 Synthesis of *N*-Boc-2-bromoethylamine (**2.46**).

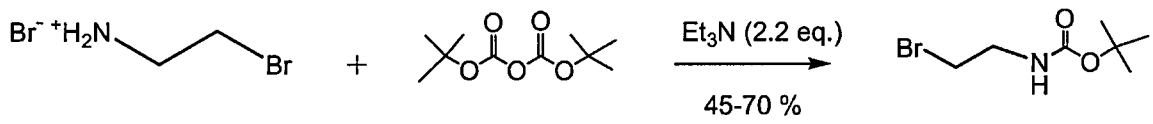

2.44 (1 eq.) 1.2 eq. **2.46**

2-bromoethylamine hydrobromide (0.41 g, 2 mmol) and Et_3N (4.4 mmol, 0.48 g) were added to a 1:1 mixture of dioxane and H_2O (40 ml) on an ice bath. Di-*tert*-butyldicarbonate (0.148 g, 2.2 mmol) was added in portions over approximately 10 min. The ice bath was removed and the mixture was allowed to stir at RT for 24 hours. As the pH of the solution was adjusted to 2.5 with 1M HCl, an evolution of CO_2 bubbles was observed. The reaction mixture was then extracted with DCM (2 x 50 ml). The extracts were pooled, washed with water, dried over $MgSO_4$ and evaporated *in vacuo*. The product was a clear, colourless, viscous oil. TLC on silica gave a single spot with an R_f = 0.48 ($KMnO_4$; hexane-Et_2O, 80/20). ^1H NMR (300 MHz, $CDCl_3$, δ): 1.45 (s, 9H, Boc), 3.38 - 3.55 (m, 4H, 2 x CH_2), 4.99 (br s, 1H, NH); ^{13}C NMR (75 MHz, $CDCl_3$, δ): 28.31 (Boc CH_3), 32.78 (CH_2), 42.32 (CH_2), 79.75 (C_q), 156.20 (CO); IR (ν_{max} / (cm^{-1}), film): 3347 (NH), 2924, 2854, 2361, 2342, 1725 (C=O), 1709, 1503, 1462. MS (+ES): 224 ($M+H^+$). Note: yields for this reaction varied from 45 - 70 %.

6.21 Alkylation of cyclen with *N*-Boc-2-bromoethylamine.

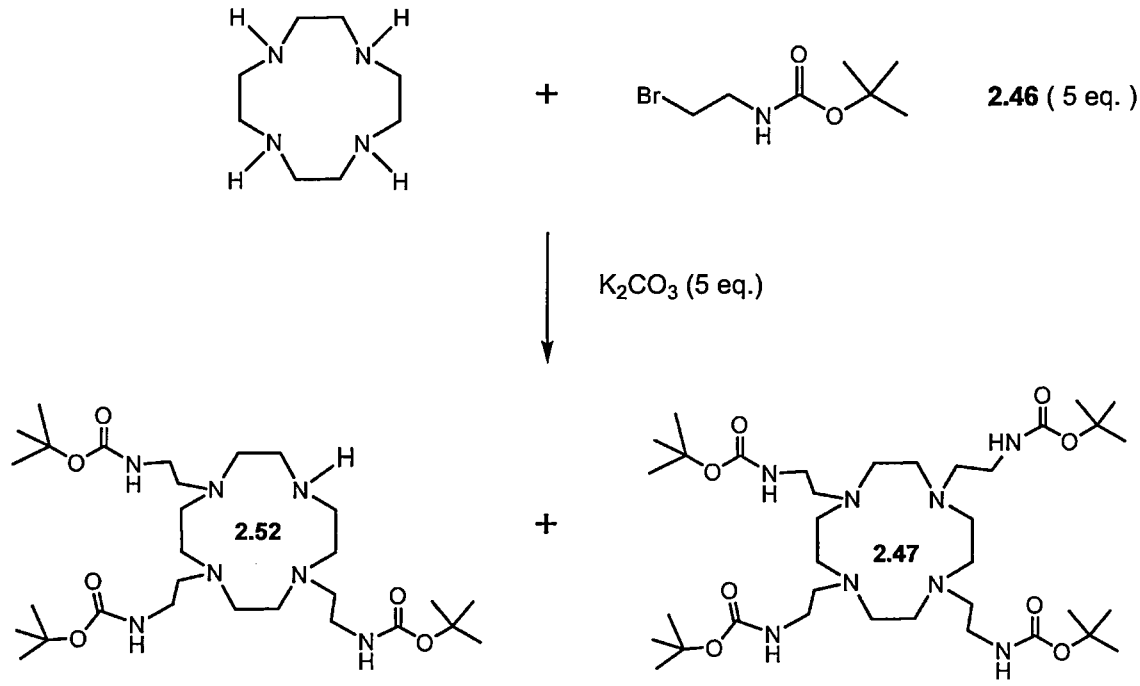

Cyclen (78.4 mg, 1 eq.) and K_2CO_3 (0.32 g, 5 eq.) were refluxed with **2.46** (0.51 g, 5 eq.) in acetonitrile for 12 hours. LC-MS (+ES) of the product residue indicated that a mixture of tri-*N*-substituted cyclen ($[M+H]^+ = 460$) and tetra-*N*-substituted cyclen ($[M+H]^+ = 603$) were formed. Attempted purification of the product residue on a silica gel column using a gradient of 0 - 15 % methanol in chloroform resulted in poor separation between **2.52** and **2.47**.

6.22 Syntheses of 1,4,7,10-tetrazacyclododecane-4,7,10-tripropanamide (**3.9**)* and 1,4,7,10-tetrazacyclododecane-1,4,7,10-tetrapropanamide (**3.10**)*.

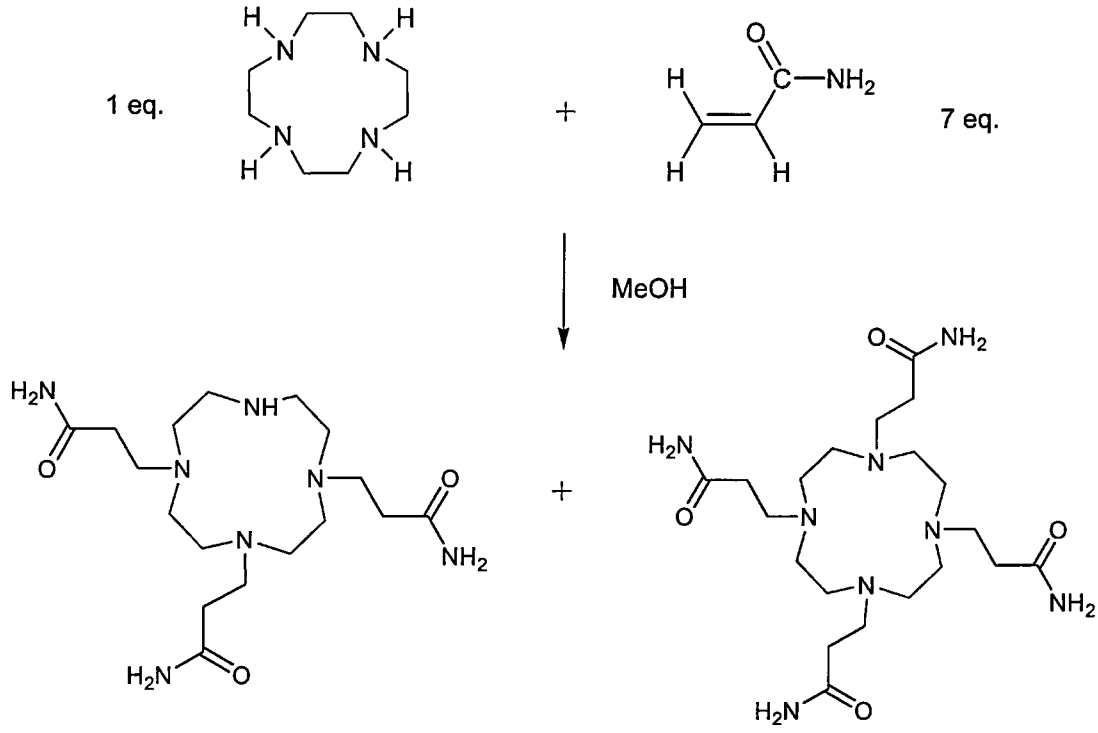

3.9 (70 %) **3.10** (8 %)

Acrylamide (2.5 g, 35 mmol) and cyclen (0.86 g, 5 mmol) were dissolved in 75 ml methanol. The solution was heated under reflux for 24 h. After most of the methanol was removed under reduced pressure, diethyl ether was added until a white solid formed. The resultant white solid was filtered, washed with ether (2 x 20 ml) and dried under vacuum. Separation of **3.9** from **3.10** was achieved on a silica gel column using 5 % ethanol in dichloromethane as eluent. **3.10** was obtained as a colourless, solid. Yield: 0.18 g hygroscopic, white solid (8 %). m.p. 174-177 °C. $R_f = 0.62$ (Ninhydrin; $CHCl_3$, MeOH, 33 % aq. NH_3, 1:1:0.5 by volume respectively. ^1H NMR (300 MHz, D_2O, δ): 2.27 (8H, t, NCH_2, $^3J = 6.8$ Hz), 2.53 (16H, s, ring CH_2), 2.60 (8H, t, CH_2CONH_2, $^3J = 6.8$ Hz). HRMS (+ES): found $[M+H]^+$ 457.3235. $C_{19}H_{45}N_4O_8$ requires 457.3232.

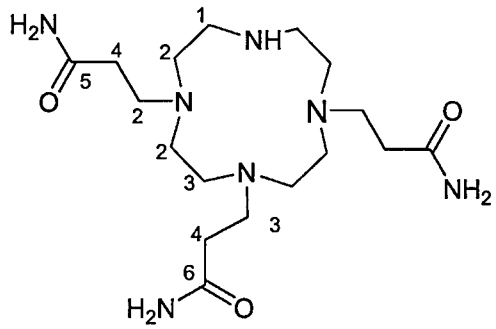

3.9

Yield **3.9**: 1.35 g hygroscopic, white solid (70 %). m.p. 170-172 °C. $R_f = 0.57$ (Ninhydrin; $CHCl_3$, MeOH, 33 % aq. NH_3, 1:1:0.5 by volume respectively). ^1H NMR (300 MHz, D_2O, δ): 2.29 (6H, t, $^3J = 6.7$ Hz, $NCH_2CH_2CONH_2$, 4), 2.42 (4H, br s, ring CH_2, 1), 2.55 (12H, br s, ring CH_2, 2+6), 2.62 (6H, t, $^3J = 6.8$ Hz, $NCH_2CH_2CONH_2$, 3); ^{13}C NMR (75 MHz, D_2O, δ); 32.36 ($\underline{C}H_2CONH_2$, 4), 45.15 (CH_2, 1), 50.01 (CH_2, 2), 50.42 (CH_2, 2), 50.59 (CH_2, 2), 51.16 (CH_2, 3), 51.33 (CH_2, 3), 178.62 (C=O, 5), 179.11 (C=O, 6). Anal. Calcd (found) for $C_{17}H_{35}N_7O_3 \cdot 1.0\ H_2O \cdot 0.37\ CH_3OH$: C, 50.23 (50.41); H, 9.34 (9.12); N, 23.60 (23.46). IR (ν_{max} / (cm^{-1}), KBr): 3349 (NH), 3154 (NH), 2969 (CH), 2837, 1673 (C=O), 1424. HRMS (+ES): found $[M+H]^+$ 386.2878. $C_{17}H_{36}N_7O_3$ requires 386.2874.

Note: Individual carbon and proton resonances were assigned by data from a ^1H - ^{13}C COSY experiment and by comparison with the spectra of structurally-similar ligands [123].

6.23 Hydrolysis of **3.9** to give 1,4,7-tris-(2-carboxylethyl)-1,4,7,10-tetrazacyclododecane (**3.11**)*.

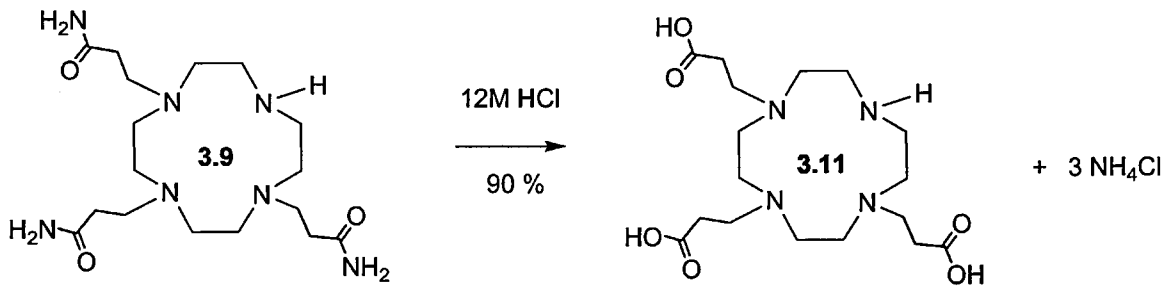

3.9 (0.3 g, 0.78 mM) was dissolved in 10 ml HCl (12 M) and refluxed vigorously for 2 h. The reaction was switched off and allowed to cool overnight. The white solid which developed was filtered off and re-dissolved in H_2O. After the H_2O was removed by lyophilisation, the white solid was recrystallised twice from aqueous methanol. The product was then dried in a vacuum oven at 50 °C for 12 h to give **3.11** as a white solid. Yield: 0.27 g (90.1 %). m.p. 180-183 °C. ^{1}H NMR (300 MHz, D_2O, δ): 2.63 (6H, t, ^3J = 6.6 Hz, CH_2CH_2COOH), 3.01 (22 H, br s, ring CH_2 + arm NCH_2CH_2); ^{13}C NMR (75 MHz, D_2O, δ); 28.83 (CH_2), 49.07 (CH_2), 176.13 (C=O). Anal. Calcd (found) for $C_{17}H_{32}N_4O_6 \cdot 1.0\ H_2O \cdot 1.0$ HCl: C, 46.1 (45.9); H, 7.9 (7.7); N, 12.7 (12.5). IR (ν_{max} / (cm^{-1}), KBr): 3076 (OH), 1753 (C=O), 1411, 798, 653. HRMS (+ES): found $[M+H]^+$ 389.2395. $C_{17}H_{33}N_4O_6$ requires 389.2395.

6.24 Reaction of cyclen with 1-cyanovinylacetate to give **3.17** (**3.21**)*.

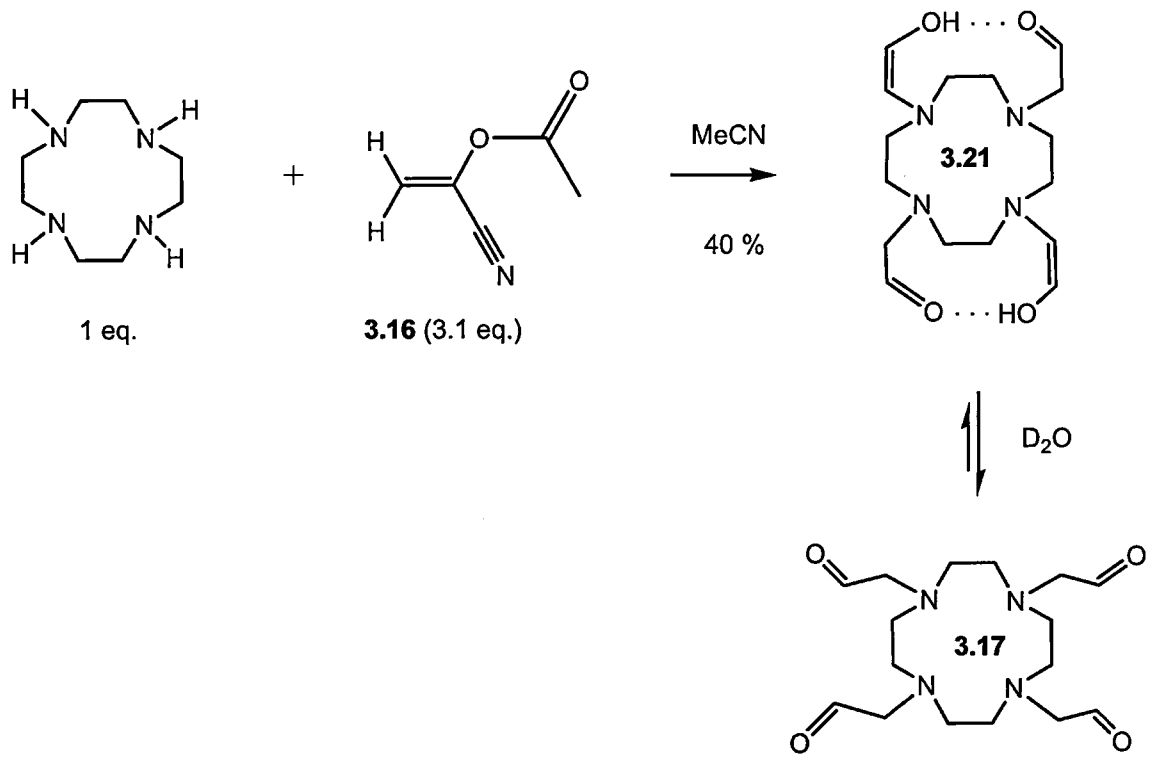

Cyclen (0.3 g, 1.74 mmol) was dissolved in dry acetonitrile (15 ml) under an argon atmosphere. Cyanovinylacetate (0.59 g, 3.1 eq.) was added in dropwise over 10 min. An off-white, solid began to precipitate out of solution after approx. 10 min. After centrifugation of the reaction mixture, the white precipitate was collected and purified by recrystallisation from aqueous acetonitrile. Yield: 0.24 g (40 %). m.p. 175 °C (with decomposition). ^{1}H NMR (300 MHz, D_2O): 2.01 (br s, 16H, CH_2), 3.52 (d, 8H, J = 6.3 Hz, CH_2), 9.73 (t, 1H, J = 6.3 Hz, CHO); ^{13}C NMR (75 MHz, D_2O, δ); 50.42 (CH_2), 65.42 (CH_2), 199.25 (CHO); Anal. Calcd (found) for $C_{16}H_{28}N_4O_4$: C, 56.45 (56.56); H, 8.29 (8.07); N, 16.45 (16.56). IR (ν_{max} / (cm^{-1}), KBr): 3431 (OH), 2987, 2837, 1652 (enol, C=C-OH). HRMS (+ES): found $[M+H]^+$ 341.2183. $C_{16}H_{28}N_4O_4$ requires 341.2183.

6.25 Synthesis of ethyl 3-hydroxy-2-nitropropanoate (**3.24**).

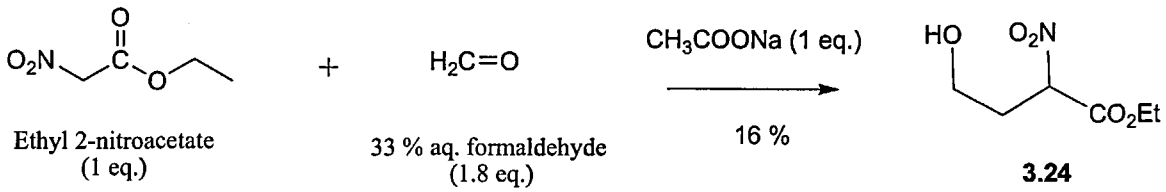

Ethyl 2-nitroacetate (1 eq.) + $H_2C{=}O$ (33 % aq. formaldehyde (1.8 eq.)) → **3.24**

An ice bath at -15 °C was prepared from ice, IMS and salt. Ethyl 2-nitroacetate (8.5 g, 0.064 moles) and 33 % aqueous formaldehyde (10 ml, 0.12 moles) were added to a small conical flask and cooled on the bath. Sodium acetate (0.16 g in 1 ml H_2O) was added with intensive mixing and the reaction was stirred for 3 h. The reaction was quenched by pouring the mixture onto 50 g crushed ice containing 1 ml conc. HCl. The oil that separated was extracted with Et_2O. The Et_2O extract was then dried over Na_2SO_4. After evaporation of the Et_2O, the oil was distilled in a short-path distillation apparatus under vacuum (0.3 mm Hg). Three fractions were collected: Fraction A; b.p. 40 °C (1.23 g); Fraction B; b.p. 44 °C (0.9 g); Fraction C; b.p. 80 - 105 °C (1.42 g). Fraction C was purified on a silica gel column (60 g) using 10 % ethyl acetate in DCM as eluent to give a colourless oil with a slight yellow tinge. Yield: 0.96 g (15.7 %). R_f = 0.39 ($KMnO_4$, UV active; 10 % ethyl acetate in CH_2Cl_2); ^{1}H NMR (300 MHz, $CDCl_3$, δ): 1.33 (3H, t, ^2J = 7.14 Hz, CH_3), 4.28 - 4.38 (4H, m, $CHCH_2CH_2OH$), 5.30 (1H, dd, ^2J = 3.84, 4.02 Hz, $CHNO_2$); ^{13}C NMR (75 MHz, $CDCl_3$, δ); 13.73 (CH_3), 60.82 (CH_2), 63.45 (CH_2), 88.36 ($CHNO_2$), 162.86 (C=O); IR (ν_{max} / (cm^{-1}), film): 3535 (OH), 1756 (CO), 1572 (NO_2), 1375 (NO_2). MS (+ES): 326.18 $[2M+H]^+$. The spectral data above agree well with published data for **3.24** [131].

6.26 Reaction of cyclen with ethyl 3-hydroxy-2-nitropropanoate (**3.24**).

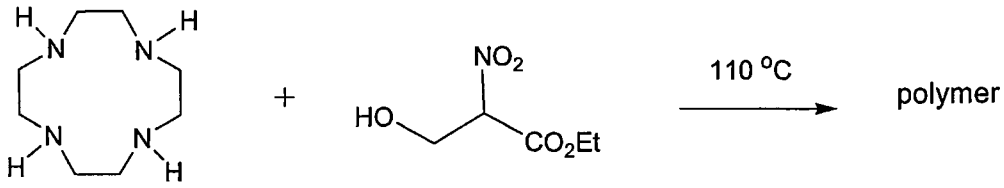

1 eq. **3.24** (4 eq.)

Chlorobenzene (b.p. 131 °C) was distilled from CaH_2 at 150 °C. Cyclen (75.4 mg, 1 eq.) was dissolved in freshly-distilled chlorobenzene (15 ml) in a 50 ml twin-necked flask. The solution was heated to 110 °C under argon. Ethyl 3-hydroxy-2-nitropropanoate (0.36 g, 1.75 mmol) was added through the side-arm. Addition of **3.24** caused the colourless reaction mixture to turn yellow and then to a deep red colour within 10 minutes. After 1 h, the reaction was stopped and the brown precipitate which had formed was filtered off. Attempts to dissolve the precipitate in methanol, chloroform and acetone were unsuccessful indicating a polymer had been formed. As the compound was insoluble in common solvents, an ^1H NMR could not be run.

6.27 Synthesis of 1-Benzyloxycarbonyl-1,4,7,10-tetraazacyclododecane (**3.28**)**.

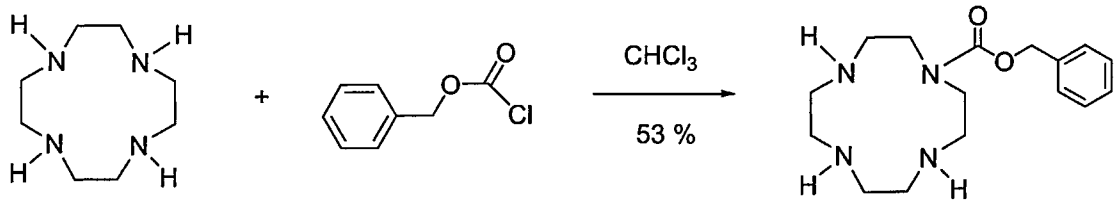

1 eq. 1.1 eq. **3.28**

A solution of benzylchloroformate (2.7 g, 15.9 mmol) in $CHCl_3$ (20 ml, dry) was added slowly over 1.5 hour to a cooled solution of cyclen (2.5 g, 14.5 mmol) in chloroform (50 ml). The reaction was allowed to reach ambient temperature and then stirred for 12 hours. Some of the organic solvent was removed under reduced pressure and the reaction stirred vigorously after the addition of 5 % NaOH (75 ml). The organic layer was separated and the aqueous layer re-extracted with $CHCl_3$ (2 x 25 ml). The organic extracts were pooled, dried over $MgSO_4$ and evaporated *in vacuo*. The resultant oil was purified on a silica gel column with 1% MeOH in $CHCl_3$ containing 0.1 % *i*$PrNH_2$ to yield an oil which after trituration with acetonitrile provided **3.28** as a white, crystalline solid (2.6 g, 53 %). A small amount of di-Z-cyclen eluted from the column first. R_f mono-Z-cyclen = 0.51 (SiO_2, 5 % MeOH in $CHCl_3$. m.p. 146-152 °C; ^{1}H NMR (300 MHz, CD_3OD, δ); 3.13 (16H, m, ring CH_2), 5.15 (2H, s, OCH_2), 7.36 (5H, m, Ph); ^{13}C NMR (75 MHz, CD_3OD, δ); 47.87 (ring CH_2), 48.44 (ring CH_2), 49.58 (ring CH_2), 50.51 (ring CH_2), 68.56 (OCH_2Ph), 128.89 (3-Ph), 128.93 (4-Ph), 129.08 (2-Ph), 129.37 (1-Ph), 157.52 (C=O): IR (ν_{max} / (cm^{-1}), KBr): 3391 (NH), 3183 (NH), 2959 (CH), 2837, 2352, 1673 (C=O), 1455, 1012, 776, 728 (arom), 558, 456. MS (+ES): 307 $[M+H]^+$. The spectral data above agree well with published data for the hydrochloride salt of **3.28** [144].

6.28 Synthesis of 1-Benzyloxycarbonyl-4,7,10-tris-(methyl-2-acetamidopropanoate)-1,4,7,10-tetraazacyclododecane (**3.29**)*.

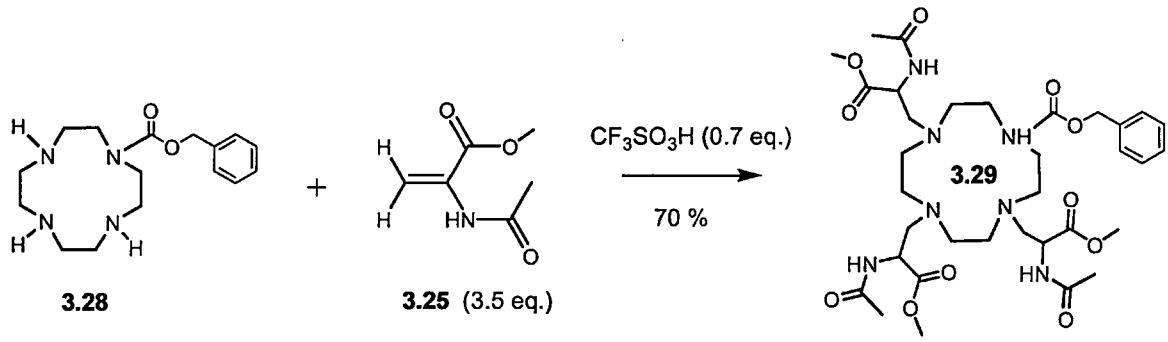

3.28 **3.25** (3.5 eq.)

3.28 (0.25 g, 0.82 mmol) was dissolved in a 3:1 mixture of CH_3Cl and CH_3CN (20 ml). Methyl 2-acetamidoacrylate (0.37 g, 2.61 mmol) was then added. Triflic acid (50 µl, 0.7 eq.) was promptly added with an automatic pipette. This resulted in a clear solution which was then stirred under argon for 24 h. After the solvent was removed *in vacuo*, the residue was partitioned between 1 M ammonia solution (10 ml) and chloroform (20 ml). After the aqueous layer was washed with another 10 ml chloroform, the organic extracts were pooled and evaporated to yield a viscous, pale yellow oil. The resulting oil was dissolved in a small amount of $CHCl_3$ and Et_2O was added to induce crystallisation. A colourless, crystalline solid was obtained. Yield: 0.42 g (70.4 %). R_f **3.29** = 0.62 (SiO_2, 3 % *i*PrNH$_2$ in CH_2Cl_2). m.p. 209 °C (with decomposition); ^{1}H NMR (300 MHz, $CDCl_3$, δ): 1.98 (6H, s, CH_3), 2.06 (3H, s, CH_3), 2.72 - 3.25 (20H, m, ring CH_2), 3.69 (9H, s, CH_3), 4.55 (m, 3H, CH), 5.80 (2H, s, OC*H*$_2$Ph), 7.24 (5H, m, Ph), 7.68 (br s, 3H, NH); ^{13}C NMR (75 MHz, $CDCl_3$, δ); 22.86 (CH_3), 23.24 (CH_3), 47.71 (CH_2), 48.65 (CH), 52.49 (CH_3), 68.56 (OCH_2Ph), 127.98 (Ph), 128.69 (Ph), 130.95 (Ph), 170.19 (C=O), 172.19 (C=O). Anal. Calcd (found) for $C_{34}H_{53}N_7O_{11}$: C, 55.50 (55.10); H, 7.26 (7.61); N, 13.32 (13.06). HRMS (+ES): found $[M+H]^+$ 736.3871. $C_{34}H_{53}N_7O_{11}$ requires 736.3876.

6.29 Deprotection of **3.29** to give **3.30***.

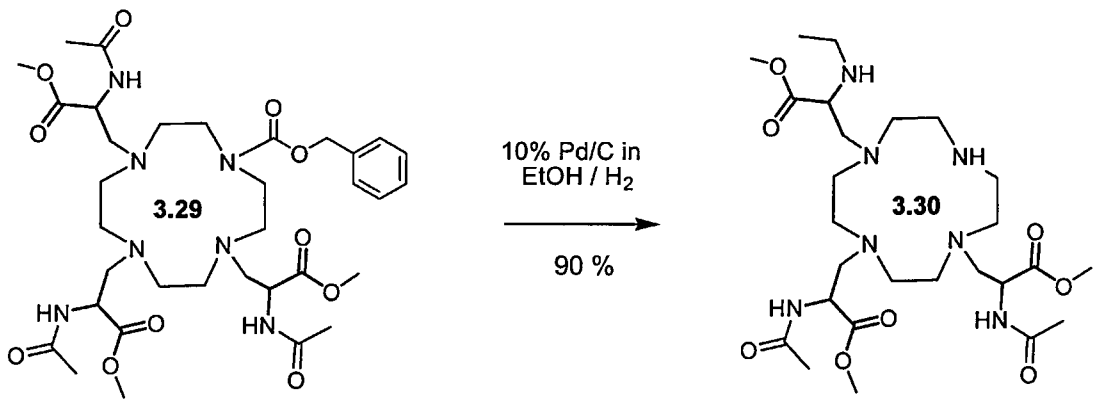

3.29 (0.40 g, 0.54 mM) was stirred in a suspension of 10 % palladium on carbon (50 mg) in ethanol (20 ml). A slow flowrate of H_2 was bubbled through the suspension in a fume cupboard. After 12 h, the reaction mixture was centrifuged to remove the catalyst. The supernatant was treated with activated charcoal and filtered through a bed of celite. After the solvent was removed under reduced pressure, a viscous oil was obtained. Yield **3.30**: 0.29 g (90 %). ^{1}H NMR (300 MHz, $CDCl_3$, δ): 1.99 (6H, s, CH_3), 2.05 (3H, s, CH_3), 2.70 - 3.20 (20H, m, ring CH_2), 3.69 (9H, s, CH_3), 4.55 (m, 3H, CH), 7.68 (br s, 3H, NH). MS (+ES): 603 $[M+H]^+$.

6.30 Hydrolysis of **3.30** with 12M HCl (aq.)

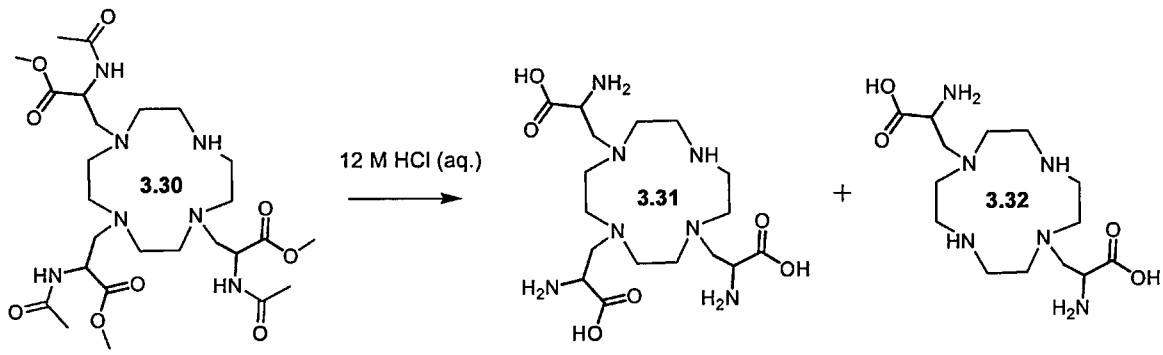

3.30 (0.28 g, 0.465 mM) was then heated with 12 M HCl (20 ml) at 60 °C for 3 h. After the acid was removed under reduced pressure, the residue was disssolve in EtOH (20 ml) and treated with activated carbon (0.25 g). The suspension was filtered through a bed of celite on a Buchner funnel and the filtrate was evaporated under reduced pressure. The resulting residue was recrystallised from aqueous EtOH to give **3.31** as an hygroscopic, white solid. Yield: 0.206 g (70 %). ^{1}H NMR (300 MHz, D_2O, δ): 1.84 (4H, s, 2 x CH_2), 2.57 - 3.10 (18H, m, ring CH_2), 4.60 - 4.70 (9H, br s, 3 x NH_3^+); ^{13}C NMR (75 MHz, D_2O, δ); 47.2, 48.6 (CH_2), 176.61 (C=O). MS (ES^+): 434 $[M+H]^+$.

Note: A peak corresponding to the disubstituted compound (**3.32**) was also observable on LC-MS ($[M+H]^+$ = 347.2). The size of this peak relative to the peak corresponding to **3.31** ($[M+H]^+$ = 434) increased in aqueous solution after 24 h.

6.31 Synthesis of 1,4,7-tris-(ethyl 2-cyanomethyl-ethanoate)-1,4,7,10-tetraazacyclododecane (**3.34**)*.

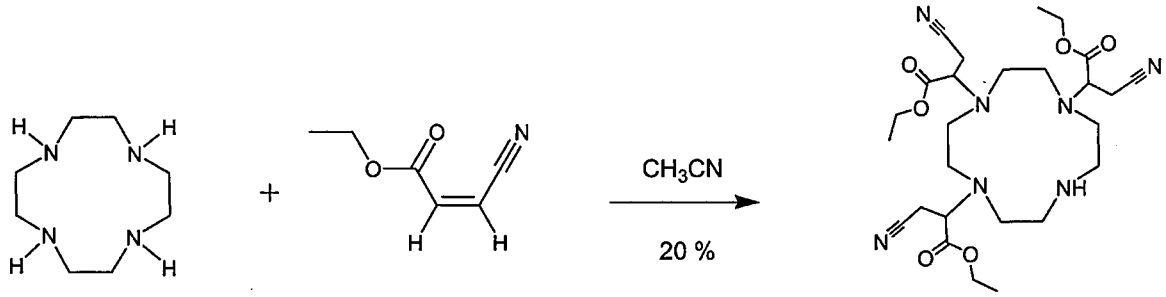

1 eq. **3.33** (3.1 eq.) **3.34**

Cyclen (0.20 g, 1.16 mmol) was dissolved in MeCN (15 ml) in a twin-necked, round-bottomed flask (25 ml). **3.33** (0.43 ml, 0.45 g, 3.59 mmol, 3.1 eq.) was added with an automatic pipette through the side-arm and the solution was stirred under argon for 12 h. The solvent was removed *in vacuo* to give an orange, viscous oil. The oil was purified by silica gel column chromatography using 20 % ethyl acetate in hexane to give a pale, yellow oil. Yield: 0.13 g (20 %). R_f **3.34** = 0.74 (SiO_2, 20 % ethyl acetate in hexane). ^{1}H NMR (300 MHz, $CDCl_3$ - CD_3OD, 7 : 1, δ) 1.22 (6H, t, J = 7.14 Hz), 1.29 (3H, t, J = 7.14 Hz), 2.28 - 2.88 (21H, m, CH_2+CH), 2.97; 2.91 (6H, dd, J = 7.5 Hz, 7.5 Hz), 4.16 (4H, q, J = 7.14 Hz), 4.22 (2H, q, J = 7.14 Hz); ^{13}C NMR (75 MHz, $CDCl_3$ - CD_3OD, 7:1, δ); 13.72 (CH_3), 13.83 (CH_3), 35.80 (CH_2), 36.36 (CH_2), 43.39 (CH_2), 45.24 (CH_2), 47.67 (CH_2), 49.41 (CH), 61.16 (ethyl CH_2), 61.83 (ethyl CH_2), 114.11 (CN), 116.83 (CN), 168.77 (C=O), 169.33 (C=O). IR (ν_{max} / (cm^{-1}) neat, film): 3435 (broad NH), 2963, 2852, 2362, 1747, 1655, 1542, 1438, 1376, 1262, 1218, 1095, 1032, 801.6. HRMS (+ES): found $[M+H]^+$ 548.3191, $C_{17}H_{36}N_7O_3$ requires 548.3195.

6.32 Deionization of **3.11•HCl** using anion exchange chromatography to give **4.1**[*].

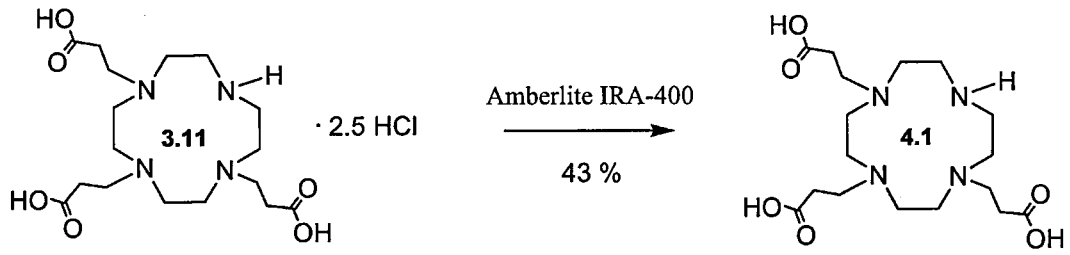

Amberlite IRA-400 (Aldrich, chloride form, 40 g) was stirred with 10 % NaOH (200 ml) in a 1L beaker for 10 minutes. The colour of the resin changed from a light to a dark brown colour. Using a batch process, the resin was stirred vigorously with deionized H_2O (250 ml) on a magnetic stirrer. After a few minutes stirring, the stirrer was switched off and the resin allowed to settle. After careful decantation of H_2O, this procedure of washing-decantation was repeated with a further 8 volumes (250 ml) of H_2O. The pH of the resin was 9.4. Three further washings of H_2O (3 x 500 ml) were required to bring the pH of the resin to 7.0. The resin was then packed into a squat glass column (3.5 x 15 cm) which was plugged with glass wool just above the on/off tap. Meanwhile, **3.11** (1.0 g) was dissolved in H_2O (50 ml) and the pH was adjusted from 1.9 to 9.5 with 3.5 % aq. NH_3 (~ 15 ml). The solution was applied to the ion-exchange column and successively eluted with water (spot-testing of the H_2O eluate with $AgNO_3$ solution revealed eluted fractions were positive for chloride ions) and then with formic acid of increasing concentrations; 0.1, 0.25, 0.5, 0.75 M. **4.1**, which eluted from the column as a colourless oil with 0.5 M formic acid, was crystallized from EtOH and acetone. Yield: 0.39 g white, mobile powder (42.7 %). ^{1}H NMR (300 MHz, D_2O, δ): 2.63 (6H, t, ^3J = 6.6 Hz, CH_2CH_2COOH), 3.00 - 3.03 (22 H, br s, ring CH_2 + arm NCH_2CH_2). MS (+ES): 386.9 $[M+H]^+$.

6.33 Synthesis of Gd(DO3P) (**4.2**)*.

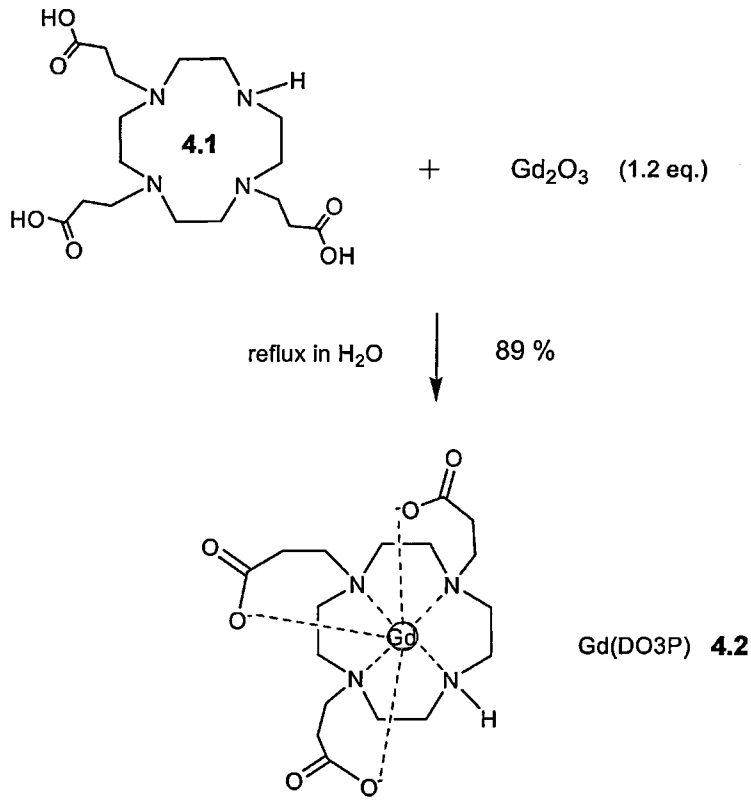

4.1 (0.28 g, 0.72 mmol) and Gd_2O_3 (0.126 g, 0.45 mmol) were refluxed in 8 ml water overnight. After 1 h, some white precipitate was observed in the flask. After the reaction was stopped, the suspension was filtered through a 0.20 micron polypropylene filter (Minisart RC 15, Sartorius) and lyophilised to give a white solid. Yield **4.2**: 0.35 g (89.4 %). m.p. > 250 °C. IR (ν_{max} / (cm^{-1}), KBr): 3435 (broad NH), 2843, 1560, 1440, 1316, 755.9. Anal. Calcd (found) for $C_{17}H_{29}GdN_4O_6 \cdot H_2O$: C, 37.63 (36.42); H, 5.57 (5.39); N, 9.99 (10.32); Gd, 28.05 (28.98). HRMS (+ES): found $[M+H]^+$ 544.1407. $C_{34}H_{53}N_7O_{11}$ requires 544.1401.

6.34 Synthesis of Gd(DO3PAM), **4.3** *.

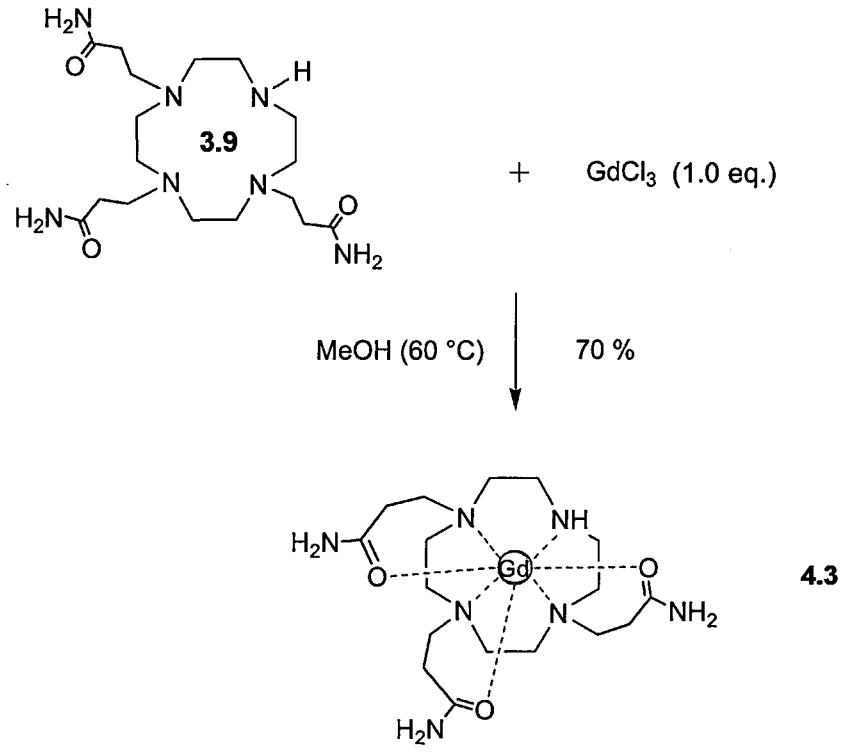

4.3

3.9 (0.15 g, 0.39 mmol) was suspended in anhydrous methanol under an inert atmosphere. Addition of $GdCl_3$ (anhydrous) to the ligand caused it to become fully-soluble. The solution was heated at 60 °C overnight under argon. After the reaction was stopped, most of the MeOH was removed at 40 °C under reduced pressure. Et_2O was added dropwise until turbidity just began. After cooling in the freezer overnight, the white, dense precipitate (**4.3**) which developed was collected by centrifugation. Yield: 0.19 g (70 %). m.p. > 250 °C. One spot on TLC with R_f = 0.4 (Silica plate, acetonitrile-water-*t*BuOH, 2:9:2 v/v). IR (ν_{max} / (cm^{-1}), KBr): 3371 (broad), 2860, 1652, 1457, 1094, 968, 728. Anal. Calcd (found) for $C_{17}H_{35}GdN_7O_3 \cdot (H_2O)_2 \cdot (Cl^-)_3 \cdot (CH_3OH)$: C, 32.15 (32.65); H, 6.61 (6.81); N, 13.12 (13.27); Gd, 21.04 (21.82). HRMS (+ES): found $[M+2(NH_4Cl)+Cl+H]^+$ 681.1776. $[M+2(NH_4Cl)+Cl+H]^+$ requires 681.1775.

6.35 Deionization of **3.31** using cation exchange chromatography to give **4.4***.

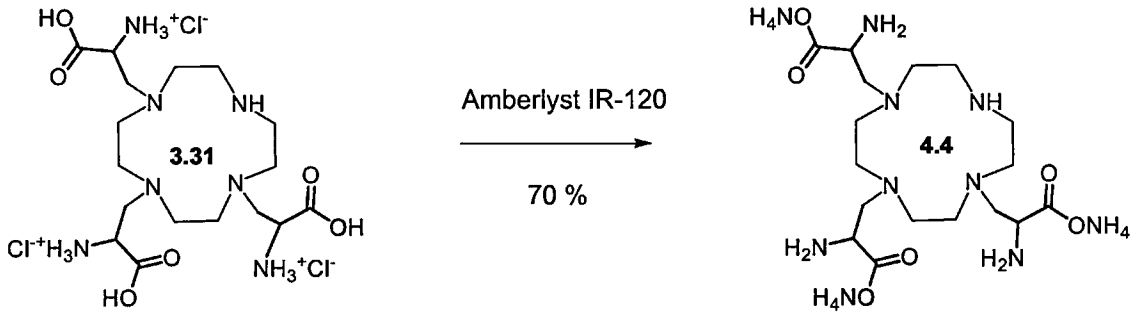

Amberlite IR-120 (Fluka, H^+ form, 16-45 mesh, 70 g) was stirred with 5 % HCl (250 ml) in a 1 L beaker for 10 minutes. The orange supernatant was decanted. Using a batch process, the resin was stirred vigorously with deionized H_2O (250 ml) on a magnetic stirrer. After a few minutes stirring, the stirrer was switched off and the resin allowed to settle. After the H_2O was carefully decanted, this procedure of washing-decantation was repeated with a further 6 volumes of H_2O (250 ml). The pH of the resin was measured (~ 5.4). Meanwhile, **3.31** (0.2 g) was dissolved in 15 ml H_2O (pH ~ 1.3). The solution was applied to the ion-exchange column and successively eluted with water (100 ml fractions) and then with 0.5 M NH_4OH. Spot-testing of the H_2O eluate with $AgNO_3$ solution revealed specific fractions were +ve for chloride. As the product did not elute with 0.5 M NH_4OH, the column was eluted with 7.5 % NH_4OH (43 ml 33 % aq. NH_3 in 150 ml H_2O). **4.4** eluted as a viscous, yellow oil which afforded an off-white solid upon trituration with EtOH and acetone. Yield: 0.13 g (70 %). ^1H NMR (300 MHz, D_2O, δ): 1.84 (4H, s, 2 x CH_2), 2.57 - 3.10 (18H, m, ring CH_2), 4.65 (9H, br s, 3 x NH_3^+). MS (+ES): 473.7 $[M+K]^+$.

6.36 Synthesis of Gd(DO3-2AP), **4.6** *.

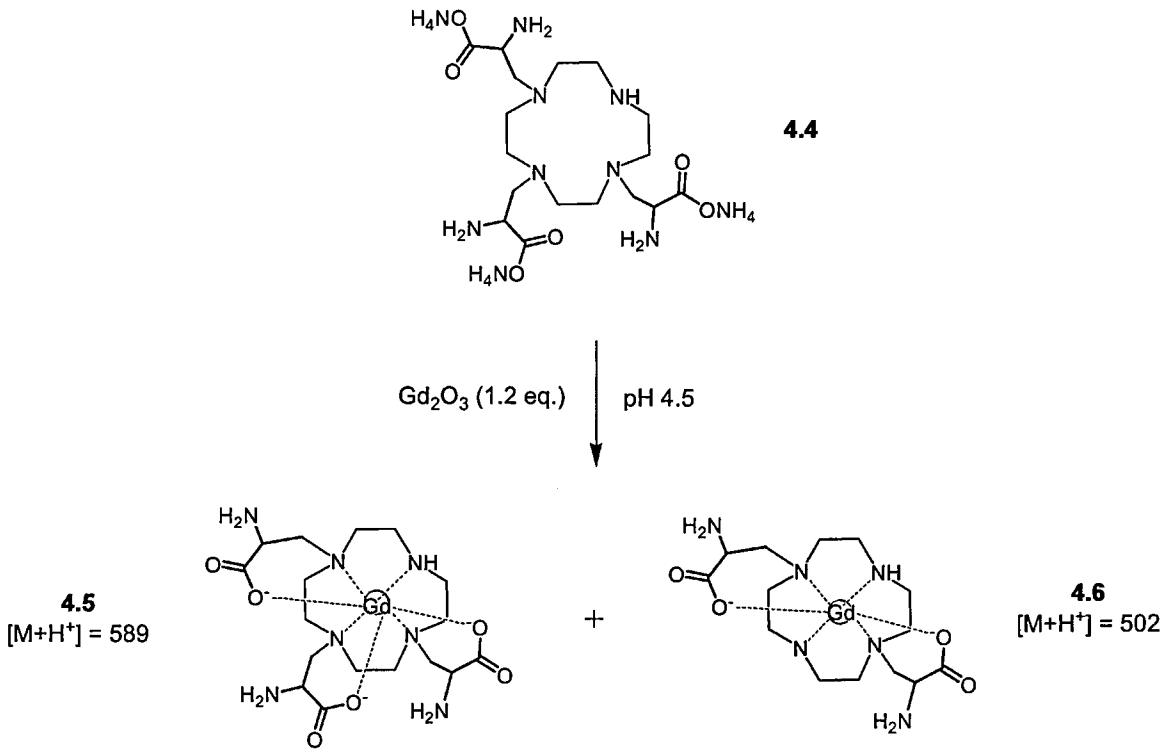

The ammonium salt (68 mg) of the ligand **4.4** was reacted with gadolinium oxide at pH 4.5 (pH was adjusted with dilute acetic acid). After 1 hour, the pH was checked and it had risen to pH 4.8. The reaction was allowed to stir overnight and then the pH was readjusted to 7.0 using dilute ammonia. After the solvent was removed *in vacuo*, the residue was resuspended in ethanol and acetone was added until a white turbidity appeared. The suspension was then put in the freezer overnight and the filtered precipitate dried under high vacuum for 24 hours. Yield: 56 mg (30 %). m.p. > 250 °C. 2 spots on TLC with R_f = 0.45, 0.57 (Silica plate, acetonitrile-water-*t*BuOH, 2:9:2, v/v). LC-MS (+ES) of the product gave 2 peaks one with an $[M+H]^+$ = 589 (which corresponds to the title product, **4.5**) and the other peak had an $[M+H]^+$ = 502 (which corresponds to the disubstituted complex, **4.6**).

6.37 Synthesis of Gd(DOTA), **4.7**.

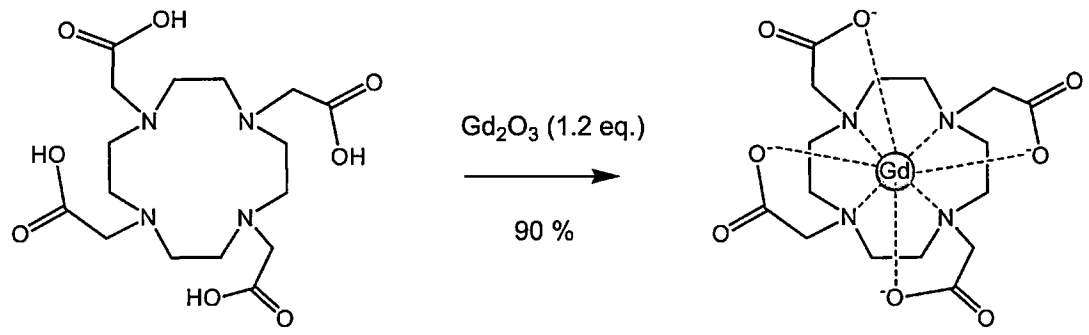

DOTA Gd(DOTA), **4.7**

DOTA (0.10 g, 0.247 mmol) and Gd_2O_3 (55.5 mg, 0.15 mmol, 0.625 eq.) were dissolved in water (8 ml) and refluxed under argon overnight. After the reaction was stopped, the suspension was filtered through a 0.22 micron polypropylene filter and lyophilised to give **4.7** as a white solid. Yield: 0.135 g (90.4 %). m.p. > 250 °C. IR (ν_{max} / (cm^{-1}), KBr): 3400, 2916, 2361, 1579, 1448. Anal. Calcd (found) for $C_{16}H_{24}GdN_4O_8 \cdot 2.5\ H_2O$: C, 31.89 (31.10); H, 4.85 (4.65); Gd, 26.09 (26.54); N, 9.30 (10.01). MS (+ES): 559.2 $[M+H]^+$.

Appendix A - TLC spray reagents [90]

Fluoroscein-peroxide spray (specific for brominated compounds)

Preparation: Solution A. 2 M NaOH.
Solution B. Half saturated fluoroscein in glacial acetic acid.
Solution C. 30 % H_2O_2.
Solution D. 0.5 % copper acetate.

Procedure: The chromatogram is sprayed with Solution A, heated under a heat gun for 1-2 minutes. It is then sprayed with a mixture of equal volumes of B and C containing a drop of D and reheated as before (the B-C-D reagent is stable in the fridge for 1-2 days).

Results: Brominated compounds appear as intense pink spots on a bright yellow background.

Phosphomolybdic acid spray (useful for steroids such as cholic acid)

Preparation: Phosphomolybdic acid (4.8 g) is dissolved in ethanol (100 ml). It is stable indefinitely.

Procedure: Chromatograms are sprayed with the reagent and heated with a heat gun until spots develop (1-2 min).

Results: Compounds containing cholic acid appear as blue spots on a pale yellow background.

Ninhydrin (0.2 %) in ethanol (useful for amines such as cyclen and amino acids)

Preparation: Ninhydrin (0.2 g) is dissolved in ethanol (100 ml). The spray is freshly prepared.

Procedure: Chromatograms are sprayed with the reagent and heated at 125 °C for 10 min.

Results: Amines appear as blue-purple spots.

Appendix B - crystallographic data for the ligand **3.10**

Table 1. Crystal data and structure refinement.

Identification code	**2006src0632 (POC 1)**	
Empirical formula	$C_{20}H_{42}N_8O_5$	
Formula weight	474.62	
Temperature	120(2) K	
Wavelength	0.71073 Å	
Crystal system	Monoclinic	
Space group	*C*2/*c*	
Unit cell dimensions	a = 16.1654(5) Å	α = 90°
	b = 10.1413(2) Å	β = 116.3670(10)°
	c = 17.0495(5) Å	γ = 90°
Volume	2504.29(12) Å^3	
Z	4	
Density (calculated)	1.259 Mg / m^3	
Absorption coefficient	0.092 mm^{-1}	
F(000)	1032	
Crystal	Block; colourless	
Crystal size	0.25 × 0.20 × 0.20 mm^3	
θ range for data collection	4.06 – 27.50°	
Index ranges	$-20 \le h \le 20$, $-12 \le k \le 13$, $-22 \le l \le 18$	
Reflections collected	15776	
Independent reflections	2864 [R_{int} = 0.0384]	
Completeness to θ = 27.50°	99.5 %	
Absorption correction	Semi–empirical from equivalents	
Max. and min. transmission	0.9818 and 0.9774	
Refinement method	Full-matrix least-squares on F^2	
Data / restraints / parameters	2864 / 0 / 170	
Goodness-of-fit on F^2	1.024	
Final *R* indices [$F^2 > 2\sigma(F^2)$]	*R1* = 0.0399, *wR2* = 0.0880	
R indices (all data)	*R1* = 0.0602, *wR2* = 0.0980	
Largest diff. peak and hole	0.247 and –0.235 e Å^{-3}	

Diffractometer: *Nonius KappaCCD* area detector (ϕ scans and ω scans to fill *asymmetric unit* sphere). **Cell determination:** DirAx (Duisenberg, A.J.M.(1992). J. Appl. Cryst. 25, 92-96.) **Data collection:** Collect (Collect: Data collection software, R. Hooft, Nonius B.V., 1998). **Data reduction and cell refinement**: *Denzo* (Z. Otwinowski & W. Minor, *Methods in Enzymology* (1997) Vol. **276**: *Macromolecular Crystallography*, part A, pp. 307–326; C. W. Carter, Jr. & R. M. Sweet, Eds., Academic Press). **Absorption correction**: *SORTAV* (R. H. Blessing, Acta Cryst. A**51** (1995) 33–37; R. H. Blessing, J. Appl. Cryst. **30** (1997) 421–426). **Structure solution**: *SHELXS97* (G. M. Sheldrick, Acta Cryst. (1990) A**46** 467–473). **Structure refinement**: *SHELXL97* (G. M. Sheldrick (1997), University of Göttingen, Germany). **Graphics:** Cameron - A Molecular Graphics Package. (D. M. Watkin, L. Pearce and C. K. Prout, Chemical Crystallography Laboratory, University of Oxford, 1993).

Table 2. Bond lengths [Å].

C1–N1	1.4753(16)
C1–C4^{i}	1.5219(17)
C2–N1	1.4732(16)
C2–C3	1.5237(17)
C3–N2	1.4775(16)
C4–N2	1.4822(16)
C4–C1^{i}	1.5219(17)
C5–N1	1.4649(17)
C5–C6	1.5282(19)
C6–C7	1.512(2)
C7–O1	1.2428(16)
C7–N3	1.3323(19)
C8–N2	1.4802(16)
C8–C9	1.5382(18)
C9–C10	1.5175(18)
C10–O2	1.2429(16)
C10–N4	1.3249(18)

Table 3. Bond angles [°].

N1–C1–C4^{i}	110.70(10)
N1–C2–C3	115.77(10)
N2–C3–C2	113.90(10)
N2–C4–C1^{i}	111.79(10)
N1–C5–C6	112.80(10)
C7–C6–C5	111.21(11)
O1–C7–N3	122.84(14)
O1–C7–C6	120.61(13)
N3–C7–C6	116.54(12)
N2–C8–C9	111.56(10)
C10–C9–C8	110.78(11)
O2–C10–N4	123.03(12)
O2–C10–C9	119.87(12)
N4–C10–C9	117.09(12)
C5–N1–C2	109.84(10)
C5–N1–C1	112.33(10)
C2–N1–C1	109.81(10)
C3–N2–C8	108.57(9)
C3–N2–C4	110.41(10)
C8–N2–C4	109.64(10)

Symmetry transformations used to generate equivalent atoms: (i) –x–1/2,–y+3/2,–z

References

1 McRobbie, D.; Moore, E.; Graves, M.; Prince, M., *MRI: From Picture to Proton.* Cambridge University Press: Cambridge, 2003.

2 Merbach, A. E.; Toth, E., *The chemistry of contrast agents in medical magnetic resonance imaging.* J. Wiley & Sons: New York, 2001.

3 http://www.uams.edu/radiology/default.asp. (Sep 2008).

4 Aime, S.; Geninatti Crich, S.; Gianolio, E.; Giovenzana, G. B.; Tei, L.; Terreno, E., High sensitivity lanthanide(III) based probes for MR-medical imaging. *Coord. Chem. Rev.* 2006, 250, (11-12), 1562-1579.

5 Huda, W.; Slone, R., *Review of Radiological Physics.* Lippincott, Williams & Wilkins: Philadelphia, 1995.

6 Lauterbur, P., Image formation by induced local interactions: Examples employing nuclear magnetic resonance. *Nature* 1973, 242, 190-191.

7 Schild, H. H., *MRI made easy.* Schering AG: Berlin, 1999.

8 Westbrook, C.; Kaut Roth, C., *MRI in Practice.* Blackwell: 1998.

9 Tweedle, M. F., Relaxation agents in NMR imaging. In *Lanthanide Probes in Life, Chemical and Earth sciences*, Bunzli, J.; Choppin, G.. Elsevier: Amsterdam, 1989.

10 Williams, D. A. R., *Nuclear Magnetic Resonance Spectroscopy (Analytical Chemistry By Open Learning).* John Wiley & Sons Inc: London, 1986.

11 Webb, S., *The Physics of Medical Imaging.* Taylor & Francis: London, 1988.

12 Wolf, G.; Popp, C., *NMR, a primer for medical imaging.* Slack Inc: New York, 1984.

13 Fullerton, G.; Potter, J.; Dornbluth, N., NMR relaxation of protons in tissues and other macromolecular water solutions. *Magn. Reson. Imag.* 1982, 1, 209-228.

14 Nelson, K.; Runge, V., Principles of MR contrast. In *Contrast-enhanced clinical magnetic resonance imaging*, Runge, V. M.. The University Press of Kentucky: 1996.

15 Caravan, P., Strategies for increasing the sensitivities of gadolinium-based contrast agents. *Chem. Soc. Rev.* 2006, 35, 512-523.

16 Hendrick, R. E.; Haacke, E. M., Basic physics of MR contrast agents and maximization of image contrast. *J. Magn. Reson. Imag.* 1993, 3, (1), 137-148.

17 Vlaardingerbroek, M.; Boer Den, J., *Magnetic Resonance Imaging. Theory and Practice.* Springer Verlag: Germany, 1996.

18 Cotton, F. A.; Wilkinson, G.; Gaus, P. L., *Basic Inorganic Chemistry.* John Wiley & Sons: 1995.

19 Tweedle, M. F., The ProHance story: the making of a novel MRI contrast agent. *Eur. Radiol.* 1997, 7 (Suppl. 5), 54225 - 5230.

20 Kohl, S. W.; Kuse, K.; Hummert, M.; Schumann, H.; Mügge, H. C.; Janek, K.; Weißhoff, H., New synthetic routes for 1-benzyl-1,4,7,10-tetraazacyclododecane and 1,4,7,10-tetraazacyclododecane-1-acetic acid ethyl ester, important starting materials for metal-coded DOTA-based affinity tags. *Z. Naturforsch.* 2007, 62b, 397-406.

21 Perez-Mayoral, E.; Soler-Padros, J.; Negri, V.; Cerdan, S.; Ballesteros, P., Synthetic approaches to heterocyclic ligands for Gd-based MRI contrast agents. *Molecules* 2007, 12, 1771-1795.

22 Wang, X.; Jin, T.; Comblin, V.; Lopez-Mut, A.; Merciny, E.; Desreux, J., A kinetic investigation of the lanthanide DOTA chelates. Stability and rates of formation and of dissociation of a macrocyclic gadolinium(III) polyaza polycarboxylic MRI contrast agent. *Inorg. Chem.* 1992, 31, 1095–1099.

23 Guo-Ping, Y.; Robinson, L.; Hogg, P., Magnetic resonance imaging contrast agents: Overview and perspectives. *Radiography* 2007, 13, e5-e19.

24 Caravan, P.; Ellison, J. J.; McMurry, T. J.; Lauffer, R. B., Gadolinium(III) chelates as MRI contrast agents: structure, dynamics, and applications. *Chem. Rev.* 1999, 99, 2293-2352.

25 Cacheris, W. P.; Quay, S. C.; Rocklage, S. M., The relationship between thermodynamics and the toxicity of gadolinium complexes. *Magn. Reson. Imag.* 1990, 8, 467.

26 Helm, L., Relaxivity in paramagnetic systems: Theory and mechanisms. *Progress in Nuclear Magnetic Resonance Spectroscopy* 2006, 49, 45 - 64.

27 Chan, K. W.-Y.; Wong, W.-T., Small molecular gadolinium (III) complexes as MRI contrast agents for diagnostic imaging. *Coord. Chem. Rev.* 2007, 251, 2428-2451.

28 Aime, S.; Botta, M.; Fasano, M.; Crich, S.; Terreno, E., Gd(III) complexes as contrast agents for magnetic resonance imaging: a proton relaxation enhancement study of the interaction with human serum albumin. *J. Biol. Inorg. Chem.* 1996, 1, 312-319.

29 Kang, S. I.; Ranganathan, R. S.; Emswiler, J.; Kumar, K.; Gougoutas, J.; Malley, M.; Tweedle, M. F., Synthesis, characterisation, and crystal structure of the gadolinium(III) chelate of (1R,4R,7R)-α,α',α''-trimethyl-1,4,7,10-tetraazacyclododecane-1,4,7-triacetic Acid (DO3MA). *Inorg. Chem.* 1993, 32, 2912-2918.

30 Rangathan, R. S.; Kang, S. I.; Nunn, A. D.; Ratsep, P. C.; Pillai, K. M. R.; Zhang, X.; Tweedle, M. F., New multimeric magnetic resonance imaging agents. *Invest. Radiol.* 1998, 33, 779-797.

31 Brasch, R. C., Rationale and applications for macromolecular Gd-based contrast agents. *Magnetic Resonance in Medicine* 1991, 22, 282-287.

32 Jacques, V.; Desreux, J. F., New Classes of MRI Contrast Agents. In *Topics in Current Chemistry*, Springer-Verlag: Berlin Heidelberg, 2002.

33 Bellin, M. F., MRI contrast agents, the old and the new. *Eur. J. Radiol.* 2006, 60, 314-323.

34 Steed, J. W., *Supramolecular Chemistry*. John Wiley & Sons Ltd.: Chichester, 2000.

35 Bottrill, M.; Kwok, L.; Long, N., Lanthanides in magnetic resonance imaging. *Chem. Soc. Rev.* 2006, 35, 557-571.

36 Young, P., A new age of imaging agents. *American Chemical Society Magazine* 2006 (Spring Edition), 42-47.

37 Rinck, P. A., *Magnetic Resonance in Medicine*. Blackwell Scientific Publications: Oxford, UK, 1993.

38 Martin, V. V.; Ralston, W. H.; Hynes, M. R.; Keana, J. F. W., Gadolinium(III) di- and tetrachelates designed for *in vivo* noncovalent complexation with plasma proteins: A novel molecular design for blood pool MRI contrast enhancing agents. *Bioconj. Chem.* 1995, 6, (61), 6-623.

39 Lauffer, R. B.; Parmalee, D.; Dunham, S.; Quellet, H.; Dolan, R.; Witte, S.; McMurry, T.; Walovitch, R., MS-325: Albumin-targeted contrast agent for MR angiography. *Radiology* 1998, 207, (2), 529-537.

40 Cavagna, F.; Dapra, P.; Castelli, P.; Maggioni, F.; Kirchin, M., Trends and developments in MRI contrast agent research. *Eur. Radiol.* 1997, 7(suppl. 5), 222-224.

41 Takehara, Y., Assessment of a potential tumour-seeking manganese metalloporphyrin contrast agent in a mouse model. *Magn. Reson. Imag.* 2002, 47, (3), 549-553.

42 Nunn, A. D.; Linder, K. E.; Tweedle, M. F., Can receptors be imaged with MRI agents ? *Q. J. Nucl. Med.* 1997, 41.

43 Allen, M. J.; Meade, T. J., Synthesis and visualisation of a membrane-permeable MRI contrast agent. *J. Biol. Inorg. Chem.* 2003, 8, 746-750.

44 Lattuada, L.; Dematttio, S.; Vincenzi, V.; Cabella, C.; Visigalli, M.; Aime, S.; Geninatti Crich, S.; Gianolio, E., Magnetic resonance imaging of tumor cells by targeting the amino acid transport sytem. *Bioorg. Med. Chem. Lett.* 2006, 16, (15), 4111-4114.

45 Meade, T. J.; Taylor, A. K.; Bull, S. R., New magnetic resonance contrast agents as biochemical reporters. *Current opinion in neurobiology* 2003, 13, 1-6.

46 Austen, B. M.; Cheng, E.; Mohammed, Y., The development of smart contrast agents for MRI imaging of Alzheimer's disease. *Alzheimer's and Dementia* 2008, 4, (4), T74-T75.

47 Sigurdsson, E. M.; Blind, J. A.; Knudsen, E.; Asuni, A.; Scholtzova, H.; Tsui, W. H.; Li, Y.; Sadowski, M.; Turnbull, D. H.; De Leon, M. J.; Wisniewski, T., A non-toxic ligand for voxel-based MRI analysis of plaques in AD transgenic mice. *Neurobiology of Aging* 2008, 29, (6), 836 - 847.

48 Lewis, M.; Kao, J.; Anderson, A.; Shively, J.; Raubitschek, A., An improved method for conjugating monoclonal antibodies with N-hydroxysulfosuccinimidyl DOTA. *Bioconjug. Chem.* 2001, 12, (2), 320-324.

49 Flacke, S.; Fischer, S.; Scott, M. J.; Fuhrhop, R. J.; Allen, J. S.; McLean, M.; Winter, P.; Sicard, G. A.; Gaffney, P. J.; Wickline, S. A.; Lanza, G. M., Novel MRI contrast agent for molecular imaging of fibrin: Implications for detecting vulnerable plaques. *Circulation* 2001, 104, 1280.

50 Waters, E. A.; Wickline, S. A., Contrast agents for MRI. *Basic Res. Cardiol.* 2008, 103, 114-121.

51 Yoo, B.; Pagel, M. D., A paracest MRI contrast agent to detect enzyme activity. *J. Am. Chem. Soc.* 2006, 128, (43), 14032-14033.

52 Que, E. L.; Chang, C. J., A smart magnetic resonance contrast agent for selective copper sensing. *J. Am. Chem. Soc.* 2006, 128, (50), 15942 -15943.

53 Moats, R.; Fraser, S.; Meade, T., A "smart" magnetic resonance imaging agent that reports on specific enzymatic activity. *Angew. Chem. Int. Engl.* 1997, 36, (7), 726-728.

54 Modo, M.; Cash, D.; Mellodew, K.; Williams, S.; Fraser, S.; Price, J.; Hodges, H., Tracking transplanted stem cell migration using bifunctional contrast agent-enhanced magnetic resonance imaging. *Neuroimage* 2002, 17, 803-811.

55 Louie, A. Y.; Huber, M. M.; Ahrens, E. T.; Rothbacher, U.; Moats, R.; Jacobs, R. E.; Fraser, S. E.; Meade, T. J., *In vivo* visualization of gene expression using magnetic resonance imaging. *Nat. Biotechnol. Markers* 2000, 18, 321-325.

56 Meade, T.; Li, W.-h.; Fraser, S., A calcium-sensitive magnetic resonance imaging contrast agent. *J. Am. Chem. Soc.* 1999, 121, 1413-1418.

57 Lowe, M., MRI contrast agents: The next generation. *Aust. J. Chem.* 2002, 55, 551-556.

58 Pérez-Mayoral, E.; Negri, V.; Soler-Padrós, J.; Cerdán, S.; Ballesteros, P., Chemistry of paramagnetic and diamagnetic contrast agents for Magnetic Resonance Imaging and spectroscopy pH responsive contrast agents. *Eur. J. Radiol.* 2008, 67, (3), 453 - 458.

59 Lowe, M. P.; Parker, D., Controllable pH modulation of lanthanide luminescence by intramolecular switching of the hydration state. *Chem. Comm.* 2000, 707-708.

60 Zhang, S.; Kuangcong, W.; Sherry, A. D., A Novel pH-sensitive MRI Contrast Agent. *Angew. Chem. Int. Ed.* 1999, 38, (21), 3192-3194.

61 Woods, M.; Kiefer, G. E.; Sherry, A. D., Synthesis, relaxometric, and photophysical properties of a new pH-responsive MRI contrast agent: The effect of other ligating groups on the dissociation of a *p*-nitrophenolic pendant arm. *J. Am. Chem. Soc.* 2004, 126, 9248 - 9256.

62 Kalman, F. K.; Woods, M.; Caravan, P.; Jurek, P.; Spiller, M.; Tircsó, G.; Kiraly, R.; Brücher, E.; Sherry, A. D., Potentiometric and relaxometric properties of a gadolinium-based MRI contrast agent for sensing tissue pH. *Inorg. Chem.* 2007, 46, (13), 5260-70.

63 Bernal, I., *Stereochemical and stereophysical behaviour of macrocycles*. Elsevier: Amsterdam, 1987.

64 Kodama, M.; Kimura, J., Reaction of cobalt (II) macrocyclic tetra-amine complexes with dioxygen. *J. Chem. Soc. Dalton Trans.* 1980, 327-333.

65 Schrodt, A.; Neubrand, A.; Van Eldik, R., Fixation of CO_2 by Zinc(II) Chelates in alcoholic medium. *Inorg. Chem.* 1997, 36, 4579 - 4584.

66 Richman, J.; Atkins, T., Nitrogen analogs of crown ethers. *J. Am. Chem. Soc.* 1974, 96, 2268 - 2270.

67 Gilchrist, T. L., *Heterocyclic Chemistry*. J Wiley & Sons: New York, 1985.

68 Sainsbury, M., *Heterocyclic Chemistry*. Royal Society Of Chemistry: Cambridge, 2001.

69 Dischino, D. D.; Delaney, E. J.; Emswiler, J. E.; Gaughan, G. T.; Prasad, J. S.; Srivastava, S. K.; Tweedle, M. F., Synthesis of nonionic gadolinium chelates useful as contrast agents for magnetic resonance imaging. *Inorg. Chem.* 1991, 39, 1265-1269.

70 McMurry, J., *Organic Chemistry*. Brooks Cole: 2003.

71 Griffin, J. M. M.; Skwierawska, A. M.; Manning, H. C.; Marx, J. N.; Bornhop, D. J., Simple, high yielding synthesis of trifunctional fluorescent lanthanide chelates. *Tet. Lett.* 2001, 42, (23), 3823-3825.

72 Kaden, T., Ten-membered rings or larger with one or more nitrogen atoms. In *Comprehensive Heterocyclic Chemistry II. Seven-membered And Larger Rings And Fused Derivatives*, Newkome, G. R.. Pergamon Press: Oxford, 1996.

73 Zheng, Q.; Dai, H.; Merritt, M.; Malloy, C.; Pan, C.; Li, W., A new class of macrocyclic lanthanide complexes for cell labelling and magnetic resonance imaging applications. *J. Am. Chem. Soc.* 2005, 127, 16178-16188.

74 Sosnovik, D.; Weissleder, R., Emerging concepts in molecular MRI. *Current Opinion in Biotechnolgy* 2006, 17, 1-7.

75 Britz-Cunningham, S.; Adelstein, S., Molecular targeting with radionucleotides: State of the science. *J. Nucl. Med.* 2003, 44, (12), 1945 -1961.

76 Dzik-Jurasz, A., Are targeted contrast agents realistically going to reach the clinic ? *Br. J. Radiol.* 2006, 79, 870-872.

77 Hermanson, G. T., *Bioconjugate Techniques*. Academic Press: 2008.

78 Manfredi, S.; Pavan, B.; Vertauni, S.; Scaglianti, M.; Compagnone, D.; Biondi, C.; Scatturin, A.; Tanganelli, S.; Ferraro, L.; Prasad, P.; Dalpiaz, A., Design, synthesis and activity of ascorbic acid prodrugs of nipecotic, kynurenic and diclophenamic acids, liable to increase neurotrophic activity. *J. Med. Chem.* 2002, 45, 559-562.

79 Majoros, I. J.; Myc, A.; Thomas, T.; Mehta, C. B.; Baker, J. R., PAMAM dendrimer-based multifunctional conjugate for cancer therapy: synthesis, characterization, and functionality. *Biomacromolecules* 2006, 7, 572-579.

80 Partridge, W. J., Drug and gene targeting to the brain with molecular trojan horses. *Nature Rev: Drug Discovery* 2002, 1, 131-139.

81 Jones, J. H., *Amino acid and peptide synthesis*. Oxford University Press: New York, 1997.

82 Bodanszky, M.; Bodanszky, A., *The practice of peptide synthesis*. Springer-Verlag: New York, 1984.

83 Norman, R. O. C.; Tomlinson, M. J.; Waddington, D. J., *Mechanisms in Organic Chemistry*. Mills: London, 1978.

84 Fieser, L. F.; Fieser, M.; Smith, J., *Reagents for Organic Synthesis*. J. Wiley & Sons: New York, 1990.

85 Silverstein, R.; Webster, F. X.; Kiemle, D., *Spectrometric identification of organic compounds*. John Wiley & Sons: New York, 2005.

86 Pollastri, M. P.; Sagal, J. F.; Chang, G., The conversion of alcohols to halides using a filterable phosphine source. *Tet. Lett.* 2001, 42, 2459 - 2460.

87 O'Neil, I.; Thompson, S.; Murray, C.; Kalindjian, S., DPPE: A convenient replacement for triphenylphosphine in the Staudinger and Mitsunobu reactions. *Tet. Lett.* 1998, 39, 7787.

88 Hudson, R., *Structure and mechanism in organo-phosphorus chemistry*. Academic Press: London & New York, 1965.

89 Sykes, P., *A guidebook to mechanism in organic chemistry*. Longman, Inc.: New York, 1986.

90 Zweig, G.; Sherma, J., *Handbook of Chromatography*. CRC Press: Cleveland, Ohio, 1972.

91 Herbert, C. G.; Alexander, R., *Mass Spectrometry Basics*. CRC Press: 2002.

92 Harwood, L. M.; Moody, C. J., *Experimental Organic Chemistry: Principles and Practice*. Blackwell: Oxford, 1989.

93 Meyer, M.; Dahaoui-Gindrey, V.; Lecomte, C.; Guilard, R., Conformations and coordination schemes of carboxylate and carbamoyl derivatives of the tetraazamacrocycles cyclen and cyclam, and the relation to their protonation states. *Coord. Chem. Rev.* 1998, 178-180, 1313 -1405.

94 Clogard, C.; Hovland, R.; Fossheim, S. L.; Aasen, A. J.; Klaveness, J., Synthesis and physicochemical characterisation of new amphiphilic gadolinium DO3A complexes as contrast agents for MRI. *J. Chem. Soc., Perkin Trans. 2,* 2000, 1047-1052.

95 Kimura, E.; Aoki, S.; Koike, T.; Shiro, M., A Tris(Zn^{II}-1,4,7,10-tetraazacyclododecane) complex as a new receptor for phosphate dianions in aqueous solution. *J. Am. Chem. Soc.* 1997, 119, 3068-3076.

96 Greene, T. W.; Wuts, P., *Protective Groups in Organic Synthesis*. J. Wiley & Sons: 2006.

97 Maruyama, K.; Hashimoto, M.; Tamiaki, H., Intramolecular photoreaction of synthetic oligopeptide-linked anthraquinone molecules. *J. Org. Chem.* 1992, 57, 6143- 6150.

98 Kirby, A. J., *Stereoelectronic Effects*. Oxford University Press: New York, 1996.

99 Photaki, I., Transformation of serine to cysteine. β-elimination in serine derivatives. *J. Am. Chem. Soc.* 1962, 85, 1123 - 1126.

100 Dugave, C.; Menez, A., Stereoconservative synthesis of orthogonally protected - functionalized amino acids using *N*-trityl derivatives. *J. Org. Chem.* 1996, 61, 6067-6070.

101 Lattuada, L.; Lux, G., Synthesis of Gd-DPTA-cholesterol: a new lipophilic gadolinium complex as a potential MRI contrast agent. *Tet. Lett.* 2003, 44, 3893-3895.

102 Hovland, R.; Glogard, C.; Klaveness, J., Preparation and *in vitro* evaluation of GdPCTA-[12] derivative: a micellar MRI contrast agent. *Org. Biomol. Chem.* 2003, 1, 644 - 647.

103 Brane, S.; Kirk, D. N., *The Bile Acids, Chemistry, Physiology and Metabolism.* Plenum: New York, 1988.

104 Goto, J.; Kato, H.; Hasegawa, F.; Nambara, T., Synthesis of monosulfates of unconjugated and conjugated bile acids. *Chem. Pharm. Bull.* 1979, 27, (6), 1402-11.

105 Hirayama, Y.; Iwamura, M.; Furuta, T., Design, Synthesis and Photochemical Properties of Caged Bile Acids,. *Bioorg. Med. Chem. Lett.* 2003, 13, 905-908.

106 Bellini, A. M.; Quaglio, M. P.; Guarneri, M., Antimicrobial activity of cholane compounds; cholic and deoxycholic acids derivatives (Part I). *Eur. J. Med. Chem.* 1983, 18, (2), 185-190.

107 Ronsin, G.; Kirby, A. J.; Rittenhouse, S.; Woodnutt, G.; Camilleri, P., Structure and antimicrobial activity of new bile acid-based gemini surfactants. *J. Chem. Soc., Perkin Trans. 2,* 2002, 1302 -1306.

108 Borbas, K. E.; Bruce, J. I., Synthesis of asymmetrically substituted cyclen-based ligands for the controlled sensitisation of lanthanides. *Org. Biomol. Chem.* 2007, 5, 2274 - 2282.

109 De Leon Rodriguez, L.; Kovacs, Z.; Esqueda-Oliva, A.; Miranda-Olvera, A., Highly regioselective *N*-trans symmetrical diprotection of cyclen. *Tet. Lett.* 2006, 47, 6937-6940.

110 Denat, F.; Brandes, S.; Guilard, R., Strategies for the regioselective N-functionalization of tetraazacycloalkanes. From cyclam and cyclen towards more sophisticated molecules. *Synlett* 2000, 5, 561-574.

111 Li, W.; Wong, W., A convenient method for the preparation of mono *N*-alkylated cyclams and cyclens in high yields. *Tet. Lett.* 2002, 43, 3217-3220.

112 Kruper, W. J.; Rudolf, P. R.; Langhoff, C. A., Unexpected Selectivity in the Alkylation of Polyazamacrocycles. *J. Org. Chem.* 1993, 58, 3869-3856.

113 Li, W.; Wong, W., A convenient method for the preparation of mono N-alkylated cyclams and cyclens in high yields. *Tetrahedron Letters* 2002, 43, 3217-3220.

114 Norman, R. O. C., *Principles of organic synthesis*. Chapman & Hall: London, 1978.

115 Perlmutter, P., *Conjugate Addition Reactions In Organic Synthesis*. Elsevier Science Ltd: Oxford, UK, 1992.

116 Mather, B. D.; Viswanathan, K.; Miller, K. M.; Long, T. E., Michael addition reactions in macromolecular design for emerging technologies. *Prog. Polym. Sci.* 2006, 31, 487-531.

117 Rolland-Fulcrand, V.; Haroune, N.; Roumestant, M.-L.; Martinez, J., Efficient chemoenzymatic synthesis of enantiomerically pure β-heterocyclic amino acid derivatives. *Tetrahedron: Asymmetry* 2000, 11, 4719 -4724.

118 Cocolios, P.; Guilard, R.; Gros, C. Polyazacycloalkanes derivatives, their metal complexes and pharmaceutical products incorporating these complexes. World Patent Number WO 96/11189, 1995.

119 Fensterbank, H.; Zhu, J.; Riou, D.; Larpent, C., A convenient one-step synthesis of mono-N-functionalized tetraazamacrocycles. *J. Chem. Soc., Perkin Trans. 1* 1999, 811-815.

120 Wainwright, K., Chemistry of structurally developed macrocycles. Part 1. Complexation properties of *N, N', N'', N'''*-Tetra(2-cyanoethyl)-1,4,8,11-tetra-aza-cyclotetradecane with nickel(II). *J. Chem. Soc., Dalton Trans.* 1980, 2117-2120.

121 Freeman, G. M.; Kent barefield, E.; Van Der Veer, D. G., Studies on Nickel(II) complexes of cyclam ligands containing functionalised nitrogen substituents: synthesis, isomerization, and *N*-dealkylation. *Inorg. Chem.* 1984, 23, 3092-3103.

122 Li, C.; Wong, W., A selective one-step synthesis of tris *N*-alkylated cyclens. *Tetrahedron* 2004, 60, 5595-5601.

123 Fensterbank, H.; Berthault, P.; Larpent, C., A tunable one-step *N,N'*-disubstitution of 1,4,8,11-tetraazacyclotetradecane with acrylamide. *Eur. J. Org. Chem.* 2003, 3985-3990.

124 Southam, R., Studies for the organic qualitative laboratory. *J. Chem. Educ.* 1976, 53, (1), 34 - 36.

125 Dischino, D. D.; Delaney, E. J.; Tweedle, M. F., Synthesis of Nonionic Contrast Agents Useful as Contrast Agents for Magnetic Resonance Imaging. *Inorg. Chem.* 1991, 30, 1265-1269.

126 Reibenspies, J. H., Structure of 1,4,7,10-tetraazacyclododecane (trihydrate). *Acta Cryst.* 1992, C48, 1717-1718.

127 Emsley, J., Very strong hydrogen bonding. *Chem. Soc. Rev.* 1981, 9, 91-124.

128 Holton, R. A.; Williams, A. D.; Kennedy, R. M., Formation of quaternary centers via the Michael reaction. Electronic compensation for steric congestion. *J. Org. Chem.* 1986, 51, 5480 -5482.

129 Klemarczyk, P., The isolation of a zwitterionic initiating species for ethyl cyanoacrylate (ECA) polymerization and the identification of the reaction products between 1°, 2°, and 3° amines with ECA. *Polymer* 2001, 42, 2837-2848.

130 Dawber, J. G.; Crane, M. M., Keto-enol tautomerization; A thermodynamic and kinetic study. *J. Chem. Educ.* 1967, 44, (3), 150-152.

131 Babievskii, K. K.; Belikov, V. M.; Tikhonova, N. A., On the production of α-nitroacrylic ester. *Russ. Chem. Rev.* 1965, 160, (1), 103-105.

132 Perez, M.; Pleixats, R., $FeCl_3$-catalysed conjugate addition of secondary amines, imidazole and pyrazole to methyl 2-acetamidoacrylate: Preparation of β-dialkylamino-α-alanine and β-(N-Heteroaryl)-α-alanine Derivatives. *Tetrahedron* 1995, 51, (30), 8355-8362.

133 Srivastava, N.; Banik, B. K., Bismuth nitrate-catalyzed versatile Michael reactions. *J. Org. Chem.* 2003, 68 (6), 2109 -2114.

134 Firouzabadi, H.; Iranpoor, N.; Jafari, A. A., Micellar solution of sodium dodecyl sulfate (SDS) catalyzes facile Michael addition of amines and thiols to α,β-unsaturated ketones in water under neutral conditions. *Adv. Synth. Catal.* 2005, 347, 655-661.

135 Wabnitz, T. C.; Spencer, J. B., A general Bronsted acid-catalysed hetero-Michael addition of nitrogen, oxygen, and sulfur nucleophiles. *Org. Lett.* 2003, 5, (12), 2141-2144.

136 Greene, T. W., *Protective Groups in Organic Synthesis.* J Wiley & Sons: 1981.

137 Comprehensive Organic Chemistry. In *Additions to and Substitutions at C-C π bonds*, Trost, B. M.. Elsevier Science: 1991.

138 Constable, E. C., *Coordination Chemistry of Macrocyclic Compounds.* Oxford University Press: Oxford, 1999.

139 Midura-Nowaczek, K., Syntheses of Methylketones of Peptides with C-Terminal Optically Active Lysine: Removal of the Benzyloxycarbonyl group. *Monatshefte fur Chemie* 1997, 128, 207-210.

140 Dygos, J.; Yonan, E.; Scaros, M.; Goodmonson, O.; Getman, D.; Periana, R.; Beck, G., A convenient asymmetric synthesis of the unnatural amino acid 2,6-dimethyl-L-tyrosine. *Synthesis* 1992, August.

141 Vogel, A. I.; Jeffery, G. H., *Vogel's Textbook of quantitative chemical analysis*. Longman Scientific & Technical.: Harlow (UK), 1989.

142 Gunnlaugsson, T.; Leonard, J. P.; Mulready, S.; Nieuwenhuyzen, M., Three step vs one pot synthesis and X-ray crystallographic investigation of heptadentate triamide cyclen-based ligands and some of their lanthanide ion complexes. *Tetrahedron* 2004, 60, 105-113.

143 Van Der Elst, L.; Laurent, S.; Muller, R. N., Multinuclear magnetic resonance characterization of paramagnetic contrast agents. The manifold effects of concentration and counterions. *Invest. Radiol.* 1998, 33, (11), 828 -834.

144 Woods, M.; Kiefer, G. E.; Sherry, A. D., Synthesis, Relaxometric, and Photophysical Properties of a New pH-Responsive MRI Contrast Agent: The Effect of Other Ligating Groups on the Dissociation of a *p*-Nitrophenolic Pendant Arm. *J. Am. Chem. Soc.* 2004, 126, 9248-9256.

145 Barge, A.; Botta, M.; Parker, D.; Puschmann, H., The nature of the counter-anion can determine the rate of water exchange in a metal aqua complex. *Chem. Comm.* 2003, 1386-1387.

146 Bruce, J. I.; Dickins, R. S.; Govenlock, L. J.; Gunlaugsson, T.; Lopinski, S.; Lowe, M. P.; Parker, D.; Peacock, R.; Perry, J.; Aime, S.; Botta, M. J., The selectivity of reversible oxy-anion binding in aqueous solution at a chiral europium and terbium center: Signaling of carbonate chelation by changes in the form and circular polarization of luminescence emission. *J. Am. Chem. Soc.* 2000, 122, 9674-9684.

147 Aime, S.; Bombieri, G.; Cavallotti, C.; Giovenzana, G. B.; Imperio, D.; Marchini, N., An unusual gadolinium ten-coordinated dimeric complex in the series of MRI contrast agents: Na[Gd(H2O)AAZTA]. $3H_2O$. *Inorg. Chim. Acta* 2007, 361, (5), 1534-1541.

148 Raymond, K. N.; Pierre, V. C., Next generation, high relaxivity gadolinium MRI agents. *Bioconj. Chem.* 2005, 16, 3 - 8.

149 Mishra, A.; Pfeuffer, J.; Mishra, R.; Engelmann, J.; Mishra, A. K.; Ugurbil, K.; Logothetis, N. K., A new class of Gd-based DO3A-ethylamine-derived targeted contrast agents for MR and optical imaging. *Bioconj. Chem.* 2006, 17, (3), 773-780.

150 Parker, D.; Morphy, J. R.; Jankowski, K.; Cox, J., Implementation of macrocycle conjugated antibodies for tumour-targeting. *Pure & Appl. Chem.* 1989, 61, (9), 1637-1641.

151 Umino, N., Sodium acetoxyborohydride as a new reducing agent. *Tet. Lett.* 1976, 10, 763-766.

152 Tweedle, M. F.; Gaughan, G. T.; Hagan, J. T. 1-substituted-1,4,7-triscarboxymethyl-1,4,7,10-tetraazacyclododecane and analogs. US Patent Number 4885363, 1989.

153 Liu, S., The role of coordination chemistry in the development of target-specific radiopharmaceuticals. *Chem. Soc. Rev.* 2004, 33, 445-461.

154 Borbas, K. E.; Ferreira, C. S. M.; Perkins, A.; Bruce, J. I.; Missailidis, S., Design and synthesis of mono- and multimeric targeted radiopharmaceuticals based on novel cyclen ligands coupled to anti-MUC1 aptamers for the diagnostic imaging and targeted radiotherapy of cancer. *Bioconj. Chem.* 2007, 18, (4), 1205 -1212.

155 Storr, T.; Thompson, K.; Orvig, C., Design of targeting ligands in medicinal inorganic chemistry. *Chem. Soc. Rev.* 2006, 35, 534 - 544.